Polarised polyphase current differential protection for distribution feeder circuits using a digital voice frequency communications channel

Chiwaya, A. A. W.

Award date:
1994

Awarding institution:
University of Bath

POLARISED POLYPHASE CURRENT DIFFERENTIAL PROTECTION FOR DISTRIBUTION FEEDER CIRCUITS USING A DIGITAL VOICE FREQUENCY COMMUNICATIONS CHANNEL.

Submitted by A A W Chiwaya, BSc, REng (Malawi)

for the degree of PhD

of the University of Bath

1994.

COPYRIGHT

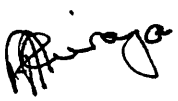

ProQuest LLC
789 East Eisenhower Parkway
P.O. Box 1346
Ann Arbor, MI 48106-1346

SYNOPSIS.

Utilities use various methods of protection of distribution feeder circuits such as fuses, overcurrent relays, and current differential relays. The latter provides the much desired Unit protection for high speed operation, sensitivity to in-zone faults, and inherent stability for external faults.

A major limitation for digital current differential protection for distribution feeders is the cost and availability of suitable data communication systems. Considering a simplistic approach to current differential protection, the volume of data required to correctly define the sampled waveforms at the feeder terminals and the need to immediately provide this data at other terminals requires high data rate communications. Invariably, this high data rate communications attracts higher costs which undermines the appeal of a digital unit protection scheme.

This thesis describes a new approach to digital unit protection for distribution feeder circuits which uses limited data, and therefore in-expensive, communications. To take advantage of the low cost communications systems available, the protection is designed to use a voice frequency channel. As this offers only a limited data rate, specialised algorithms were used which dramatically reduce the data required to define the current signals. Based on equations used to derive power in a three phase system, these use polyphase polarised current measurements made at the feeder's terminals. The polarising reference phasors were first derived from the phase voltages at the terminals. However, as the use of voltage transformers may be unattractive in distribution feeder systems, positive phase sequence currents were also used to provide the reference.

Details are given of the algorithm's performance under a variety of power system fault conditions on overhead line feeders, underground cable feeders, and on composite feeders of both overhead lines and underground cables. It has been demonstrated that the algorithm provided a desirable level of protection while working within the limited capability of a voice frequency data communications channel.

ACKNOWLEDGEMENTS.

I would like to express my sincere gratitude to my supervisor, Dr. M. A. Redfern, for his excellent supervision. I thank him for his untiring help, advice, encouragement, comments, criticism, guidance, and friendly attitude throughout the course of the research and preparation of this thesis. I appreciate his general support beyond this research.

I would like to thank Prof. A T Johns for permitting this research to be done and providing the facilities.

I acknowledge the assistance given by J I Barrett and J Grzejewski both from the School of Electronic and Electrical Engineering.

My special thanks go thousands of miles away to my wife Janet and my children Allan and Yolanda whose patience, understanding and waiting I greatly value.

The financial support from Electricity Supply Commission of Malawi, ESCOM, is highly appreciated, and my thanks go to the Management of ESCOM for their encouragement and interest.

CONTENTS.

LIST OF SYMBOLS AND ABBREVIATIONS

A, B, C or a, b, c	power system phases
ω	angular frequency
ωC	susceptance
ωL	inductive reactance
R	resistance
sec	seconds
i or I	current
A	Amps
v or V	voltage
kV	kilovolts
kw	kilowatts
MW	megawatts
s	reference phasor
Hz	frequency
km	kilometre
PCM	Pulse Code Modulation
CCITT	International Telegraph and Telephone Consultative Committee
ITU	International Telecommunication Union
ANSI	American National International Standards
ISO	International Standards Organisation
IEC	International Electrotechnical Commission
IEE	Institute of Electrical Engineers
IEEE	Institute of Electronic and Electrical Engineers
TDM	Time Division Multiplexing
FDM	Frequency Division Multiplexing
FM	Frequency modulation
ADC	Analogue to Digital Convertor

S/N	signal to noise ratio
ac	alternating current
dc	direct current
bits	binary digits
PLL	Phase Locked Loop
EMTP	Electromagnetic Transients Program
h	120 degrees operator
n_s	number of samples per power system cycle
CT	Current Transformer
VT	Voltage Transformer
k	bias setting for current differential relaying
P	real power
Q	reactive power
Subscript *0, 1, 2*	zero, positive, negative phase sequences
VCO	Voltage Controlled Oscillator
ms	milliseconds
θ	phase angle between, say, voltage and current
Φ	phase displacement of say current from a reference point
ϕ	phase displacement of say current from a reference point
$\surd$	square root
Σ	summation
ρ	resistivity
μ	relative permeability
ε	relative permittivity
$\rangle$	greater than
BCH	Bose Chaudhuri-Hocquenghen code
ESCOM	Electricity Supply Commission of Malawi
ACSR	Aluminium Conductor Steel Reinforced
AAA	All Aluminium Alloy

Chapter 1

INTRODUCTION.

1.1 AN OVERVIEW OF POWER SYSTEM PROTECTION.

Feeder circuits are one of the most vulnerable points in power systems[1] that are prone to disruptions due to accidents or equipment failure which lead to short circuits. For safe and secure operation of the electrical power supply network, the objective of short circuit protection is to detect the presence of a short circuit on the system and initiate isolation of the faulted section from the rest of the supply network in the shortest time achievable. It is essential that, in order to minimise disruption to the network, the protection remains inoperative for all healthy conditions and faults on the other plant. The basic idea is to define the undesirable conditions and look for any discrepancies between the undesirable and permissible conditions that the protection system can sense. This requires clear understanding of the conditions existing during short circuit faults, protection requirements and their constraints. The basic process of power system protection is as shown in figure 1.1, while figure 1.2 illustrates the functional requirements and the constraints that influence their fulfilment[2].

Protection systems are generally divided into Unit and Non-unit systems[3]. Unit protection, also referred to as Restricted protection, is provided when a section of the power system is protected individually without reference to the other sections, and thus, coordination with protection in adjacent zones is eliminated, resulting in high speed tripping. It is based on comparison of zone boundary conditions to decide whether or not a fault exists in the protected zone. Non-unit protection, also referred to as Unrestricted protection, is based on measurements taken at one location, the relaying point, on the supply network. Protection schemes comprise CT's and/or VT's, circuit breakers, relays

and sometimes a communications system. With the power system divided into zones as illustrated in figure 1.3, with the CT's and VT's providing the boundaries, a protection scheme can provide primary protection offering first line of defense, or back-up protection offering second line of defense. Although the fundamentals of protection are quite similar, each of the zone categories has protective relays specifically designed for the primary protection which are based on the characteristics of the equipment being protected. Table 1.1 gives relay device numbers.

1.2 CONVENTIONAL FEEDER CURRENT DIFFERENTIAL RELAYING.

Unit protection is mainly used as the main protection and current differential protection provides the much desired unit protection of feeders. To compare the zone boundary conditions of a feeder circuit, a communications channel is used to transfer electrical quantities from the remote terminal to the local terminal. The local relay then compares quantities from the remote terminals with the corresponding local quantities for a decision to be made as to whether or not a fault exists and if it does, to send a trip signal to a circuit breaker. If a fault does not exist or it is not in the designated zone of protection, the relay restrains from tripping.

The relay in Unit protection uses the principle, first established by Merz and Price in the early 1900's, that on a healthy power system circuit the vector sum of the terminal currents flowing in the protected zone is zero in accordance with Kirchoff's law. Only an in-zone shunt fault establishes an alternative current path resulting in vector differences in the currents measured at the terminals. When these differences exceed a predetermined value, a trip condition is established. An external fault results in the vector differences not exceeding the trip limits and therefore causes no trip. Figure 1.4 summarises these concepts.

In practice, current differential relaying of feeders, also called pilot relaying because of the use of a communications channel, is typically applied to short feeder circuits of up to 80 km[4, 5, 6]. The distances are limited due to the effects on relay sensitivity and restraint under through fault conditions because of the transmission line effects which result in the high impedance of the wires, their charging currents and the phase shifts suffered by the voltages. The communications system may use metallic conductors, optical fibres, or free space via radio, or microwave, as the communications medium, as illustrated in figure 1.5[3, 7]. The system may be dedicated to one user or shared between several. The choice depends on availability, costs and geography.

Three relay technologies are presently used in power system protection:-

- electromechanical relays, introduced in the early 1900's,
- solid state relays introduced in the late 1950's,
- microprocessor relays introduced in the 1980's.

Traditional current differential relaying uses either electromechanical or analogue static relays together with copper wires to provide the communications circuit. In these schemes, the pilot circuit is an integral part of the decision making process since it provides the electrical signal summation circuit[6, 8]. A typical arrangement is shown in figure 1.6. The typical operating times of these relays varies from one and a half to three cycles depending on the type of relay[9], its settings and the fault. As they have been used for so long, there is a good appreciation of their performance limitations. When the pilots are used in microprocessor-based relaying, instead of being part of the differential circuit, they are used merely to convey information between the relays at the feeder's terminals. The passage of signals can take place simultaneously in both directions, with the differential connections formed locally at each terminal. The problem then becomes simply one of communications.

Digital networks offer excellent opportunities to convey protection signals. However, uncertainties arise as to how the Unit protection schemes will perform over the long term. Questions have risen about whether networks and equipment designed for business use properly fit the needs of protection which include requirement to have all failure modes as random and not systematic, consistent send and receive times, no re-bunching of data, no queuing in modems, and no random re-routing.

1.3 THE IMPACT OF MICROPROCESSOR-BASED RELAYS.

Microprocessors have revolutionised the science of protective relaying. Evolution of relays for the protection of transmission lines started with electromechanical relays in the 1920's[10]. Development work on static relays started in the period of 1940 - 50, initially using thermionic valves which were eventually abandoned by the advent in 1950 - 60 of transistors and other solid state components. However, the introduction of digital computers in the 1950's, and their subsequent use for the protection of power system equipment first proposed in 1969[11], has brought about alternative approaches to the traditional methods used with electromechanical and static relays. These alternative approaches have made available modern equipment in the form of protection relays, communication channels, substation controllers, test equipment, personal computers and software packages that provide a medium for improved performance and greater information availability. The advanced analytical techniques now possible enable rigorous studies to be performed in order to better understand the behaviour of the power system especially under fault conditions. This leads to overall improvements in the protection. On the applications point of view, the performance of protection schemes can be verified without any shut-downs by simulating contingencies at any location of the system.

Modern relays are characterised by the ability to execute various algorithms that efficiently perform functions carried out by traditional relays and perform investigative tasks in depth. Several protection algorithms can be included in one package, reducing the differences between relays based on Unit and Non-Unit protection. In feeder circuits, with Unit protection and its associated shorter operating times as the main scheme, the additional schemes which can be included in a digital relay include back-up features[12] of Non-Unit protection. As local data relating to the operation of the power system is available, the non-operation of the Unit protection can therefore be overcome should the communications channel be lost.

The key in the algorithms is to determine the quantities that exist to distinguish between tolerable and intolerable conditions. As in traditional relaying, voltage, current, temperature, frequency and pressure[13, 14] are such quantities. The most common shunt fault indicator is a sudden and generally significant increase in the current[5]. In feeder circuits, current is used in such schemes as differential, overcurrent, directional and distance protection. Distribution system protection schemes depend on whether or not the feeders form parallel circuits, ring-mains or radials, have voltage transformers, data links, and also good economics.

The use of digital data communications in microprocessor relaying has complicated rather than simplified the design of current differential relaying. The signals cannot be summated in the communications circuit in the manner used in traditional relaying. Full duplex data transmission is used for simultaneous and independent decision making by the relays at the feeder's terminals. A simplified representation of a typical digital current differential scheme is shown in figure 1.7. The relays are designed assuming that bidirectional propagation times are essentially equal in each directional. Bidirectional time symmetry is not a critical requirement for normal data transfer. The V.35 CCITT standard, for example, has no restriction to the amount of propagation time

asymmetry for communications equipment[15]. The communications may thus produce some significant difference between transmit signal delays and receive signal delays causing misalignment of the data and resulting in calculating non-existent spill current by the difference process.

The normal requirement in digital differential relaying, therefore, is to effect precise time alignment of measured quantities from the ends in order to arrive at a correct decision. The process includes accurate measurements of the propagation time delay introduced by the communications system. The volume of data thus required to correctly define a sampled sinusoidal waveform at a terminal with any accuracy is relatively high.

Ideally, the communications system should instantaneously transfer all the data required for the protection. Unfortunately, practical communication systems are limited in the quantity of data that they can handle in a specified time period, and they introduce time delays from when the data is made available for transfer at one terminal and provided for use at others. This has led to research into new differential relaying algorithms which can tolerate the limited capacity and associated time delays of the communications systems[16, 17, 18, 19].

Wideband communications such as available in fibre optic data transmission would offer good opportunities to convey the mass of data required for protection and thereby provide less problems with the use of sophisticated encoding. However, as this protection is intended for distribution feeder circuits, a low cost communications system is considered to be very advantageous.

1.4 PROTECTION USED IN MALAWI SYSTEM.

Malawi is situated in Southern Central Africa. Roughly the size of England, but with a population of around 10 million, it has a maximum demand of 140.2 MW and a generation capacity of 189.5 MW. Transmission voltages are 132 kV and 66 kV, with distribution voltages at 33 kV and 11 kV. Services on the network include a SCADA system that uses pilot wires and power line carrier for communications.

To protect the Malawi system, overcurrent and earth fault schemes are widely used both as the main protection and also as back-up protection. Distance protection is the main protection on the transmission network. Some short feeders are protected using current differential schemes. Currently, feeder differential protection uses the biased differential 'Translay' HO4 relays and the high speed biased differential DS7 relays in conjunction with private pilot wires which provide the electrical signal summation circuits. Both types use the balanced voltage schemes.

The HO4 relays are for general use on three phase feeders. A high degree of stability on through faults and good sensitivity on internal faults is achieved. Least sensitive earth fault setting of 40% of rated current is used. The DS7 is a higher speed class otherwise similar to HO4. It can use least sensitive earth fault setting of 20% of rating. Figure 1.8 summarises the typical time/current characteristics.

Simplicity, reliability and cost, in addition to high speed operation, are important for any new digital unit protection for distribution feeder circuits and particularly so for such a small size of the power system as in Malawi, which could be characteristic of many developing countries. As voice frequency channels are widely used on pilot wires, either rented or privately owned, for protection and control, any new service that uses them

will be attractive. Thus a new digital low cost unit protection scheme that uses voice frequency channels over pilot wires can be welcome.

The performance of a new differential protection needs to be in line with the performance of the HO4 and the DS7. Required tripping times would therefore need to be in the region of two and a half cycles of the 50 Hz power system waveform.

1.5 RESEARCH OBJECTIVES.

To take advantage of the low cost communication systems available for use over telephone circuits, a voice frequency channel appeared to be an ideal solution to use in unit protection of distribution feeder circuits. The objective of this research was thus to formulate new unit protection algorithms for distribution feeder circuits which provide the capabilities of conventional pilot wire differential protection while using the limited data transfer capabilities of digital data voice frequency communication channel and carry out their evaluation using computer simulation.

Voice frequency communication channels are the most commonly used systems having been extensively developed commercially for mass communications. They provide a standardised communications environment operating over a variety of media and, thus, provide a convenient standard for use with distribution system protection schemes. With an operating bandwidth of 4 kHz they can use a dedicated medium or share a medium with other channels. Since the available bandwidth is limited, the volume of data which can be handled is also limited.

Modems provide the interface between the digital protection and the communications medium, offering standard data rates ranging from 75 bits/sec to 14400 bits/sec operating in full or half duplex mode. After careful consideration of the characteristics of

communications systems, it was decided to base the research on a full duplex 2400 bits per second channel. Although this may be considered modest in light of currently available systems, the inherent communications security and its tolerance to interference generally vary with the inverse of the data rate[20]. It also provides a useful challenge to examine the level of performance which can be achieved with the system.

1.6 OUTLINE OF PROCEDURE.

To overcome the need to transmit the mass of data required to define the sampled current waveform and operate with a data transfer rate of 2400 bits/sec, it was essential to dramatically reduce the data used to define the current signals. The technique used a directional element on the measured quantity and was based on the equations used to derive instantaneous power in a three phase power circuit. This involved multiplying the locally obtained instantaneous values of the sampled phase currents i_a, i_b and i_c, with the locally derived instantaneous values of three phase reference phasors s_a, s_b and s_c on phases a, b, and c respectively, to provide a measurement which contained a steady dc component. The reference phasors are a set of three unit amplitude rotating sinusoidal waveforms, 120 degrees apart. Signals synchronised to the power system frequency and ideally having the same phase at all of the feeder's terminals were used to derive the polarising reference. Since this protection is principally aimed at short distribution feeders and assuming a heavily interconnected power system, the phase difference of the prefault local versus remote voltages is small, and therefore the three phase voltages were used to derive unit amplitude polarising reference phasors. To cater for conditions when there are no VT's, an alternative method used positive phase sequence current for the reference phasors.

Unbalanced conditions introduce second harmonics. Therefore a low pass filter is introduced by averaging the derived measurements over half a power system cycle to

remove any second harmonic terms leaving the steady dc term which contains both magnitude and phase information.

At the terminals of the protected feeder, i_a, i_b and i_c, and s_a, s_b and s_c, provided the polyphase polarised current measurement I_p. A second measurement, using an orthogonal set of reference phasors, (s_a-s_b), (s_b-s_c), and (s_c-s_a) gave polyphase polarised current measurement I_q which provided complimentary information, and hence the two measurements fully characterised the monitored terminal currents. The measurements I_p and I_q were transmitted alternatively and were given as[21];

$$I_p = i_a s_a + i_b s_b + i_c s_c \tag{1.1}$$

$$I_q = I_a(s_b - s_c) + i_b(s_c - s_a) + i_c(s_a - s_b) \tag{1.2}$$

These measurements were used in the differential process to detect shunt faults on the feeder by comparing received values with the corresponding local values delayed by the communications system delay time. This delay time included the message transmission time and the propagation delay time. As the polyphase polarised current measurements were steady DC signals, they reduced the demands on the communication channels. This technique, therefore, overcomes the normal requirement of digital differential relaying to synchronise data obtained at different terminals and also reduces the volume of data required to be transferred between relays. The system can thus operate with both telephone type communications circuits and copper pilot circuits.

The protection algorithm was evaluated using the EMTP power system simulation package to model a typical 33 kV network of 20 km long feeders. Both overhead lines

and underground cables were modelled with a variety of faults at different fault positions. Composite feeders were also modelled which had a mixture of overhead lines and underground cables. Both internal and external faults were considered. Points-on-wave at fault were varied. The communications being normally free running, synchronism variations between fault occurrence and data transmission were considered by randomising the transmission start time.

To provide security against mal-operation due to transitions in the measured I_p and I_q signals after the fault, two trip indications were required before allowing the algorithm to trip.

The algorithm was sensitive to all in-zone faults, producing relay trip outputs in average time of under two and a half power system cycles. It restrained from tripping for all external faults, including a terminal fault.

1.7 PRESENTATION FORMAT OF THE THESIS.

The thesis covers the work done in deriving the new digital current differential protection for distribution feeder circuits which only requires a voice frequency channel for digital data communications. Background information, objectives of the research, methods used, power system model studied, results obtained from the simulation, the conclusion and scope for further work are all given.

There are ten chapters, each chapter having its own figures, tables and appendices where applicable. Apart from this introductory one, each chapter starts with an introduction, continues with the main body, and ends with a summary.

Chapter 1 serves as an introduction of the work. Briefly, the role of protection in a power system has been discussed, giving examples of protection schemes with respect to feeder circuits. The use and impact of microprocessor-based systems in protection is mentioned. Communications-related problems in feeder differential protection have been briefly mentioned, highlighting the need for the type of research undertaken and how it is proposed to tackle them. The basis of the protection algorithms used has also been outlined, and an outline of the whole work is given.

Chapter 2 summarises the concepts of current differential protection, mentioning some of the strengths and weaknesses. Work carried out by some researchers in addressing some of the weaknesses is mentioned. The new approach aims at addressing some of the communications-related problems without compromising the strengths. It overcomes the need to transmit the mass of data required to define the sampled current waveforms and operate with a low data transfer capacity by dramatically reducing the data used to define the current signals.

Chapter 3 presents the new technique. The derivation of the reference phasors is discussed. At the terminals of the protected feeder the reference phasors and the measured three phase currents provide polyphase polarised current measurements. Each relay system transmits these measurements to the other relay, and compares its local signals with those received from the other relay in order to detect shunt faults on the feeder.

Chapter 4 discusses the communications aspects. The choice of voice frequency channels, and not wideband communication channels, has been discussed. A justification is given of using a 2400 bit per second data transfer operating on full duplex, briefly comparing it with other V-series CCITT standards[22, 23, 24], by citing switching durations, speed and noise.

The technique to reduce the data used to define the current signals was based on the equations used to derive the instantaneous power in a three-phase circuit. Power is basically voltage polarised current and has different terminologies depending upon the polarisation[25]. Chapter 5 discusses the equations for real power and reactive power. Both balanced and unbalanced system conditions are considered, with the method of symmetrical components being used to explain the phenomenon of unbalance in a three phase power system. The relevance to the new technique is given.

Chapter 6 presents the model of the power system used in the algorithm's evaluation. The EMTP package was used to model a typical 33 kV feeder network of overhead lines, of cables, and of composite overhead line and cable sections. The power system test model has a parallel configuration with single circuits as supply lines. One line of the parallel circuit has the differential scheme, and the other line together with the supply lines serve to provide the protection algorithm with external faults.

Chapter 7 presents the performance of the algorithm with the reference phasors being derived from the system voltage waveforms. Various faults at different fault positions have been studied.

Chapter 8 presents the performance of the algorithm with the positive phase sequence currents providing the reference phasors. As in chapter 7, various faults at different fault positions have been studied.

Conclusion of the work and proposal for further work is given in Chapter 9. Chapter 10 lists the references.

The new technique may be tested on systems such as that of Malawi. Appendix A gives an overview of the Malawi power network and its suitability for field tests.

1.8 FIGURES.

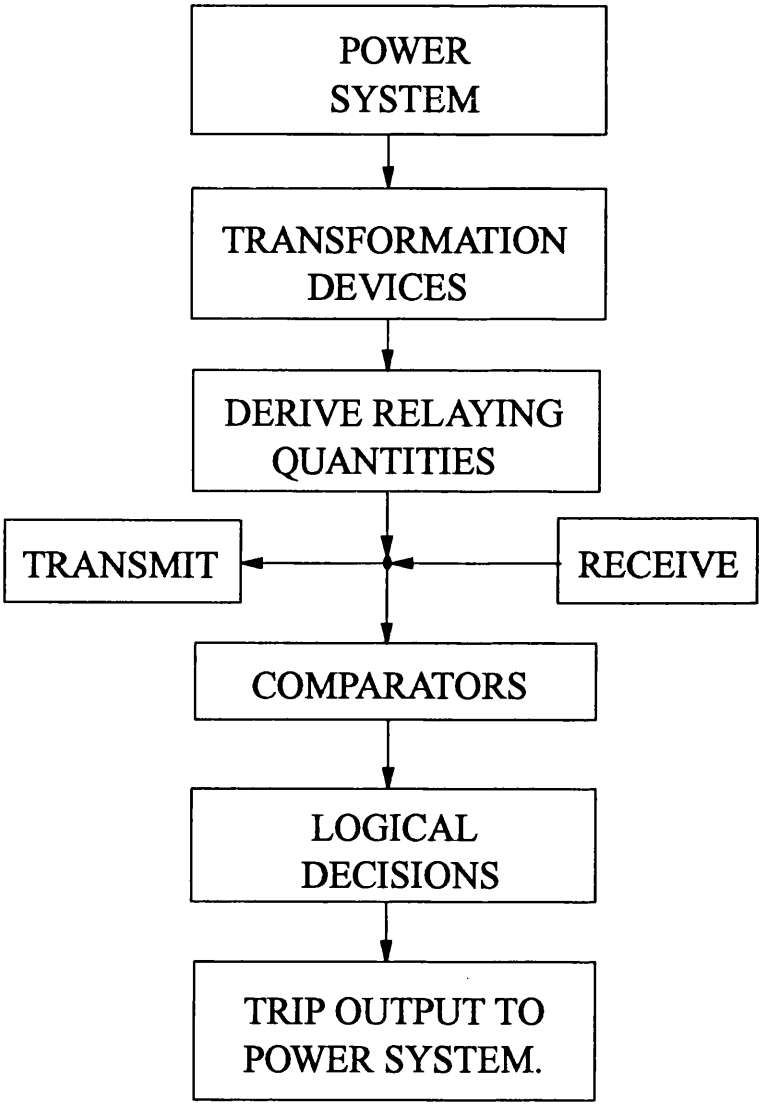

Figure 1.1 Basic Process of Power System Protection.

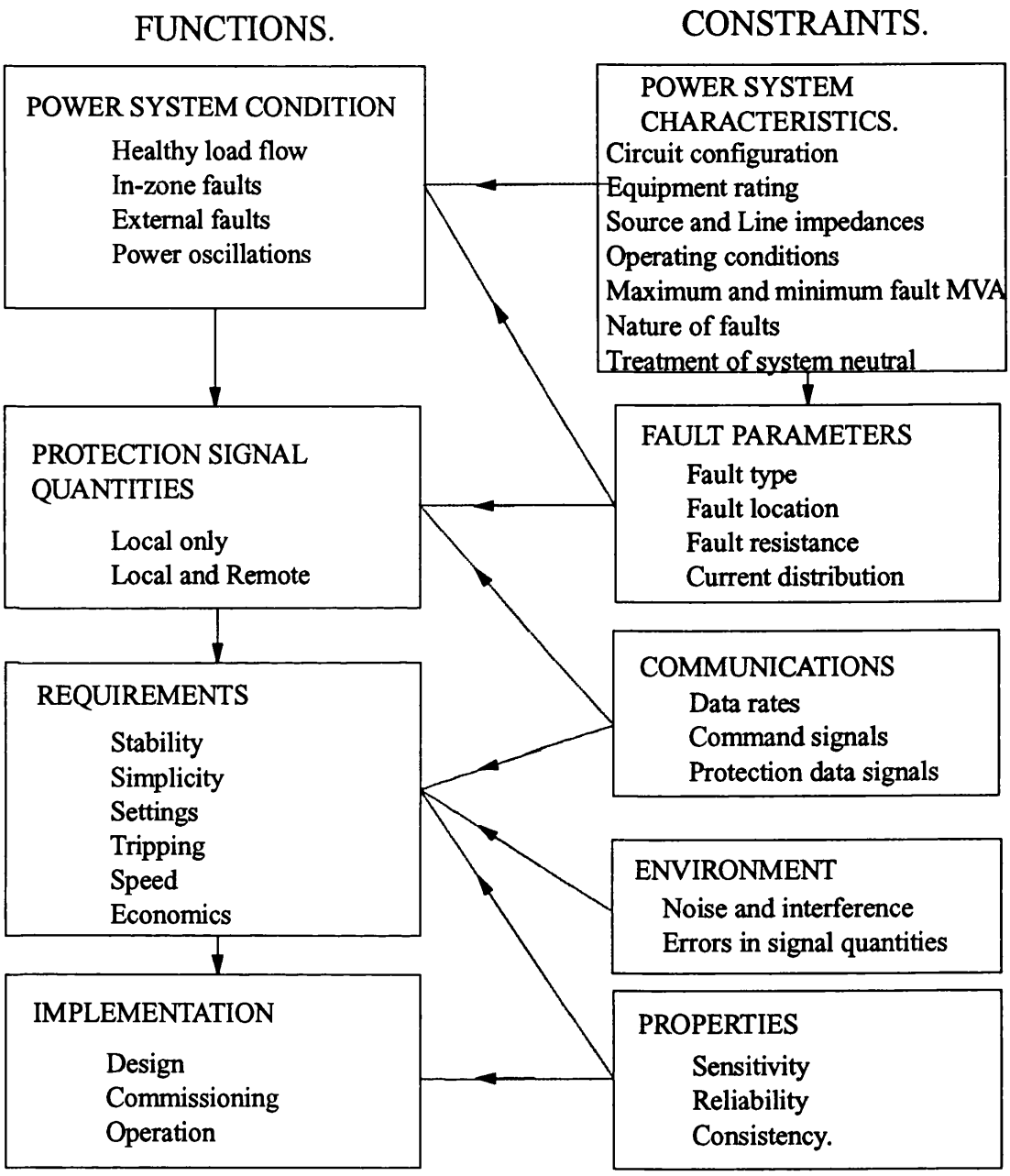

Figure 1.2 Functional Requirements and Constraints of Protection.

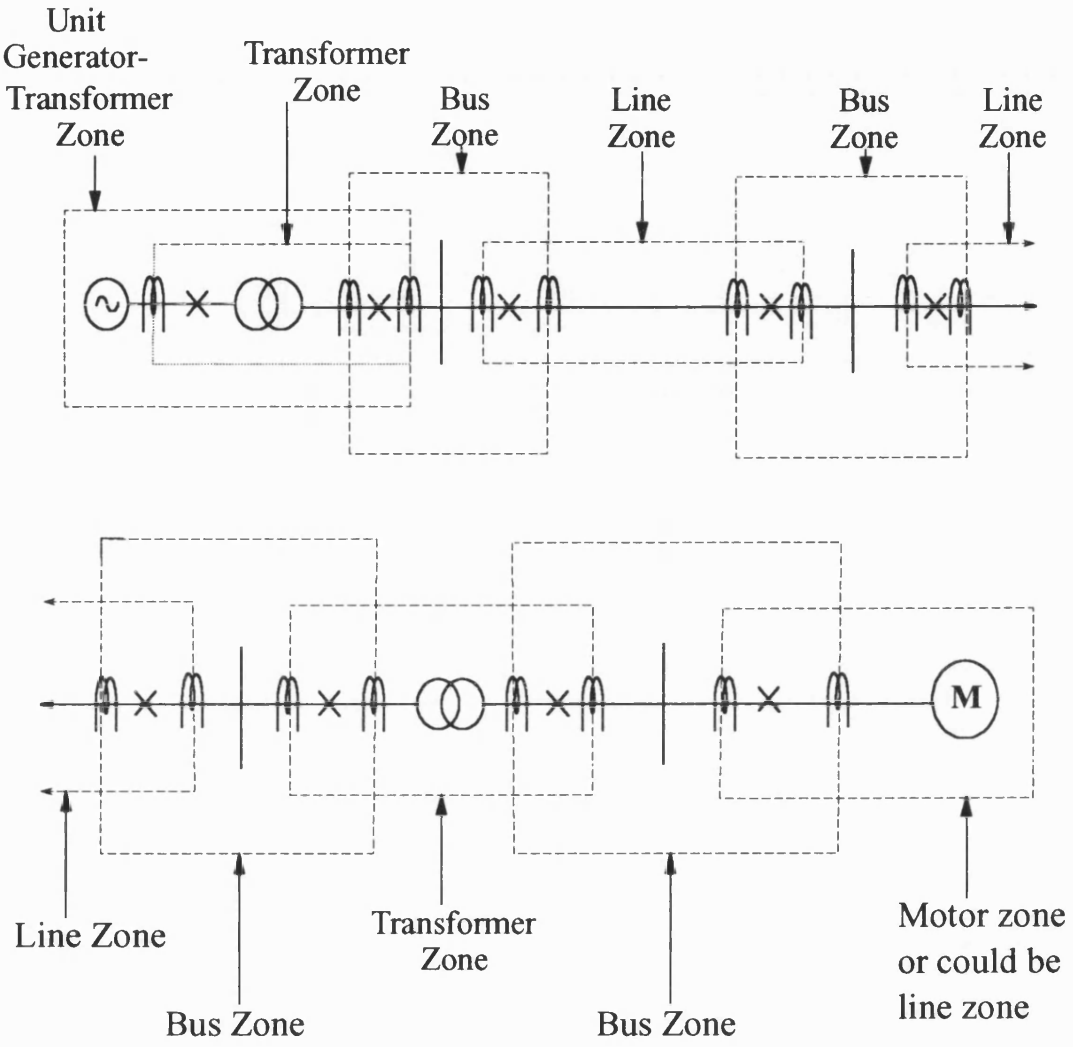

Figure 1.3 Power System Primary Protection Zones.

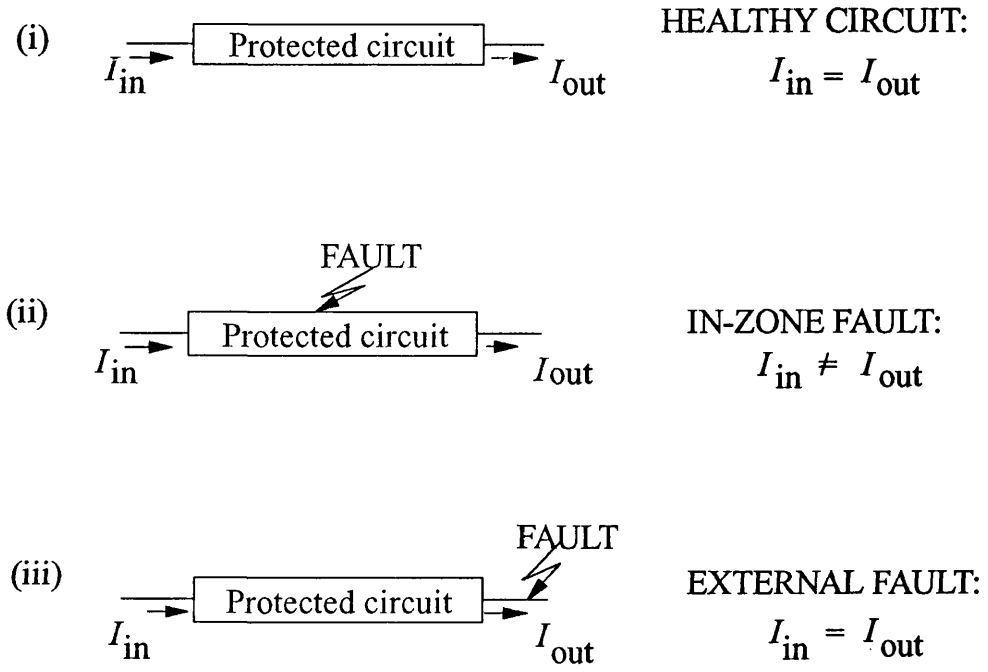

Figure 1.4 Concepts of Differential Protection.

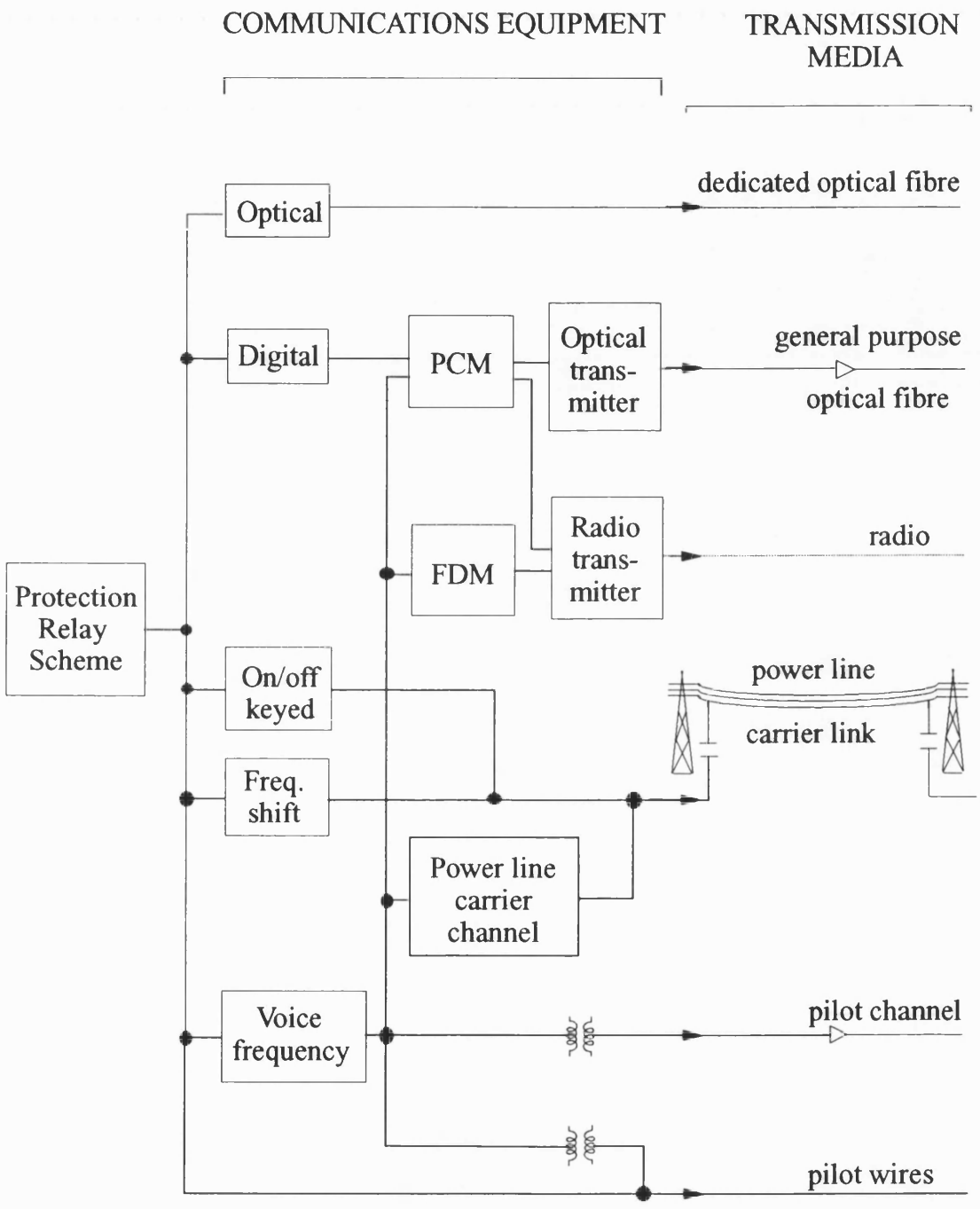

Figure 1.5 Communication Channels available for Protection.

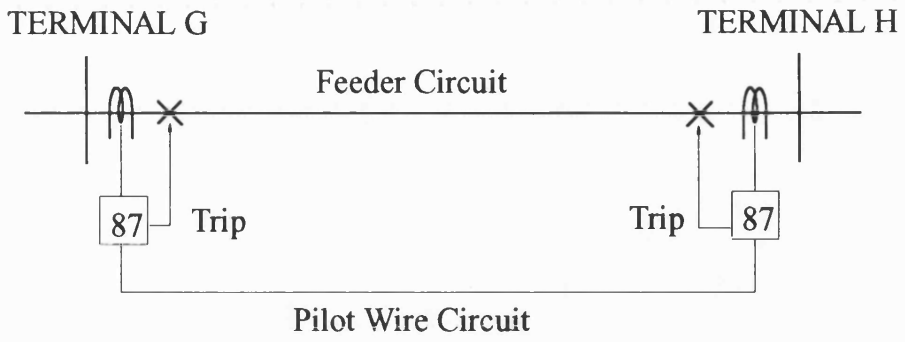

Figure 1.6 Typical Feeder Differential Protection Scheme.

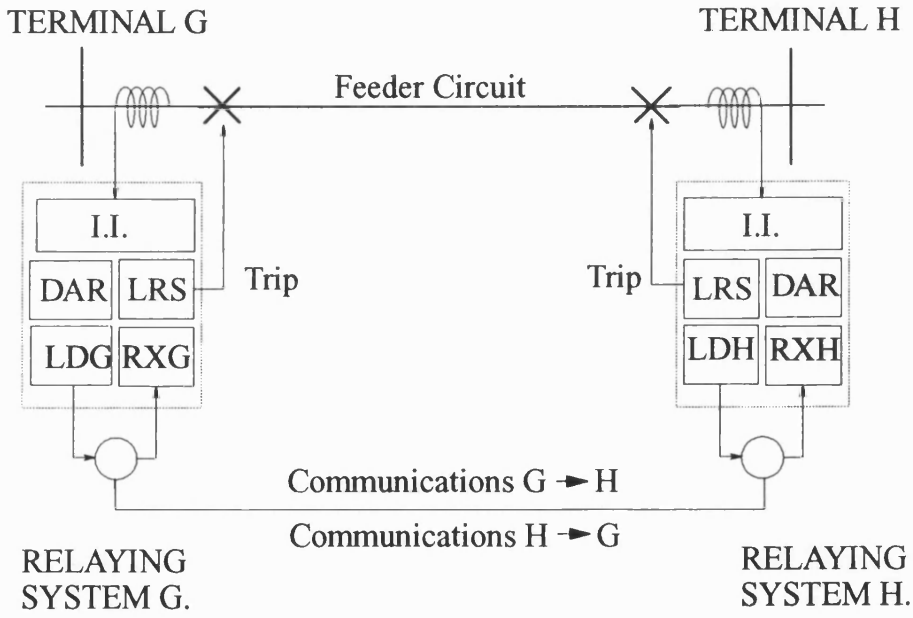

I.I. Input Interface.
DAR Data Acquisition for Remote Relay.
LRS Local Relay System.
LDG Line Driver - Relay G (H).
RXG Receiver - Relay G(H).

Figure 1.7 Simplfied Block Diagram of a Digital Current Feeder Differential Protection Scheme.

(i) HO4.

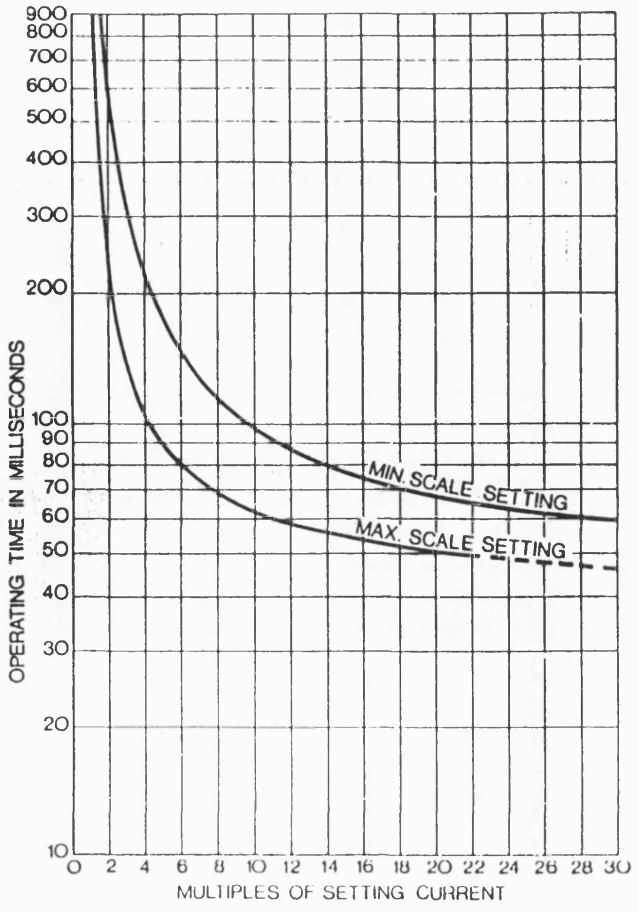

(ii) DS7.

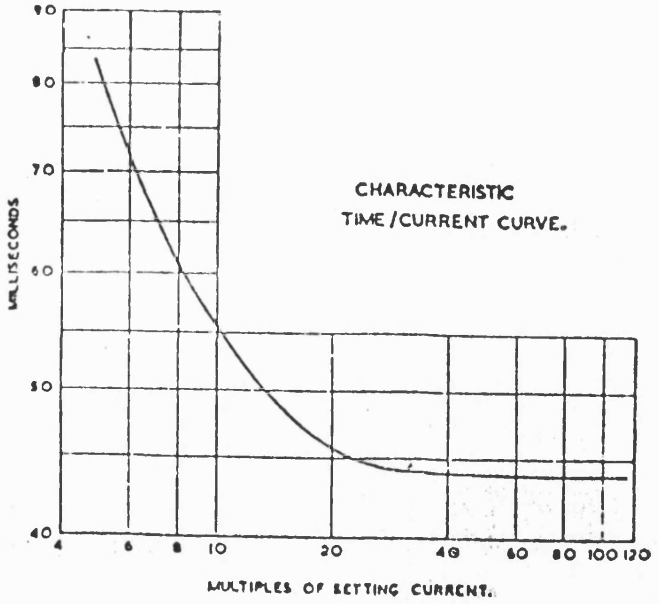

Figure 1.8 Typical Time/Current Characteristics of the HO4 and DS7 Feeder Current Differential Relays.

1.9 TABLES.

Device No.	Definition
2	Time delay starting or closing relay: except device 48, 62, 79
3	Checking or interlocking relay
21	Distance relay
25	Synchronising or synchronism check relay
27	Undervoltage relay
30	Annunciator relay
32	Directional power relay
37	Undercurrent or underpower relay
40	Field failure relay
46	Reverse phase or phase balance current relay
47	Phase-sequence voltage relay
48	Incomplete-sequence relay
49	Machine or transformer thermal relay
50	Instantaneous overcurrent or rate-of-rise relay
51	Ac time overcurrent relay
53	Exciter or DC generator relay
55	Power factor relay
56	Field application relay
59	Overvoltage relay
60	Voltage or current balance relay
62	Time delay stopping or opening relay
64	Earth fault protective relay
67	Ac directional overcurrent relay
68	Blocking relay
74	Alarm relay
76	Dc overcurrent relay
78	Phase angle measuring or out-of-step protective relay
79	Ac reclosing relay
81	Frequency relay
82	Dc reclosing relay
83	Automatic selective control or transfer relay
85	Carrier or pilot wire receive relay
86	Lock-out relay
87	Differential protective relay
91	Voltage directional relay
92	Voltage and power directional relay
94	Tripping or trip-free relay.

Table 1.1 Relay Standard Device Function Numbers.

Chapter 2

FEEDER CURRENT DIFFERENTIAL RELAYING.

2.1 INTRODUCTION.

In the early days of power transmission, over-current relays were mostly used for the protection of transmission lines[10]. The growing complexity of the power system and the requirement for fast and selective clearance of faults have led to the introduction of other relays, such as directional over-current, differential and distance relays.

Current differential protection inherently provides Unit protection offering, in principle, ideal fault selectivity and high speed operation. The basic requirement of any Unit protection scheme is that it must operate for all faults within the protected power circuit. Equally, it must remain inoperative both during healthy power system conditions and for faults external to the protected circuit. Unit protection fulfils these requirements by comparing zone boundary conditions. In the protection of feeder circuits, a pilot circuit[26] may be used as a medium to transmit current information between the relays at the feeder's terminals so that the relays can continuously carry out comparisons for decision making. Thus the relays located at the terminals of the protected feeder monitor the local electrical quantities, compare local with received quantities from other relays in order to make a trip decision, provide data for other relays in the scheme, and initiate local circuit breaker operation.

In microprocessor-based relays, analogue relaying signals are sampled at regular intervals, converted into digital data, processed and transmitted through the communications link. A complication arises in that digital data, unlike continuous analogue signals, represent information at discrete time intervals. Moreover, the relays interface with communications equipment which is not specifically designed for protection applications. Relays at the feeder's terminals must therefore effect precise time alignment of the measurements from the ends before effective comparison can take place. Generally, then, the volume of data required to define a sampled waveform and transmit to the other end(s) is relatively high.

In this chapter, a review of principles of digital current differential protection is given. Some techniques offered to reduce the amount of data required to define a sampled waveform and transmit to the other end(s) have been discussed. The chapter also includes a summary of the strengths and weaknesses in current differential relaying.

2.2 PRINCIPLES OF OPERATION.

In differential protection the vector sum of the terminal currents flowing into the protected zone should equal to zero in accordance with Kirchoff's first law, any residual current representing either capacitive or fault current. Ideally Merz-Price systems should provide little or no differential or operate current for through faults and little or no restraint or bias current for internal faults. In practice this is modified to allow for current transformer saturation and capacitance in the primary system and there is compensation for communications-related complications.

The method generally applied has a trip output point linearly proportional to a value of load or fault current expressed as a percentage bias current which acts as a restraining quantity. The general formulae used for decision making are given as:-

$$I_{op} = | I_L - I_R |$$
$$I_{bias} = \frac{1}{2} (| I_L | + | I_R |) \quad (2.1)$$

where I_{op} is the differential or operate current and I_{bias} is the restraint or bias current. The trip indication is generally given when the following applies:-

$$I_{op} > I_{min} \quad AND \quad I_{op} > k\, I_{bias} \quad (2.2)$$

where I_{min} is the set minimum current or relay nominal current and k is the percentage bias setting. Figure 2.1 illustrates the characteristics.

To implement these principles, the microprocessor at each feeder's terminal handles the local data acquisition. This is done by filtering the input signals using anti-aliasing filters to ensure that frequencies greater than half the sampling rate are removed, and sampling them using the Analogue to Digital Converter (ADC) to obtain numerical values ready for processing and transmission through a communications link. A sample and hold stage precedes the ADC to prevent the input signal from varying during the conversion period. This is necessary because the ADC takes finite time, about 25μsec, to perform a conversion. On receiving data from the remote terminal(s), the local relay performs a comparison with the local data in order to make a decision as to whether or not an in-zone shunt fault exists and have a trip output to the local circuit breaker. The role of the communications is simply to transfer information from one relaying point to another. With reference to a local relay, therefore, the other relays in the scheme provide remote data acquisition for that unit. A general summary is that the protection function at each terminal includes local input interface and data acquisition, remote terminal input interface and data acquisition, data transfer from remote to local, and local relay decision

making and trip output circuit, and this is as in the scheme shown in figure 1.7 of the previous chapter.

2.3 EXISTING SCHEMES.

One approach adopted in reference 19 could use either Pulse Code Modulation (PCM) digital or Frequency Modulated (FM) analogue communications. The PCM option used a 64 kbits/sec channel whereas the FM option could operate over voice frequency communication channels. Using the later option, the power system waveform was frequency modulated onto a 1750 Hz audio tone carrier frequency. This carrier frequency places the frequency spectrum of the transmitted signal on the flattest part of the channel's group delay characteristic and thus provided the least probability of distortion in the demodulated signal.

Reference 18 describes an approach which uses a wideband communications system as demanded by the volume of data together with the communications system protocols and error detection coding. The system uses elaborate data polling and channel delay time measurements. The communications requirements are met by a CCITT standard 64 kbits/sec communications operating on full duplex. Taking eight samples per cycle, the resulting average relay operating time was about 26 milliseconds.

Another approach is described in reference 27 which has a facility where if the channel propagation time is known and fixed, the associated time delay can be preset accordingly, otherwise this can be continuously computed and adjusted by the protection. It offers a choice of baud rates, ranging from 75 bits per second to 19.2 kbits per second. A carrier frequency of 1800 Hz has been selected which places the frequency spectrum of the transmitted signal on the flattest part of the channel's group delay

characteristic. With twelve samples per cycle, the typical operating time was 40 milliseconds.

A different approach was investigated in reference 28 where the difference currents obtained from post- and pre-fault line currents are used to minimise the desensitizing effect of load and line charging currents. The principle uses the theory of superposition, forming delta currents which are the differences in currents obtained by subtracting pre-fault values from post-fault values. The trip criteria is based on a comparison of delta current phasors from the ends where the angle information of resultant delta current phasors is used to determine if the fault is inside or outside of the protected zone. Taking 12 samples per cycle, the relay detected all internal faults on a short transmission line within half a cycle.

In examining techniques to reduce the volume of data required to be transferred between relays in a current differential scheme, reference 16 describes the protection concepts of the technique of using charge comparison to provide a new solution to the difficulties of current differential protection with limited communications capabilities. Reference 17 describes the communication concepts of the charge comparison. The charge comparison technique is based on the principle of conservation of charge at a node, using Kirchoff's law. At each relay location, the half-cycle area under each waveform is measured by integrating current samples between zero-crossings. The resultant ampere-second area is the coulombs of charge which is stored in memory along with start/finish time tags. The charge information is transmitted to the other relay(s) in the scheme together with timing information. This technique targeted the critical disadvantages of current differential relaying which are loss of protection on channel failure, high-capacity channel requirements, and requirements of precise channel delay compensation. The communications requirements were satisfied by a 7.2 kbits/sec data rate channel suitable for transmission over a voice frequency communications channel. With 40 samples per

cycle, the relay reached a trip decision in about 16 milliseconds, one cycle of the 60 Hz waveform.

2.4 STRENGTHS OF FEEDER DIFFERENTIAL RELAYING.

In very general terms, the relative strengths are presented of current differential relaying of feeder circuits against other feeder relaying schemes such as distance-based and directional overcurrent schemes.

Differential current protection provides Unit protection, and hence, does not respond in principle to external faults. It does not therefore require time co-ordination with protection of adjacent zones.

It operates correctly for internal faults even with out-feed at one terminal on Teed feeders or in-feed that may cause change in effective reach of distance relays[29]. In addition, it provides simultaneous high speed tripping of all terminals even for high resistance ground faults[30] near the strong terminal where the weak terminal sees essentially no fault current at all due to the in-feed effect at the strong terminal, until the strong terminal trips.

When used to protect parallel lines, it is unaffected by mutual coupling between parallel lines causing directionality loss of zero sequence polarised ground directional relays and change of effective reach of ground distance relays. It provides security during current reversal due to sequential clearing of parallel line faults. High speed trip occurs for schemes for evolving faults without the current reversal security delay associated with directional comparison schemes. There is no effect from the line side potential that provides spurious voltage to relays protecting a de-energised line, with coupling to a parallel energised line.

Another attractive feature is that it inherently does not operate for power swing[31, 32, 33] conditions, which can cause difficulties for other types of relays.

Another strength of current differential relaying is that it does not require voltage transformers. As a result it is not subject to blown potential fuse problems. Neither is it subject to relaying voltage problems associated with short lines with high source impedance ratios[34]. Even faults that cause voltage collapse will not cause confusion in the decision making. In addition it is not subject to the transient response problems associated with capacitive voltage transformers[35].

It can tolerate increased line loading without affecting relaying characteristics or requiring relay setting changes.

It also protects 100% of the line, unlike in the case of impedance relays where most consistent and fastest operating time is for faults less than 80% of the reach setting[34].

In general, current differential relaying is easily applied on Teed feeders, unlike in the application of directional relays which would need a pair of relays for any pair of terminal ends.

2.5 WEAKNESSES OF FEEDER DIFFERENTIAL RELAYING.

There are numerous relative weaknesses in feeder circuit current differential protection. Amongst them is that there is no provision of remote bus fault time-delayed back-up although preference is often on local back-up for bus fault protection. There is also a problem of lacking fault locating provisions. Though the lack of AC voltage source is regarded as a strength, it brings in a weakness in that the scheme cannot serve as AC voltage source for data acquisition.

The communications requirements are the classical weaknesses of differential protection. There is a requirement for precise channel delay compensation and this increases the computational burden because of increased data handling. Because of the volume of data required to correctly define a relaying electrical signal sample at a feeder terminal and transmit to other feeder(s) in the scheme, feeder current differential relaying generally requires a large capacity communications channel, which unfortunately highlights the system cost. The communications also introduce an undesired element in that there is a loss of protection when the communications channel fails.

2.6 AN OVERVIEW OF THE NEW PROTECTION SCHEME.

Figure 2.2 illustrates the proposed protection scheme for distribution feeder circuits at the local terminal. The primary power transducers (voltage transformers and current transformers) provided the power system's current and voltage signals. The input signals were filtered using anti-aliasing filters and then sampled using the A/D converter. The voltage samples were used to generate a set of three unit amplitude rotating sinusoidal reference waveforms s_a, s_b and s_c in phase with the phase voltages. Similarly, an orthogonal set of reference phasors $(s_a\text{-}s_b)$, $(s_b\text{-}s_c)$, and $(s_c\text{-}s_a)$ was generated. Since the protection is required to operate during faults causing voltage collapse, a memory feature is included. In the event that there are no VT's, the positive phase sequence currents are used to provide the reference.

Based on equations used to derive the instantaneous power in a three phase circuit, the reference phasors are multiplied with the current signals to obtain polyphase polarised current measurement I_p. The orthogonal set of reference phasors provide I_q. I_p and I_q are steady dc terms. These dc terms are transmitted consecutively to the remote relay for comparison with the locally obtained data.

As the algorithms decouple the measurements from the power system frequency and its waveform, they have a high inherent tolerance to the complications introduced by communication delays and their fluctuations. The demands on the communications are thus reduced. For this research, the communications requirements have been limited to a full duplex 2400 bits per second system suitable for operation over a voice frequency channel. This requirement was provided by a CCITT V.26 modem standard. This data rate however only offers 48 bits of data per cycle. A major constraint is the design of the coding. To ensure effective error detection and rejection of bad data, and at the same time maximise throughput of actual data, the data stream for the relaying scheme is a thirty-two bit message, comprising a six bit header followed by two Hamming (13,9) code blocks. Thus a message requires 13.33 milliseconds transmission time.

As soon as an incoming message is received and decoded, its value together with the value obtained from local measurements is provided for the trip comparator. This received value is compared to the corresponding locally measured signal delayed by the message transmission delay together with an allowance for signal propagation delays and marshalling. A total of 17 milliseconds is allowed as the communications system delay time. This is composed of the 13.33ms message transmission time, 2ms for worst case scenario propagation delay time, and about 2ms marshalling time. Thus the total delay time can vary. Based on the local and remote data, the differential or operate and the restraint or bias current measurements are derived. A decision is then made by the relay to trip the local circuit breaker if the fault condition is inside the protected zone.

2.7 SUMMARY.

Feeder current differential relaying provides a solution to unit protection of feeders. It has characteristic high speed operation, sensitivity to in-zone faults and stability during external faults. Using the concepts established in the early 1900's by Merz and Prize,

feeder differential protection has seen its advancements from the use of electromechanical relays, analogue static relays, to the state-of-the-art microprocessor-based relays. The communications industry has meanwhile advanced from the use of metallic pilots to the modern optical fibre technology. These channels are not specifically developed for use in protection schemes. The result is that protection algorithms must take into account the complications introduced by the channels. This has led to investigations into new approaches to differential relaying to formulate algorithms which are tolerant to the various constraints. To this effect, a brief statement of a selection of a few schemes has been made.

Briefly, some of the strengths and weaknesses of feeder current differential protection have been mentioned. In this research, it is desired to overcome the weaknesses without compromising the strengths. Specialised algorithms are used to decouple the signals from the power system waveforms and their frequency, thereby reducing demands on the communications system. A low cost communications system is thus used in providing effective protection.

2.8 FIGURES.

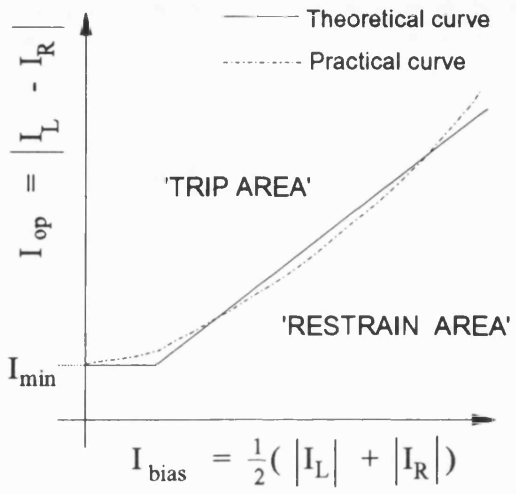

Figure 2.1 Biased Current Differential Trip Characteristic.

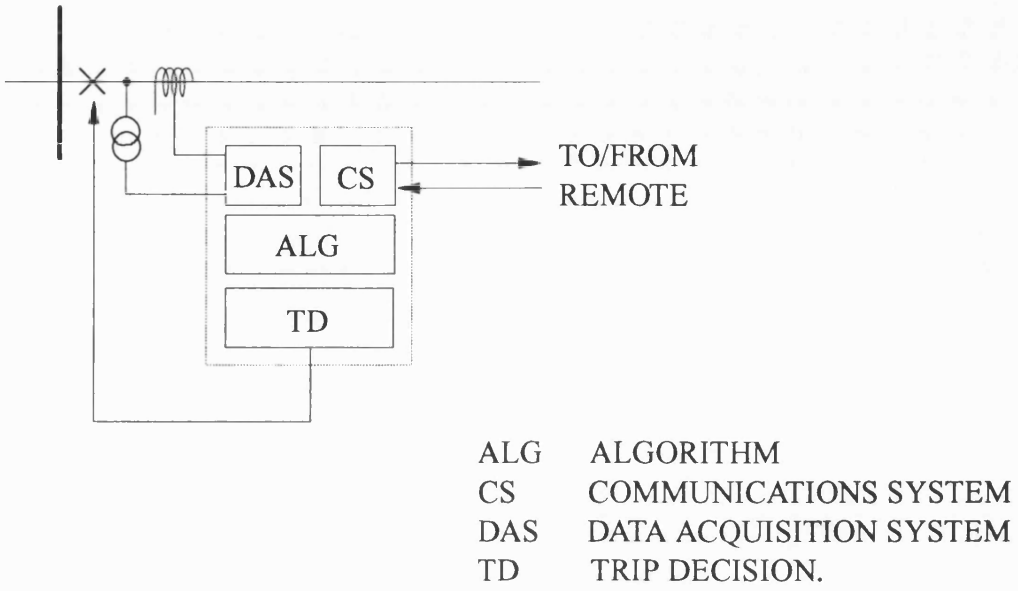

Figure 2.2 Overview of the new Protection Scheme as seen at one terminal.

Chapter 3

THE CURRENT DIFFERENTIAL PROTECTION ALGORITHM.

3.1 INTRODUCTION.

In digital differential relaying it is a normal requirement to effect precise time alignment of the measured quantities from the feeder terminals in order to reach a correct trip decision. Combining the raw data, the communication protocols and the error control coding, the volume of data to be transferred between the relays is high. Wideband communications offer good opportunities to transmit the mass of data thus required for the protection. However, as this protection is for distribution feeder circuits, a low cost communications system is required.

To take advantage of the low cost communication systems available, a voice frequency channel was chosen as an ideal solution to use in the Unit protection of distribution feeder circuits. The limited voice frequency channel bandwidth of 4 kHz means that the volume of data which can be handled is also limited. It was therefore required to dramatically reduce the data that defines the current signals in order to overcome the need to transmit the mass of data required to define the sampled current waveform. After careful consideration of the characteristics of communication systems, it was decided to base the research on a full duplex 2400 bits/second channel.

The use of such a low data transfer rate introduces problems. 2400 bits/second corresponds to a data rate of 48 bits for each power system cycle. Allowing for a nominal fifty percent overhead for communications protocols and error detection coding, the data transfer capacity becomes 24 bits per cycle.

This chapter describes the techniques used to overcome the need to transmit the mass of data required to define the sampled current waveform and operate with this low data transfer capacity. The technique uses a directional element on the measured quantity and is based on the equations used to derive instantaneous power in a three phase power circuit. The operation of the algorithm is also presented.

3.2 DATA REDUCTION.

The mass of data required to define the sampled current waveform is reduced so as to operate with the low data transfer capacity. The algorithm achieves this by using locally obtained reference phasors as polarising signals to obtain polyphase polarised measurements of the current waveforms at the feeder's terminals. An orthogonal set of reference phasors provides complimentary information. The polarised current measurements are steady signals containing both amplitude and phase information of monitored three-phase currents with respect to the reference phasors.

The equations used to derive instantaneous power in a three-phase circuit form the basis of the algorithm. Real power P and reactive power Q are given as[36]:-

$$P = i_a v_a + i_b v_b + i_c v_c \tag{3.1}$$

$$Q = \frac{1}{\sqrt{3}} [i_a(v_b - v_c) + i_b(v_c - v_a) + i_c(v_a - v_b)] \tag{3.2}$$

Equations (3.1) and (3.2) are constants under balanced conditions[37, 38, 39].

Based on these power equations, the algorithm multiplies the instantaneous values of the sampled phase currents, i_a, i_b and i_c, by instantaneous values of three phase reference

phasors, s_a, s_b and s_c, for phases a, b and c respectively, to provide a constant polarised measurement I_p which represents the amplitude of the current in phase with the reference phasors. An orthogonal set of reference phasors, (s_a-s_b), (s_b-s_c) and (s_c-s_a) produces a constant polarised measurement I_q which represents the amplitude of the current orthogonal to the reference phasors.

Letting the reference phasors have unity amplitudes, I_p and I_q may be written as:-

$$I_p = i_a s_a + i_b s_b + i_c s_c \tag{3.3}$$

$$I_p = 3\, I \cos(\phi) \tag{3.4}$$

and,

$$I_q = i_a(s_b - s_c) + i_b(s_c - s_a) + i_c(s_a - s_b) \tag{3.5}$$

$$I_q = 3\sqrt{3}\, I \sin(\phi) \tag{3.6}$$

where I_p and I_q are non-oscillating constants.

Unbalance conditions introduce second harmonics as to be discussed in chapter 5. Therefore, a low pass filter is introduced by averaging I_p and I_q over half a power system cycle to remove these terms, leaving the steady, dc term which contains both the magnitude and phase information.

Analysis of equation (3.3) to consider unbalanced currents involves replacing the three-phase currents by three balanced systems containing positive, negative and zero phase sequence components.

Let[21]

$$i_{a0} = i_{b0} = i_{c0} = I_0 \sin(\omega t + \Theta_0 + \phi_0) \tag{3.7}$$

$$\begin{aligned} i_{a1} &= I_1 \sin(\omega t + \Theta_1 + \phi_1) \\ i_{b1} &= I_1 \sin\left(\omega t + \Theta_1 + \phi_1 + \frac{4\pi}{3} \right) \\ i_{c1} &= I_1 \sin\left(\omega t + \Theta_1 + \phi_1 + \frac{2\pi}{3} \right) \end{aligned} \tag{3.8}$$

$$\begin{aligned} i_{a2} &= I_2 \sin(\omega t + \Theta_2 + \phi_2) \\ i_{b2} &= I_2 \sin\left(\omega t + \Theta_2 + \phi_2 + \frac{2\pi}{3} \right) \\ i_{c2} &= I_2 \sin\left(\omega t + \Theta_2 + \phi_2 + \frac{4\pi}{3} \right) \end{aligned} \tag{3.9}$$

and,

$$\begin{aligned} s_a &= \sin(\omega t + \Theta) \\ s_b &= \sin\left(\omega t + \Theta + \frac{4\pi}{3} \right) \\ s_c &= \sin\left(\omega t + \Theta + \frac{2\pi}{3} \right) \end{aligned} \tag{3.10}$$

With reference to equation (5.27) to be discussed later, equation (3.3) becomes;

$$I_p = 3 I_1 \cos(\phi_1) - 3 I_2 \cos(2\omega t + \Theta + \Theta_2 + \phi_2) \tag{3.11}$$

Although this technique removes the zero phase sequence currents immediately, the negative phase sequence components produce the second harmonic term. Averaging the measurements of I_p and I_q over half a power system cycle, removes these terms leaving the steady, dc term.

A variety of power system derived signals could have been used for the reference phasors. These should be synchronised to the power system frequency and ideally have the same phase at all of the feeder's terminals. Since this protection is principally aimed at short distribution feeders and assuming a heavily interconnected power system, the phase difference between prefault local versus remote voltages is small, and hence the terminal's three phase voltages were used to derive the reference. To cater for conditions when there are no VT's, an alternative method used positive phase sequence currents to derive the reference.

3.2.1 REFERENCE PHASORS FROM PHASE VOLTAGES.

A unit amplitude reference phasor is derived in step with each phase voltage waveform. There are therefore three reference phasors forming a set of three unit amplitude rotating sinusoidal waveforms 120 degrees apart. The set of reference phasors, s_a, s_b, and s_c, corresponds to the phase to ground voltages and the orthogonal set, (s_a-s_b), (s_b-s_c), and (s_c-s_a) corresponds to the phase to phase voltages.

As the system waveforms are generated using the EMTP power simulation package, the system frequency is known to be 50 Hz, the phase displacement is known, and the start of the simulation, and therefore the start of the waveforms, is also known. Thus, the reference phasors can easily be derived. The principle of phase locked loop, PLL[40, 41, 42, 43], can be adopted to derive the reference phasors.

3.2.1.1 PHASE LOCKED LOOP.

In principle, the PLL is composed of a phase detector, a loop filter, an amplifier and a voltage controlled oscillator, VCO, as illustrated in the block diagram in figure 3.1. Its essential property is the restitution of the phase, and thereby the frequency, of an input

signal which can then be coherently detected. The operation of the PLL can be summarised as below, with a mathematical description given in appendix 3.1.

i. Phase Detector stage.

With reference to figure 3.1, the phase detector compares the phase of a periodic input signal against the output of the VCO and generates a voltage output that is a measure of their phase difference. The difference voltage is then filtered by the loop filter and applied to the VCO as its control voltage. Assuming the input is a per unit, pu, value of the system phase voltage, then this provides the PLL with f_{in}. The output of the VCO, which is f_{VCO}, is a locally generated free-running frequency set equal to the expected input frequency. f_{VCO} tracks f_{in} closely to stay in lock. The VCO is able to acquire lock in the whole frequency range generally known as capture range centred about its free-running frequency. Once in lock, the VCO maintains the lock for a wider range than the capture range. The range of frequency for which the lock is held when the frequency is swept in one direction is known as the lock range. The ranges centred about the VCO free-running frequency are illustrated in figure 3.2. If f_{VCO} and f_{in} are not equal, then the phase error signal, after filtering and amplification, causes f_{VCO} to deviate in the direction of f_{in}. When conditions are right, the VCO quickly locks to f_{in}, maintaining a fixed phase relationship with the input signal. Thus a clean replica of the input waveform is provided.

Generally, the phase detector is a multiplier. The inputs may have phase shifts, and may have noise present. Invariably, a number of terms are produced, including one proportional to the difference between the phases.

ii. Loop Filter stage.

This stage removes all high frequency sum terms from the output of the phase detector. It also provides a short term memory of the frequency and hence ensures a rapid recapture of the signal if the loop falls out of lock due to external fading or loss of signal.

iii. Voltage Controlled Oscillator stage.

In the absence of an input signal the VCO output oscillates at its natural frequency, and there is no output from the phase detector. When an input voltage is applied, the output frequency changes and the change in frequency is directly proportional to the input voltage.

If the input frequency is outside the capture range, the product of the input signal and the VCO output result in beats. The beats consist of two sinusoidal components which have the sum and difference frequencies. As they lie outside the loop filter bandwidth, they are attenuated. The VCO input is thus negligible, resulting in the VCO continuing to oscillate at its natural frequency. The loop is thus out of lock.

If the input signal is inside the capture range, the difference frequency component of the phase detector output passes through the loop filter unattenuated. As it now has an input, the VCO output frequency moves away from its natural frequency. The frequency moves closer to the input frequency and rapidly falls into phase synchronism with the input signal. At this point the two frequencies are identical and the phase difference between the two signals is fixed, giving a constant voltage output from the filter. The magnitude of this voltage is related to the steady phase difference and the difference between the input signal frequency and the natural frequency of the VCO.

3.2.1.2 MEMORY FEATURE ON THE REFERENCE PHASOR.

Ideally, the reference signals should follow the voltage waveforms until the phase waveforms drop to near-zero, where-upon the signals assume the previous cycle until the waveforms recover. In this work, in order to avoid the complications of the resulting transients and phase shifts, the reference signals assume the previous cycle for the next six cycles when a fault is detected. The number six is chosen as the EMTP simulation gives six cycles after the fault. Moreover, for fault conditions for which the algorithm should trip, the trip output should occur inside six cycles after the fault.

This facility ensures the availability of a reference phasor when it is most needed, that is when there is a fault, where otherwise complicated processing is required due to the transients and phase shifts as a result of the fault and thereby introducing undesirable delays in decision making. In particular, the memory feature is useful with fault conditions that result in voltage collapse[44, 45, 46, 47, 48] at a terminal where otherwise the reference phasors are lost. Voltage collapse conditions may occur when control is lost and voltage falls progressively when heavily loaded systems reach a state where sensitivities are such that control actions actually make the situations worse[46]. A system is prone to collapse if there are heavy power flows into an area with insufficient local reactive reserves[46]. A feature of this phenomenon is the speed with which it can occur resulting in there being insufficient time for post-fault correction action. Thus, the phenomenon of voltage collapse on a transmission system, due to operation near the maximum transmissible power, is characterised by a fall in voltage, which is at first gradual and then rapid. The later is aggravated by certain control systems, in particular the transformer tap-changer becoming unstable[44]. Normally, thermal rating constraints at the lower voltages prevent demands reaching the critical levels for voltage collapse[44].

A direct way to model these phasors for simulation purposes can be to use a sine wave generating function[49]. The unit amplitude reference phasors are then as follows:-

$$s_a = \sin(\ ref.\ Angle\ )$$

$$s_b = \sin\left(\ ref.\ Angle\ + \frac{4\pi}{3}\right) \qquad (3.12)$$

$$s_c = \sin\left(\ ref.\ Angle\ + \frac{2\pi}{3}\right)$$

$$where\ \ ref.\ Angle\ = (\ timeStep\ * \frac{2\pi}{T}\ )\ *\ DTOR$$

with T as the period of the system waveform, and DTOR stands for 'Degrees TO Radians' conversion which is simply $\pi/180.0$. The sine wave generation terminates with the end of simulation.

3.2.2 REFERENCE PHASORS FROM A SINGLE PHASE VOLTAGE.

This is similar to the above derivation of the reference phasors from the systems three phase voltages, the only difference being that only one phase quantities are used. Applying a phase shift of 120 degrees lagging and also leading onto a one phase reference phasor, say s_a, produces the other reference phasors s_b and s_c. This section is relevant assuming there are no VT's available, and installing one new VT will be cheaper than installing three.

3.2.3 REFERENCE PHASORS FROM POSITIVE PHASE SEQUENCE CURRENT.

However, in the event that the use of VT's proves to be undesirable, positive phase sequence current can be used to derive the reference. This in effect still uses a voltage component indirectly as the positive phase sequence current is system generated as it is

produced by the positive phase sequence voltage.

If both the three-phase excitation, which is the generation, and the three-phase network, which is the transmission and distribution network, are balanced, the three phase system may be solved as a single phase system using a positive sequence parameter[10] since all the three voltages or currents are equal in magnitude and displaced by an equal angle of 120 degrees. This is the situation when conducting load flow or planning studies of a given power system[10]. However, during disturbances, such as faults, either the excitation or the network, or both, may become unbalanced. In such cases, the unbalance can be explained by transforming the phasor quantities into component quantities of positive sequence, negative sequence and zero sequence to be discussed in Chapter 5.

The positive sequence current is generated by the positive phase sequence voltages which are system generated. As such, the positive phase sequence current provides good polarising reference phasors since they are synchronised to the power system frequency, and have the same phase at all of the feeder's terminals. It is given as:-

$$I_1 = \frac{1}{3}\left[I_a + hI_b + h^2 I_c \right]$$

In terms of discrete sample values, the instantaneous values of the positive phase sequence components can thus be derived as:-

$$\begin{aligned} i_{a1} &= \frac{1}{3}\left[i_{a,\,n} + i_{b,\,(n-\frac{2}{3}n_s)} + i_{c,\,(n-\frac{1}{3}n_s)} \right] \\ i_{b1} &= \frac{1}{3}\left[i_{b,\,n} + i_{c,\,(n-\frac{2}{3}n_s)} + i_{a,\,(n-\frac{1}{3}n_s)} \right] \\ i_{c1} &= \frac{1}{3}\left[i_{c,\,n} + i_{a,\,(n-\frac{2}{3}n_s)} + i_{b,\,(n-\frac{1}{3}n_s)} \right] \end{aligned} \qquad (3.13)$$

where n represents the instant that the last sample was taken and n_s is the number of samples per cycle.

Dividing each sequence component phasor by its magnitude gives unity amplitude rotating waveforms. A unit amplitude reference phasor is derived in step with each phase's positive sequence component. There are therefore three reference phasors forming a set of three unit amplitude rotating sinusoidal waveforms s_a, s_b, and s_c, 120 degrees apart. Just as above, I_p and I_q can be represented as in equations (3.3) and (3.5), that is:-

$$I_p = i_a s_a + i_b s_b + i_c s_c$$

$$I_q = i_a(s_b - s_c) + i_b(s_c - s_a) + i_c(s_a - s_b)$$

3.3. ALGORITHM OPERATION.

The algorithms are structured such that the various functions of a differential protection relay are divided into modules as illustrated in figure 3.3. The top end functions process the system data on its way from the primary transformers. The bottom end handles the data interchange on two one-way communication channels between the feeder terminals. In between the top end and the bottom end is the module that carries out the calculations and logic steps required for the trip decision. This stage is described in appendix 3.2

The main stages of the protection algorithm are summarised in figure 3.4. They include initialisation and data input, data processing and interchange, and data comparison to reach a trip decision. The program is written in C[50, 51]

3.3.1 SYSTEM INITIALISATION AND DATA INPUT.

The algorithms have a number of parameters which must be given correct default values to operate correctly. The parameters may need to be modified to alter the behaviour of

the program. Thus they are run-time set-able parameters. An overview is given below;

The input data for a relay passes through may stages of processing and the stages are summarised in figure 3.5. At every stage some distortion may be introduced:-

- The measurement apparatus (CT's and VT's)[52, 53] may introduce errors.
- The Analogue-to-Digital conversion stage has a number of effects:
  - Anti-aliasing filters are used on the analogue side to prevent frequencies higher than the Nyquist[54, 55] frequency from causing beat frequencies to appear in the output. This is basically a low-pass filter which is set around the Nyquist frequency (half of the sampling frequency).
  - The sampling frequency of the ADC[56] may be substantially lower than the input data frequency. This could result in distortion of the data.
  - Since the digital output has only a limited accuracy (usually 12 bits) a quantisation error will be present in the output. The analogue input value will have to be truncated to a multiple of the bit step.
  - Analogue input values which fall outside of the range of operation of the converter will be truncated to the minimum or maximum output. Any values which exceed these limits may also generate warnings. The output of the converter is digital and as such is no longer prone to loss of accuracy.
- A differential protection algorithm requires the data for remote ends of the protected feeder to be transmitted to the local relay for decision making. The transmission introduces effects as will be discussed in chapter 4, (the severity of some of them, like noise, may well be affected by the fault occurrence, especially in the application with pilot wires):
  - There is a significant delay associated with the transmission of the data. The delay is due to the propagation delay characteristic of the medium, A to D conversion, and buffering for transmission.

- The communication line may experience some temporary outage. This may be due to any disturbance which results in un-recoverable bit errors in the message. (As the bandwidth of the communications channel is barely sufficient for the data, extensive CRC may not be used as will become evident in chapter 4).

The set-able parameters are included in appendix 3.3.

3.3.2 DATA PROCESSING AND INTERCHANGE.

As mentioned above, the reference phasors are derived, these being either from the phase voltage waveforms or from the positive phase sequence currents as will be detailed respectively in chapters 7 and 8 in the evaluation of the algorithm.

Equations (3.3) and (3.5) are then evaluated to get the polarised current measurements I_p and I_q respectively. As the protection scheme is principally aimed for 33kV distribution feeder circuits which have very small X/R ratios[4, 38, 57] as in table 3.1, a simple filter can be used on the measurements. Using a half power cycle filter[58] to remove any second harmonic terms, the measurements are smoothed.

As table 3.1 shows, generally the X/R ratio increases with voltage. Therefore at low voltages, the small X/R ratio means that transients due to a fault die down very quickly because the large resistances act as dampers. The filter process therefore uses only a half cycle moving average filter:-

$$y = \frac{\sum_{i=0}^{n} x_i}{n} \tag{3.14}$$

where n is the number of samples in half a cycle. Thus the function takes a

measurement x and returns its smoothed equivalent y.

The smoothed measurements are then transmitted to the other terminals. The data stream used for the relaying scheme is organised as shown in figure 3.6. As will be discussed in chapter 4 each block of code is started with a six bit header followed by two Hamming (13,9) code blocks. The six bit header is a pre-defined set of bits which provides data synchronism. Each Hamming code[59, 60, 61, 62] block contains thirteen bits, nine of which are data bits. Each message block therefore contains eighteen data bits. As per operation of the V.26 modem standard, the data stream to be transmitted is divided into pairs of consecutive bits (dibits). Each dibit is encoded as a phase change relative to the phase of the immediately preceding signal element. At the receiver, the dibits are decoded and the bits are reassembled in correct order. Thus the eighteen bit message block comprise two identifier bits, two bits reserved for other applications and fourteen data bits relating to I_p and I_q alternatively. The identifier bits are used to define the measurements as corresponding to I_p ('0' '0') or I_q ('1' '1'). The remaining eight parity bits are used for error detection such that the security of the protection is not compromised should the data be corrupted.

There are thus thirty two bits for a message and at 2400 bits/sec bit rate, each message requires 13.33 milliseconds transmission time. Marshalling times and propagation delays increase this time to 17 milliseconds considering the worst case scenario of 2 milliseconds propagation delay time in pilot wires. However, since the data stream can be considered to be continuous, data is available each 13.33 milliseconds.

Shortly before the end of one message's transmission period, the next value of I_p or I_q is provided in rotation to the data sending unit for coding and transmission. If the last transmission was of the measurement I_p, the next would be I_q, and vice versa.

Once an incoming message has been received and decoded, its value is compared with the value obtained from the local measurements. This received value is compared to the corresponding locally measured signal delayed by the message transmission delay together with an allowance for signal propagation delays and marshalling. With the message structure described above, a 17 millisecond delay is introduced to the locally derived measurement, and the decision process is executed after receipt of a message, that is, every 13.33 milliseconds.

Similar comparison is used for both I_p and I_q. The data comparison involves calculating the operate signals, $(I_p)_{op}$ and $(I_q)_{op}$, and bias signals, $(I_p)_{bias}$ and $(I_q)_{bias}$;

$$\begin{aligned} (I_p)_{op} &= | I_{p_L} - I_{p_R} | \\ (I_p)_{bias} &= \frac{1}{2} (| I_{p_L} | + | I_{p_R} |) \\ (I_q)_{op} &= | I_{q_L} - I_{q_R} | \\ (I_q)_{bias} &= \frac{1}{2} (| I_{q_L} | + | I_{q_R} |) \end{aligned} \qquad (3.15)$$

The processing and interchange stage is summarised in the flow diagram in figure 3.7.

3.3.3 DIFFERENTIAL DECISION MAKING.

Two trip conditions are required before the relay trip output is given. These could either be consecutive trip decisions, that is, I_p and then I_q, or vice versa, or alternatively two subsequent I_p or I_q trips. Thus the trip indication is given when either of the following applies:-

$$(I_p)_{op} \succ (I_p)_{\min} \quad AND \quad (I_p)_{op} \succ k_p\,(I_p)_{bias}$$
$$(I_q)_{op} \succ (I_q)_{\min} \quad AND \quad (I_q)_{op} \succ k_q\,(I_q)_{bias} \qquad (3.16)$$

As in chapter 2 section 2.2 and illustrated in figure 2.1, the bias setting k is the slope of a plot of the operate quantity versus the bias quantity and the $(Ip)_{min}$ and $(Iq)_{min}$ are the trip settings of the polarised currents. Figure 3.8 illustrates the basic method of differential relaying to explain the bias and operate settings.

With reference to figure 3.8, for normal operation and for a fault outside the zone between the two sets of CTs, current I_G entering this zone equals current I_H leaving, neglecting charging currents. Therefore, assuming identical CTs, $I'_G = I'_H$. For this case the current I'_G-I'_H in the operate coil is zero and the relay does not operate. In practice, however, no two CTs will give exactly the same secondary current for the same primary current, and the difference current I'_G-I'_H can become appreciable for external faults even though I_G=I_H. The percentage bias setting k desensitises the relay to short circuit currents flowing to an external fault. As such k indicates the operate current required to operate the relay as a percentage of the smallest restraint current[95].

On the other hand, a fault inside the zone between the CTs causes I_G to increase suddenly while I_H either decreases or increases and flows in the opposite direction. Either way, $I_G \neq I_H$, and consequently $I'_G \neq I'_H$. Therefore, a difference current I'_G-I'_H flows in the relay operate coil which may cause the relay to operate. To ensure that the relay does not operate for low currents when charging currents and any error current due to CT mismatch are significant, a threshold setting of I_{min} is included.

Hence the trip criterion

$$I_{op} > I_{min} \quad AND \quad I_{op} > kI_{bias}.$$

Separating the trip decisions as in equation (3.16) so that they are based on I_p or I_q, and requiring two trip decisions before tripping the relay provides a faster trip output than combining the two measurements.

The decision making process is summarised in the flow diagram in figure 3.9 while figure 3.10 is the block diagram showing the general operation of the relay. The running of the program is summarised in appendix 3.4.

3.4 SUMMARY.

The current differential protection algorithm has been developed to accommodate the modest communications capabilities associated with digital data voice frequency communications channel. To avoid the need to accurately synchronise the data at the local and remote ends of the protected feeder, two reference phasor sets are derived which are used to provide a polarised measurement of the three phase currents. A variety of power system derived signals are used for the reference, and these are the terminal's three phase voltages and the positive phase sequence currents.

The current measurement system, when coupled with a half cycle filter to remove second harmonic terms, provides a steady, dc, output. Using two orthogonal reference phasor sets provides the data required to characterise the currents measured. Requiring two trip indications before allowing the algorithm to trip provides security against mal-operation due to the transitions in the measured I_p and I_q signals after the fault.

3.5 FIGURES.

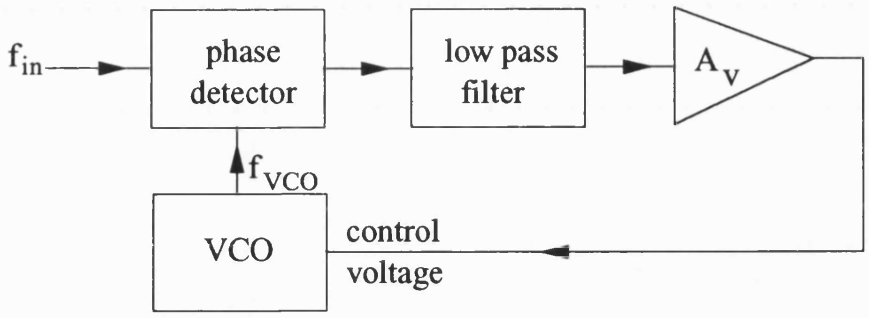

Figure 3.1 Block Digram of a Phase Locked Loop.

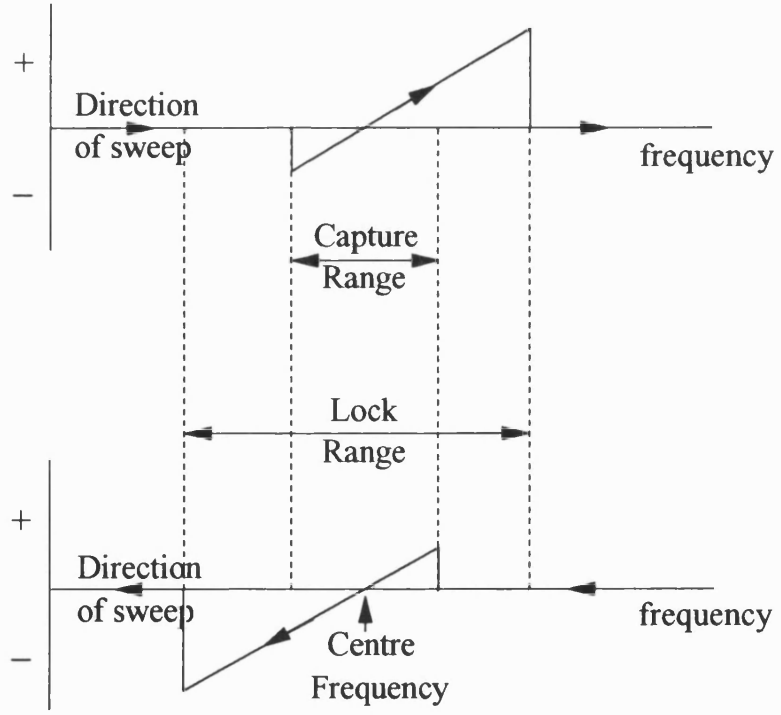

Figure 3.2 PLL Capture Range and Lock Range.

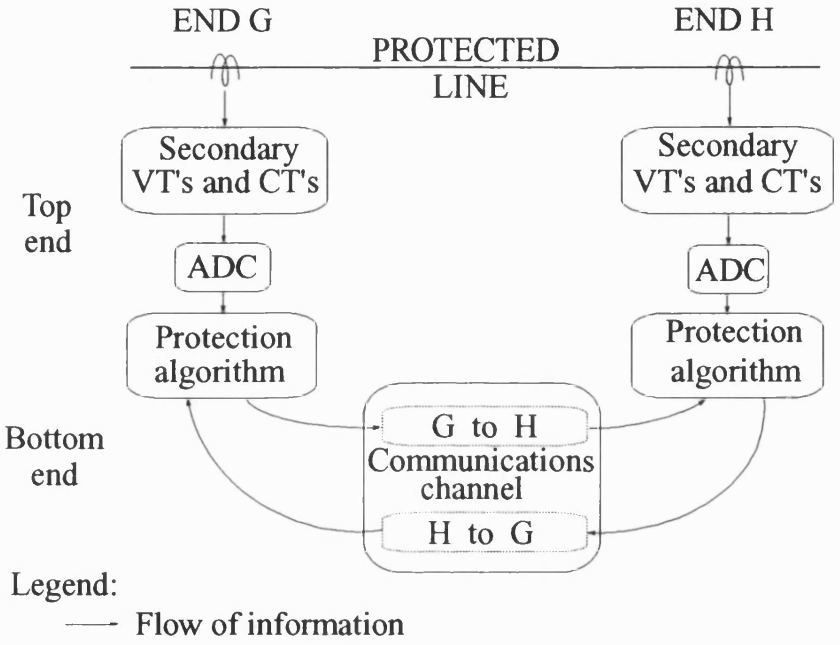

Figure 3.3 Pictorial Representation of the Scheme.

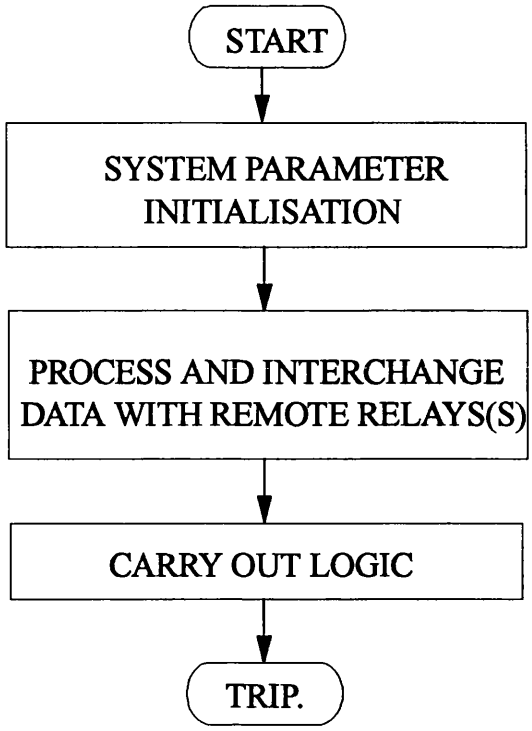

Figure 3.4 Main Stages of the Protection Algorithm.

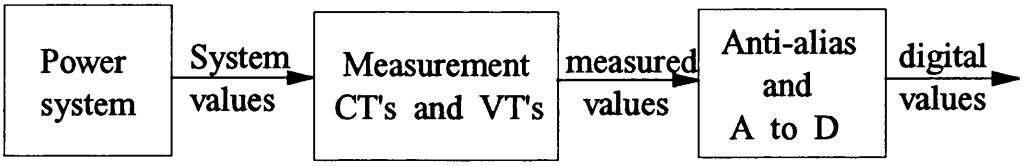

Figure 3.5 Input Data Processing Stages.

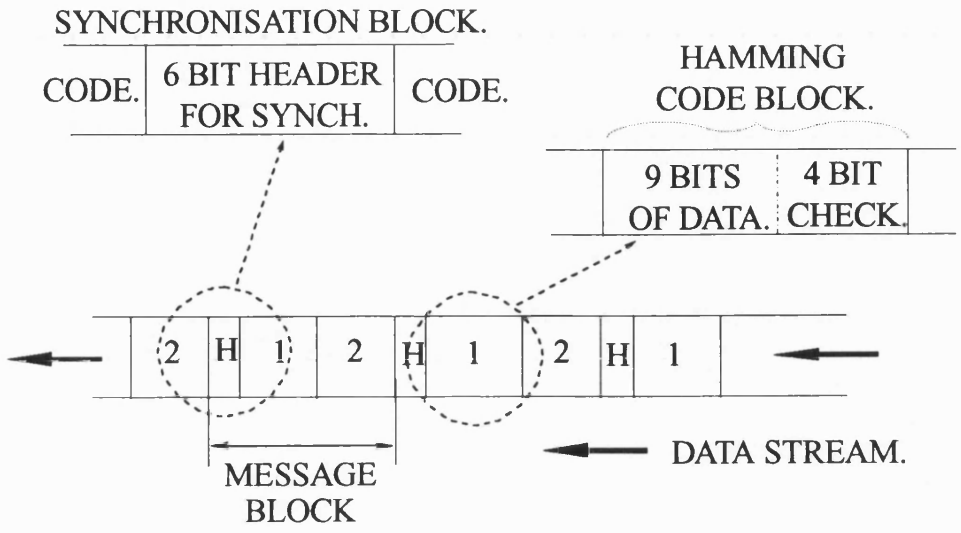

Figure 3.6 Data Stream Organisation.

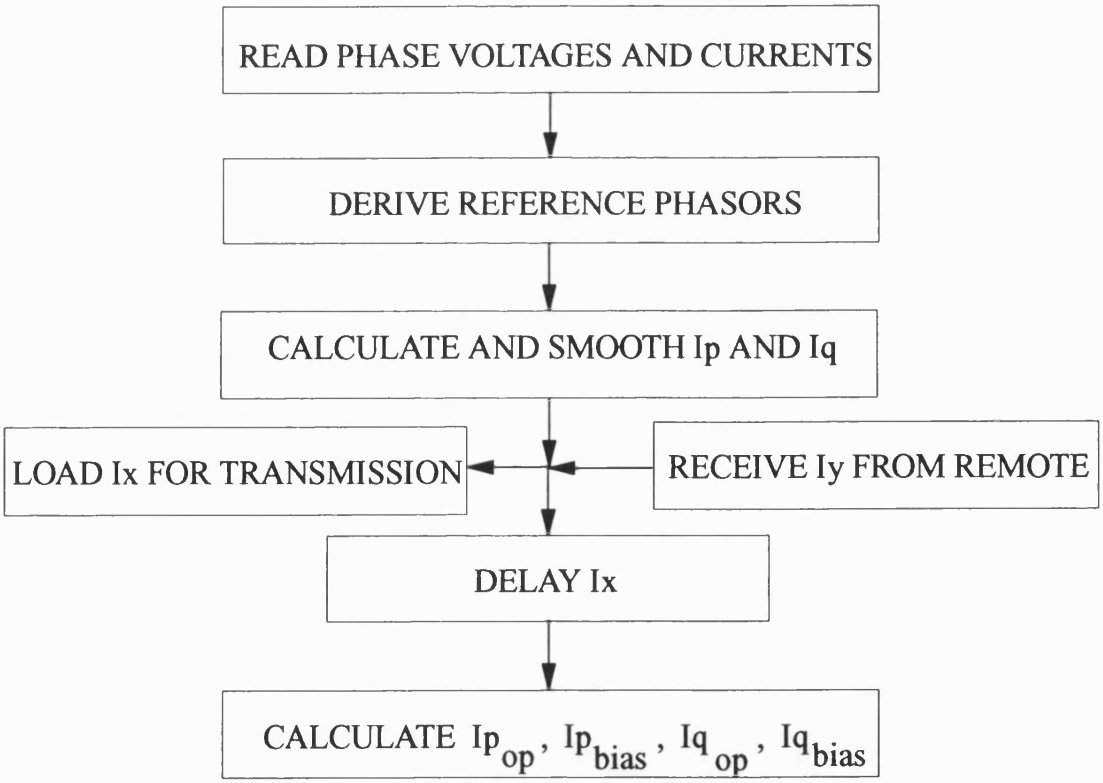

Figure 3.7 Data Processing and Interchange.

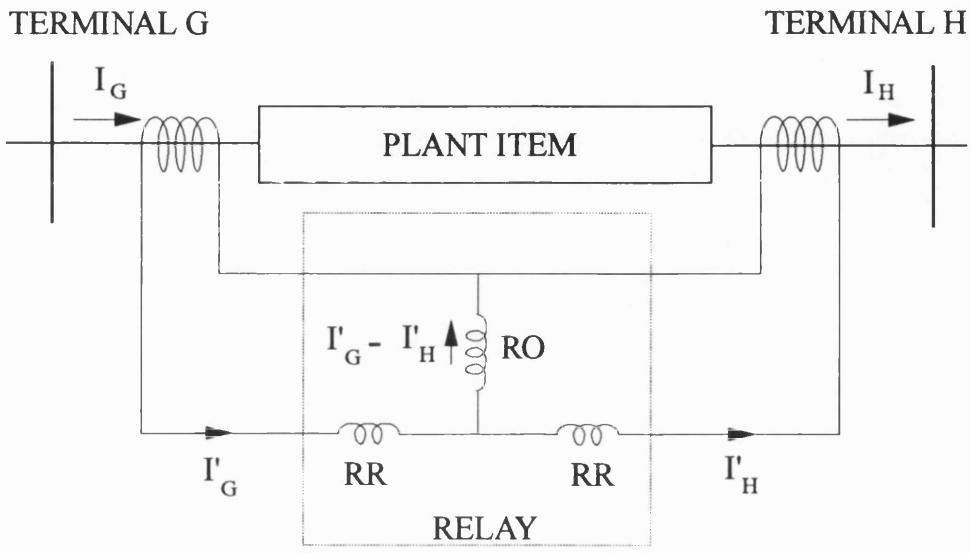

RO Relay operating coil
RR Relay restraining coil
I_G Primary current at terminal G
I'_G Secondary current at terminal G
I_H Primary current at terminal H
I'_H secondary current at terminal H.

Figure 3.8 The basic Differential Protection of a plant item.

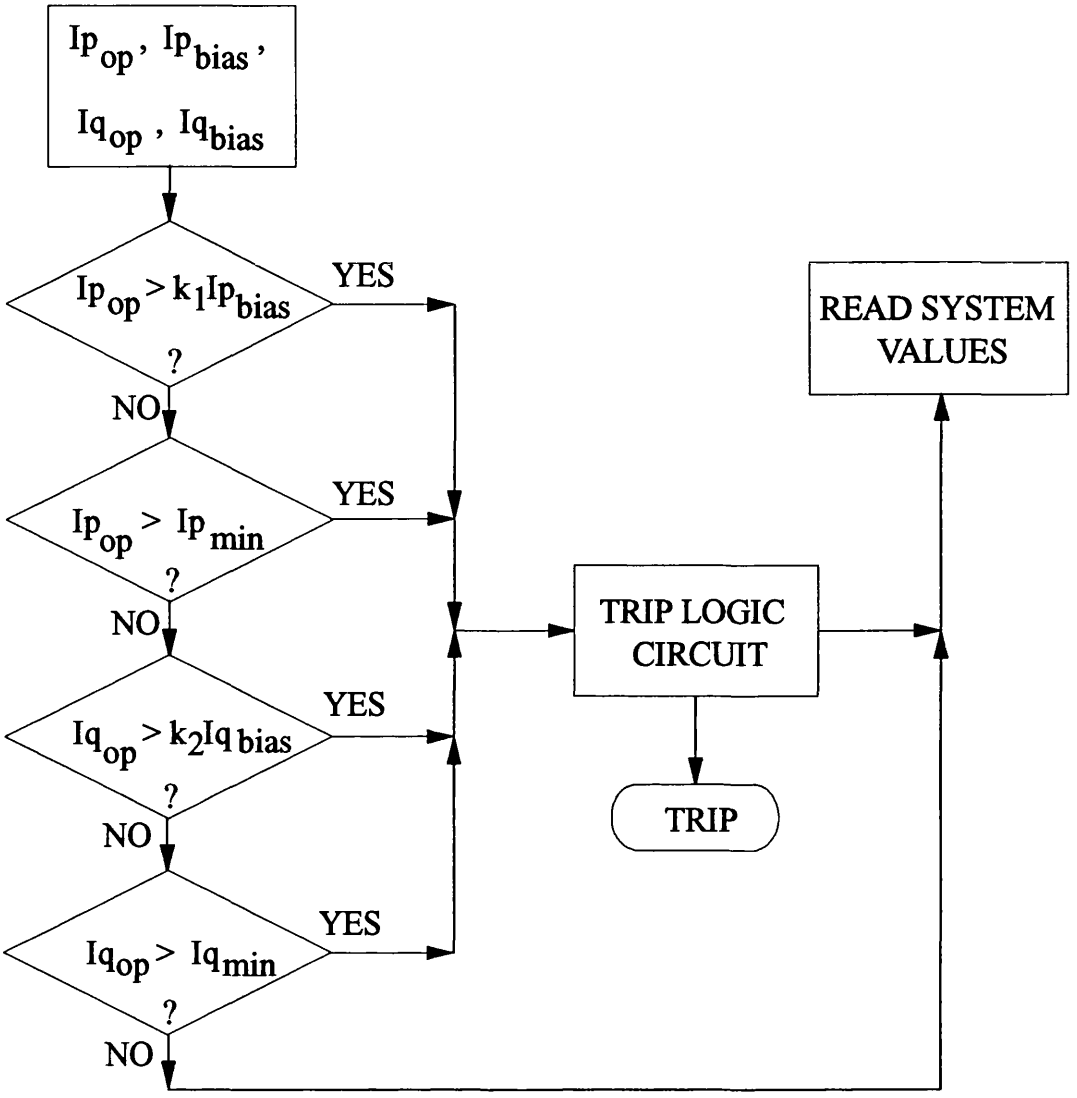

Figure 3.9 Logic Stage of the Protection Algorithm.

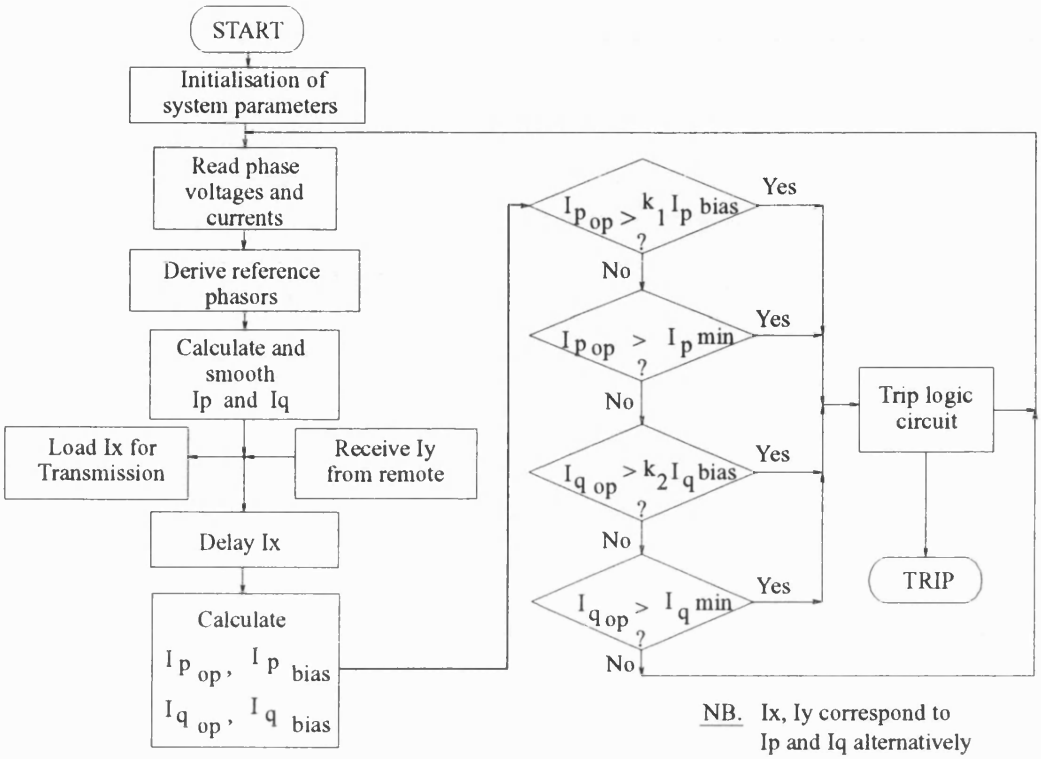

Figure 3.10 General Operation of the Protection Algorithm.

3.6 TABLES.

Table 3.1 Typical X/R ratios for cables and overhead lines.

PLANT	NOMINAL RATING (MVA)	X/R RATIO[57]
400 kV overhead line	1800	14
400 kV cable	1800	18.4
132 kV overhead line	200	3.4
132 kV cable	200	4.5
33 kV overhead line	25	1.9
33 kV cable	25	0.78

3.7 APPENDICES.

Appendix 3.1 Mathematical description of the Phase Lock Loop, PLL.

Let V_1 be the input signal to the PLL:

$$V_1(t) = E_1\cos(\omega_1 t + \theta_1) \tag{A3.1}$$

The output from the VCO then will be;

$$V_2(t) = E_2\cos(\omega_2 t + \phi_2(t)) \tag{A3.2}$$

The VCO oscillates at its natural frequency ω_2 when the loop is out of lock so that $\phi_2(t)$ is constant and equal to ϕ_2. The output voltage V_d of the phase detector is;

$$V_d(t) = V_1(t) \times V_2(t)$$

$$= E_1\cos(\omega_1 t + \theta_1) \times E_2\cos(\omega_2 t + \phi_2)$$

$$= \frac{E_1E_2}{2}\left[\cos((\omega_1 - \omega_2)t + (\theta_1 - \phi_2)) + \cos((\omega_1 + \omega_2)t + (\theta_1 + \phi_2))\right]$$

This output thus takes the form of beats. As the low frequency component is outside the filter bandwidth and is attenuated, the VCO control voltage is negligible. If the input frequency is moved closer to the VCO natural frequency such that it falls inside the capture range, the loop quickly pulls the VCO output into phase synchronism with the input. With some complicated mathematics about the transient state while the loop becomes locked, the final result is that the VCO frequency equals the input frequency:

$$V_2(t) = E_2\cos(\omega_1 t + \theta_2) \tag{A3.3}$$

From equation (A3.2), $\Phi_2(t)$ has become time variable;

$$\phi_2(t) = (\omega_1 - \omega_2)t + \theta_2 \tag{A3.4}$$

V_d reduces to

$$V_d(t) = \frac{E_1E_2}{2}\left[\cos(\theta_1 - \theta_2) + \cos(2\omega_1 t + (\theta_1 + \theta_2))\right]$$

This is passed through the loop filter which removes the high frequency component and leaves the dc component unattenuated. The control voltage of the VCO thus becomes

$$V_c(t) = k_d \bullet \cos(\theta_1 - \theta_2) \qquad \text{(A3.5)}$$

where $k_d = E_1E_2/2$.

The change in output frequency $\Delta\omega$ is related to the control voltage $V_c(t)$ by

$$\Delta\omega = k_o V_c(t) \qquad \text{A(3.6)}$$

With the instantaneous frequency of the VCO output voltage given as

$$\omega_{inst} = \frac{d}{dt}\left[\omega_2 t + \phi_2(t)\right]$$

$$= \omega_2 + \frac{d}{dt}\phi_2(t)$$

The change in frequency, $\Delta\omega$, is thus given as

$$\Delta\omega = \omega_{inst} - \omega_2 = \frac{d}{dt}\phi_2(t) \qquad \text{(A3.7)}$$

Equations (A3.4) and (A3.7) make

$$\Delta\omega = \omega_1 - \omega_2 \qquad \text{(A3.8)}$$

Thus substituting for $\Delta\omega$ and $V_c(t)$ in equation (A3.6),

$$\omega_1 - \omega_2 = k_0 k_d \cos(\theta_1 - \theta_2)$$
$$= k_0 k_d \cos\theta' \qquad \text{(A3.9)}$$

where $\theta' = \theta_1 - \theta_2$, which is the phase difference between the input and output signals. θ' is equal to 90° ($\pi/2$ radians) when $\omega_1 = \omega_2$. Thus the input and output signals are said to be in phase quadrature. A slight alteration in the input frequency results in a phase error θ_e:

$$\theta' = \frac{\pi}{2} - \theta_e \qquad \text{(A3.10)}$$

From equation (A3.9)

$$\begin{aligned} \omega_1 - \omega_2 &= k_0 \, k_d \cos\left(\frac{\pi}{2} - \theta_e \right) \\ &= k_0 \, k_d \sin \theta_e \end{aligned} \qquad \text{(A3.11)}$$

From equations (A3.6) and (A3.8),

$$V_c(t) = \frac{\omega_1 - \omega_2}{k_o}$$

Therefore from equation (A3.11)

$$\begin{aligned} V_c(t) &= k_d \sin \theta_e \\ &\approx k_d \, \theta_e \end{aligned} \qquad \text{(A3.12)}$$

for small θ. This is the defining equation for phase sensitive detector.

Rearranging equation (A3.11)

$$\theta_e = \sin^{-1} \left(\frac{\omega_1 - \omega_2}{k_o k_d} \right) \qquad \text{(A3.13)}$$

The sign of θ_e indicates the direction the output frequency has to change. Edges of the lock range can be found from this equation (A3.13). When $\theta_e = 90°$, $\omega_1 - \omega_2 = k_o k_d$. Similarly, when $\theta_e = -90°$, $\omega_1 - \omega_2 = -k_o k_d$. These are the maximum and minimum values the frequency difference ($\omega_1 - \omega_2$) can have.

The lock range therefore has a bandwidth equal to $2k_o k_d$ about the centre frequency of the VCO. When the input frequency is pushed outside this range, the loop falls out of lock and the VCO returns to its centre frequency.

The above analysis assumes unity dc gain of the loop filter. Otherwise the term $k_o k_d$ should be replaced by $k_o k_d \, |F(o)|$ where F(o) is the loop filter gain at dc.

The capture range of the loop depends on the transient response of the loop and is approximately equal to $2k_ok_d \mid F(j\omega_c) \mid$, where ω_c is half of the two sided capture range. For a loop with a simple lag filter,

$$2\omega_c = 2\sqrt{\frac{k_ok_d}{\tau}}$$

where τ = filter time constant.

Appendix 3.2 The Differential Protection Algorithm.

```
/* File:    algo.c
 * Version: 1.10
 * Date:    November-1993
 * Author: Allexon Chiwaya
 * Support: ANSI-C
 * Proj:    alex/operate
 * Algorith definition (used in conjunction with SIMUL DPES package)
 */

#include <assert.h>
#include <math.h>
#include <stddef.h>
#include <stdio.h>

#include "simul.h"

#define SM_LEN      (12)          /* length of moving-average filter */
#define MAX_DELAY   (50)          /* maximum delay */

#define ABS(x)      ((x) < 0 ? -(x) : (x))

typedef struct {
    const char  *name;            /* name of the quantity */
    double      sum;              /* sum of the values */
    double      past[SM_LEN];     /* circ. buffer of past values */
    Count       index;            /* index into past[] to current */
    Count       valid;            /* index of last valid value */
} Smooth;

typedef struct {
    double      past[MAX_DELAY];  /* circular delay buffer */
    Count       in, out;          /* reader and writer indexes */
    Count       delay;            /* should be fixed */
    Count       valid;            /* number of valid data points */
} Delay;

const double pi = 3.141592654;

Smooth ipFilter[2], iqFilter[2];
Delay  ipDelay[2], iqDelay[2];
Delay  iAdelay8[2], iBdelay8[2], iCdelay8[2];
Delay  iAdelay16[2], iBdelay16[2], iCdelay16[2];

/* Debugging flags */
#define DBA_ALGO    (0x1001)        /* basic algorithm outline */
#define DBA_NORM    (0x1002)        /* normalisation */
#define DBA_REFS    (0x1004)        /* reference phasors */
#define DBA_IPQ     (0x1008)        /* Ip and Iq calculations */
#define DBA_XMIT    (0x1010)        /* tranmsmission of values */
#define DBA_RECV    (0x1020)        /* reception of values */
#define DBA_DELAY   (0x1040)        /* transmission compensating delay */
#define DBA_CALC    (0x1080)        /* calculations */
#define DBA_LOGIC   (0x1100)        /* decision logic */
#define DBA_SMOOTH  (0x1200)        /* smoothing */

/* debugging macro - print debugging if flag is set */
#define DBGA(x, y)  (((debug & DBA_##x) == DBA_##x) ? algoInfo y: (void)0)
char *algoDbFlags[] = {"algo", "norm", "refs", "ipq", "xmit", "recv",
    "delay", "calc", "logic", "smooth", NULL};
```

```
/* Indexes for permanent values */
#define IPR         (0)
#define IQR         (1)
#define N           (2)
#define IP_NORM     (3)         /* normal Ip (pre fault) */
#define FAULTED     (4)         /* has fault occured ? */

/* multiply by DTOR to convert Degrees -> Radians */
#define DTOR        (pi/180.0)


/* - smooth a value through a moving-average filter
 * args: filter, original value
 * rtns: smoothed value
 * note: filter length is set by SM_LEN
 */

static double smooth (Smooth *filter, double next)
{
    double ave;         /* average */

    assert (filter->name != NULL);
    assert (filter->index >= 0 && filter->index < SM_LEN);
    DBGA (SMOOTH, ("SMOOTH: filter %s %dth value %lf", filter->name,
        filter->index, next));
    /*
     * Drop the least recent value
     */
    if (filter->valid < SM_LEN) {
        /* filter in pre-run. No output */
        filter->valid++;
    } else {
        DBGA (SMOOTH, ("SMOOTH: filter %s dropping %lf", filter->name,
            filter->past[filter->index]));
        filter->sum -= filter->past[filter->index];
    }
    /*
     * Add in the new value and find average
     */
    filter->sum += filter->past[filter->index] = next;
    filter->index = (filter->index+1) % SM_LEN;
    ave = filter->sum / filter->valid;
    DBGA (SMOOTH, ("SMOOTH: filter %s returning %lf", filter->name, ave));
    return ave;
}


/* - delay a value by a fixed amount (using a circular buffer)
 * args: delay line, current value
 * rtns: value of 'delay' steps ago
 */
static double delay (Delay *del, double val)
{
    double old = 0;

    assert (del->delay < MAX_DELAY);
    if (del->valid < del->delay) del->valid++;
    else {
        old = del->past[del->out];
        del->out = (del->out + 1) % MAX_DELAY;
    }
    del->past[del->in] = val;
    del->in = (del->in + 1) % MAX_DELAY;
    return old;
}
```

```
/* - main protection algorithm implementation
 * args: current time step
 * rtns: TRUE to trip, FALSE otherwise
 */

Bool protect (Count timeStep, Count end)
{
   Value Ipr, Iqr;
   Count n;
   Bool trip;
   double  Va = localV (A),
           Vb = localV (B),
           Vc = localV (C);
   double  Ia = localI (A),
           Ib = localI (B),
           Ic = localI (C);
   double  Sa, Sb, Sc;
   double  Ia8,  Ib8,  Ic8;
   double  Ia16, Ib16, Ic16;
   double  Ia1, Ib1, Ic1;
   double  Ip, Iq;
   double  Ip_op, Iq_op, Ip_bias, Iq_bias;
   double  k1, k2, Ip_min, Iq_min;
   static Count   timedel;

   plot ("Va", Va);
   plot ("Vb", Vb);
   plot ("Vc", Vc);
   plot ("Ia", Ia);
   plot ("Ib", Ib);
   plot ("Ic", Ic);
   Ipr = getPerm (IPR);
   Iqr = getPerm (IQR);
   n = getPerm (N);
   if (timeStep == 1) {
      /* initialise */
      ipFilter[end].name = "Ip filter";
      iqFilter[end].name = "Iq filter";

      if (end == 0) timedel = rand () % 16;
      printf ("Start exchanging values at time-step %u\n", timedel);
      ipDelay[end].delay = /* 16 + */ (Count) param ("delay");
      iqDelay[end].delay = /* 16 +  */ (Count) param ("delay");
      setPerm (FAULTED, 0);          /* starts un-faulted */
      iAdelay8[end].delay = iBdelay8[end].delay = iCdelay8[end].delay
         = 8;
      iAdelay16[end].delay = iBdelay16[end].delay = iCdelay16[end].delay
         = 16;
   }
   DBGA (ALGO, ("ALGO VALS: time %u V=<%lf,%lf,%lf> I=<%lf,%lf,%lf>", timeStep,
      Va, Vb, Vc, Ia, Ib, Ic));
   Ia16 = delay (&iAdelay16[end], Ia);
   Ia8  = delay (&iAdelay8[end],  Ia);
   Ib16 = delay (&iBdelay16[end], Ib);
   Ib8  = delay (&iBdelay8[end],  Ib);
   Ic16 = delay (&iCdelay16[end], Ic);
   Ic8  = delay (&iCdelay8[end],  Ic);
   /* 1: Derive reference phasors
    * Normalise the phase voltages
    */
   Va =  Va / param ("norm-A");
   Vb =  Vb / param ("norm-B");
   Vc =  Vc / param ("norm-C");
   DBGA (NORM, ("ALGO NORM: normalised V=<%lf,%lf,%lf>", Va, Vb, Vc));
```

```
/* 1:...
 * generate sine waves of unity amplitude synched to the voltages
 * and call them Sa, Sb, and Sc
 */
/* Implementation:  assume the voltage waveforms are modelled by:
 *      Va = V_A * sin ((2 * pi / 20) * time)
 *      Vb = V_B * sin ((2 * pi / 20) * time + 4*pi/3)
 *      Vc = V_C * sin ((2 * pi / 20) * time + 2*pi/3)
 * where time = current time step and V_A, V_B, V_C are amplitudes.
 * Note: there are 24 time-steps per system cycle
 *The above comments are irrelevant when using Ia1, Ib1, Ic1 for ref.
 */
{
   double refAngle = timeStep * 2.0 * pi / 20.0;

   DBGA (REFS, ("ALGO REFS: offset angle = %lf", param ("ang-~")*DTOR));
   refAngle += param ("ang-~") * DTOR;
   /*Sa = sin (refAngle); */
   /*if (! getPerm (FAULTED) && Va == 0.0 && Sa != 0.0) */
         /*algoInfo ("Error: Va & Sa don't match (%f, %f)", Sa, Va);*/
   /*plot ("Sa", Sa);*/
   /*Sb = sin (refAngle + 4.0*pi/3.0); */
   /*plot ("Sb", Sb);*/
   /*Sc = sin (refAngle + 2.0*pi/3.0); */
   /*plot ("Sc", Sc);*/
   Ia1 = (Ia + Ib16 + Ic8)/3;
   /*Sa = Ia1; */
   Sa = Va;
   plot ("Sa", Sa);
   Ib1 = (Ib + Ic16 + Ia8)/3;
   /*Sb = Ib1; */
   Sb = Vb;
   plot ("Sb", Sb);
   Ic1 = (Ic + Ia16 + Ib8)/3;
   /*Sc = Ic1; */
   Sc = Vc;
   plot ("Sc", Sc);
}
DBGA (REFS, ("ALGO REFS: reference waves S=<%lf,%lf,%lf>", Sa, Sb, Sc));
/* 1:...
 * provide a memory feature in case of voltage collapse for
 * reference phasors (This is implicit)
 */
DBGA (ALGO, ("ALGO: finished box 1"));


/* 2: calculate and smooth Ip and Iq
 * Calculate Ip and Iq according to formulas given
 */
Ip = Ia*Sa + Ib*Sb + Ic*Sc;
Iq = Ia * (Sb-Sc) + Ib * (Sc-Sa) + Ic * (Sa - Sb);
DBGA (IPQ, ("ALGO IPQ: Ip = %u, Iq = %u", Ip, Iq));

/* 2:...
 * Smooth Ip and Iq with a 12 points moving average filter
 */
Ip = smooth (&ipFilter[end], Ip);
plot("Ip", Ip);
Iq = smooth (&iqFilter[end], Iq);
plot("Iq", Iq);
DBGA (IPQ, ("ALGO IPQ: smooth Ip = %lf, smooth Iq = %lf", Ip, Iq));
DBGA (ALGO, ("ALGO: finished box 2"));
```

```
/* We detect a change in Ip (after the first 24 timesteps)
 * to detect a fault (- or after first 24 steps when using I1)
 */
if (timeStep == 24) {
    setPerm (IP_NORM, Ip);
} else if (timeStep > 24) {
    double deltIp =  Ip - getPerm (IP_NORM);
    if (ABS (deltIp) / (ABS (getPerm (IP_NORM)) + 0.05) > 0.05)
        setPerm (FAULTED, 1);
}


/* 3: exchange values with other end
 * Transmit the value of Ip to the other end iff
 *      (timeStep - timedel) mod 32 = 0
 */
if ((timeStep - timedel) % 32 == 0) {
    DBGA (XMIT, ("ALGO XMIT: transmitting Ip (=%lf)", Ip));
    send (Ip);
}
/* 3:...
 * Transmit the value of Iq to the other end iff
 *    (timeStep - timedel + 16) mod 32 = 0
 */
if ((timeStep - timedel + 16) % 32 == 0) {
    DBGA (XMIT, ("ALGO XMIT: transmitting Iq (=%lf)", Iq));
    send (Iq);
}
/* 3:...
 * Recieve Ip from the other end iff
 *      (timeStep - timedel - delay) mod 32 = 0
 * and timeStep > delay (other end has transmitted 1st value)
 */
if ((timeStep - timedel - (Count) param ("delay")) % 32 == 0
  && timeStep > (Count) param ("delay")) {
    Ipr = recv ();
    DBGA (RECV, ("ALGO RECV: receiving Ip (=%lf)", Ip));
}
/* 3:...
 * Receive Iq from the other end iff
 *      (timeStep - timedel - delay + 16) mod 32 = 0
 * and timeStep > delay (other end has transmitted 1st value)
 */
if ((timeStep - timedel - (Count) param ("delay") + 16) % 32 == 0
  && timeStep > (Count) param ("delay")) {
    Iqr = recv ();
    DBGA (RECV, ("ALGO RECV: receiving Iq (=%lf)", Iq));
}


/* 4: Delay local Ip/Iq
 * Received data shall be available. Delay of transmission shall
 * be compensated for, by delaying local values by 17 ms
 */
Ip = delay (&ipDelay[end], Ip);
Iq = delay (&iqDelay[end], Iq);
DBGA (DELAY, ("ALGO DELAY: delayed Ip = %lf, Iq = %lf", Ip, Iq));


/* 5: Calculate formulae
 * Calculations valid iff
 *      (timeStep - timedel - delay) mod 16 = 0
 * and timeStep > delay (other end has transmitted 1st value)
*/
if ((timeStep - (Count) param ("delay")) % 16 == timedel
```

```
    && timeStep > (Count) param ("delay")) {
      Ip_op = ABS (Ip - Ipr);
      Ip_bias = (ABS (Ip) + ABS (Ipr)) / 2;
      Iq_op = ABS (Iq - Iqr);
      Iq_bias = (ABS (Iq) + ABS (Iqr)) / 2;
      DBGA (CALC, ("ALGO CALC: Ip_op=%lf, Ip_bias=%lf, Iq_op=%lf, Iq_bias=%lf",
          Ip_op, Ip_bias, Iq_op, Iq_bias));
  }


  /* 6: perform logic as described on flowchart
   * logic done iff
   * other end has transmitted
   */
  k1 = param ("k1");
  k2 = param ("k2");
  Ip_min = param ("Ip_min");
  Iq_min = param ("Iq_min");
  if ((timeStep - (Count) param ("delay")) % 16 == timedel
    && timeStep > (Count) param ("delay")) {
      if (Ip_op > k1*Ip_bias && Ip_op > Ip_min)   goto trip;
      if (Iq_op > k2*Iq_bias && Iq_op > Iq_min)   goto trip;
      n=0;
      DBGA (LOGIC, ("ALGO LOGIC: logic in box 6 false; box 7 n set to %u", n));
      setPerm (IPR, Ipr);
      setPerm (IQR, Iqr);
      setPerm (N, n);
      return FALSE;
  }
  DBGA (LOGIC, ("ALGO LOGIC: awaiting to receive data for comparison"));
  setPerm (IPR, Ipr);
  setPerm (IQR, Iqr);
  return FALSE;
trip:
  if (++n >= 2) trip = TRUE; else trip = FALSE;
  DBGA (LOGIC, ("ALGO LOGIC: box 7 n=%u", n));
  setPerm (IPR, Ipr);
  setPerm (IQR, Iqr);
  setPerm (N, n);
  return trip;
}
```

Appendix 3.3 The Configuration File of the Algorithm.

On starting, the system reads a configuration file which contains default values of a number of parameters required by the relay. These include:-

- values required by the computer simulation environment, which include:
  - paths where input data files are stored and where plot files can be written,
  - names of plots which are of interest on this run;
- values which define the modelled part of the system, top and bottom, and include:
  - CT and VT parameters (turns ratio and knee point);
  - ADCs' range and number of bits,
  - communications channel delays;
- names and range of values for user parameters (used to alter the behaviour of the algorithm without recompiling).

In the program, the input files handle the three voltages and the three currents at either terminal of the feeder. A counter *timeStep* holds the current input data file time-step for use to process the main algorithm.

The dummy types of *Variable*, *Phase*, and *End* are used to differentiate between different variables present in the system and index the arrays. *Variable* indicates whether the value is a voltage (V) or a current (I). The *Phase* type represents one of the three phases on the system. The *End* type represents one of the feeder, and by convention, the end G is considered to be local and the end H is remote.

Variable declarations are split into two parts. The first part declares the internal system variables used to process the data. These variables are all declared as *static* to make them inaccessible from the outside of the module, and they include the time step and the input and output files. The second part declares variables used directly in the algorithm, and they include the bias factor, k, and the trip settings of the polarised current.

A listing of the configuration file is given below.

```
-- The following statements can occur in the configuration file:
--      Comments start with -- and end with the end of line
--      ECHO some text   displays some text when the program is run
--      USE 'filename'   uses the filename as part of the configuration
        ECHO Case for typical internal fault in system with overhead line feeders.
        ECHO Fault is introduced at time-step 60.

-- All plots are performed for one end of the system at a time
-- 'Swop' provides plots for the other end
-- The plot directive has the format:
--      PLOT <var> '<file>'     {<options>}
-- where <options> are a combination of the following flags:
--              B - put a banner in the file
--              + - sum values across runs
--              A - arithmetic mean across runs
--              G - geometric mean across runs
--              R - RMS across runs
--              # - separate files across runs
-- The following system variables are available for plotting:
--      *out-g, *out-h          : output of protect() algorithm
--      *trip-g, *trip-h        : trip output (only 1st TRUE)
--      *time-step                      : current time step
--      *run-number                     : current run (1-...)
--        PLOT    *out-local        'trip'          {+}
--        PLOT    Ip                'Ip'
--        PLOT    Iq                'Iq'
--        PLOT    calc_Ip           'calc_ip'

        PATH    DATA 'ohldata/1phein2' PLOT 'plots'

--      CT phases ends  kneep knees [turns μ, turns σ]
        CT  *     *     1     1     [300, 0]
        VT  *     *     1     1     [300, 0]

--      ADC quan bits swing
        ADC  I    12    2048
        ADC  V    12    2048

--      CHAN end capa; delay [duration μ, duration σ] [mtbf μ, mtbf σ]
        CHAN  *    14;17              [0, 0]            [1000, 0]

--      PARAM   name    min, default, max       {units}
        PARAM   norm-A  0,1,2000        {A}
        PARAM   norm-B  0,1,2000        {A}
        PARAM   norm-C  0,1,2000        {A}
        PARAM   delay   0,17,100        {cycles}

        PARAM   k1      0.01, 0.02, 1   { }
        PARAM   k2      0.01, 0.02, 1   { }

        PARAM   Ip_min  0, 0.3, 1000   {A}
        PARAM   Iq_min  0, 0.3, 1000   {A}

        PARAM   ang-G   0, 90, 360      {°}
        PARAM   ang-H   0, 110, 360     {°}
```

Appendix 3.4 Program Running.

The Hewlett Packard Vectra RS/25C 386 25MHz computer in the University of Bath Power and Energy System Group laboratory is used. The program is installed in the 'D' drive under the directory **OPERATE**. Using the Q editor, the steps below may be followed to execute the program for a data case:-

q algo.c This command loads in the differential protection algorithm file as in appendix 3.2. Debugging messages can easily be re-worded to suit the user's style. The file must be saved before quitting in order to save any changes and amendments.

q dpes.cnf This command loads in the configuration file as in appendix 3.3. The file specifies the paths where the input data files are stored and where plot files and their names can be written. This file can be used to change the behaviour of the algorithm and to change the default values of the settings. Again any changes must be saved.

There are a number of options provided. The command below may be used:-

algo < options >

Valid options include:

-cases <int>	Specify number of cases
-debug <flags>	Turn on some debugging
-default	Use default values for parameters
-help	Display this help message
-repeat <int>	Repeat the simulation for a specified number of times
-seed <int>	Set the random seed
-swap	Swap ends (G and H) for plots
-simple	Use a linear model for CT's and VT's
-time	Time the real time performance of simulator
<parm>=<val>	Set the value of a parameter

For example, to get some help on *debug* facility, the following command can be used:-

algo -help debug

This command when executed will show the valid algorithm debugging flags:-

algo, refs, ipq,
xmit, recv, delay,
calc, logic, smooth

A typical command to run a data case using default values of the configuration file and a linear model for CT's and VT's for example, and repeating the simulation a specified number of times, say ten, is:-

algo -default -simple -repeat 10

On-line changing of some parameters can be done by running the program without using *default*, and the following will appear, where the user is prompted for an input and hitting 'return' on the keyboard enters the default value:-

Please input the required values for the following:

ang-H in degrees = *[<val>]*
ang-G in degrees = *[<val>]*
Iq_min in A = *[<val>]*
Ip_min in A = *[<val>]*
k2 = *[<val>]*
k1 = *[<val>]*
delay in samples = *[<val>]*

Chapter 4

THE COMMUNICATIONS SYSTEM.

4.1 INTRODUCTION.

Many protection schemes incorporate the need for end to end communications in order to achieve overall protection of feeder circuits. Examples include the transfer tripping operations associated with distance and other relays[3, 29, 63, 64], and the transmission of continuous signals related to phase or amplitude associated with differential current relaying schemes. The times required to make the data transfer are critical to the operation of the protection and can not be allowed to increase above strict limits. The communications, thus, need to operate in real time.

For digital relays, the communications system uses a modem[65, 66] to provide the interface between the digital protection system and the communications medium. Secure data transfer between the relaying points in unit protection of feeders is ensured by the coding controls and error detection techniques[67, 68]. A variety of communications media[69] are used, ranging from an elementary copper pair to power line carrier, microwave and optical fibre links. Each service offers advantages and limitations depending on the particular application.

Transfer of data enjoys a choice between using a 4 kHz bandwidth voice frequency communications and wideband communications using a CCITT (The International Telegraph and Telephone Consultative Committee, which is part of the International Telecommunication Union, ITU) standard on 64 kbits/s time slots which is an ANSI (American National International Standards) equivalent of 56 kbits/s time slots. Voice frequency communication channels are the most commonly used systems having been

developed for telephone communications. As they have been extensively developed for mass communications, they provide a convenient standard for use with distribution system protection schemes.

This chapter presents the choice of the voice frequency communications for the work undertaken. An overview of communications for protection is given. A summary is given of the 2400 bits per second modem used, comparing it with other V-series CCITT modem standards. Here, switching durations, speed and noise have been highlighted.

4.2 OVERVIEW OF COMMUNICATIONS PRINCIPLES.

Long term historical performance statistics show that the ultimate reliability and dependability of Unit schemes of protection are linked to that of the communications system. Due to the long period of time for which pilot wires, for example, have been used, there is a good understanding of their performance limitations. Some of the limitations are that normally only single phase quantities can be transmitted and this may result in loss of information derived from the three phase system. Also signal levels may exceed regulatory limits. For systems transmitting tones continuously, for example frequency modulation systems, the maximum power level at the zero relative level point is -13dBm. This, when combined with the high noise levels often associated with power system faults, give unfavourable signal to noise ratio for the communications channel. Carrier frequency is around 1800 Hz[24], this being the flattest part of the voice frequency channel's group delay characteristic and hence provide the least probability of distortion in the demodulated signal.

Since the launch of the first digital current differential relays in the mid 1980's[70] there is now a desire to understand more the performance limitations of digital communications. The limitations are better understood with some appreciation of the

operating principles. As voice frequency communications is the main subject, a brief summary of operating principles is centred around it.

Several techniques[69, 71, 72], exist which can be used to provide bi-directional data transfer, and they include Time Division Multiplexing (TDM), Frequency Division Multiplexing (FDM), echo compensation, and analogue hybrids, which is a simplified subset of echo compensation. TDM is most suited for high data rates where Pulse Code Mode (PCM)[73] is typical in digital communications using CCITT standard 64 kbits/sec communications. Frequency multiplexing options could operate on voice frequency communications channels. They allow independent communication paths separated in frequency and can, therefore be used in four-wire operations to provide the required full duplex operation in feeder differential protection schemes. Using frequency division multiplexing alone requires high order filters to ensure that the local receiver can distinguish between the signal from the remote transmitter and that generated locally. The use of hybrids alone to couple the transmitter's output and the receiver's input to a pilot circuit, for example, also requires a complex system to provide the necessary channel separation. Using these two systems together would provide both a relatively simple and cost effective solution with the required separation between the two channels of data transfer. Thus, at each relaying terminal, the communications comprises a modem, transmitter and receiver subsystems, and a hybrid.

4.3 CHOICE OF MODEM.

Communication channel characteristics maybe specified in terms of a frequency and phase response. A signal that carries information, however, and which the communications system transmits, varies in an unpredictable or random manner. Such a signal may not be defined in terms of a specific amplitude and phase spectrum, but may be specified by its power spectrum or by a probability distribution function[74, 75].

Thus, a signal may be of a nature which makes it incompatible with effective transmission through a given channel. An interface between the digital protection system and the communications medium is therefore required.

The basis of the interface between the digital protection system and the communications medium is the modem. It converts digital signals into a form suitable for transmission over the voice frequency channel. For transmission from one modem to another over the communications medium, a carrier signal as mentioned above is used to modulate the data signal. Demodulation is a process that is invoked at the receiving modem to recover the original digital signal. The modem is sometimes referred to as a Data Circuit-terminating Equipment (DCE) and the corresponding computer, terminal or any device connected to it is referred to as a Data Terminal Equipment (DTE). A CCITT recommendation V.24[24] standard describes the interconnecting circuits, called Interchange Circuits, at the interface between DTE and DCE for the transfer of binary data, control and timing signals. A summary of the most widely used circuits is given in table 4.1.

Modems operate over a wide range of operating speeds varying from 75 bits/sec to 14.4kbits/sec in full or half duplex and offer different advantages for different applications. A host of national and international standards[24] have been agreed upon to define the characteristics of the different modems in ensuring connectivity between various equipments[22, 76]. The standardisation of signal conversion terminal equipment or modem is the province of the CCITT. The standardisation of the junction or interface between the modem and the DTE is a matter of agreement between the CCITT and the International Standards Organisation, ISO, or the International Electrotechnical Commission, IEC.

The CCITT V-series recommendations include specifications for modems, interfaces, test equipment and line quality. In the field of telecommunications, there are a number of significant advantages in having standards:

- Connectivity is ensured between various equipment
- Dependency on particular suppliers is removed
- Guarantee of quality is provided
- Even barriers to trade caused by differences in national practices can be removed
- Safety and protection is ensured.

Some of the standards are illustrated in figure 4.1. It is noted that the higher speed modems may normally have modes that allow compatibility with lower speed modem standards. An example of this is that the V.32 modem can operate in a mode compatible with a V.29 modem.

One consideration when selecting modems is whether the combination of the modem and the line is required to provide a full duplex or a half duplex link. A full duplex link allows serial data transmission in both directions at the same time while a half duplex link allows serial data transmission in only one direction at a time. The CCITT V.26 standard with its data rate of 2400 bits per second operating on full duplex was chosen for this application. Although this may be considered modest in light of currently available systems, the inherent communications security and tolerance to interference generally vary with the inverse of the data rate. Tolerance to interference is related to the system's energy per bit to noise ratio, E_b/N_o[20], defined by:-

$$\frac{E_b}{N_o} = \frac{\left(\frac{S}{R}\right)}{N_o} \qquad (4.1)$$

where,

E_b is the signal energy per bit
N_o is the noise energy per hertz
S is the sending signal strength

and,

R is the data bit rate.

For a constant sending signal and interference level, an increase in the data rate decreases the energy per bit to interference energy ratio and hence increases the possibility of data corruption. Here, then, the V.26 modem standard scores against the V.33 modem standard. Another favourable factor is that the V.26 has a short initialisation time after a disturbance in the communications. Although the V.33 boasts a higher data rate of 14400 bits per second, its initialisation time is greater than 50 msec compared to the 15 msec of the V.26[22]. A fall in level of the incoming line signal to -31 dBm or lower for more then 10 ± 5 ms will cause the V.26 to be turned off[24]. An increase in level to -26 dBm or higher will, within 10 ± 5 ms, turn the circuit on. The condition for levels between -26 dBm and -31 dBm is not specified except that the signal level detector exhibits a hysteresis action such that the level at which the off to on transition occurs is at least 2dB greater than that for the on to off transition.

4.4 CHOICE OF TRANSMISSION MEDIUM.

There are several communication channels that can be used for power system protection purposes. A channel may take the form of a pair of metallic conductors. It may also take the form of glass fibre along which a beam of light is transmitted, or free space through which an electromagnetic beam is transmitted. Each service offers advantages and

limitations depending on the particular application. The choice of a particular system depends on such factors as economics, geography and technical requirements, among others.

In choosing media for communications in protection applications, various factors are considered. These include the type of scheme, bandwidth, length of circuit, availability of channel, and cost. A general summary of comparison between two extremes, pilot wire and optical fibre systems, is illustrated in table 4.2[3, 5, 7, 65, 69, 77, 78].

One of the important elements in choosing a medium is the channel capacity. The information capacity of a channel is related to the bandwidth and noise according to Shannon's law[22, 79, 80] which states that if a channel has a bandwidth B and mean signal-to-ratio of S/N, the maximum rate at which information may be transmitted is C bits per second. The basic formula is:-

$$C = B \log[\, 2(\, 1 + S/N) \,] \quad bits/sec \tag{4.2}$$

where,

C is the channel capacity
B is the bandwidth
S/N is the signal-to-noise ratio.

For large S/N, Shannon's law approximates to;

$$C = B \log[\, 2(S/N) \,] \tag{4.3}$$

Thus, the communications link, because of the limited bandwidth, is restricted to the transfer of data.

4.5 TRANSMISSION EFFECTS.

In exchanging data over a communications transmission system between protection relaying points, undesirable effects are experienced. These occur as a result of the line properties and disturbances.

The quality of circuit for voice transmission is often expressed only in terms of the maximum insertion loss (for example at the reference frequency of 800 Hz) which can be tolerated by the equipment. For data transmission, modems are, however, more demanding in their requirements and their effective operation depends on the nature of other circuit characteristics in addition to insertion loss. Some of the characteristics are summarised in appendix 4.1 which gives the performance specification of a typical line available from the British Telecom which conforms to CCITT specification M1020[24]. Circuits meeting the requirements of this specification are intended for use with modems that do not contain equalisers. Note that high speed modems use equalisation to reduce the effects of attenuation and group delay.

Transmission effects may generally lead to any of the following:-

(i) There is a significant delay associated with transmission of the data. The delay is due to processing, that is, analogue to digital conversion and buffering for transmission, and also due to transmission line parameters which result in propagation delays. Other effects in this category include retrials which succeed resulting in large delays.

(ii) The data channel may experience temporary outages. This may be due to any disturbances, as summarised under appendix 4.1, which result in unrecoverable bit errors in the message.

(iii) Noise is associated with any data transmission.

4.6 NOISE AND ERRORS.

The preceding section has established that there is always a possibility that received data will contain errors whenever data is transmitted over a channel. General reference to one major contributor, noise, is now made here. At all times the communications is subject to random interference. Many and varied sources cause uncorrelated electrical noise which give rise to random fluctuations in the received signals. Noise may come from within the electronic part such as thermal noise in resistors, shot effects in amplifiers, and impulse noise caused by switching in communication networks. It may come from outside the electronic parts such as lightning discharge and other atmospherics, and arcing contacts in electrical machinery.

In digital transmission the noise may give rise to two distinct kinds of error condition. One kind is that of random errors that involve no correlation between the digits in error, and characterises channel corrupted with Gaussian noise[74]. The other kind involves burst errors where a number of consecutive, rather than individual and probably widely spaced, digits are corrupted. Bursts can be generated from a number of sources such as arcs that accompany power system short circuit faults and switchings in communication networks.

4.7 COMMUNICATIONS FAILURE MODES.

Ideally the Unit power system protection should clear all in-zone faults. In practice, however, faults may not always be cleared. Among the factors contributing to this most undesirable scenario are the failure of the relay 'element' to detect the fault, the failure of the communications, and the failure of the circuit breaker to trip. The failure of the communications is the topic of discussion here.

Failures in communications can either be random, that is, appearing as one-off events isolated from other failures, or systematic, that is, occurring every time the particular conditions arise. Thus systematic failures are less difficult to isolate.

Examples of failures in metallic pilots include open circuits and short circuits which are random, and impaired insulation which may be random or systematic. Fault induced interferences are systematic. To circumvent random failures circuit duplication can be used. Other effective methods to circumvent random failures include the use of alternative routes, back-up systems, and the use of test tones.

Digital communications has an advantage in that good on-line fault reporting is possible. Common problems especially with multiplexing is that the multiplexer may send messages to wrong ports. Concerns for the future include risk of systematic failure modes, automatic rerouting of the communications circuit may become common, and also communications problems could occur when protection is required to operate

Other problems between protection and communications include the fact that the general communications specifications may not meet protection demands. The protection signal is unique. Consistent send and receive times are desired. It is needed that there is no queuing in the modems, no re-bunching of data, no need to repeat or resend, and no rerouting except when there is a communications system failure.

4.8 DATA CODING.

The various effects on the transmission of data introduce the need for proper identification of any corrupt blocks of data and insurance that there is minimum likelihood that they will be accepted as being healthy. There are several techniques of enhancing the communications system to handle errors in the received signals, and

inevitably and unfortunately, they increase the cost of the system. The enhancements can be introduced either by enhancing the transmitter and receiver hardware, using a wider operating bandwidth, using higher transmission powers, or by employing coding techniques to provide error detection and correction. Error detection and correction is the main interest here.

The discipline of coding for error detection and correction has two main types, and these are the linear block coding and convolutional coding[73, 59]. An immediate advantage of linear block coding for protection applications is that each block of data is a self contained package and the error detection and correction coding is not linked to other blocks, as is the case with the convolutional codes. Therefore, corrupted blocks of data can be identified and discarded if appropriate. Linear block coding is applicable in this work.

The linear block code packages an information data stream of k bits into a block of n bits. A block has therefore (n-k) parity bits and these are used for error detection and correction. The parity bits represents an overhead because n bits have to be transferred to convey k bits of information. This overhead is important as it provides a mechanism to detect and correct corrupted data, thereby enhancing system security by providing effective interconnection and meaningful intercommunication. To ensure that maximum throughput of actual data is obtained from the communications system, it is essential to minimise the overheads introduced by the coding strategy. A compromise is therefore required between the level of error detection and correction provided by the coding and the percentage of power system data included in the message.

The Hamming code[59, 60, 61, 81], described by (n,k), is a simple code relative to a Bose-Chaudhuri-Hocquenghen (BCH) code[59] which is described by (n,k,d) where d is a measure of how many corrupted bits in the block can be corrected. However, the extra

sophistication of the BCH code offers the possibility of detecting and correcting a higher number of corrupted data bits. A comparison between the Hamming code and the BCH code is illustrated in figures 4.2 and 4.3[59]. Figure 4.2 illustrates the ability of the Hamming (7,4), (13,9), (26,21), and (45,39) codes to provide error free blocks in the presence of Gaussian noise, and shows the probability of incorrectly decoding a block plotted against the signal to noise power ratio expressed as the ratio of the uncoded energy per bit to the noise power spectral density. The figure shows that the longer Hamming codes are better able to handle the noise until the signal to noise ratio increases above 10 or 12 dB. Similarly figure 4.3 is for the BCH (7,4,1), (31,21,2), and (63,39,4), and it shows that the longer BCH codes are also better able to handle the noise until the signal to noise ratio increases above about 6dB.

Because of the limited data transfer rate of 2400 bits per second, the Hamming (13,9) code was used in this application. This code provides an information data stream of 9 bits into a block of 13 bits. Therefore, in a code there are 4 parity bits which are used to provide a mechanism to detect and correct corrupted data. The shortness of this code makes it suitable for use in low data transfer systems as proposed in this work.

4.9 SUMMARY.

A communications system provides secure data transfer between the relaying points of Unit protection schemes of feeder circuits. It is basically composed of a communications source and communications sink connected by a channel. Modems provide the interface between the digital protection system and the communications medium.

Considerable expertise and investment has been applied to telephone based digital data communication systems. They, therefore, provide an almost ready made communications platform which can be used for feeder protection schemes. For this application, it has

been proposed to use a voice frequency channel for the digital data communications, operating with both standard telephone type communication circuits and copper pilot circuits, if they have already been installed. A CCITT V.26 standard modem using 2400 bits per second operating in full duplex mode is used.

Whenever data is transmitted over a communications channel there is a possibility that the received data will be corrupted. It is important in protection applications that any corrupted blocks of data are properly identified. Since the protection data is continually being updated, corrupted data is best rejected. Coding techniques offer the potential of greatly enhancing a communications system's ability to detect errors in the received signal.

To ensure that maximum throughput of actual data is obtained from the communications system, it is essential to minimise the overheads introduced by the coding strategy. Considering that only a modest communications data rate is used, a Hamming (13,9) code is used. This code provides an information data stream of 9 bits into a block of 13 bits, offering 4 parity bits to handle errors.

4.10 FIGURES.

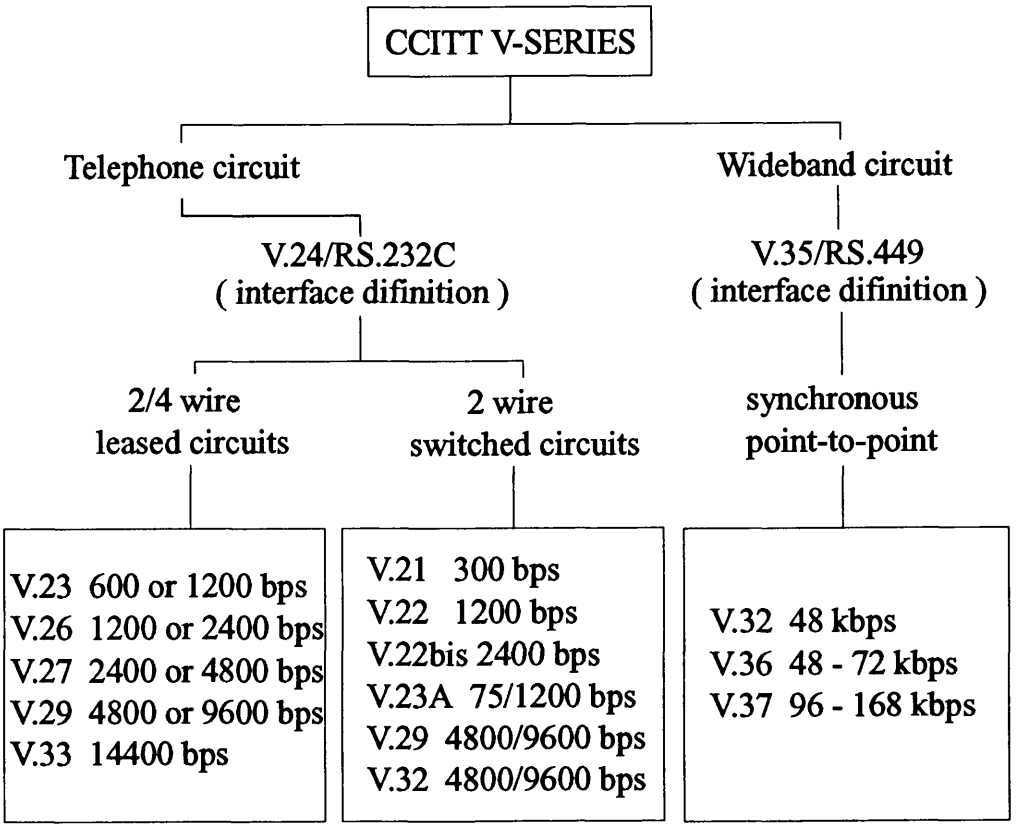

Figure 4.1 Summary of CCITT V-Series Modem Standards.

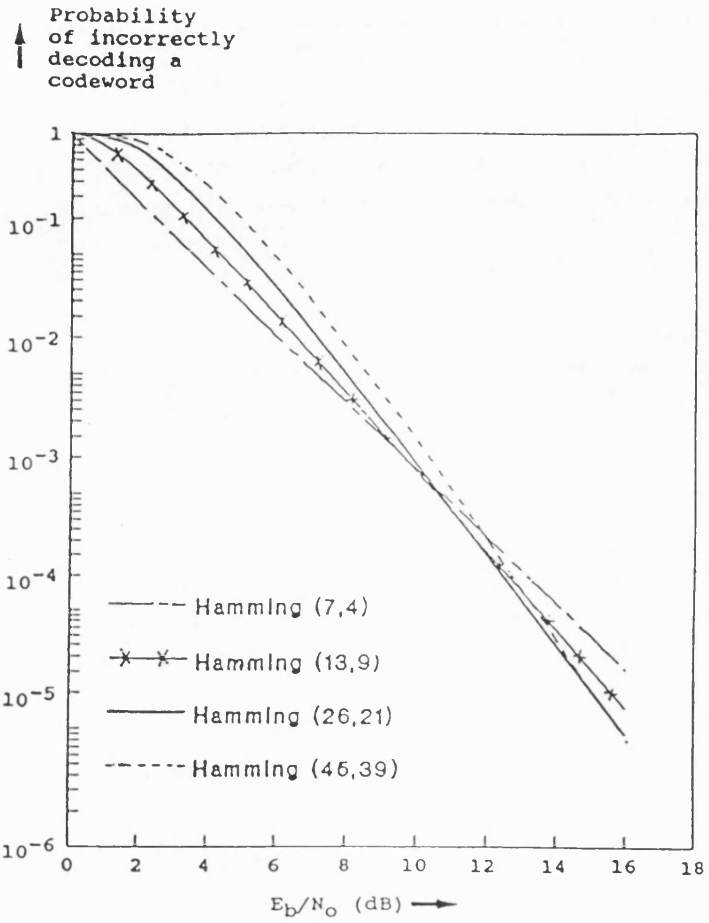

Figure 4.2 Probability of an Error in a Code Block when using Hamming Codes during exposure to Gaussian Noise.

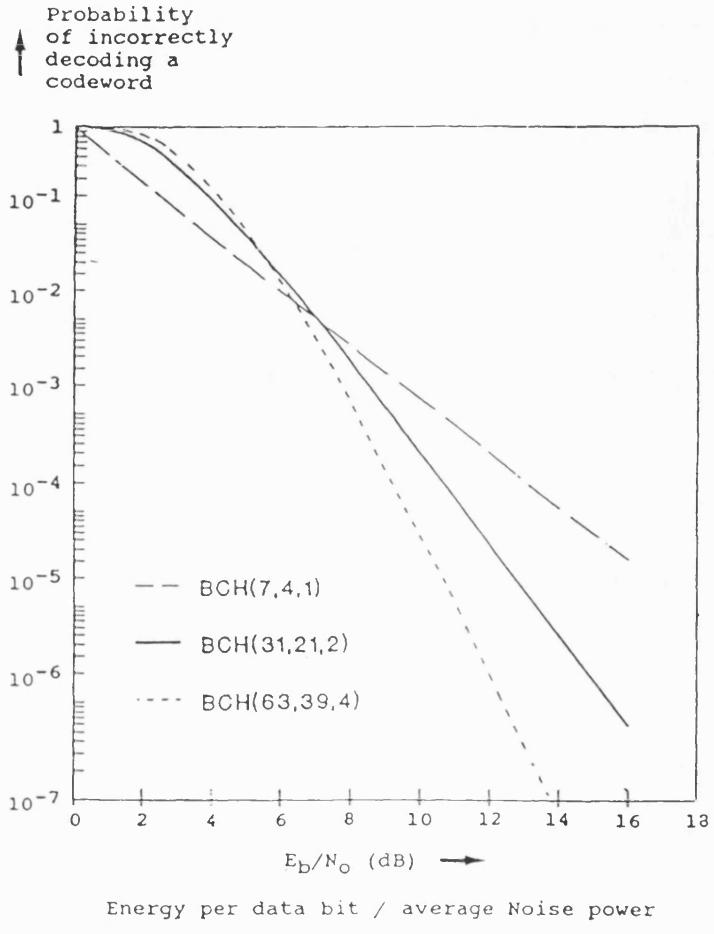

Figure 4.3 Probability of an Error in a Code Block when using BCH Codes during exposure to Gaussian Noise.

4.11 TABLES.

Table 4.1 Summary of most widely used Interchange Circuits (of the V.24 standard) between DTE and DCE.

INTERCHANGE CIRCUIT No.	DESIGNATION
102	Signal ground or common return
103	Transmitted data
104	Received data
105	Request to send
106	Ready for sending
107	Data set ready
108	Connect data set to line
109	Data channel received line signal detector
113	Transmitter signal element timing (DTE)
114	Transmitter signal element timing (DCE)
115	Receiver signal element timing (DCE)
125	Calling indicator.

Table 4.2 Summary Comparison of Pilot Wires and Optical Fibres.

CHARACTERISTIC	PILOT WIRE	OPTICAL FIBRE
Power line length[5, 38]	short*, (40 km)	short, (30 km)
Typical data rate[65, 77]	low, eg voice frequency	high, eg 140 Mbit/s
Propagation delay[3]	2 milliseconds	〈 0.2microseconds
Velocity, (length/delay)	2E+07 m/s	〉 1.5E+11m/s
Message length	short to medium	can be long
Communication protocol[65, 69]	Asynchronous/synchronous	Synchronous
Operational wavelength	〉 5000m	850 - 1300 nm
Operational Frequency[3]	Up to 4 kHz (audio range)	____
Attenuation[77, 78], (dB/km)	〈 1	〈 1
Charact. impedance[78], (Ω)	105.7 - 111.5	not applicable -insulator
Miscellaneous	Small information capacity	Large info. capacity
	High material costs	Quantity-related cost
	Small cable size	Small cable size
	Interference prone	Interference immune
	Some cross talk	Negligible cross talk
	Suffer induced voltage	Elliminates induction
	Light weight	Complete electrical isolation
		Light weight
		Rugged

* power line length:

short = line ≤ 80 km

medium = 80 〈 line ≤ 240 km

long = line 〉 240 km.

4.12 APPENDICES.

Appendix 4.1 Typical Leased Line Performance Specifications (cont. next page).

Nominal insertion loss at 800 Hz is: 3dB for a 2-wire presentation 0dB for a 4-wire presentation		
CHARACTERISTIC	FREQUENCY BAND (Hz)	LIMITS
		(dB)
Loss/Frequency response	300 - 500	-2 to +6
between customer's premises	500 - 2000	-1 to +3
relative to the loss at 800 Hz	2000 - 2600	-1 to +3
	2600 - 2800	-1 to +3
	2800 - 3000	-2 to +6
		(μs)
Group delay/Frequency	500 - 600	3000
response between customer's	600 - 1000	1500
premises relative to minimum	1000 - 2600	500
delay	2600 - 2800	3000

Appendix 4.1 (continued from previous page).

CHARACTERISTIC	QUANTITY
Impulsive Noise level	-45dBmOp
Impulsive Noise Threshold (no more than 18 impulsive noise counts to exceed the threshold in any period of 15 minutes)	-21dBmO
Signal to quantising noise ratio	22dB
Signal to listener echo ratio	20dB
Cross-talk Attenuation	45dB
Maximum Frequency error	2Hz

GLOSSARY

Insertion Loss:- This is the term in decibels used to define the difference between the power input to and power output from a circuit measured at a specified frequency, for example at 800Hz. The insertion loss of a circuit will vary over time, normally within ±3dB of the nominal loss. Changes of the loss within this range may occur gradually or instantaneously.

Loss/Frequency response (relative to 800Hz):- On any telephone circuit, some frequencies transmitted will be weakened or attenuated more than others. Loss/Frequency

response describes the variation in losses which can be expected in different sections of the available bandwidth of a circuit. In data transmission, the distortion introduced by a poor loss/frequency response may impair a receiver modem's ability to interpret the signals correctly. Generally, higher frequencies are attenuated more than lower frequencies.

Group Delay/Frequency response:- Just as attenuation varies with frequency, the propagation time of a signal through the medium is also dependent on frequency. Delay distortion is the condition which causes some frequencies to be slower than others. In data transmission, information is transmitted through rapid changes in the signal state and the term group delay/frequency response refers to a time measurement of a change in a signal at different frequencies through a system.

Random circuit noise:- Random circuit noise, or white noise, can be of any frequency and, when severe, can cause hissing sound. It is measured in dBmOp, where dBmO refers to the ratio of the noise power to the test level at a particular point in a transmission path known as the relative zero level point. The 'p' shows that the measurement is taken using a psophometer which is a device which measures only significant noise.

Impulsive noise:- A form of distortion characterised by high amplitude and short duration (peaks). Both random and impulsive noise depend on route length.

Signal to Quantising noise:- Signals, especially on PCM channels, could suffer from quantising distortion as a result of coding and decoding. Limits of signal to quantising noise may be included for the convenience of manufacturers.

Signal to Listener Echo ratio:- This is a reflection effect which occurs whenever there

is a change in the electrical characteristics of a circuit, for example a two wire connected to a four wire circuit. Signal to listener echoes can cause errors if they are of sufficient high order.

Cross-talk Attenuation:- Cross talk is caused by induction between different telephone channels. For example, on a poor telephone connection faint conversation may be overhead in the background. Cross talk attenuation is of a very low level such that it is not significant in data transmission.

Maximum Frequency error:- Carriers systems used in multiplexing telephone channels may introduce slight changes in the frequencies of signals transmitted. This is known as frequency error or frequency offset.

Other impairments:-

i. *Gain hits*:- Gain hits result in a short term increase or decrease in the data signal amplitude, and if greater than, say ±3dB, can cause bit errors in data communications. Gain hits may result from transients or overshoots occurring in poorly stabilised communications equipment. According to CCITT Recommendation M.1060 that covers the maintenance of leased lines[24] there ought not to be more than 10 gain hits of ±3dB within a 15 minute period.

ii. *Dropouts*:- A sudden drop of 10dB or more in the level of data signal is termed a 'dropout'. Impairments of this type, which may be caused by power failures, short circuits in the cable network, or similar short term interruptions, could lead to bit errors. According to CCITT Recommendation M.1060, within an observation period of 15 minutes, in general, no interruptions of length 3 milliseconds to 1 minute should appear.

Chapter 5

POWER IN THREE PHASE CIRCUITS.

5.1 INTRODUCTION.

As the new algorithm involves the polarisation of the feeder's terminal currents and is based on the equations used to derive the instantaneous power in a three phase circuit, the basic definitions of power[25] in an electrical power system have been briefly given in this chapter. Commonly known power terms, which are real power, P, and reactive power, Q, have been discussed, and symmetrical components are used to explain unbalanced conditions. These two power terms form the basis of the power algorithm where two sets of three phase phasors are reduced to dc terms plus oscillatory terms operating at twice the power system frequency. A low pass filter would remove the oscillatory terms to remain only with the steady, dc, output. The implication of this approach for the protection algorithm is that the algorithms thereby have a high inherent tolerance to the complications introduced by communication channel delays and their fluctuations.

5.2 OVERVIEW OF POWER.

Power is a loosely defined quantity which basically describes the ability to do work. For electricity, it is the combination of current and voltage. Although this appears to be straightforward, it is far from simple. Being the product of current and voltage, various power terms are defined depending on the components used or the type of polarisation of the current by the voltage. As many electrical devices used in power systems are designed to operate and be tested with sinusoidal voltages and currents, power is a familiar term in uncorrupted sinusoidal waveforms. It can be described as Instantaneous

Power, Real Power, Reactive Power, and Apparent Power[82, 83, 84].

The use in power systems of such devices as power transformers and power electronic equipment, however, contribute to the distortion of voltage and current waveforms due to harmonics[85]. These result in secondary power terms being derived such as Distortion Power, Fictitious Power, Non-reactive Power, Complex Power and Vector Power[25, 86, 87]. In distribution systems, there are many sources of harmonic distortion. Rotating machines cause harmonics due to varying magnetic field reluctance caused by slots in the stator and rotor. Arc welding equipment generate harmonics due to the non-linear voltage-current characteristic of the arc[86]. Electronic control and power conversion equipment produce harmonics by imposing cyclic changes of impedance in the power supply circuit switching.

Of immediate interest as a basis for the algorithm is the Real Power flowing at the terminals of the feeders, that is, the rate at which energy is provided or absorbed in a power circuit. If time were not a constraint, this could be measured accurately with an integrating algorithm, however for protection applications, minimising the decision making time of the algorithm is an important criterion of the system's success. If the power system was balanced, an instantaneous measurement is possible since under these conditions the *Real Power* is the same as the *Instantaneous Power.*

The widely known formula of *Instantaneous Power p* is expressed as the product of voltage *v* and current *i*. Voltage is work per unit charge and current is charge transfer per unit time. Therefore, the instantaneous power may be defined as the rate of change of energy. It may be given as;

$$v\,i = \frac{dw}{dq}.\frac{dq}{dt} = \frac{dw}{dt} = p \qquad (5.1)$$

The voltage or current may be represented as a sinusoidal waveform;

$$x(t) = X\,Cos(\omega t + \Phi) \qquad (5.2)$$

where

X is the amplitude of the measured quantity, v or i,

ω is the angular velocity or radian frequency in radians per second,

Φ is the phase angle measured in radians.

The solution of a problem involving a balanced three phase system may be found by considering only one phase in which the voltage, or current is taken as the reference vector and solving for that phase alone as in the case of a single phase. The magnitude of the currents and voltages in the other two phases will then be the same as in the reference phase but there will be a corresponding phase displacement of ±120 degrees as appropriate. This is possible because in a balanced three phase system, the phase voltages and currents are balanced as they are sinusoidal and, can be represented by vectors of equal magnitude and displaced from each other by equal phase angles of 120 degrees. Balanced or symmetrical conditions also exist when each of the three phases contain equal impedances. Furthermore, if a balanced system of three phase voltages is applied across the terminals of a balanced three phase network, then the currents flowing in each of the three phases will also be balanced.

The voltages and currents in a balanced three phase power system exist as shown in figure 5.1. With the phasors drawn to form a triangle, as shown in figure 5.2, it is clear that the summation of the phase voltages is zero, and the summation of the currents is also zero. The voltages and currents can be written as:-

$$
\begin{aligned}
v_a &= V\,Cos(\,\omega t\,) & i_a &= I\,Cos(\,\omega t + \phi\,) \\
v_b &= V\,Cos(\,\omega t + \frac{4\pi}{3}\,) & i_b &= I\,Cos(\,\omega t + \frac{4\pi}{3} + \phi\,) \\
v_c &= V\,Cos(\,\omega t + \frac{2\pi}{3}\,) & i_c &= I\,Cos(\,\omega t + \frac{2\pi}{3} + \phi\,)
\end{aligned}
\qquad (5.3)
$$

The philosophy of power is best discussed using single phase systems.

5.3 SINGLE PHASE TREATMENT OF POWER.

INSTANTANEOUS POWER, *p*

The fundamental formula of power given in equation (5.1) shows that the product of instantaneous voltage *v* and instantaneous current *i* gives the instantaneous power *p*, i.e:

$$p = v\,i \qquad (5.4)$$

REAL POWER, P

Under balanced conditions, the Instantaneous Power is the same as Real Power[88]. Generally, Real Power P at any time t_0 is:-

$$P = \frac{1}{T}\int_{t_0 - T}^{t_0 + T} v\,i\,dt \qquad (5.5)$$

where T is the measurement interval which can be taken as one period or more of the AC voltage or current waveform. Assuming that the input waveforms are sampled at sampling frequency of f_s, the discrete equation for P, which is also known as average or effective power[87], is then[89, 37]:-

$$P = \frac{1}{N} \sum_{j-1}^{N} (v_j \, i_j) \qquad (5.6)$$

where N is the number of samples per period, for example 24, and v_j and i_j respectively represent the j^{th} samples of the voltage and current waveforms. The physical nature of Real Power P can be defined as the power delivered by a generator or absorbed by a load. If both the voltage and current are sinusoidal, and taking V and I as the rms values, P can be written as

$$P = V I \, Cos\phi \qquad (5.7)$$

where ϕ is the angular phase difference by which the voltage leads the current. With nonsinusoidal waveforms, real power is

$$P = \sum_{n} V_n \, I_n \, Cos\phi_n \qquad (5.8)$$

where V_n, I_n and ϕ_n are as in equation (5.7), but for the n^{th} harmonic. Change in the angle ϕ in these equations causes instantaneous power, and consequently real power, to change in form and amplitude. This can be shown by considering that any electrical system is characterised by R, L and C which are the energy storage and dissipation elements. Resistance is responsible for the energy dissipation. The energy storage is effected by the properties of the capacitors and inductors which store energy in the electric and magnetic field respectively.

P can be illustrated across the circuit elements. Assuming an alternating voltage is applied to a resistive load, figure 5.3 shows the resulting waveforms. The current follows exactly the voltage waveform. At each time instant Ohm's Law (I = V/R) is obeyed. The power dissipated in the resistance is the instantaneous product of voltage and current, and is a direct current component with a component alternating at double the power system frequency. However, the power dissipated is positive.

If the alternating voltage is applied to a pure inductor, figure 5.4 shows the resulting waveforms. At the instant of switching on, because of electrical inertia inherent in magnetic circuits, inductance causes the current to lag behind the voltage waveform. After a few cycles the current settles to a steady alternating value, but its waveform lags by 90° behind that of the voltage. The power flow oscillates positively and negatively at double the system frequency. Unlike in the purely resistive case, the magnetising current carries no power as the mean value of the product of voltage and current is zero.

The case of capacitance can be explained considering an alternating voltage being applied to an open-circuited line or cable. In this case the line can absorb electric charge owing to capacitance. The surge of current into the line occurs at the instant of switching on which decays to the steady alternating value required to keep the line electrically charged at the applied voltage. In this case the current leads the voltage waveform by 90°. As in the case of inductance, there is no transfer of real power, but power oscillates forwards and reverse at double the system frequency.

Thus in a power circuit, elements operate ideally as:-

(a) resistance R where $\Phi = 0°$

(b) inductance L where $\Phi = -90°$

(c) capacitance C where $\Phi = 90°$.

If the case with R determines the dissipation function

$$W_D = R\, i^2 / 2, \tag{5.9}$$

and is associated with real power, then the case with pure inductor L and pure capacitance C would determine the reactive kinetic and potential energies

$$\begin{aligned} W_T &= L\, i^2 / 2 \quad (\textit{kinetic energy}) \\ W_P &= C\, v^2 / 2 \quad (\textit{potential energy}), \end{aligned} \tag{5.10}$$

according to general principles using Maxwell's equations[83].

REACTIVE POWER, Q

Whereas the real power is the product of current and its in-phase voltage component, Reactive Power Q^{90} is the product of voltage and the associated lagging or leading current waveform. With sinusoidal waveforms, reactive power is:-

$$Q = V I \sin\phi. \tag{5.11}$$

With nonsinusoidal waveforms, reactive power is equal to the sum of the values of the reactive power for every harmonic component. The physical nature of Q can be defined as the component of power responsible for the transfer of energy to and from the source[83, 87]. Q is associated with the kinetic energy W_T and/or potential energy W_P as in equation (5.10).

APPARENT POWER, U

Apparent power is basically the product of the rms values of voltage and current:-

$$U = V I \tag{5.12}$$

In using the rms values of voltage and current, apparent power takes the meaning of maximum effective power which may be transferred. Thus U in sinusoidal conditions is also calculated as a sum of powers P and Q:

$$U = \sqrt{P^2 + Q^2} \tag{5.13}$$

and is equivalent to phasor power[25]. It is used to define the maximum ratings of electrical apparatus such as transformers, generators and motors. It is also used as a reference value for power factor calculations. For network analysis, apparent power is used as a reference value for network analysis on a per unit basis.

PHASOR POWER, S

The geometrical sum of real and reactive powers is the phasor power;

$$S = P + jQ \tag{5.14}$$

The magnitude of S equals to the apparent power. For nonsinusoidal conditions, phasor power is equal to the phasor sum of the values of the phasor power of every harmonic.

POWER FACTOR, PF

The division of real power P by the apparent power U defines the power factor:

$$PF = \frac{P}{U} \tag{5.15}$$

It is identical to the cosine of the angle Φ by which the voltage leads the current.

5.4 POLYPHASE TREATMENT OF POWER.

Practical systems are three phase systems. In these systems, instantaneous, real, and reactive powers represent the corresponding algebraic sums of the instantaneous, real and reactive powers. In this case, the voltages are all determined with respect to the same common reference point which is the neutral point.

In a three phase system, instantaneous power is given as per equation (5.4):-

$$p = v_a i_a + v_b i_b + v_c i_c \tag{5.16}$$

where a, b, and c are the three phases. The real power, P is then given as:

$$P = \frac{1}{T} \int_{t - T/2}^{t_o + T/2} (v_a i_a + v_b i_b + v_c i_c) \, dt \tag{5.17}$$

In discrete form, real power is given as:

$$P = \frac{1}{N} \sum_{j-1}^{N} (v_{aj}\, i_{aj} + v_{bj}\, i_{bj} + v_{cj}\, i_{cj}) \qquad (5.18)$$

For a balanced three phase system the equations (5.16), (5.17), and (5.18) are equal to[37]:

$$P = 3\ V\ I\ Cos\phi \qquad (5.19)$$

Similarly, reactive power in a balanced three phase system is a constant and is equal to[37]:

$$Q = 3\ \sqrt{3}\ V\ I\ Sin\phi \qquad (5.20)$$

5.5 UNBALANCE IN A POWER SYSTEM.

If the applied voltage is unbalanced, or the impedances in each phase are no longer identical due to asymmetrical faults or loads[91], the three phase currents also become unbalanced and the solution of considering a single phase as in the above method becomes complicated. It is to be noted that asymmetrical faults involve one or two phases and asymmetrical loads may be due to inadequate line transpositions and also due to the fact that industrial loads may not be perfectly balanced.

The method of symmetrical components[38, 92, 93, 94, 95, 96, 122] can be used to explain unbalance in a system. Quoting from C L Fortesque as in reference 97, the method shows that "a system of n vectors or quantities may be resolved when n is prime into n different symmetrical groups or system, one of which consists of n equal vectors and the remaining (n-1) systems consist of n equal-spaced vectors which with the first mentioned groups of equal vectors forms an equal number of symmetrical n-phase systems. When n is not prime some of the n-phase systems degenerate into repetitions of systems having numbers of phases corresponding to the factors of n." Thus this method resolves an unbalanced system of polyphase vectors into a number of balanced

sy systems which forms the basis of the method of symmetrical components.

In In terms of a three phase system this means that an unbalanced set of voltages or cu currents can be resolved into two symmetrical three phase systems having opposite phase se sequence (that is, positive and negative phase sequence designated with subscripts 1 and 2, 2, respectively) plus a third set of equal vectors having zero phase displacement (that is, ze zero phase sequence designated with subscript 0) as shown in figure 5.5. Consideration of of one phase only of each of the three balanced systems solves the unbalanced three ph phase problem by adding together the corresponding symmetrical components of each ph phase.

Th The first step is to consider the equation (5.16) for instantaneous power:

$$p = v_a \,.\, i_a + v_b \,.\, i_b + v_c \,.\, i_c$$

Th Thus, using symmetrical components for voltage and current, this expression becomes:-

$$\begin{aligned} P = \quad & (\, v_{a0} + v_{a1} + v_{a2} \,).(\, i_{a0} + i_{a1} + i_{a2} \,) \\ & + (\, v_{b0} + v_{b1} + v_{b2} \,).(\, i_{b0} + i_{b1} + i_{b2} \,) \\ & + (\, v_{c0} + v_{c1} + v_{c2} \,).(\, i_{c0} + i_{c1} + i_{c2} \,) \end{aligned} \qquad (5.21)$$

Sir Since

$$v_{a0} = v_{b0} = v_{c0} \text{ , and } \; i_{a0} = i_{b0} = i_{c0} \text{ ,}$$

eq equation (5.21) becomes

$$
\begin{aligned}
P \;=\; & 3\,v_{a0}i_{a0} + v_{a0}(\,i_{a1} + i_{b1} + i_{c1}\,) + v_{a0}(\,i_{a2} + i_{b2} + i_{c2}\,) \\
& + i_{a0}(\,v_{a1} + v_{b1} + v_{c1}\,) + i_{a0}(\,v_{a2} + v_{b2} + v_{c2}\,) \\
& + v_{a1}i_{a1} + v_{b1}i_{b1} + v_{c1}i_{c1} + v_{a2}i_{a2} + v_{b2}i_{b2} + v_{c2}i_{c2} \\
& + v_{a1}i_{a2} + v_{b1}i_{b2} + v_{c1}i_{c2} + v_{a2}i_{a1} + v_{b2}i_{b1} + v_{c2}i_{c1}
\end{aligned}
\qquad (5.22)
$$

Symmetrical components represent balanced systems. Thus

$$
i_{a1} + i_{b1} + i_{c1} = 0 \qquad v_{a1} + v_{b1} + v_{c1} = 0
$$

$$
i_{a2} + i_{b2} + i_{c2} = 0 \qquad v_{a2} + v_{b2} + v_{c2} + 0
$$

Therefore, equation (5.22) reduces to

$$
\begin{aligned}
P \;=\; & 3v_{a0}\,i_{a0} \\
& + (\,v_{a1}i_{a1} + v_{b1}i_{b1} + v_{c1}i_{c1}\,) + (v_{a2}i_{a2} + v_{b2}i_{b2} + v_{c2}i_{c2}\,) \\
& + (\,v_{a1}i_{a2} + v_{b1}i_{b2} + v_{c1}i_{c2}\,) + (\,v_{a2}i_{a1} + v_{b2}i_{b1} + v_{c2}i_{c1}\,)
\end{aligned}
\qquad (5.23)
$$

Let V and I be peak values of voltage and current simultaneously, and let

$$
v_{a0}=v_{b0}=v_{c0}=V_{a0}Sin(\omega t + \Theta_0) \qquad i_{a0}=i_{b0}=i_{c0}=I_{ao}Sin(\omega t + \Theta_0 + \phi_0) \qquad (5.24)
$$

$$
\begin{aligned}
v_{a1} &= V_{a1}\,Sin(\omega t+\Theta_1\,) & i_{a1} &= I_{a1}\,Sin(\omega t+\Theta_1+\phi_1) \\
v_{b1} &= V_{a1}\,Sin(\omega t+\Theta_1+4\pi/3) & i_{b1} &= I_{a1}\,Sin(\omega t+\Theta_1+\phi_1+4\pi/3) \\
v_{c1} &= V_{a1}\,Sin(\omega t+\Theta_1+2\pi/3) & i_{c1} &= I_{a1}\,Sin(\omega t+\Theta_1+\phi_1+2\pi/3)
\end{aligned}
\qquad (5.25)
$$

$$
\begin{aligned}
v_{a2} &= V_{a2}\,Sin(\omega t+\Theta_2) & i_{a2} &= I_{a2}\,Sin(\omega t+\Theta_2+\phi_2) \\
v_{b2} &= V_{a2}\,Sin(\omega t+\Theta_2+2\pi/3) & i_{b2} &= I_{a2}\,Sin(\omega t+\Theta_2+\phi_2+2\pi/3) \\
v_{c2} &= V_{a2}\,Sin(\omega t+\Theta_2+4\pi/3) & i_{c2} &= I_{a2}\,\sin(\omega t+\Theta_2+\phi_2+4\pi/3)
\end{aligned}
\qquad (5.26)
$$

Using SinA.SinB = ½ [Cos(A-B) - Cos(A+B)], equation (5.23) becomes

$$P = 3\frac{V_{a0}I_{a0}}{2}[Cos\phi_0 - Cos(2\omega t + 2\Theta_0 + \phi_0)]$$

$$+ \frac{V_{a1}I_{a1}}{2}[Cos\phi_1 - Cos(2\omega t+2\Theta_1+\phi_1)] + \frac{V_{a1}I_{a1}}{2}[Cos\phi_1 - Cos(2\omega t+2\Theta_1+\phi_1+2$$

$$+ \frac{V_{a1}I_{a1}}{2}[Cos\phi_1 - Cos(2\omega t + 2\Theta_1 + \phi_1 + 4\pi/3)]$$

$$+ \frac{V_{a2}I_{a2}}{2}[Cos\phi_2 - Cos(2\omega t+2\Theta_2+\phi_2)] + \frac{V_{a2}I_{a2}}{2}[Cos\phi_2 - Cos(2\omega t+2\Theta_2+\phi_2+4$$

$$+ \frac{V_{a2}I_{a2}}{2}[Cos\phi_2 - Cos(2\omega t + 2\Theta_2 + \phi_2 + 2\pi/3)]$$

$$+ \frac{V_{a1}I_{a2}}{2}[Cos(\phi_2 + \Theta_2 - \Theta_1) - Cos(2\omega t + \Theta_1 + \Theta_2 + \phi_2)]$$

$$+ \frac{V_{a1}I_{a2}}{2}[Cos(\phi_2 + \Theta_2 - \Theta_1 - 2\pi/3) - Cos(2\omega t + \Theta_1 + \Theta_2 + \phi_2)]$$

$$+ \frac{V_{a1}I_{a2}}{2}[Cos(\phi_2 + \Theta_2 - \Theta_1 + 2\pi/3) - Cos(2\omega t + \Theta_1 + \Theta_2 + \phi_2)]$$

$$+ \frac{V_{a2}I_{a1}}{2}[Cos(\phi_1 + \Theta_1 - \Theta_2) - Cos(2\omega t + \Theta_1 + \Theta_2 + \phi_1)]$$

$$+ \frac{V_{a2}I_{a1}}{2}[Cos(\phi_1 + \Theta_1 - \Theta_2 + 2\pi/3) - Cos(2\omega t + \Theta_1 + \Theta_2 + \phi_1)]$$

$$+ \frac{V_{a2}I_{a1}}{2}[Cos(\phi_1 + \Theta_1 - \Theta_2 - 2\pi/3) - Cos(2\omega t + \Theta_1 + \Theta_2 + \phi_1)]$$

Using rms values and simplifying, equation (5.23) becomes[88]

$$
\begin{aligned}
P \;=\; & 3\,[\, V_{a0}\, I_{a0}\, Cos\phi_0 + V_{a1}\, I_{a1}\, Cos\phi_1 + V_{a2}\, I_{a2}\, Cos\phi_2 \,] \\
& - 3\, V_{a0}\, I_{a0}\, Cos(\, 2\omega t + 2\theta_0 + \phi_0 \,) \\
& - 3\, V_{a1}\, I_{a2}\, Cos(\, 2\omega t + \theta_1 + \theta_2 + \phi_2 \,) \\
& - 3\, V_{a2}\, I_{a1}\, Cos(\, 2\omega t + \theta_1 + \theta_2 + \phi_1 \,)
\end{aligned}
\qquad (5.27)
$$

In the above equations, ϕ are the phase angles between the voltage and current phasors and θ are the phase displacements of the positive, negative and zero sequence components.

Equation (5.27) shows that the real power P is composed of zero sequence component P_o, positive sequence component P_1, and negative sequence component P_2 which are all non-oscillatory. It also comprises double frequency terms that have positive sequence voltage coupling with negative sequence current and vice versa. It is noted that the zero sequence components do not couple with any other sequence component but produce both a constant term and an oscillatory term. The double frequency terms are responsible for the oscillatory nature of the waveforms and they average to zero over each half cycle of the power system waveform leaving the power as an average constant.

Filtering could remove the sinusoidal terms and leave the power measurement as a non-oscillating steady DC signal decoupled from the power system frequency and its waveform. The implications for the feeder current differential protection algorithm are phenomenal. The use of non-oscillating steady dc signals in feeder differential protection implies that there will be no requirement for precise data alignment between the feeder's terminals. This reduces the demands on the communications, and thereby enabling the use of limited data rates.

5.6 SUMMARY.

In order to highlight the basis of the new algorithm, this chapter has given a brief analysis of instantaneous power in a three phase circuit. Real power and reactive power have been briefly defined. The method of symmetrical components has been used to explain the oscillatory nature of waveforms during system unbalance. It has been shown that power contains a steady DC component plus second harmonic terms. Averaging over half a power system cycle would remove the second harmonic terms leaving only steady DC terms.

This formed the basis of the protection algorithm. Two sets of three phase phasors were reduced to measurements containing dc terms plus oscillatory terms operating at twice the power system frequency. Averaging the measurements over half a power system cycle removed these terms leaving the steady, dc terms. The use of dc terms reduced the demands on the communications and thereby enabled the use of low data rates.

5.7 FIGURES.

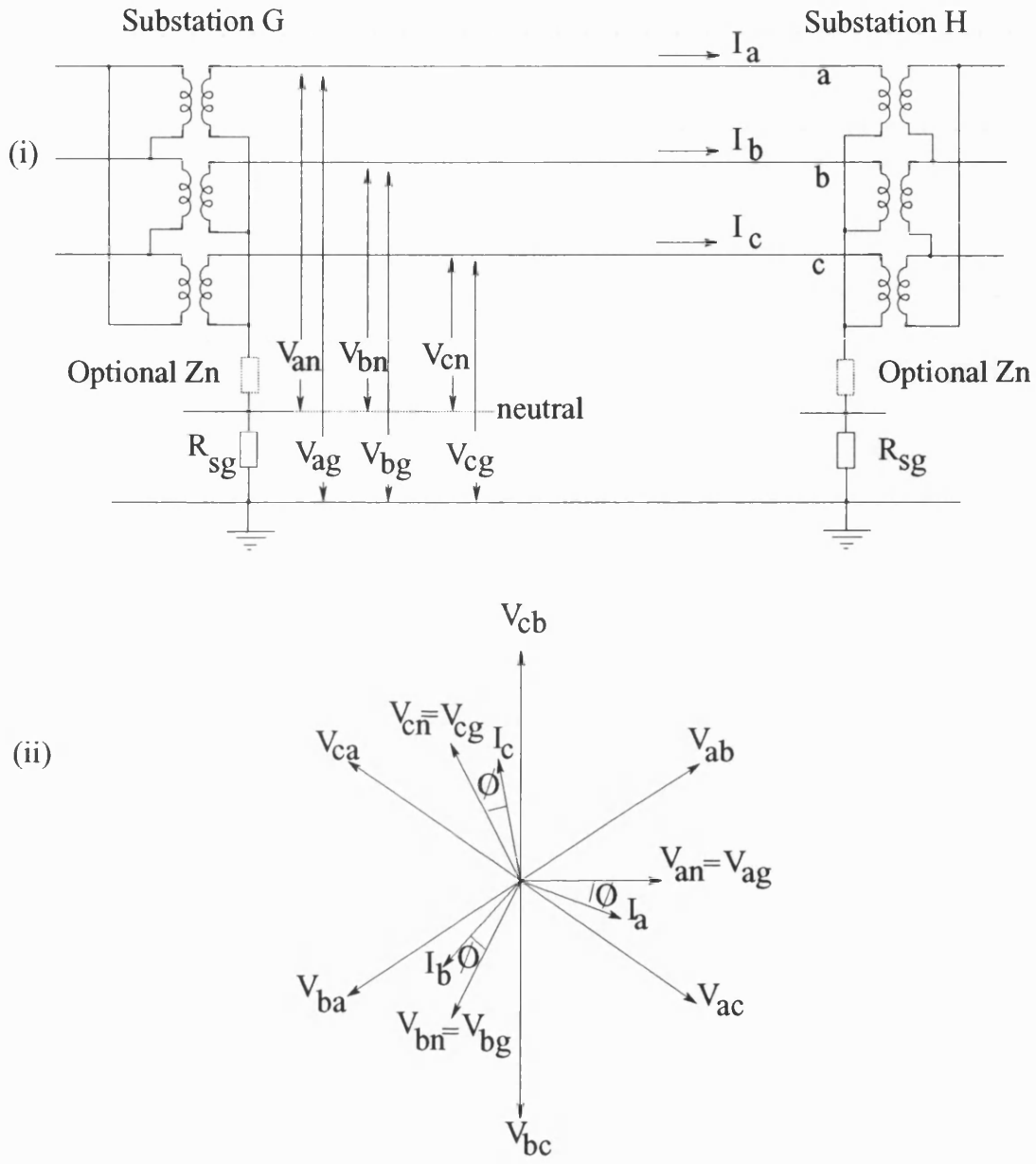

(i) Feeder Circuit Diagram.

(ii) Corresponding Phasor Diagram at one Treminal.

Figure 5.1 Voltages and Currents under Balanced Conditions.

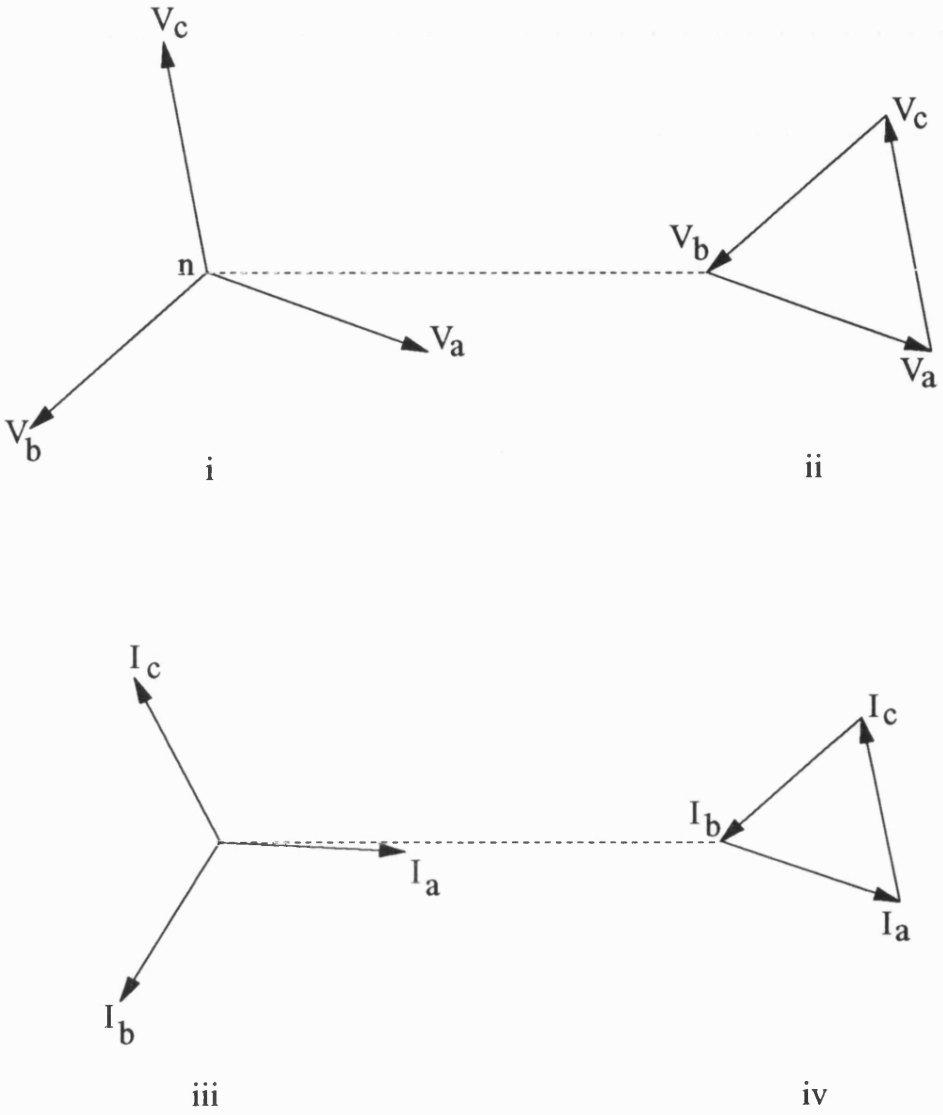

i. Voltage Phasors.
ii. Sum of Voltage Phasors is Zero.
iii. Current Phasors
iv. Sum of Current Phasors is Zero.

Figure 5.2 Summation of Phase Voltages, as well as Currents, is Zero under Balanced Conditions.

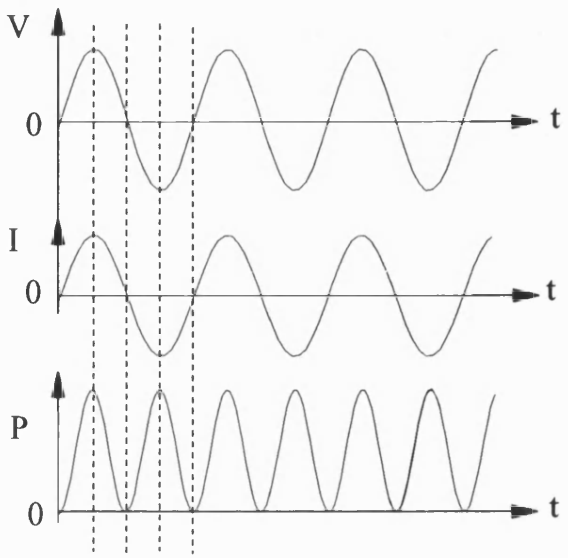

Figure 5.3 Waveforms With Alternating Voltage Applied To a Resistive Load.

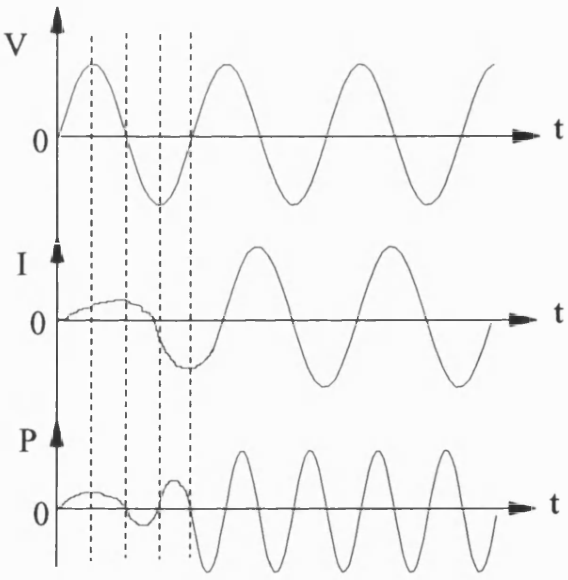

Figure 5.4 Waveforms With Alternating Voltage Applied To a Pure Inductor.

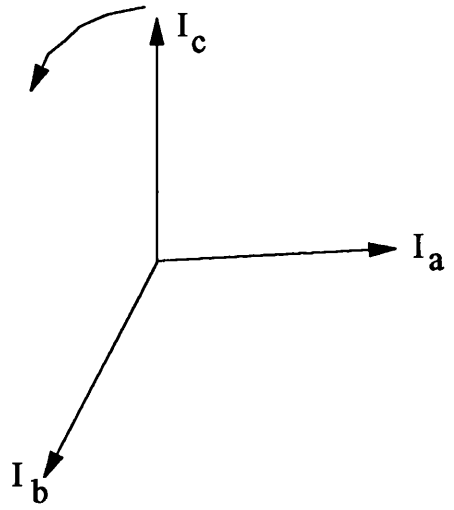

Unbalanced System Currents.

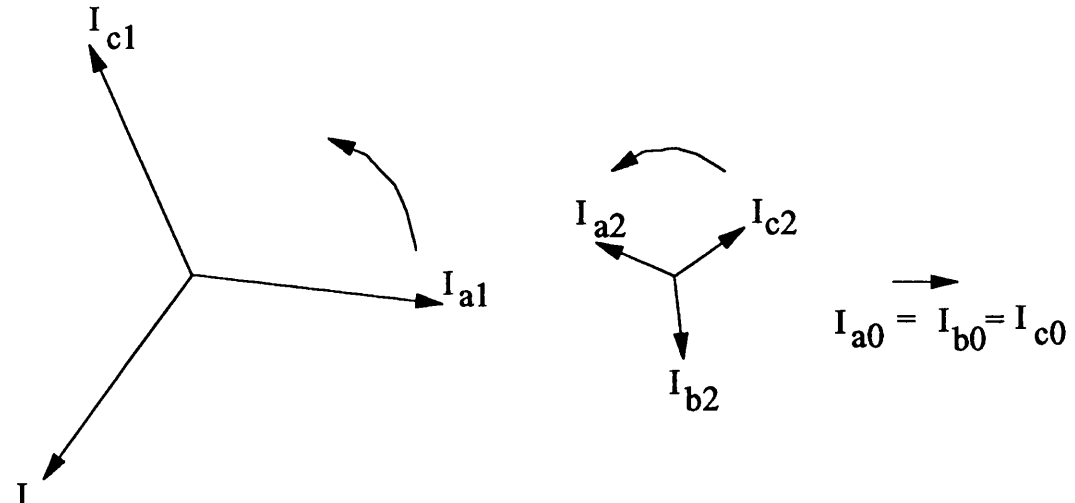

Positive Phase Sequence Currents.

Negative Phase Sequence Currents.

Zero Phase Sequence.

Figure 5.5 Unbalanced System and Corresponding Symmetrical Components.

Chapter 6

THE POWER SYSTEM TEST MODEL.

6.1 INTRODUCTION.

Overhead lines are used extensively where power is transmitted over open country or distributed in small towns, villages, or sparsely populated rural areas. Because of the concern for safety and amenities in densely populated areas, underground cables provide alternatives for distribution networks. In rural areas, underground cables may be used to preserve values of the locality. However, since underground cables are more expensive than overhead lines for the same voltage and load capacity as shown in table 6.1[98], overhead construction is adopted wherever possible. A construction may also consist of both overhead line sections and underground cable sections such as in feeders supplying airports.

The feeder circuits may be arranged in radial, parallel, ring or interconnected modes as shown in figure 6.1, the circuits being represented by the conventional single line diagram. The choice of the arrangement largely depends on the load that may have to be supplied, this varying from as high as 100 MW per square mile in city areas to as low as 25 kW per square mile in a sparsely populated rural area[99]. The general observation on the arrangements are:-

- A closely interconnected network interconnects all circuits in a heavily loaded area.
- The interconnected network is a development of the ring circuit.
- The ring circuit gives alternative supplies to a number of scattered substations.
- Parallel circuits, as compared to radial circuits, give improved reliability of

supply.

- The radial circuit is cheap but gives no alternative supply.

The parallel feeder circuit was modelled using the EMTP power simulation package[100]. One of the characteristics of distribution feeders being short lengths, 20 km long feeders were modelled. These distances also suit the use of pilot wires for communications as discussed above.

As discussed in chapter 5, an electrical system is characterised by R, L and C, and in conductors, these elements affect the ability to fulfil their function as part of a power system. The EMTP package was used to derive these parameters for both the underground construction and overhead line construction. Also modelled was a composite circuit of overhead line sections and underground cable sections. This chapter presents the feeder circuit model using the three types of constructions. The conductors are discussed first followed by the feeder circuit.

6.2 UNDERGROUND CABLE MODEL.

Paper-insulated[101] metal-sheathed power cables were introduced in the 1890's with the 1920's seeing the advent of 33 kV cables[102]. Together with polymeric-insulated power cables[101], they have a proven service history in underground transmission and distribution of power. They can be divided into two categories, solid-type and pressurised type[103]. Solid-type cables are normally for operation at voltages up to and including 33kV[104]. There is no control over the internal pressure in this type of cables. Pressurised cables have their insulation maintained at a pressure above atmospheric pressure by means of pressure reservoirs suitably located along the route. They are normally used at and above 33 kV.

Cables can be supplied in single core or three core form. Single core cables have the simplicity of construction, consisting of a stranded conductor insulated with layers of impregnated paper insulation, and an overall metal sheath. Three core cables have the three insulated conductors forming the cores and placed inside a metal pipe[105].

A three core solid-type cable was modelled using the EMTP Cable Constants routine[100]. Its cross section was that of a 3 x 1.5625 square centimetre 33kV oil filled, manufactured by Pirelli General Cable Works Ltd., Southampton. Figure 6.2 illustrates the cross section, showing three conductors enclosed in a metal pipe which acts as neutral conductor for a three phase cable system[106].

As per EMTP format, the input data case was as in appendix 6.1. The Cable Constants output matrices of R and ωL for the series impedance, and G and ωC for the shunt admittance, are shown in appendix 6.2. PI equivalents were requested. These PI equivalents provide for the lumped-element resistance, inductance and capacitance matrices (for a kilometre, in this case) as in figure 6.3, and by connecting many such short sections in series, keeping track of any actual transpositions in case of an overhead line construction, a model for a length of a line can be made.

All matrices are assumed to be symmetrical. They have common diagonal self-coupling values and common off-diagonal mutual-coupling values. The zero conductance values in the output can be explained. The conductance, which is between the conductors and between the conductors and the ground, accounts for the leakage current through the insulation of cables and at the insulators in the case of overhead lines. However, the conductance is to be practically zero since the leakage is negligible.

6.3. OVERHEAD LINE MODEL.

The main attraction for the use of bare overhead line conductors is the electrical insulating property of air which removes the necessity of insulation and protective coverings that contribute to the high cost of underground cables. In distribution networks, the wood pole support is largely used, especially when wood is plentiful. The supports may assume the A-frame or H-frame construction, or simply a single pole as in this work.

The phase conductors are not symmetrically disposed to each other, and this results in electrostatic and electromagnetic unbalance[3] which can be largely eliminated by transposition. However, modern practice is to build overhead lines without transposition towers to reduce costs[3]. With AC systems, the geometry of conductors introduces electromagnetic and electrostatic coupling between the conductors, and between conductors and ground. This results in self and mutual components for the parameters, resistance, inductance, capacitance and conductance. The EMTP Line Constants routine was used to calculate these parameters for single and double circuit 33 kV overhead line constructions. Aluminium Conductor Steel Reinforced (ACSR)[3, 107] conductors supported on wooden poles were modelled as illustrated in figure 6.4. It should be noted that the line configuration and conductor spacings are influenced, not only by voltage, but also by many other factors, including the type of insulators, support, span length, conductor sag and the nature of terrain and external climatic loadings. There can, thus, be large variations in spacings between different line designs for the same voltage level. Figure 6.4 depicts spacings from an arbitrary centre reference line in typical constructions.

Various conductors are named after birds, insects, flowers and animals such as the Parakeet, Osprey, Wasp, Daffodil, Tiger, just to mention a few[107]. A type Raven ACSR conductor was assumed. The input data case is as in appendix 6.3 with the output data

as in appendix 6.4. As in the Cable Constants routine, the standard EMTP Line Constants output includes a sorted line-conductor table before the requested matrices, and ends with standard EMTP output terminating information. All this was edited out in the appendix 6.4. Since all matrices are symmetrical, the output gives values only in and below the diagonal.

6.4 POWER SYSTEM CIRCUIT MODEL.

The power system model was of a typical 33 kV feeder network containing parallel feeders, 20 km long, as shown in figure 6.5. The model was used for the system with overhead lines construction, then with underground cable construction, and also for system with composite feeders consisting of overhead line sections and underground cable sections. Conveniently, the sections of the composite feeders were each 10 km long in the protected line, the parallel line, and the incoming lines. It is noted that real life construction may not necessarily have equal lengths of such sections in composite feeder circuits.

Protective relays are located at the feeder terminals at substations G and H, with substation G acting as the local station and substation H acting as the remote station. The point P1 on the model serve to introduce in-zone faults. Point P2 serve to introduce faults on parallel feeders. Points F1 and F2 are for the introduction of external faults. The voltage sources are such that the phase angle difference between the two ends determines the current flow.

The model data cases to run in the EMTP are as in appendices 6.5, 6.6, 6.7 for the case with overhead lines, underground cables and the composite feeders, respectively.

6.5 SUMMARY.

Using EMTP power simulation package, a typical 33 kV feeder network has been modelled containing parallel feeders, 20 kilometres in length. Since distribution feeder circuits may consist of either overhead lines, underground cables, or composite construction of both overhead lines and underground cables, the model uses firstly overhead line construction only, then underground cable construction only, and lastly composite network of both overhead line sections and underground cable sections.

Cable Constants routine and Line Constants routine of the EMTP were used to calculate respectively the cable parameters and line parameters R for resistance, L for inductance and C for capacitance for the circuit modelling. In the model feeder network, arbitrary points were included for the simulation of in-zone faults and external faults, with external faults to be applied on the parallel feeder as well as on the supply feeders.

6.6 FIGURES.

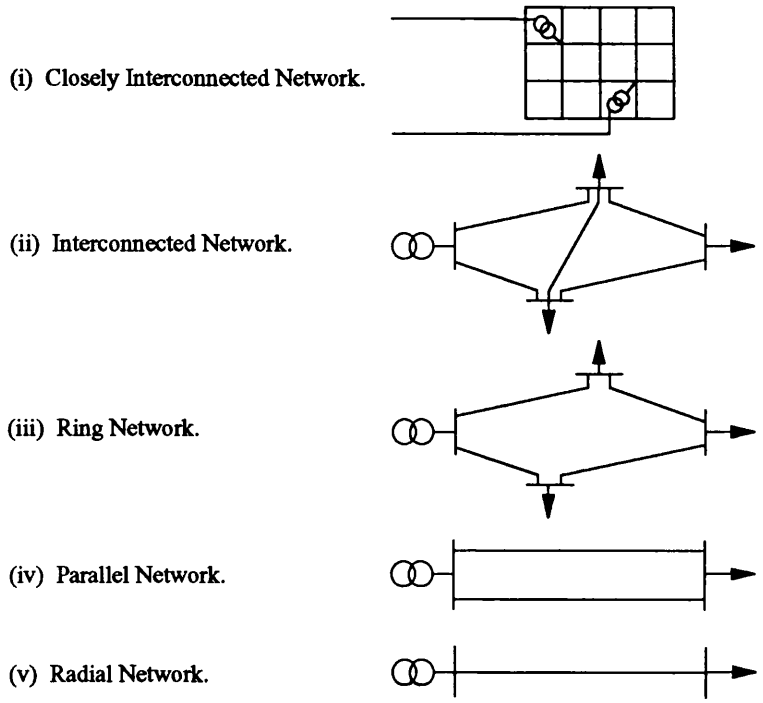

Figure 6.1 Distribution Feeder Circuit Arrangements.

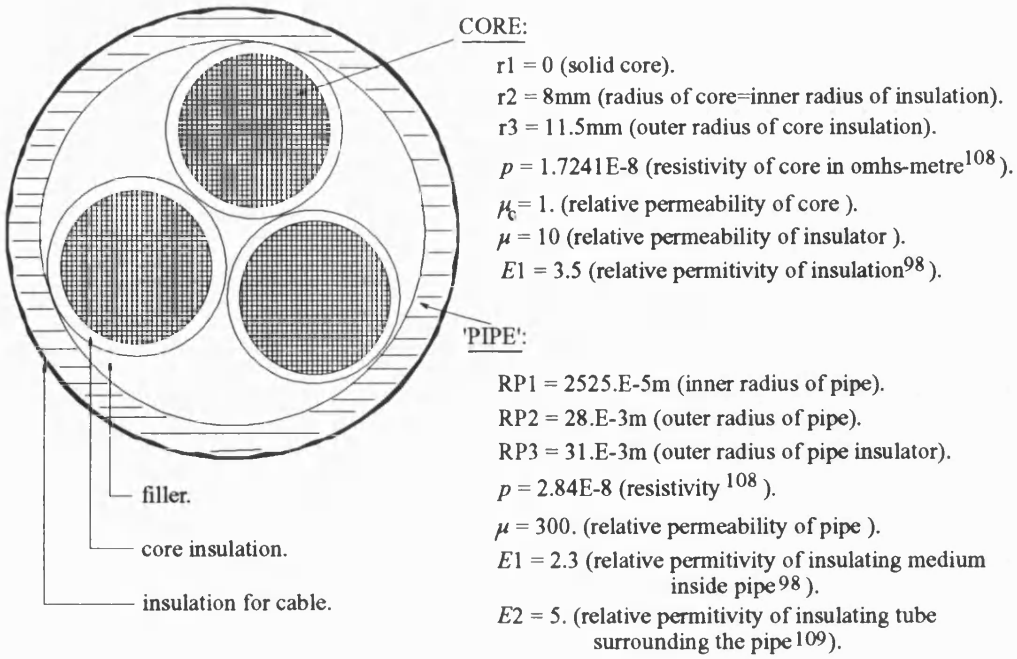

Figure 6.2 Cross Section of Underground Cable.

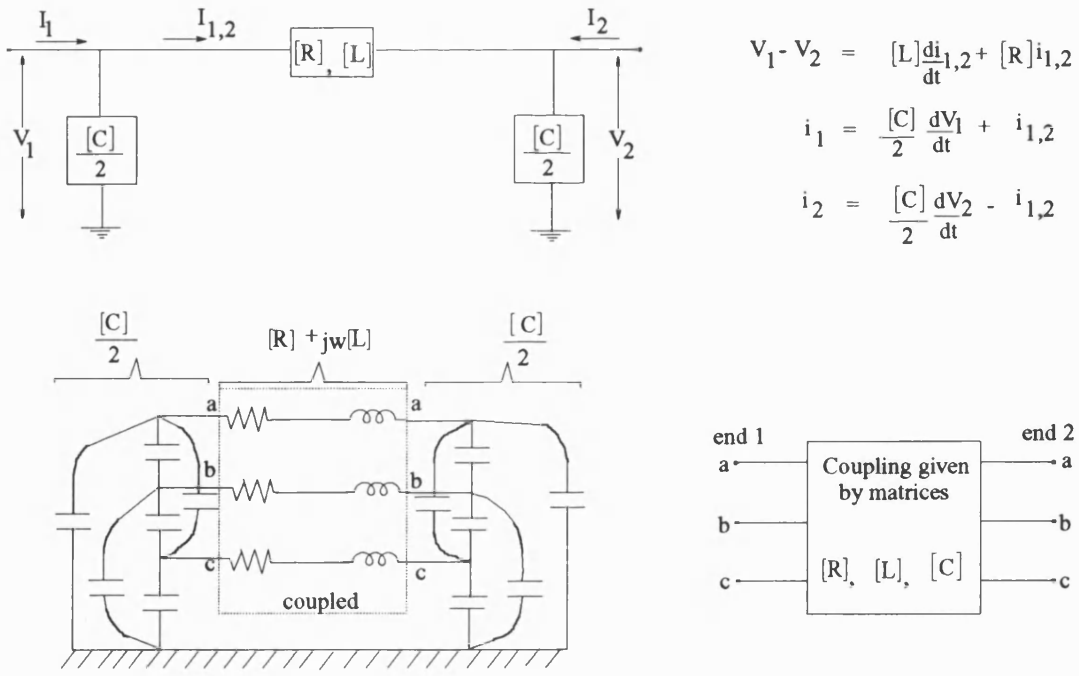

Figure 6.3 PI representation of lumped element Resistance, Inductance, and Capacitance.

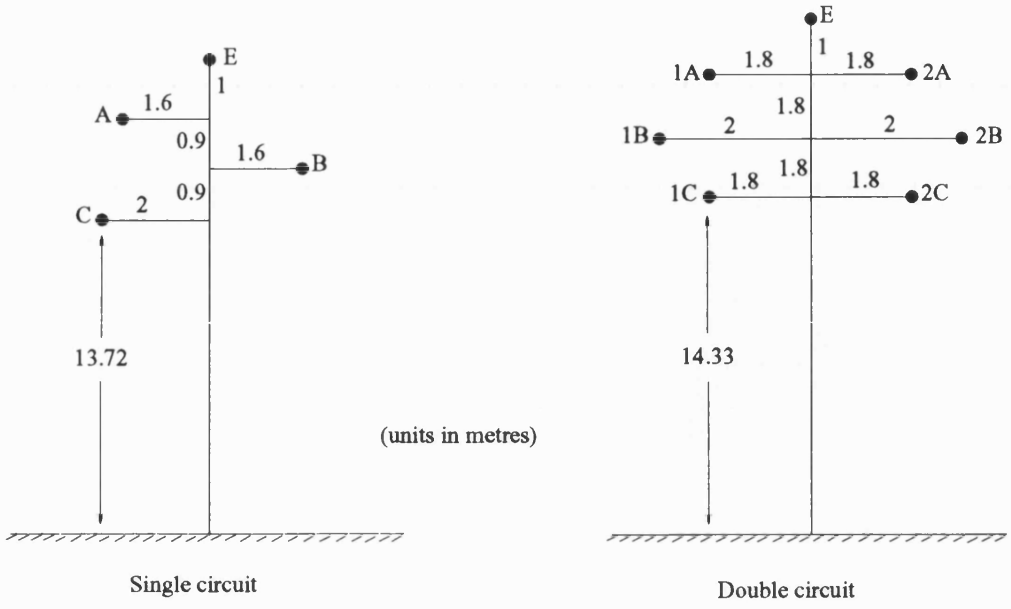

Figure 6.4 Overhead Line Configuration.

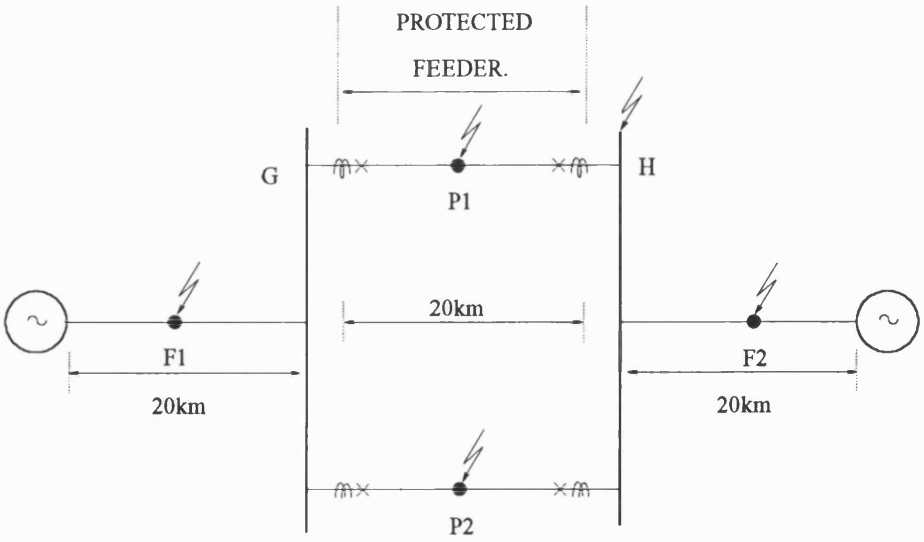

Figure 6.5 Power System Test Model.

6.7 TABLES.

Table 6.1 Cost Comparison of Underground Cables and Overhead Lines.

Voltage (kV)	Ratio = $\frac{\text{cost of underground cable}}{\text{cost of overhead line}}$
0.415	2 or less
11	3
33	5
66	7
132	8
275	13 (7 for heavy duty)
400	18 (23 for heavy duty)

6.8 APPENDICES.

Appendix 6.1 EMTP Input Data Case for 33kV Underground Cable of figure 6.2.

```
BEGIN NEW DATA CASE
C     Data case for a model of an underground 3-phase SC cable system.
C     Cables enclosed in a conducting pipe which is earthed.
C     'CABLE CONSTANTS' routine is used to calculate the parameters.
C     Homogeneous (Carson's) earth is assumed.
C     Call this data case CABLES01.DOC.
C
3456789012345678901234567890123456789012345678901234567890123456789012345
67890
CABLE CONSTANTS                                                    1
C Miscellaneous data card.
   3  -1    3         1    1    1    1    1
C Parameters of the pipe.
 2525.E-5    28.E-3    31.E-3   2.84E-8      300.       2.3        5.
C Location of each SC coaxial cable within the pipe.
   14.E-3         0.    14.E-3       120.    14.E-3       240.
   1    1    1
C Geometrical and physical data of SC coaxial cable.
             8.0E-3   11.5E-3
 1.7241E-8         1.        10.       3.5
             8.0E-3   11.5E-3
 1.7241E-8         1.        10.       3.5
             8.0E-3   11.5E-3
 1.7241E-8         1.        10.       3.5
      1.0
C Frequency card.
          100.             50.
C Radius of solid core = 8mm (3 cores in all)
C Displacement of centre of core = 14mm
C Inner and outer radii of core, respectively, = 25.25mm and 28mm
C Radius of outer most insulation = 31mm
BLANK CARD ENDING FREQUENCY CARDS
BLANK CARD ENDING CABLE CONSTANTS
BEGIN NEW DATA CASE
BLANK
```

Appendix 6.2 EMTP Output for the 33kV Underground Cable Modelling.. .

---------- Cable constants matrices for frequency 5.00000000E+01 Hertz. ----------

Impedance matrix [Z] follows :

3.4586035E-04	2.5315023E-04	2.5315023E-04
3.6429408E-04	2.5281756E-04	2.5281756E-04
2.5315023E-04	3.4586035E-04	2.5315023E-04
2.5281756E-04	3.6429408E-04	2.5281756E-04
2.5315023E-04	2.5315023E-04	3.4586035E-04
2.5281756E-04	2.5281756E-04	3.6429408E-04

Admittance matrix [Y] follows :

0.0000000E+00	0.0000000E+00	0.0000000E+00
7.2234972E-08	-1.7445006E-08	-1.7445006E-08
0.0000000E+00	0.0000000E+00	0.0000000E+00
-1.7445006E-08	7.2234972E-08	-1.7445006E-08
0.0000000E+00	0.0000000E+00	0.0000000E+00
-1.7445006E-08	-1.7445006E-08	7.2234972E-08

Voltage transformation matrices follow. These are complex, with the magnitude displayed above the angle in degrees. Transformation [AI], from phase to modal variables:

0.3333333	0.3333333	0.3333333
0.0000000	0.0000000	0.0000000
0.3333333	0.6666667	0.3333333
-180.0000000	0.0000000	180.0000000
0.5000000	0.0000000	0.5000000
0.0000000	-169.0111635	-180.0000000

Transformation [A], from modal to phase variables:

1.0000000	0.5000000	1.0000000
0.0000000	180.0000000	0.0000000
1.0000000	1.0000000	0.0000000
0.0000000	0.0000000	64.1451182
1.0000000	0.5000000	1.0000000
0.0000000	180.0000000	180.0000000

Characteristic impedance matrix [Zc] in phase variables:

80.9383559	43.1243372	43.1243372
-31.8605276	-18.1911469	-18.1911469
43.1243372	80.9383559	43.1243372
-18.1911469	-31.8605276	-18.1911469
43.1243372	43.1243372	80.9383559
-18.1911469	-18.1911469	-31.8605276

Appendix 6.3 EMTP Input Data Case for 33 kV Overhead Line of figure 6.4.

(i) Data for the Single Circuit Line.

```
BEGIN NEW DATA CASE
C     LINE CONSTANTS FOR OVERHEAD LINES USING 'LINE CONSTANTS' ROUTINE.
C     THIS IS A SHORT SINGLE CIRCUIT 33 kV OVERHEAD LINE WITH 1 EARTH WIRE.
C     CALL THIS DATA CASE ONECCT.DOC
C 3456789012345678901234567890123456789012345678901234567890123456789012345678901234567890
LINE CONSTANTS
METRIC
C Conductor card to define the line geometry and some of its fundamental electrical properties.
BRANCH   RGA1  PA1  RGB1   PB1  RGC1   PC1  RGA1   PA2  RGB2   PB2  RGC2   PC2
  1 0.5  0.5426  4        1.005  -1.6  15.52  7.9
  2 0.5  0.5426  4        1.005   1.6  14.62  7.0
  3 0.5  0.5426  4        1.005  -2.0  13.72  6.1
  0 0.5  0.2733  4        1.415   0.0  16.52  8.9
BLANK CARD ENDING CONDUCTOR CARDS OF  "LINE CONSTANTS" CASE
C Frequency cards.
  100.0      50.0       1    1  1         10.0            44
BLANK CARD ENDING FREQUENCY CARD
BLANK CARD ENDING "LINE CONSTANTS" CASES
BLANK
BEGIN NEW DATA CASE
BLANK
```

(ii) Data for the Double Circuit Line.

```
BEGIN NEW DATA CASE
C     LINE CONSTANTS FOR OVERHEAD LINES USING 'LINE CONSTANTS' ROUTINE.
C     THIS IS A SHORT DOUBLE CIRCUIT 33 kV OVERHEAD LINE WITH 1 EARTH WIRE.
C     CALL THIS DATA CASE TWOCCTS.DOC
C 3456789012345678901234567890123456789012345678901234567890123456789012345678901234567890
LINE CONSTANTS
METRIC
C Conductor card to define the line geometry and some of its fundamental electrical properties.
BRANCH   RGA1  PA1  RGB1   PB1  RGC1   PC1  RGA1   PA2  RGB2   PB2  RGC2   PC2
  1 0.5  0.5426  4        1.005  -1.8  17.93  10.31
  2 0.5  0.5426  4        1.005  -2.0  16.13   8.51
  3 0.5  0.5426  4        1.005  -1.8  14.33   6.71
  4 0.5  0.5426  4        1.005   1.8  17.93  10.31
  5 0.5  0.5426  4        1.005   2.0  16.13   8.51
  6 0.5  0.5426  4        1.005   1.8  14.33   6.71
  0 0.5  0.2733  4        1.415   0.0  18.93  11.31
BLANK CARD ENDING CONDUCTOR CARDS OF  "LINE CONSTANTS" CASE
C Frequency cards.
  100.0      50.0       1    1  1         10.0            44
BLANK CARD ENDING FREQUENCY CARD
BLANK CARD ENDING "LINE CONSTANTS" CASES
BLANK
BEGIN NEW DATA CASE
BLANK
```

Appendix 6.4 EMTP Output Data for the 33 kV Overhead Line Modelling.

(i) Output Data for the Case with Single Circuit Line.

Susceptance matrix, in units of [mhos/kmeter] for the system of equivalent phase conductors.
Rows and columns proceed in the same order as the sorted input.

```
 1  2.474361E-06

 2 -2.941907E-07  2.362417E-06

 3 -5.309914E-07 -2.791643E-07  2.417798E-06
```

Impedance matrix, in units of [ohms/kmeter] for the system of equivalent phase conductors.
Rows and columns proceed in the same order as the sorted input.

```
 1  6.203173E-01
    5.928957E-01

 2  7.530715E-02  6.159467E-01
    1.770386E-01  6.083879E-01

 3  7.262905E-02  7.068586E-02  6.111331E-01
    2.234525E-01  1.866924E-01  6.258947E-01
```

(ii) Output Data for the Case with Double Circuit Line.

Susceptance matrix, in units of [mhos/kmeter] for the system of equivalent phase conductors.
Rows and columns proceed in the same order as the sorted input.

```
 1  2.490776E-06

 2 -4.857959E-07  2.533936E-06

 3 -2.207461E-07 -4.964157E-07  2.457656E-06

 4 -2.176731E-07 -1.604863E-07 -1.239155E-07  2.490776E-06

 5 -1.604863E-07 -1.695292E-07 -1.726951E-07 -4.857959E-07  2.533936E-06

 6 -1.239155E-07 -1.726951E-07 -2.540225E-07 -2.207461E-07 -4.964157E-07  2.457656E-06
```

Impedance matrix, in units of [ohms/kmeter] for the system of equivalent phase conductors.
Rows and columns proceed in the same order as the sorted input.

```
 1  6.188509E-01
    5.980293E-01

 2  7.196391E-02  6.110842E-01
    2.269956E-01  6.260203E-01

 3  6.906366E-02  6.578906E-02  6.062495E-01
    1.940750E-01  2.498289E-01  6.442841E-01

 4  7.609820E-02  7.196260E-02  6.906245E-02  6.188509E-01
    1.692498E-01  1.740729E-01  1.722994E-01  5.980293E-01

 5  7.196260E-02  6.833112E-02  6.578768E-02  7.196391E-02  6.110842E-01
    1.740729E-01  1.906208E-01  1.969062E-01  2.269956E-01  6.260203E-01

 6  6.906245E-02  6.578768E-02  6.349666E-02  6.906366E-02  6.578906E-02  6.062495E-01
    1.722994E-01  1.969062E-01  2.155046E-01  1.940750E-01  2.498289E-01  6.442841E-01
```

Appendix 6.5 Typical EMTP Input Data Case for a Model of 33 kV Feeder Circuit of Overhead Lines as illustrated in figure 6.5.

```
BEGIN NEW DATA CASE
C     This data case is of a model of 33 kV feeder circuit of overhead lines.
C     It utilises the parameters calculated using
C     LINE CONSTANTS routines of data cases TWOCCTS.DOC AND ONECCT.DOC.
C     The system test model is illustrated in figure 6.5. This data case is for a mid-zone one phase fault.
C     Call this data case 1PHEIN2.DOC
$OPEN, UNIT=4 FILE=1PHEIN2.PL4    FORM=UNFORMATTED  STATUS=UNKNOWN
   .001   .180    50.    50.
     1      1      1      3      1      0             2
 1 RGA1   PA1          6.189 5.980 24.91
 2 RGB1   PB1          0.720 2.270 -4.86 6.111 6.260 25.34
 3 RGC1   PC1          0.691 1.941 -2.21 0.658 2.498 -4.96 6.062 6.443 24.58
 4 RGA2   PA2          0.761 1.692 -2.18 0.720 1.741 -1.60 0.691 1.723 -1.24
                     6.189 5.980 24.91
 5 RGB2   PB2          0.720 1.741 -1.60 0.683 1.906 -1.70 0.658 1.969 -1.73
                     0.720 2.270 -4.86 6.111 6.260 25.34
 6 RGC2   PC2          0.691 1.723 -1.24 0.658 1.969 -1.73 0.635 2.155 -2.54
                     0.691 1.941 -2.21 0.658 2.498 -4.96 6.062 6.443 24.58
 1  PA1  RHA1  RGA1   PA1
 2  PB1  RHB1
 3  PC1  RHC1
 4  PA2  RHA2
 5  PB2  RHB2
 6  PC2  RHC2
 1  FA1   GA          6.203 5.929 24.74
 2  FB1   GB          0.753 1.770 -2.94 6.159 6.084 23.62
 3  FC1   GC          0.726 2.235 -5.31 0.707 1.867 -2.79 6.111 6.259 24.18
 1STARTA  FA1  FA1   GA
 2STARTB  FB1
 3STARTC  FC1
 1        HA   FA2  FA1   GA
 2        HB   FB2
 3        HC   FC2
 1       FA2 END-A  FA1   GA
 2        FB2 END-B
 3        FC2 END-C
BLANK CARD TERMINATING BRANCH CARDS
C SWITCH CARDS FOLLOW
     GA  RGA1      -1       1                                  1
       GB  RGB1      -1       1                                  1
     GC  RGC1      -1       1                                  1
    RHA1   HA      -1       1                                  1
    RHB1   HB      -1       1                                  1
    RHC1   HC      -1       1                                  1
     GA  RGA2      -1       1
     GB  RGB2      -1       1
     GC  RGC2      -1       1
    RHA2   HA      -1       1
    RHB2   HB      -1       1
    RHC2   HC      -1       1
C    HA    HB      .06      1
```

```
C    HB   HC      .06       1
    PC1           .06       1
BLANK CARD TERMINATING SWITCHES
C     SINUSOIDAL VOLTAGE SOURCE CARDS
C       1       2       3       4       5       6       7       8
C 34567890123456789012345678901234567890123456789012345678901234567890123456789012345678901234567890
14STARTA      33000      50.       0.0                    -1.
14STARTB      33000      50.    -120.0                    -1.
14STARTC      33000      50.     120.0                    -1.
14  END-A     33000      50.     -20.0                    -1.
14  END-B     33000      50.    -140.0                    -1.
14  END-C     33000      50.     100.0                    -1.
BLANK CARD TERMINATING SOURCE CARDS
C     OUTPUT CARDS
 CALCOMP PLOT
 SCREEN PLOT
 PRINTER PLOT
C 1
   RGA1  RGB1  RGC1  RHA1  RHB1  RHC1
-1   GA  RGA1   GB  RGB1   GC  RGC1  RHA1   HA  RHB1   HB  RHC1   HC
BLANK TERMINATING OUTPUT REQUEST CARDS
C       1       2       3       4       5       6       7       8
C 34567890123456789012345678901234567890123456789012345678901234567890123456789012345678901234567890
C PLOT SPECIFICATION
 14410.    120         RGA1  RGB1  RGC1

 14410.    120         RHA1  RHB1  RGC1
 19410.    120        BRANCH
                      GA  RGA1   GB  RGB1   GC  RGC1
 19410.    120        BRANCH
                     RHA1   HA  RHB1   HB  RHC1   HC
BLANK CARD TERMINATING PLOT CARDS
BLANK
BLANK
BEGIN NEW DATA CASE
BLANK
```

Appendix 6.6 Typical EMTP Input Data Case for a Model of 33 kV Feeder Circuit of Underground Cables as illustrated in figure 6.5.

```
BEGIN NEW DATA CASE
C     This is the data case for a model of 33 kV feeder circuit of underground cables.
C     It utilises the parameters calculated using Cable Constants routine of data case CABLES01.DOC.
C     The system test model is illustrated in figure 6.5. This data case is for a mid-zone one phase fault.
C     This is data case 1PHGIN2.DOC
$OPEN, UNIT=4 FILE=1PHGIN2.PL4   FORM=UNFORMATTED STATUS=UNKNOWN
   .001   .180    50.    50.
     1      1      1      3      1      0      0      2
 1 RGA1  PA1          3.45863.64297.2E-4
 2 RGB1  PB1          2.53152.5282-17E-53.45863.64297.2E-4
 3 RGC1  PC1          2.53152.5282-17E-52.53152.5282-17E-53.45863.64297.2E-4
 1  PA1  RHA1  RGA1   PA1
 2  PB1  RHB1
 3  PC1  RHC1
 1  FA1    GA  RGA1   PA1
 2  FB1    GB
 3  FC1    GC
 1STARTA   FA1  RGA1   PA1
 2STARTB   FB1
 3STARTC   FC1
 1   HA   FA2  RGA1   PA1
 2   HB   FB2
 3   HC   FC2
 1  FA2 END-A  RGA1   PA1
 2  FB2 END-B
 3  FC2 END-C
 1 RGA2   PA2  RGA1   PA1
 2 RGB2   PB2
 3 RGC2   PC2
 1  PA2  RHA2  RGA1   PA1
 2  PB2  RHB2
 3  PC2  RHC2
BLANK CARD TERMINATING BRANCH CARDS
C SWITCH CARDS FOLLOW
     GA  RGA1       -1        1                                  1
     GB  RGB1       -1        1                                  1
     GC  RGC1       -1        1                                  1
   RHA1    HA       -1        1                                  1
   RHB1    HB       -1        1                                  1
   RHC1    HC       -1        1                                  1
     GA  RGA2       -1        1
     GB  RGB2       -1        1
     GC  RGC2       -1        1
   RHA2    HA       -1        1
   RHB2    HB       -1        1
   RHC2    HC       -1        1
C    PA1   PB1      .06        1
C    PB1   PC1      .06        1
      PC1            .06        1
BLANK CARD TERMINATING SWITCHES
```

```
C     SINUSOIDAL VOLTAGE SOURCE CARDS
C       1       2       3       4       5       6       7       8
C 34567890123456789012345678901234567890123456789012345678901234567890
14STARTA      33000      50.      0.0                      -1.
14STARTB      33000      50.   -120.0                       -1.
14STARTC      33000      50.    120.0                       -1.
14 END-A      33000      50.    -20.0                       -1.
14 END-B      33000      50.   -140.0                       -1.
14 END-C      33000      50.    100.0                       -1.
BLANK CARD TERMINATING SOURCE CARDS
C     OUTPUT CARDS
 CALCOMP PLOT
 SCREEN PLOT
 PRINTER PLOT
C 1
   RGA1  RGB1  RGC1  RHA1  RHB1  RHC1
-1   GA  RGA1   GB  RGB1   GC  RGC1  RHA1   HA  RHB1   HB  RHC1   HC
BLANK CARD TERMINATING OUTPUT REQUEST
C     PLOT SPECIFICATION CARD
C       1       2       3       4       5       6       7       8
C 34567890123456789012345678901234567890123456789012345678901234567890
C  PRINTER PLOT
C  CALCOMP PLOT
C  SCREEN PLOT
 14410.    120         RGA1  RGB1  RGC1
 14410.    120         RHA1  RHB1  RHC1
 19410.    120       BRANCH
                     GA  RGA1   GB  RGB1   GC  RGC1
 19410.    120       BRANCH
                    RHA1   HA  RHB1   HB  RHC1   HC
BLANK CARD TERMINATING PLOT CARDS
BLANK
BEGIN NEW DATA CASE
BLANK
```

Appendix 6.7 Typical EMTP Input Data Case for a Model of a Composite 33 kV Feeder Circuit of Overhead Line Sections and Undeground Cable Sections with the Test Circuit as illustrated in figure 6.5.

```
BEGIN NEW DATA CASE
C     This data case is of a model of a composite 33 kV feeder circuit of overhead line sections and
C     underground cable sections.
C     The sections are each 10km long.
C     The system test model is illustrated in figure 6.5. This data case is for a mid-zone one phase fault.
C     This is data case 1MXEIN.DOC
$OPEN, UNIT=4 FILE=1MXEIN.PL4    FORM=UNFORMATTED  STATUS=UNKNOWN
   .001   .180    50.    50.
     1      1      1      3      1      0             2
 1 RGA1   PA1          6.189 5.980 24.91
 2 RGB1   PB1          0.720 2.270 -4.86 6.111 6.260 25.34
 3 RGC1   PC1          0.691 1.941 -2.21 0.658 2.498 -4.96 6.062 6.443 24.58
 4 RGA2   PA2          0.761 1.692 -2.18 0.720 1.741 -1.60 0.691 1.723 -1.24
                     6.189 5.980 24.91
 5 RGB2   PB2          0.720 1.741 -1.60 0.683 1.906 -1.70 0.658 1.969 -1.73
                     0.720 2.270 -4.86 6.111 6.260 25.34
 6 RGC2   PC2          0.691 1.723 -1.24 0.658 1.969 -1.73 0.635 2.155 -2.54
                     0.691 1.941 -2.21 0.658 2.498 -4.96 6.062 6.443 24.58
 1  PA1  RHA1          3.45863.64297.2E-4
 2  PB1  RHB1          2.53152.5282-17E-53.45863.64297.2E-4
 3  PC1  RHC1          2.53152.5282-17E-52.53152.5282-17E-53.45863.64297.2E-4
 1  PA2  RHA2          6.203 5.929 24.74
 2  PB2  RHB2          0.753 1.770 -2.94 6.159 6.084 23.62
 3  PC2  RHC2          0.726 2.235 -5.31 0.707 1.867 -2.79 6.111 6.259 24.18
 1  FA1   GA           6.203 5.929 24.74
 2  FB1   GB           0.753 1.770 -2.94 6.159 6.084 23.62
 3  FC1   GC           0.726 2.235 -5.31 0.707 1.867 -2.79 6.111 6.259 24.18
 1STARTA  FA1  FA1   GA
 2STARTB  FB1
 3STARTC  FC1
 1   HA   FA2  FA1   GA
 2   HB   FB2
 3   HC   FC2
 1  FA2 END-A  FA1   GA
 2  FB2 END-B
 3  FC2 END-C
BLANK CARD TERMINATING BRANCH CARDS
C SWITCH CARDS FOLLOW
     GA  RGA1      -1       1                              1
     GB  RGB1      -1       1                              1
     GC  RGC1      -1       1                              1
   RHA1    HA      -1       1                              1
   RHB1    HB      -1       1                              1
   RHC1    HC      -1       1                              1
     GA  RGA2      -1       1
     GB  RGB2      -1       1
     GC  RGC2      -1       1
   RHA2    HA      -1       1
```

```
   RHB2   HB      -1       1
   RHC2   HC      -1       1
C     HA   HB     .06       1
C     HB   HC     .06       1
     PC1         .06       1
BLANK CARD TERMINATING SWITCHES
C     SINUSOIDAL VOLTAGE SOURCE CARDS
C       1       2       3       4       5       6       7       8
C 34567890123456789012345678901234567890123456789012345678901234567890123456789012345678901234567890
14STARTA      33000      50.      0.0                      -1.
14STARTB      33000      50.   -120.0                      -1.
14STARTC      33000      50.    120.0                      -1.
14  END-A     33000      50.    -20.0                      -1.
14  END-B     33000      50.   -140.0                      -1.
14  END-C     33000      50.    100.0                      -1.
BLANK CARD TERMINATING SOURCE CARDS
C     OUTPUT CARDS
 CALCOMP PLOT
 SCREEN PLOT
 PRINTER PLOT
C 1
   RGA1  RGB1  RGC1  RHA1  RHB1  RHC1
-1   GA  RGA1   GB  RGB1   GC  RGC1  RHA1   HA  RHB1   HB  RHC1   HC
BLANK TERMINATING OUTPUT REQUEST CARDS
C       1       2       3       4       5       6       7       8
C 34567890123456789012345678901234567890123456789012345678901234567890123456789012345678901234567890
C PLOT SPECIFICATION
 14410.    120         RGA1  RGB1  RGC1

 14410.    120         RHA1  RHB1  RGC1
 19410.    120       BRANCH
                     GA  RGA1   GB  RGB1   GC  RGC1
 19410.    120       BRANCH
                    RHA1   HA  RHB1   HB  RHC1   HC
BLANK CARD TERMINATING PLOT CARDS
BLANK
BLANK
BEGIN NEW DATA CASE
BLANK
```

Chapter 7

ALGORITHM EVALUATION WITH POLARISING REFERENCE PHASORS DERIVED FROM VOLTAGE WAVEFORMS.

7.1 INTRODUCTION.

An evaluation of the performance of the voltage polarised current differential algorithm is presented. The 33 kV feeder circuit modelled in chapter 6 is used with overhead lines only first, and then with underground cables only. The performance of the algorithm is also evaluated on composite feeders of overhead line and underground cable sections. A variety of in-zone and external faults are considered, and these include single phase faults, double phase faults and three phase faults. Fault inception angle is varied between 0° and 360° with the fault position varied between 0% and 100% of the line.

The start of data transmission is randomised for each simulation run as mentioned in chapter 3 in section 3.3.2 under Data Processing and Interchange. This is in view of the fact that practical communications will be free running and is therefore not synchronised with the inception of the fault.

Test results show that the algorithm is sensitive to all in-zone faults and, for the fault conditions presented for which the algorithm should trip, the tripping times were all under two and half power cycles. The algorithm remained stable for all external faults, including terminal faults.

A summary of the waveforms is given, clearly showing fault inception times and trip times where applicable. A general statement of the results is given in the summary to the chapter.

7.2 FAULT TYPES.

In a power system, lines are one of the most vulnerable points to conditions that lead to sudden changes in the normal voltage or current existing at the time[1]. In this work, only short circuit type of faults were considered, and the term 'fault' is synonymous to short-circuit.

In distribution feeder systems the major causes of faults can be generalised as:-

- Insulation failures which may be due to design defects and error, improper manufacture, inadequate insulation and insulation ageing.

- Electrical stress due to lighting surges, switching surges and dynamic over-voltages.

- Mechanical disturbances which can be as a result of wind, snow and ice, atmospheric contamination and human action.

- Thermal overload as a result of overcurrent or overvoltage.

A fault may cause currents to flow between phase and neutral or earth, between two phases and earth or without earth, or across all three phases to earth or without earth. The former two fault paths involving one or two phases are for asymmetrical faults, while the latter is for a symmetrical fault. Although three phase faults are normally assumed in the calculation of fault levels, symmetrical faults on three phase systems are the least common, with the most common being single phase faults followed by double phase to earth faults and double phase faults without earth[1, 14, 57].

It is the purpose of the protection system to detect the presence of faults on the power system, locate them, and initiate action which will isolate from the rest of the supply network the faulted plant in the shortest time achievable, thus minimising damage to plant and disturbances to the network. The protection should cope well with worst case scenario such as three phase faults and also with common fault conditions such as single phase faults. It must accurately discriminate between faults on the protected plant and those elsewhere on the network. It must also remain stable during faults on adjacent plant, however severe the fault.

7.3 TESTS ON FEEDER CIRCUIT WITH OVERHEAD LINES.

As discussed in preceding chapter, the EMTP data case of appendix 6.5 was used to model a typical 33 kV feeder network as illustrated in figure 6.5.

The current supplied to the transmission-line capacitance is called charging current. Thus, charging current is given as[4]:-

$$\begin{aligned} I_{chg} &= j\omega C \frac{V}{\sqrt{3}} \\ \therefore \quad |I_{chg}| &= \omega C \frac{V}{\sqrt{3}} \end{aligned} \tag{7.1}$$

For the 33kV system modelled in chapter 6, charging current is 3.8 Amps. There is a nominal load Ip equals to 151 Amps. An in-zone three phase fault results in Ip equals to 2047 Amps and -1858 Amps for the local and remote terminals respectively. For the same fault condition, Iq equals to 2130 Amps and -2593 Amps for the local and remote

terminals respectively. An external three phase fault results in Ip equals to -612 Amps and -658 Amps for the two terminals respectively, and Iq equals to -1146 Amps and -1065 Amps. For an in-zone single phase fault, Ip equals to 517 Amps and -364 Amps for the two terminals with Iq equals to 352 Amps and -1095 Amps. An external single phase fault results in Ip equals to -2 Amps and -60 Amps with Iq equals to -565 Amps and -595 Amps for the two terminals respectively. All these results are clearly shown in the figures below. The trip settings, as in the configuration file of appendix 3.3 in chapter 3, were satisfied with both I_{p_min} and I_{q_min} set at 200 Amps, and the bias settings k_1 and k_2 set at 2.0 percent.

7.3.1 SINGLE PHASE FAULTS.

Being the most common type of fault in sub-transmission systems and distribution systems, the first series of faults to be studied were those that involve only a single phase. Firstly, an in-zone single phase fault was introduced at point P1 on phase C. Figure 7.1 shows the EMTP output voltages and currents for each phase at the terminals of the protected feeder. There are thus 12 signals in total.

Figure 7.2 shows the C-phase current, C-phase voltage, C-phase reference signal, and the polarised current measurements Ip and Iq at the local terminal for the in-zone single phase fault. The local terminal in this case is terminal G. Both Ip and Iq are constants, confirming equations (3.4) and (3.6). The fault results in large measurements for both Ip and Iq. Within 20 milliseconds after the fault, both Ip and Iq have settled to new steady values.

Figure 7.3 shows the comparisons between the locally obtained Ip and Iq signals to those received from the remote end of the feeder. This clearly shows the differences between the measurements during the fault, and the delays between the two signals which are

caused by the communications system. A feature to be noticed also is that due to the in-zone fault, the change in direction of flow of the polarised current measurements at the remote terminal is opposite that of the local terminal. Using the trip requirement of two subsequent trip indications, this fault condition led to a trip time of 39 milliseconds. With the fault still on, the algorithm always gives a 'yes trip' decision producing a trip output every time it makes a comparison between the local and remote signals. This is illustrated by the train of spikes in the trip signal.

The histogram in figure 7.4 shows the number of trips against trip times for 100 simulation runs. As the starting time for each run is random, considering that the communications is free running and not synchronised with the fault, the trip time for these 100 runs varies from 35 milliseconds to 48 milliseconds, with the average trip time being 41.32 milliseconds.

Figure 7.5 shows the comparison between the locally obtained Ip and Iq signals to those received from the remote end of the feeder for an external single phase fault on one supply feeder at point F1 on the test system of figure 6.5. For this condition, the measurements are relatively small and although there is a difference between the local and remote signals, this is less than the trip setting. For this fault, the algorithm remains stable and does not trip.

Figures 7.6 is for an external fault on the other supply feeder at point F2 and shows the comparisons between the local end and remote end measurements. Here again, the algorithm remains stable and does not trip. Figure 7.7 is for an external fault on the parallel feeder at point P2, and shows the comparisons between the local end and remote end measurements. The polarised current measurements Ip and Iq remained about the same before and after the parallel feeder fault. This is so because the actual measured currents do not change for the type of fault, but only the voltage registers a noticeable

change as shown in figure 7.8. Again, the algorithm remains stable and does not trip. Figure 7.9 compares the local end and remote end measurements for the unlikely terminal single phase fault, and again, the algorithm remains stable and does not trip.

A feature to be noticed also for the external faults is that the direction of flow of the polarised current measurements at the remote terminal is the same as that of the local terminal.

7.3.2 DOUBLE PHASE FAULTS.

The response curves for a phase to phase to earth in-zone fault is illustrated in figure 7.10. The differences between the local and remote Ip and Iq led to the algorithm tripping after 37 milliseconds. As in the single phase case, so long as there is a fault, the algorithm keeps producing a trip output when ever it compares the remote and local signals. The response to a similar fault but external to the protected zone at point F1 is shown in figure 7.11. For this condition, the algorithm remained stable and did not trip. Figure 7.12 is for an external fault on the other supply feeder at point F2, and figure 7.13 is for an external fault on the parallel feeder at point P2. The external fault conditions did not cause the algorithm to trip at all.

The response for a phase to phase in-zone fault without earth is illustrated in figure 7.14. The differences between the local and remote Ip and Iq led to the algorithm tripping after 38 milliseconds. The response to a similar fault but external to the protected zone at point F1 is shown in figure 7.15. For this condition, the algorithm remained stable and did not trip. Figure 7.16 is for an external fault on the other supply feeder at point F2, while figure 7.17 is for an external fault on the parallel feeder at point P2 on the test system. All the external faults did not cause the algorithm to trip at all.

7.3.3 THREE PHASE FAULTS.

Similar to above, the responses to in-zone and external three phases to ground faults are illustrated in figures 7.18 to 7.21. For these, the in-zone fault resulted in tripping after 36 milliseconds, but the algorithm remained stable for the external faults.

A more demanding fault is a terminal fault resulting in voltage collapse at one terminal as clearly shown in figure 7.22. Although the disturbance was detected, the algorithm remained stable since it did not receive the second trip indication.

Also included were fault conditions at 100 meters from the relaying points both inside and outside of the protected zone. Figure 7.23 is for the response to such a fault condition inside the protected zone, while figure 7.24 is for a similar fault but external to the protected zone. The algorithm tripped at 38 milliseconds for the in-zone fault but did not trip for the external fault.

Point-on-wave at fault was varied. A typical response is presented in figure 7.25 which is for an in-zone fault at 72° on the wave. The algorithm tripped at 44 milliseconds. Figure 7.26 is for a similar fault but external to the protected zone. For this fault condition, the algorithm remained stable and did not trip.

A summary of the trip response of the system with overhead line feeders is illustrated in the histogram in figure 7.27 which is for 100 simulation runs for a typical in-zone single phase fault. The average trip time is now 40 milliseconds for the in-zone fault. Rightly, a similar number of runs for an out-of-zone fault produced no trip indication.

7.4 TESTS ON FEEDER CIRCUIT WITH UNDERGROUND CABLES.

The EMTP data case of appendix 6.6 of the preceding chapter was used to model a typical 33 kV feeder network as illustrated in figure 6.5. There is a nominal load Ip equals to 903 Amps. An in-zone three phase fault results in Ip equals to 7994 Amps and -6775 Amps for the local and remote terminals respectively. For the same fault condition, Iq equals to 13494 Amps and -15277 Amps for the local and remote terminals respectively. An external three phase fault results in Ip equals to -2094 Amps and -2358 Amps for the two terminals respectively, and Iq equals to -6359 Amps and -6081 Amps. For an in-zone single phase fault, Ip equals to 1538 Amps and -23 Amps for the two terminals with Iq equals to -68 Amps and -2702 Amps. An external single phase fault results in Ip equals to 631 Amps and 500 Amps with Iq equals to -1845 Amps and -1708 Amps for the two terminals respectively. All these results are clearly shown in the figures below. The trip settings, as in the configuration file of appendix 3.3 in chapter 3, were satisfied with both I_{p_min} and I_{q_min} set at 700 Amps, and the bias settings k_1 and k_2 set at 2.0 percent.

7.4.1 SINGLE PHASE FAULTS.

Similar to the case with overhead lines, the first series of faults to be studied were those that involve only a single phase. Firstly, an in-zone single phase fault was introduced. As in a similar fault condition with overhead line system used in figure 7.3, figure 7.28 shows the comparisons between the locally obtained Ip and Iq signals to those received from the remote end of the feeder. There are dramatic differences between the local and remote measurements after the fault and the algorithm tripped after 44 milliseconds.

The response to a typical single phase to ground fault external to the protected zone is summarised in figure 7.29. For this condition, the measurements are relatively small and

although there is a difference between the local and remote signals, this is less than the trip setting. For this fault, the algorithm remains stable and does not trip.

7.4.2 DOUBLE PHASE FAULTS.

The response curves for a phase to phase to earth in-zone fault is illustrated in figure 7.30. The differences between the local and remote Ip and Iq led to the algorithm tripping after 42 milliseconds. A typical response to a similar fault but external to the protected zone is shown in figure 7.31. For this condition, the algorithm remained stable and did not trip.

The response curves for a phase to phase in-zone fault without earth is illustrated in figure 7.32. The differences between the local and remote Ip and Iq led to the algorithm tripping after 46 milliseconds. A typical response to a similar fault but external to the protected zone is shown in figure 7.33. For this condition, the algorithm remained stable and did not trip.

7.4.3 THREE PHASE FAULTS.

Similarly, the responses to in-zone and external three phases to ground faults are illustrated in figures 7.34 and 7.35 respectively. For these, the in-zone fault resulted in tripping after 40 milliseconds, but the algorithm remained stable and did not trip for the external fault.

Figure 7.36 shows the results of a terminal fault condition. Although the disturbance was detected, the algorithm remained stable since it did not receive the second trip indication.

It is to be noted that in underground cable networks, single phase faults may result into

three phase faults with earth. The evaluation of the protection algorithm must however involve all possible cases, including single phases and double phase fault conditions as has been done above.

7.5 TESTS ON FEEDER CIRCUIT WITH COMPOSITE FEEDERS.

Distribution systems may have some feeders consisting of both overhead lines and underground cables as discussed above. This section presents responses for such networks. For simplicity, equal lengths of sections of overhead lines and underground cables were used. The EMTP data case of appendix 6.7 of the preceding chapter was used to model a typical 33 kV feeder network as illustrated in figure 6.5. The trip settings illustrated in appendix 3.3 in chapter 3 were set at 300 Amps for both $I_{p\text{-}min}$ and $I_{q\text{-}min}$, with the bias settings k_1 and k_2 equal to 2.0 percent.

7.5.1 SINGLE PHASE FAULTS.

Similar to the above cases, the first series of faults to be studied were those that involve only a single phase. Firstly, an in-zone single phase fault was introduced. Figure 7.37 shows the comparisons between the locally obtained Ip and Iq signals to those received from the remote end of the feeder. The differences between the local and remote measurements after the fault led to the algorithm tripping after 41 milliseconds.

The response to a typical single phase to ground fault external to the protected zone is summarised in figure 7.38. For this condition, the measurements are relatively small and although there is a difference between the local and remote signals, this is less than the trip setting. For this fault, the algorithm remains stable and does not trip.

7.5.2 DOUBLE PHASE FAULTS.

The response curves for a phase to phase to earth in-zone fault are illustrated in figure 7.39. The differences between the local and remote Ip and Iq led to the algorithm tripping after 39 milliseconds. A typical response to a similar fault but external to the protected zone is shown in figure 7.40. For this condition, the algorithm remained stable and did not trip.

The response curves for a two phase in-zone fault without earth are illustrated in figure 7.41. The differences between the local and remote Ip and Iq led to the algorithm tripping after 40 milliseconds. A typical response to a similar fault but external to the protected zone is shown in figure 7.42. For this condition, the algorithm remained stable and did not trip.

7.5.3 THREE PHASE FAULTS.

Similarly, the responses to in-zone and external three phases to ground faults are illustrated in figures 7.43 and 7.44 respectively. For these, the in-zone fault resulted in tripping after 39 milliseconds, but the algorithm remained stable and did not trip for the external fault.

As above, a voltage collapse condition at one terminal was studied. Figure 7.45 shows the results. Although the disturbance was detected, the algorithm remained stable since it did not receive the second trip indication.

7.6 SUMMARY.

This chapter has presented the performance evaluation of the algorithm where the polarising references were derived from the terminal's phase voltages. A memory feature was included in case of fault conditions that cause voltage collapse[110]. The resulting polyphase polarised current measurements from the feeder's terminals were used to derive the bias signal and the difference signal[111] required for the trip decision making in the differential protection algorithm.

The simulation was made as practical as possible. Feeders that can exist in a network were modelled. They included those with only overhead lines, with only underground cables, and also a mixture of both overhead lines and underground cables. Communications would normally be free running and not synchronised with the fault. This was also modelled by simply randomising the start of a simulation run.

A variety of faults at different fault positions were considered. Applied inside and external to the protected zone, with the inception angle varied, these faults involved single phases, double phases and three phases.

As mentioned above, Unit protection is provided when a section of the power system is protected individually without reference to the other sections. Thus, coordination with protection in adjacent zones is eliminated. Strictness on the setting is therefore relaxed. The trip settings $I_{p\text{-}min}$ and $I_{q\text{-}min}$ do not have to be equal. Likewise, the bias settings k_1 and k_2 do not have to be equal.

The results were very good. For the fault conditions presented for which the algorithm should trip, the tripping times were all under two and half power system cycles for in-zone faults. This tripping time is acceptable in distribution feeders[9]. Variations in the

synchronism between fault occurrence and data transmission meant that the tripping times vary within 13.33 milliseconds, as discussed in chapter 4. The principle constraint for this technique is the time required to transmit data from one terminal to another. Reducing this time, by increasing the data rate, would reduce the tripping time. For all external faults, including a terminal fault, the algorithm remained stable and did not trip.

The algorithm thus has the much desired properties in protection. It accurately discriminates between faults on the protected plant and those elsewhere on the network. For faults on the protected plant, it initiates fast isolation of the faulted plant from the rest of the supply system.

This scheme may introduce added advantages. As voltages are available, several features which use this additional information may be incorporated in the relay to increase its performance. These may include implementing a back-up distance protection or fault locating features[112, 113]. However, the requirement of this relay that voltage be supplied removes one advantage of current differential relaying.

7.7 FIGURES.

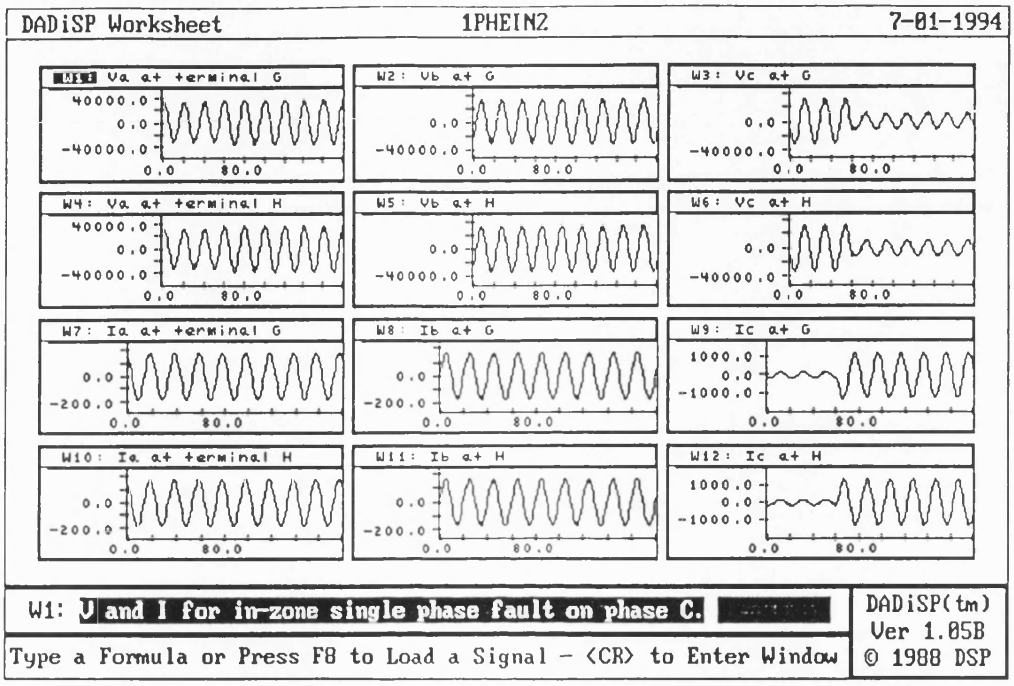

Figure 7.1 Screen dump of the EMTP output Voltages and Currents for a Mid-zone Single Phase Fault at point P1 on the Test System with Overhead Line Feeders.

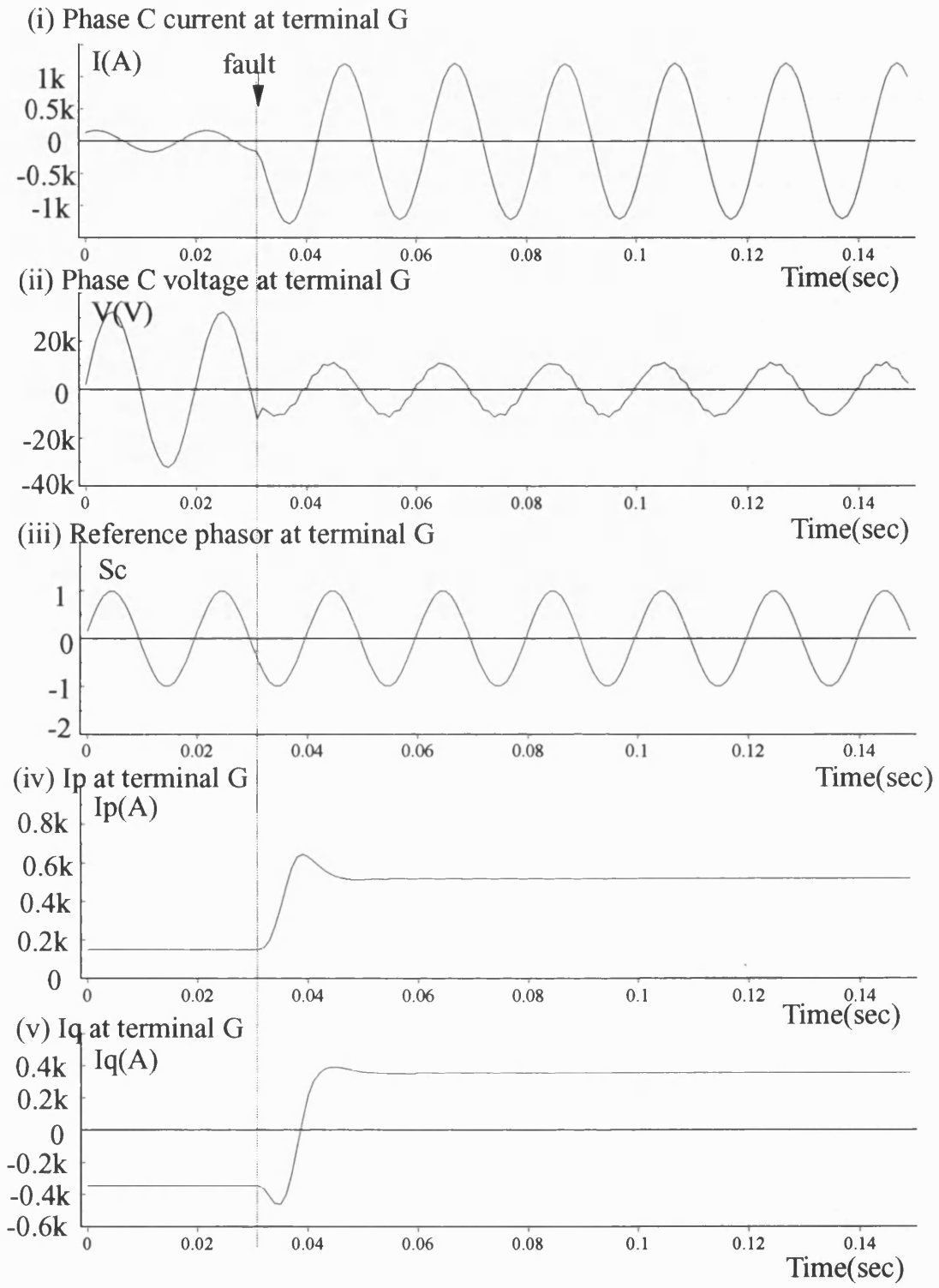

Figure 7.2 Input and Algorithm Derived Waveforms for an In-zone Single Phase Fault at Point P1 on the Test System.

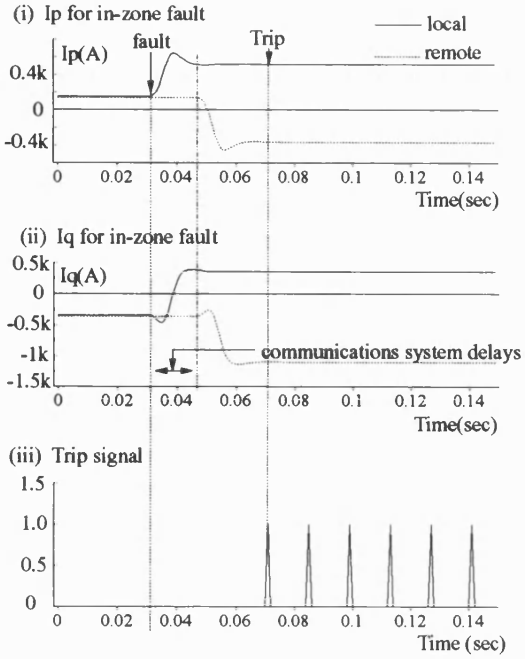

Figure 7.3 Polarised Currents for an In-zone Single Phase Fault at point P1 on the Test System with Overhead Line Feeders.

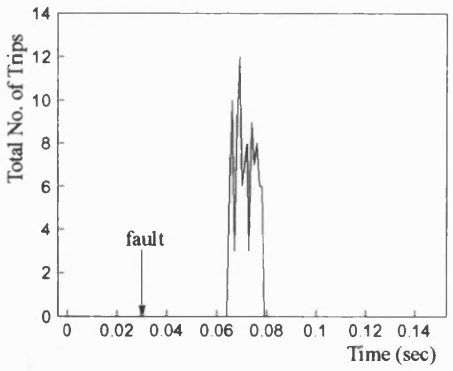

Figure 7.4 Histogram of number of trips versus time for 100 simulation runs for the above In-zone Single Phase Fault.

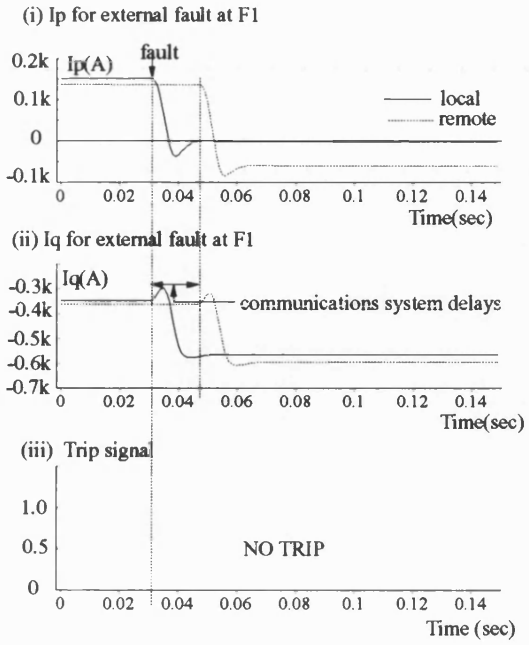

Figure 7.5 Polarised Currents for an External Single Phase Fault at point F1 on the System with Overhead Line Feeders.

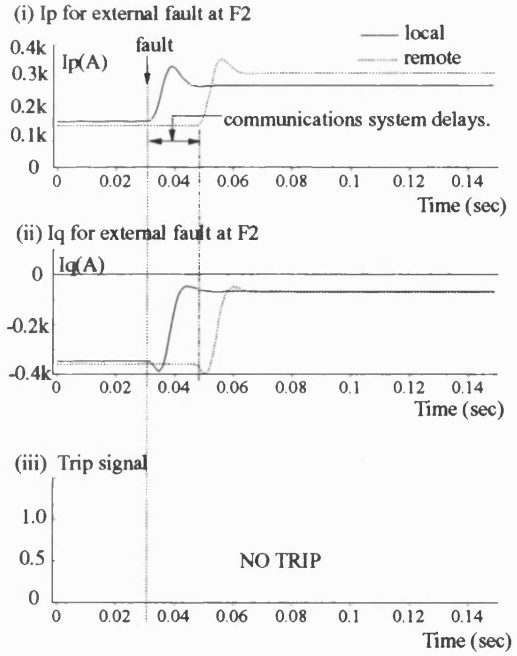

Figure 7.6 Polarised Currents for an External Single Phase Fault at point F2 on the System with Overhead Line Feeders.

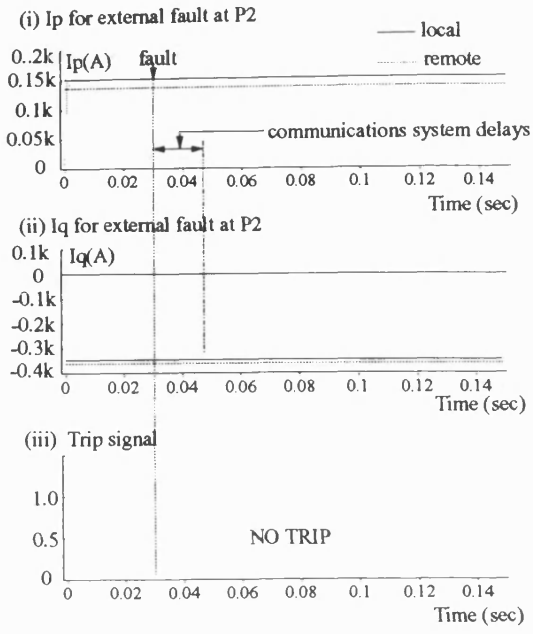

Figure 7.7 Polarised Currents for an External single phase fault on the parallel feeder on the System with Overhead Line Feeders.

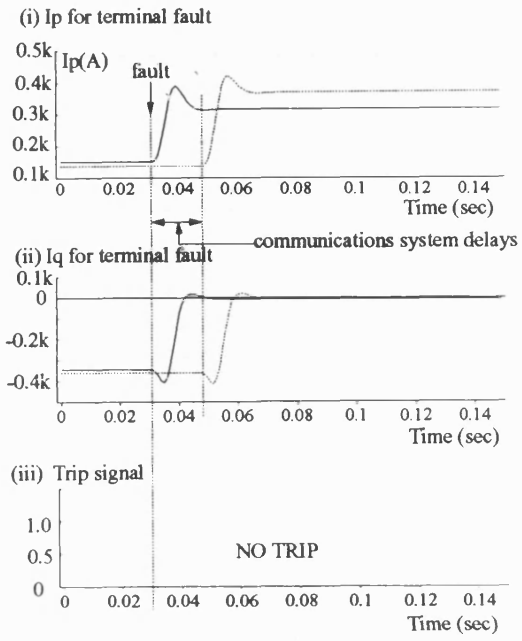

Figure 7.9 Polarised Currents for a single phase fault at Terminal H on the Test System with Overhead Line Feeders.

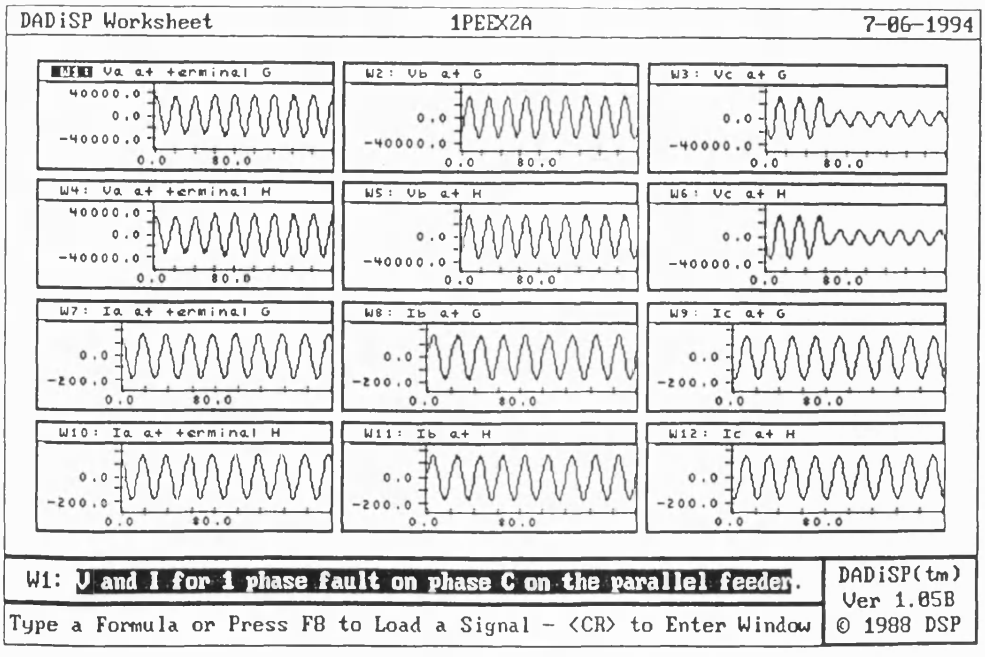

Figure 7.8 Screen dump of the EMTP output Voltages and Currents for an External Single Phase Fault on the parallel feeder at point P2 on the Test System with Overhead Line Feeders.

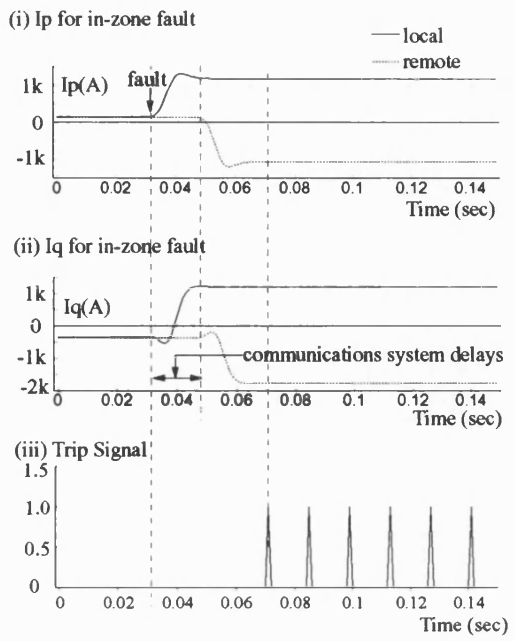

Figure 7.10 Polarised Currents for In-zone Two Phases Earth fault at Point P1 on the Test System with Overhead Line Feeders.

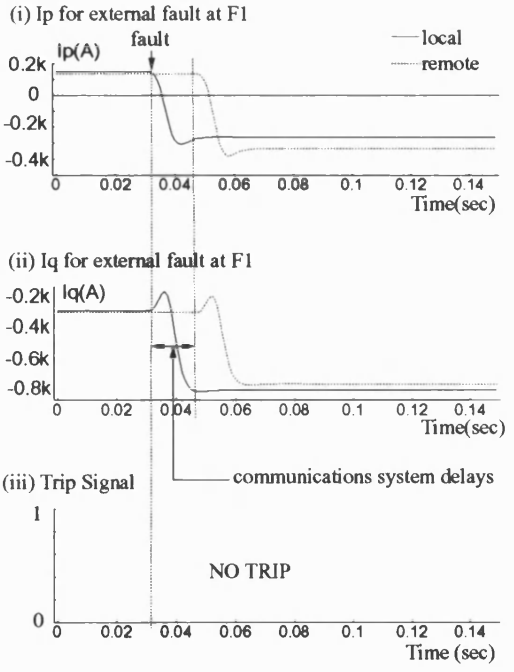

Figure 7.11 Polarised Currents for external Two Phases Earth fault at Point F1 on the Test System with Overhead Line Feeders.

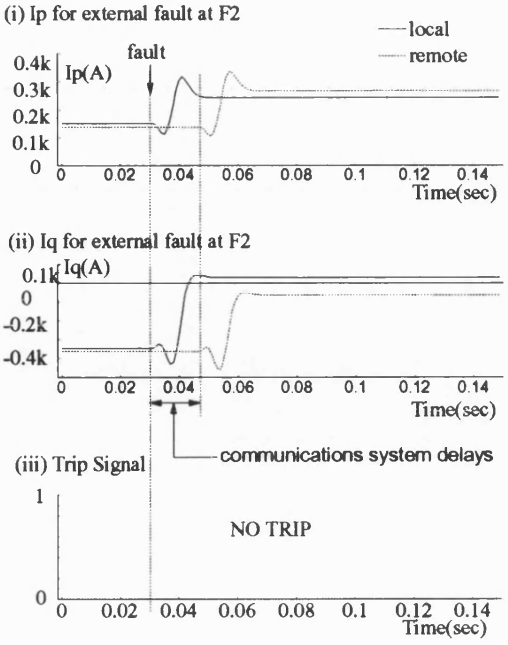

Figure 7.12 Polarised Currents for external Two Phases Earth fault at Point F2 on the Test System with Overhead Line Feeders.

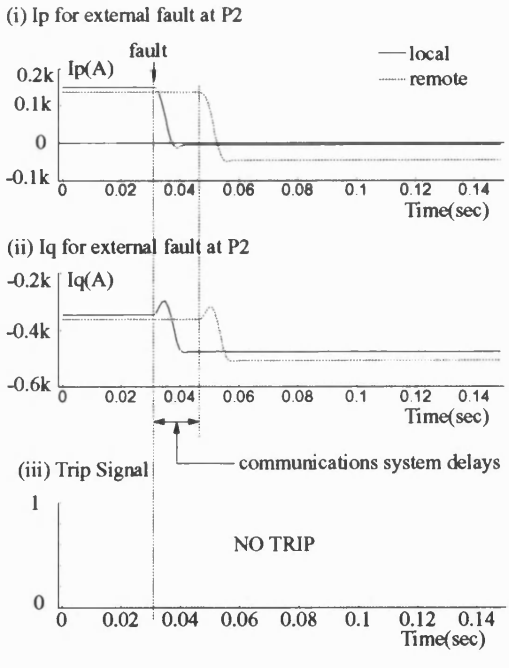

Figure 7.13 Polarised Currents for external Two Phases Earth fault at Point P2 on the Test System with Overhead Line Feeders.

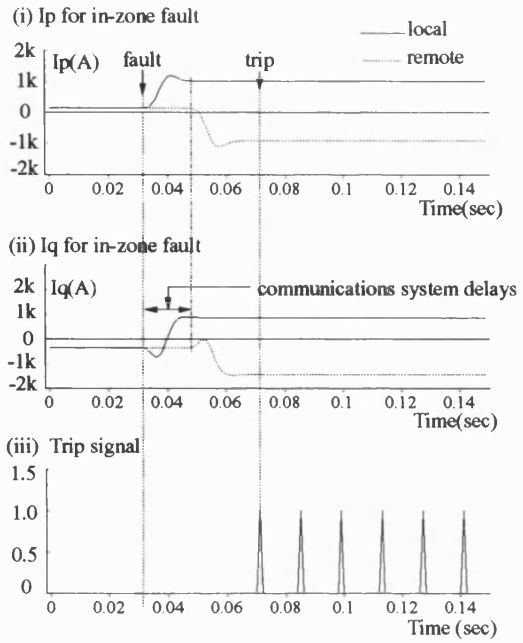

Figure 7.14 Polarised Currents for In-zone Phase to Phase fault at Point P1 on the Test System with Overhead Line Feeders.

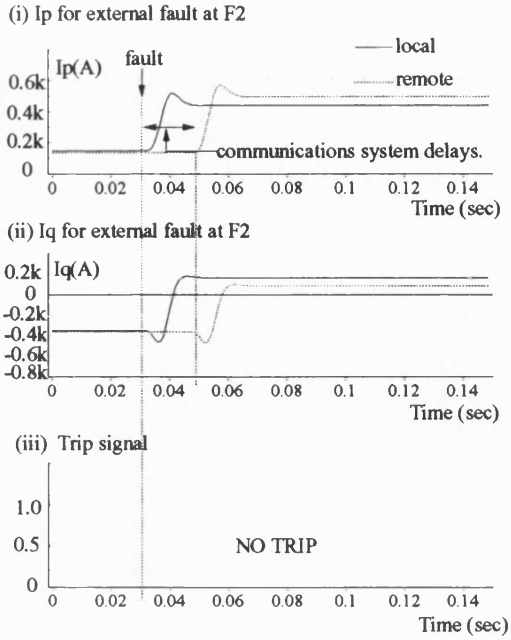

Figure 7.16 Polarised Currents for an External Phase to Phase fault at Point F2 on the Test System with Overhead Line Feeders.

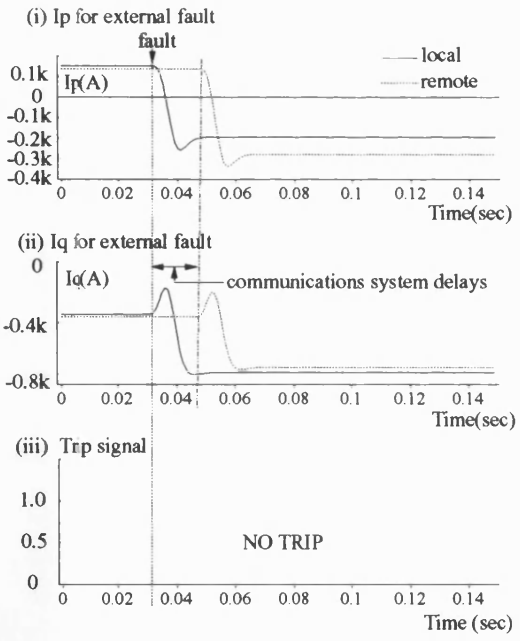

Figure 7.15 Polarised Currents for an External Phase to Phase fault at point F1 on the Test System with Overhead ine Feeders.

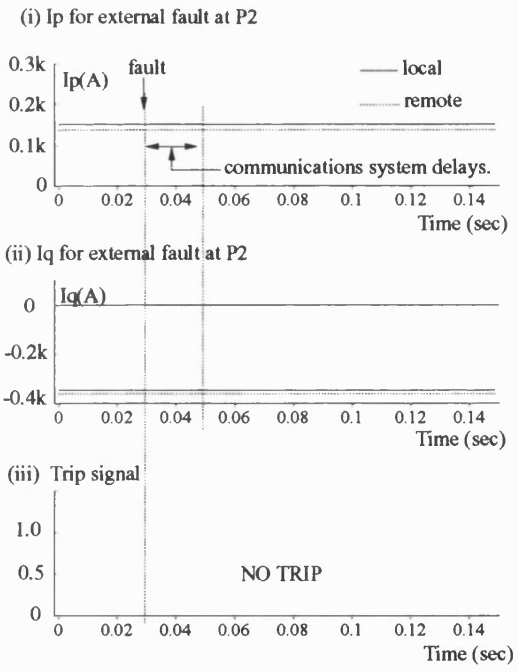

Figure 7.17 Polarised Currents for an External Phase to Phase fault at Point P2 on the Test System with Overhead Line Feeders.

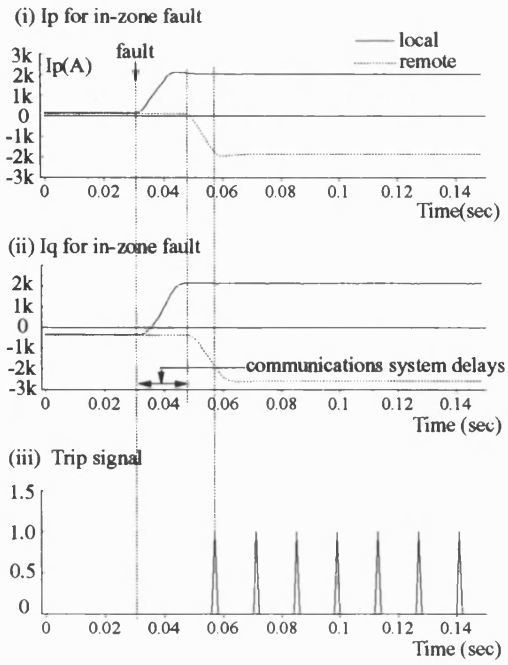

Figure 7.18 Polarised Currents for In-zone Three Phase Earth Fault at Point P1 on the Test System with Overhead Line Feeders.

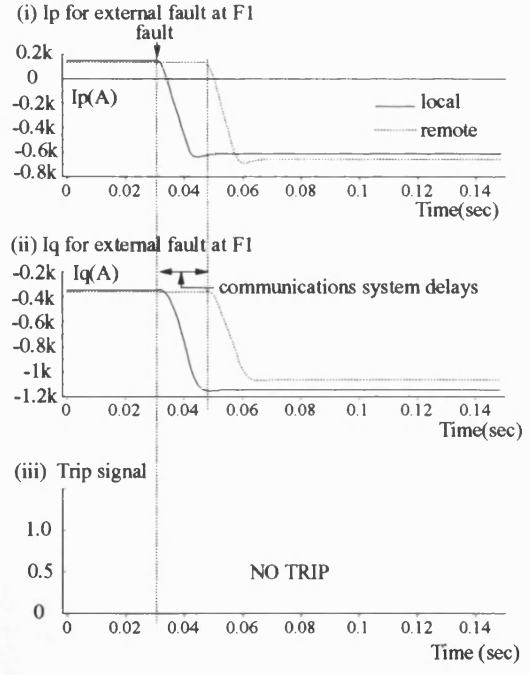

Figure 7.19 Polarised Currents for External three Phase Earth Fault at point F1 on the Test System with Overhead Line Feeders.

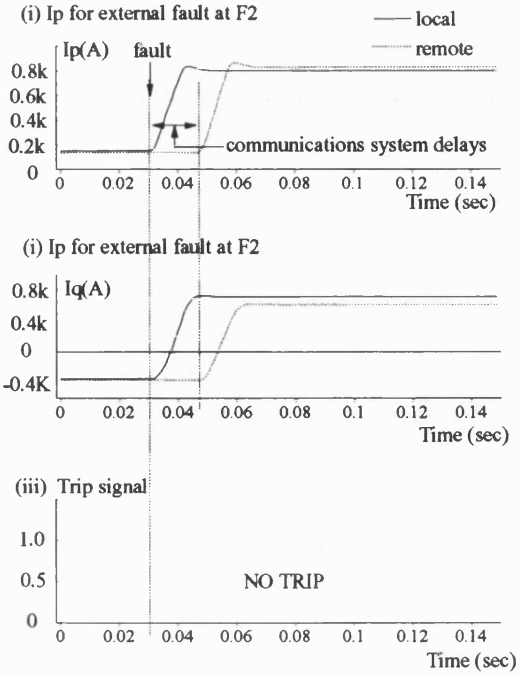

Figure 7.20 Polarised Currents for External three Phase Earth Fault at point F2 on the Test System with Overhead Line Feeders.

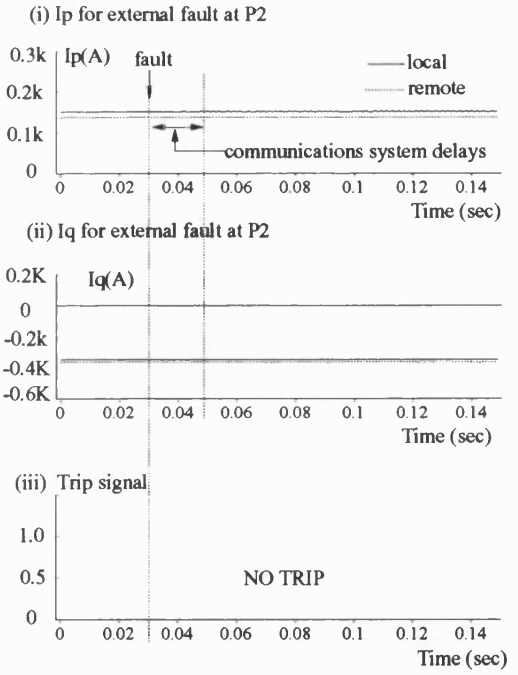

Figure 7.21 Polarised Currents for External three Phase Earth Fault at point P2 on the Test System with Overhead Line Feeders.

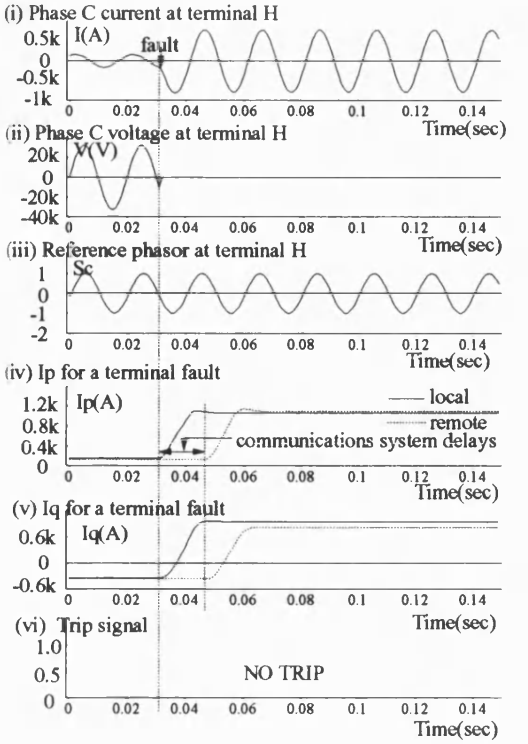

Figure 7.22 Input and Derived Waveforms for a three Phase Earth Fault at Terminal H on the Test System with Overhead Line Feeders.

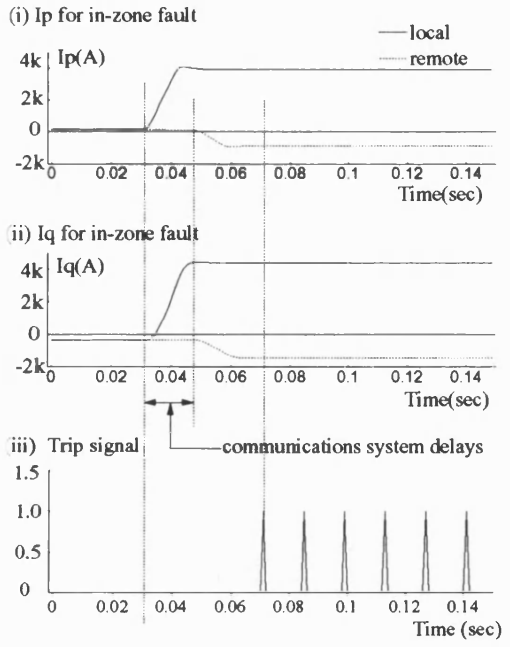

Figure 7.23 Polarised Currents for In-zone three phase earth fault 100 metres from terminal on the System with Overhead Line Feeders.

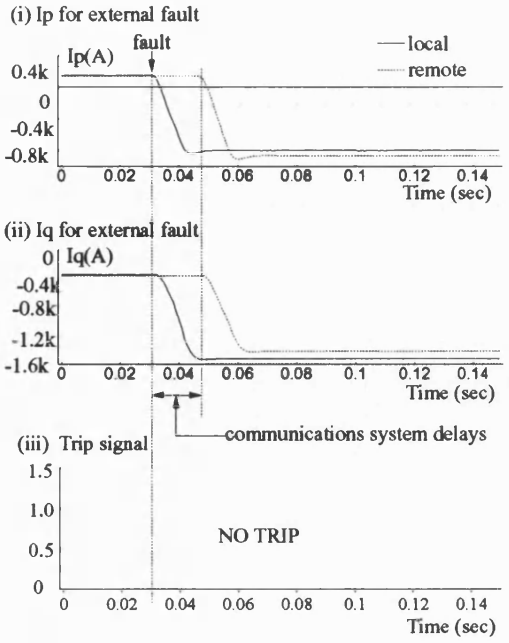

Figure 7.24 Polarised Currents for external three phase earth fault 100 metres from terminal on System with Overhead Line Feeders.

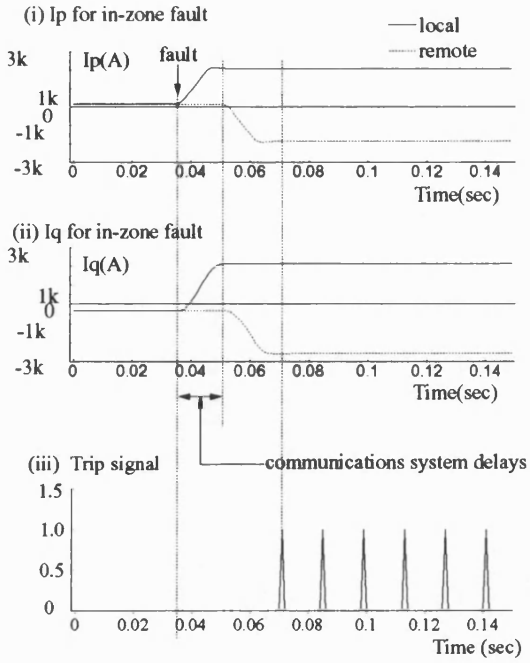

Figure 7.25 Polarised Currents for varied point-on-wave In-zone three phase earth fault on System with Overhead Line Feeders.

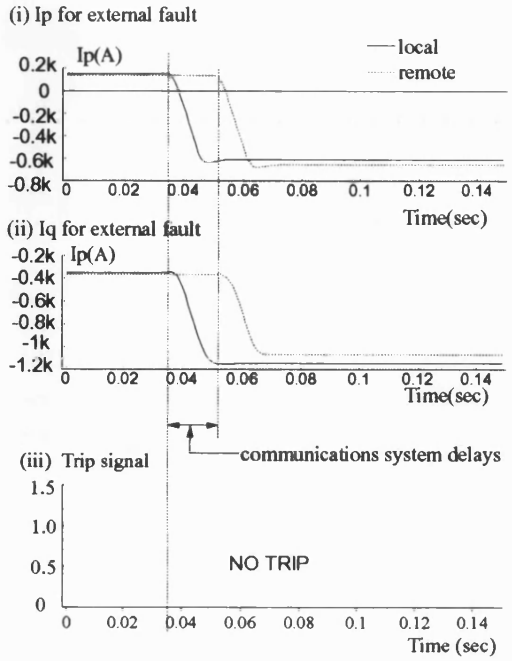

Figure 7.26 Polarised Currents for varied point-on-wave External three phase earth fault on System with Overhead Line Feeders.

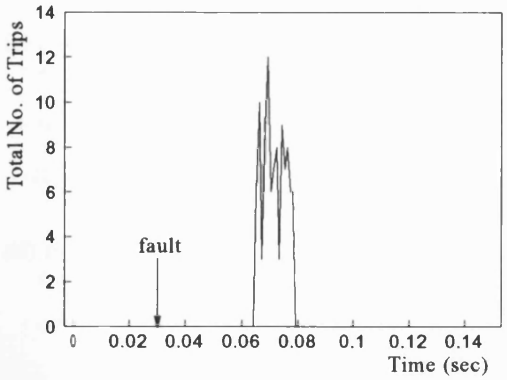

Figure 7.27 Histogram of Trip Response Summary of In-zone Faults on System with Overhead Line Feeders using 100 simulation runs.

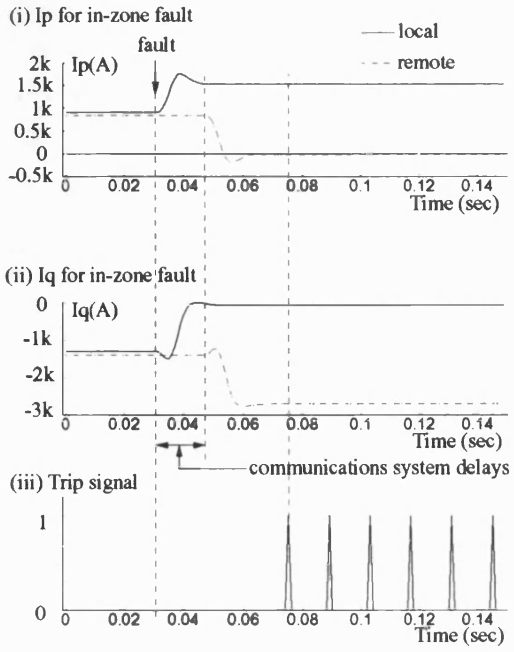

Figure 7.28 Polarised Currents for an In -zone Single Phase Fault at point P1 on the Test System with Underground Feeders.

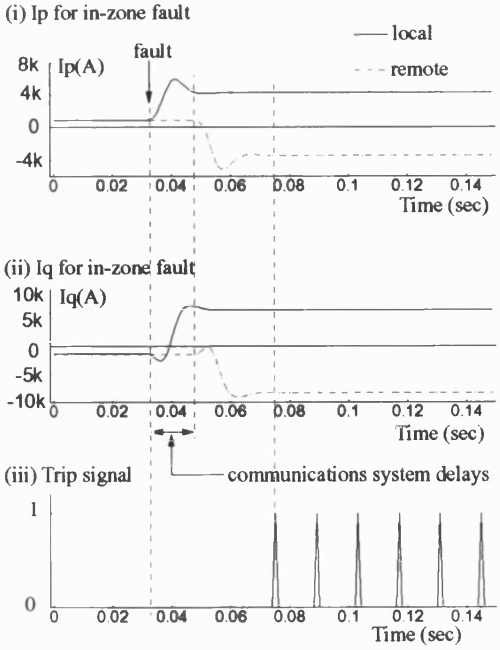

Figure 7.30 Polarised Currents for In -zone Two Phases to Earth Fault at point P1 on the Test System with Underground Feeders.

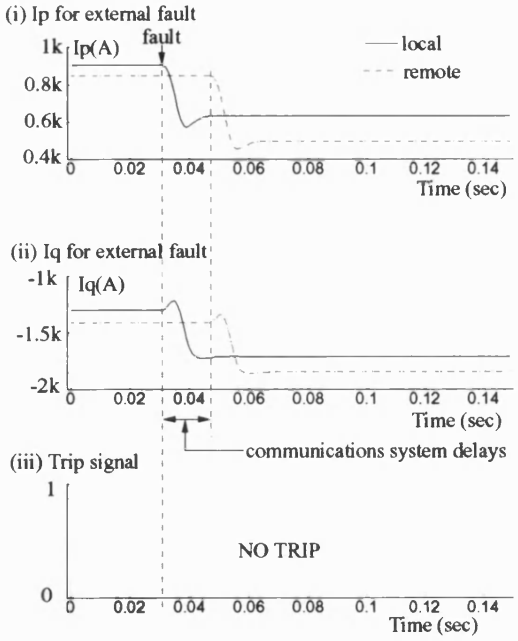

Figure 7.29 Polarised Currents for an External Single Phase Fault at point F1 on the Test System with Underground Feeders.

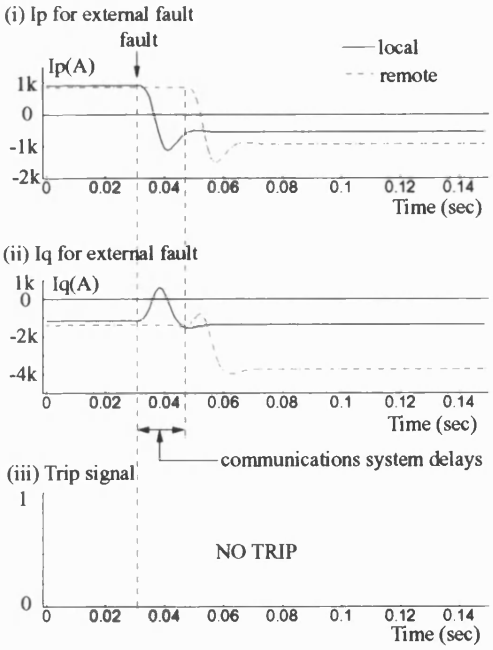

Figure 7.31 Polarised Currents for an External Two Phases to Earth Fault at point F1 on the Test System with Underground Feeders.

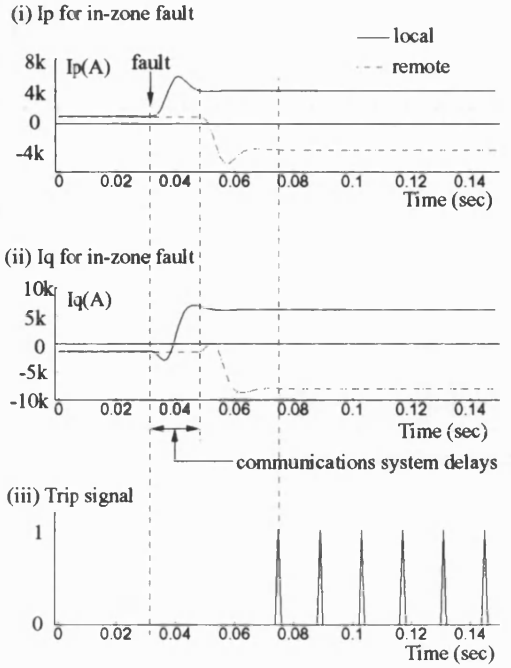

Figure 7.32 Polarised Currents for In-zone Two Phases Fault at point P1 on the Test System with Underground Feeders.

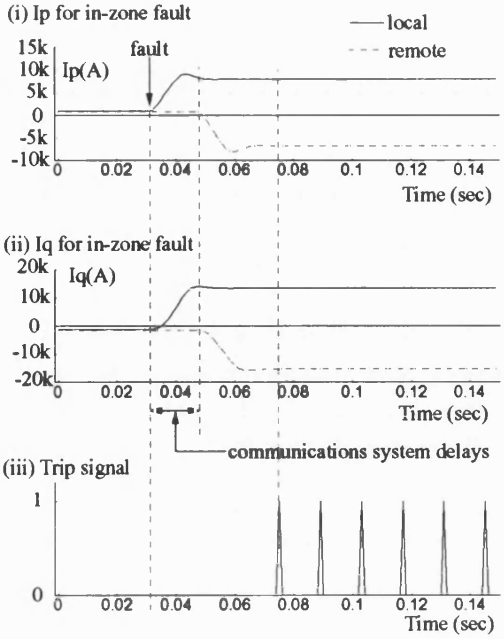

Figure 7.34 Polarised Currents for In-zone Three Phases to Earth Fault at point P1 on the Test System with Underground Feeders.

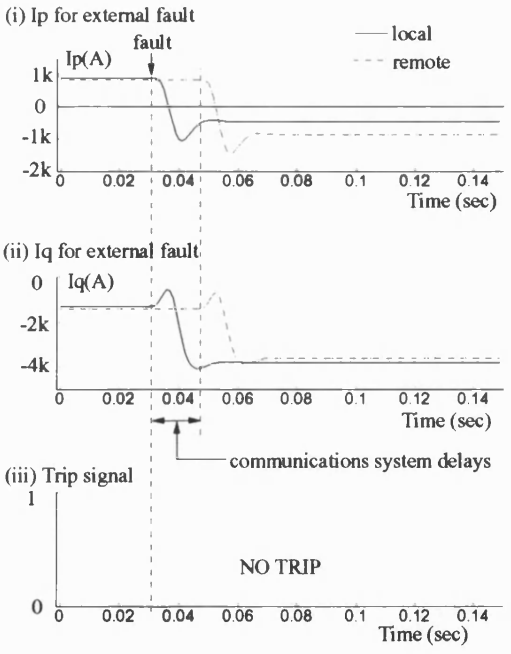

Figure 7.33 Polarised Currents for an External Two Phases Fault at point F1 on the Test System with Underground Feeders.

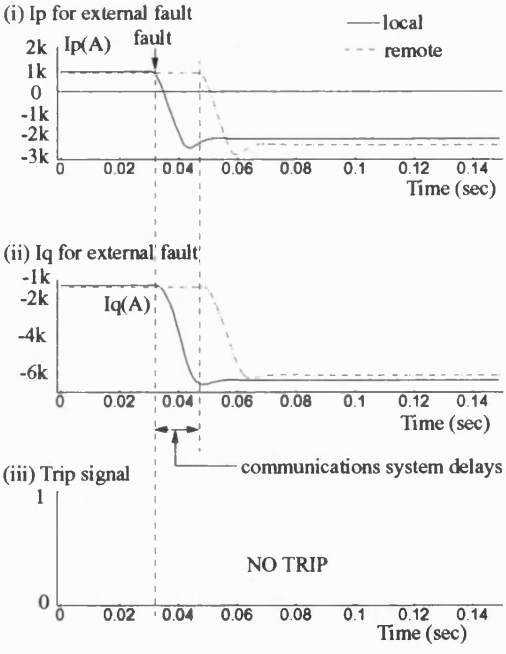

Figure 7.35 Polarised Currents for an External Three Phases to Earth Fault at point F1 on the Test System with Underground Feeders.

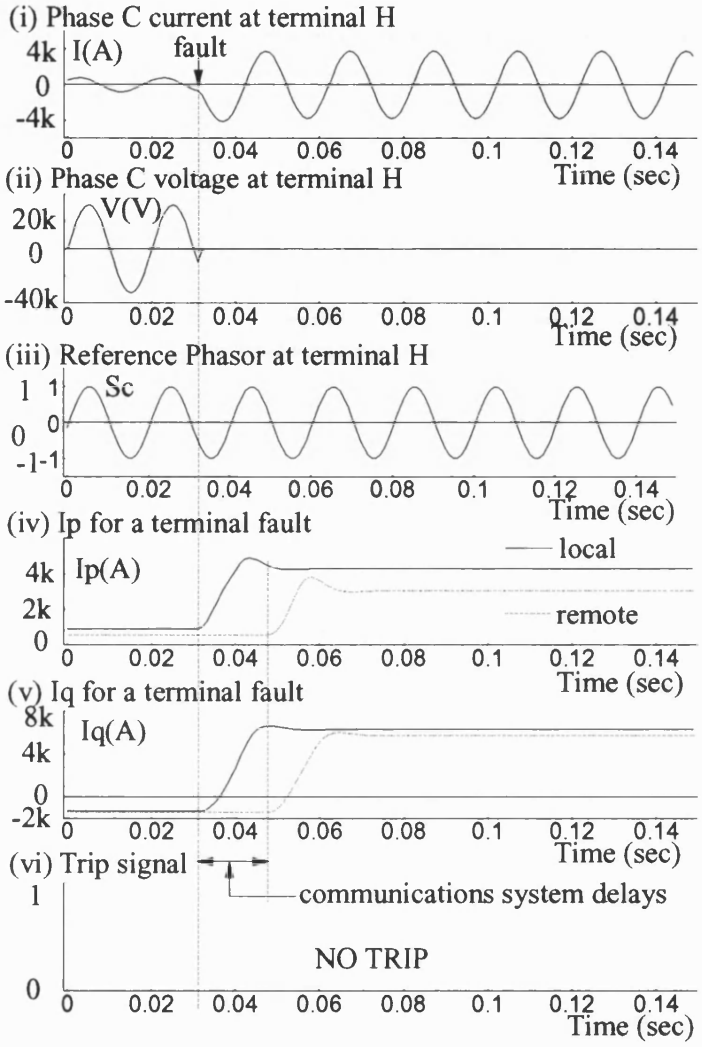

Figure 7.36 Input and Derived Waveforms for a Three Phase to Earth fault at terminal H on the Test System with Underground Feeders.

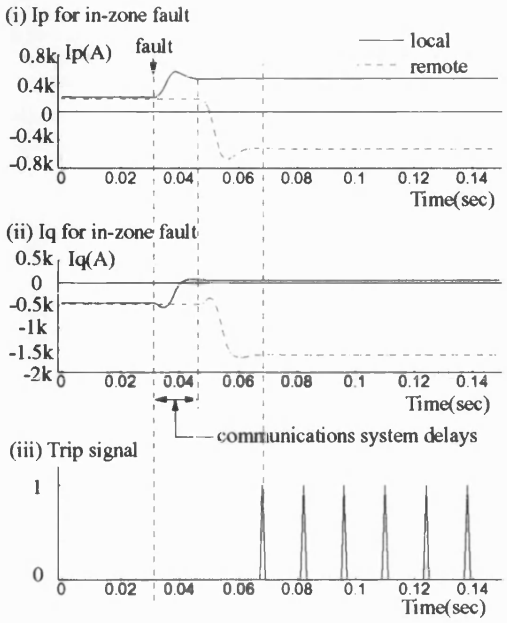

Figure 7.37 Polarised Currents for an In-zone Single Phase Fault at point P1 on the Test System with Composite Feeders.

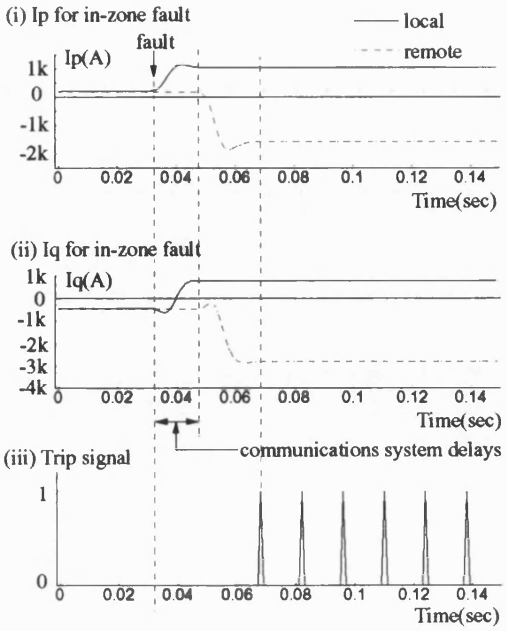

Figure 7.39 Polarised Currents for an In-zone Two Phases to Earth Fault at point P1 on the Test System with Composite Feeders.

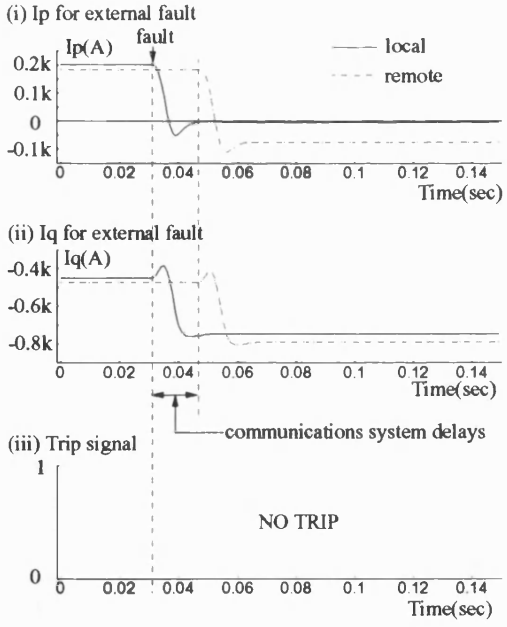

Figure 7.38 Polarised Currents for an External Single Phase Fault at point F1 on the Test System with Composite Feeders.

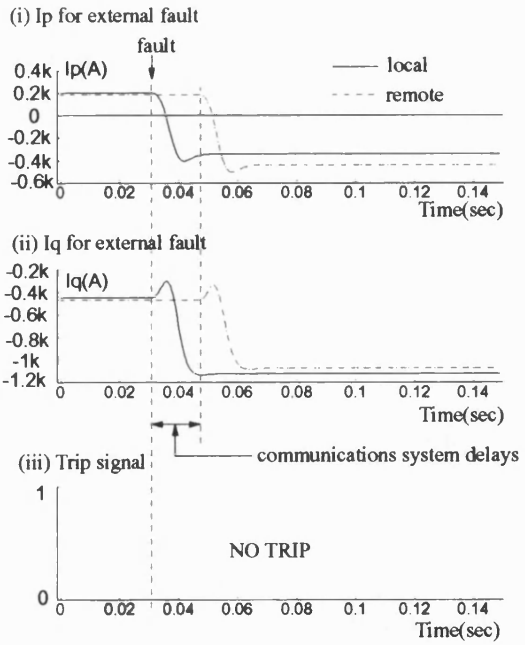

Figure 7.40 Polarised Currents for an External Two Phases to Earth Fault at point F1 on the Test System with Composite Feeders.

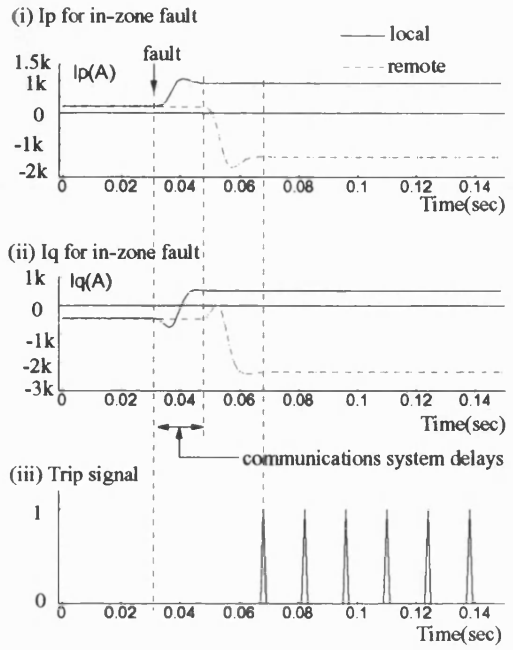

Figure 7.41 Polarised Currents for an In-zone Two Phases Fault at point P1 on the Test System with Composite Feeders.

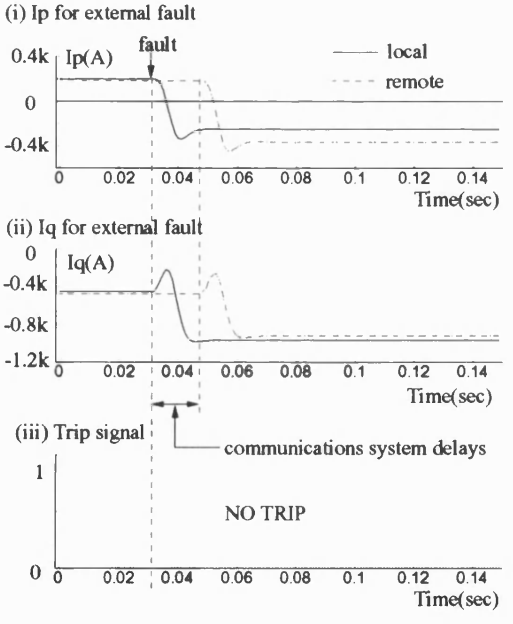

Figure 7.42 Polarised Currents for an External Two Phases Fault at point F1 on the Test System with Composite Feeders.

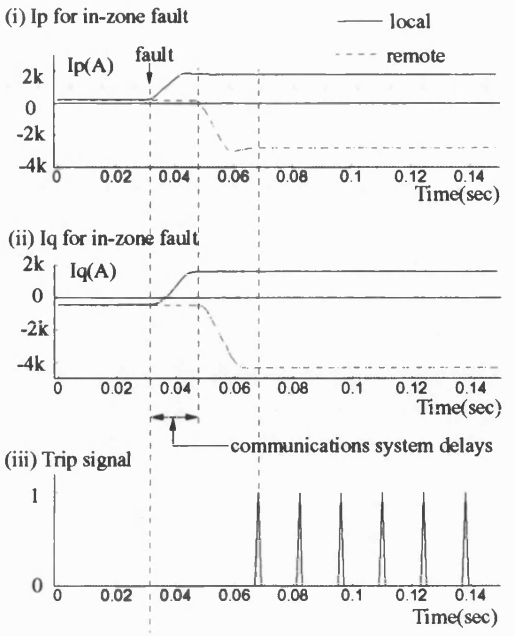

Figure 7.43 Polarised Currents for In-zone Three Phases to Earth Fault at point P1 on the Test System with Composite Feeders.

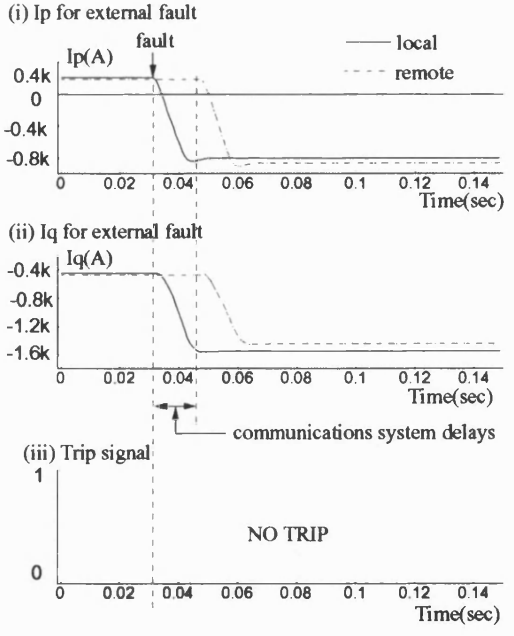

Figure 7.44 Polarised Currents for External three Phases to Earth Fault at point F1 on the Test System with Composite Feeders.

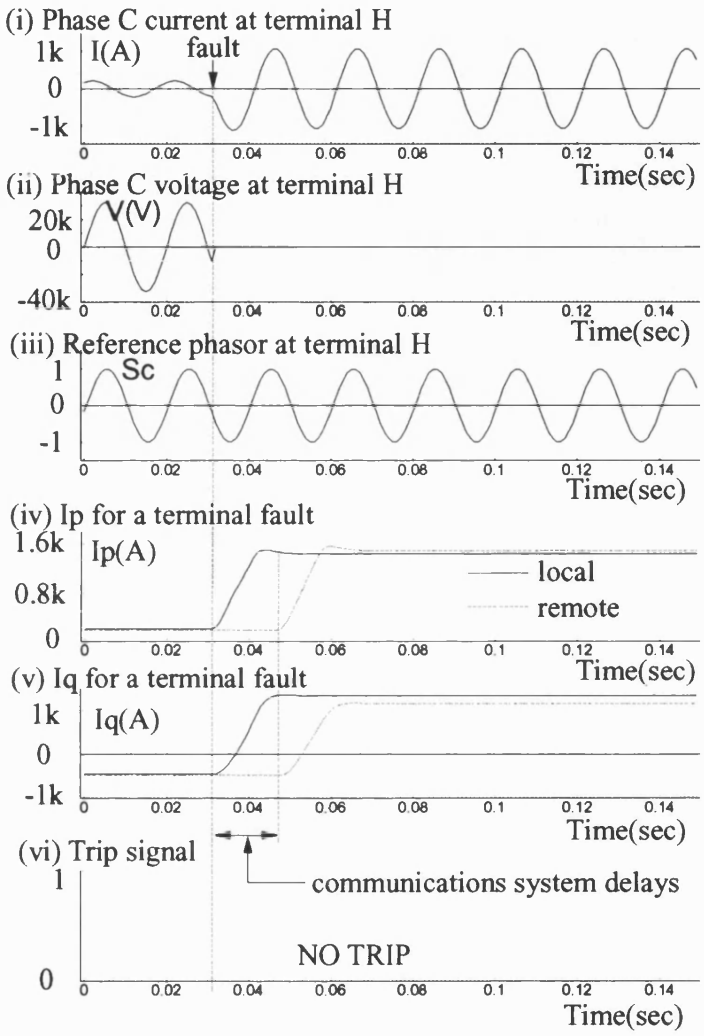

Figure 7.45 Input and Derived waveforms for a Three Phase to Earth fault at terminal H on the Test System with Composite Feeders.

Chapter 8

ALGORITHM EVALUATION WITH POLARISING REFERENCE PHASORS FROM POSITIVE PHASE SEQUENCE CURRENTS.

8.1 INTRODUCTION.

Although voltage transformers are usually present in a substation, it will be generally good to have such a protection that it does not depend on them in case of a vt failure for example. In the event that new vt's have to be installed to go with the scheme, this may make the scheme economically unattractive as vt's are expensive, especially so with the scheme targeting distribution feeder circuits.

An alternative method therefore uses positive phase sequence currents to derive the polarising reference. This chapter presents an evaluation of the performance of the algorithm with the polarising quantity derived from the positive phase sequence currents. The power system model is that of figure 6.5 described in chapter 6 and also used in the preceding chapter. Data transmission between the feeder terminals is also the same as that described above in chapter 3.

Studied were a variety of faults at various fault positions both inside and outside the zone of protection on feeder circuits individually comprising overhead lines, underground cables, and a combination of overhead lines and underground cables. Points on the parallel feeder and on the supply feeders were used for the external faults. Test results show that the algorithm is sensitive to all in-zone faults, producing relay trip outputs within two and half power system cycles after the fault. It restrained from tripping for all external faults including close-up faults.

A summary of a selection of the results is given below. The results are presented for unbalanced faults, which are the single phase and double phase faults, and balanced faults, which are faults that involve all the three phases. As in practical systems, the communications has not been synchronised to the fault, but has been made free running by randomising the start of each data transfer.

8.2 SEQUENCE COMPONENTS.

Electric power systems are essentially balanced or symmetrical from the generators to the point of single phase loading except in an area of a fault or unbalance[5]. In the balanced area,

- Positive phase sequence currents flowing in the network produce only positive phase sequence voltage drops.
- Negative phase sequence currents flowing in the network produce only negative phase sequence voltage drops.
- Zero phase sequence currents flowing in the network produce only zero phase sequence voltage drops.

However, all this is not true for any unbalance or asymmetrical condition where;

- Positive phase sequence current flowing in the unbalanced system produces positive, and negative, and possibly zero, phase sequence voltage drops.
- Negative phase sequence current flowing in the unbalanced system produces positive, negative, and possibly zero phase sequence voltage drops.
- Zero phase sequence current flowing in the unbalanced system produces all three phase sequence voltage drops.

Graphical representation of a balanced condition, as discussed in chapter 5 and illustrated in figure 5.2, can be re-illustrated for the graphical determination of zero phase sequence quantities. If the three phase values of, say currents, do not sum to zero vectorially, then a zero phase sequence component must be present. This scenario is explained in figure

8.1 where three such currents I_a, I_b, I_c are represented by vectors na, nb and nc, respectively. The line to line currents I_{ab}, I_{bc} and I_{ca} are then represented by vectors ba, cb, and ac respectively. If point n' is now determined as the centre of the triangle abc, the same line to line currents could result from the three phase currents I'_a, I'_b and I'_c, represented by vectors n'a, n'b and n'c, respectively. As I'_a, I'_b and I'_c contain only positive and negative sequence components and are the only possible solution for such phase currents having these line to line currents, they must contain the same positive and negative phase sequence components as the original phase currents I_a, I_b, and I_c[122]. Thus:-

$$\begin{aligned} I'_a &= I_{a1} + I_{a2} \\ I'_b &= I_{b1} + I_{b2} \\ I'_c &= I_{c1} + I_{b2}. \end{aligned} \qquad (8.1)$$

$$\begin{aligned} \textit{and} \qquad nn' &= I_a - I'_a \\ &= (I_{a0} + I_{a1} + I_{a2}) - (I_{a1} + I_{a2}) \\ &= I_{a0} \end{aligned}$$

Thus the vector nn' represents the zero phase sequence component of the phase currents. It is noted that the vectorial sum of the three line currents is always zero.

In the case where either the phase currents do not contain a zero phase sequence component or if the zero phase sequence component has been subtracted from the phase values, then figure 8.2[122] may be used to graphically illustrate the determination of positive and negative phase sequence components of the currents.

Using the h-operator, and in terms of the phase currents;

$$I_{a1} = \frac{1}{3} \left[I_a + hI_b + h^2 I_c \right] \qquad (8.2)$$

With zero phase sequence component absent,

$$I_a + I_b + I_c = 0,$$

$$\begin{aligned} I_{a1} &= \frac{1}{3}\left[I_a + hI_b + h^2(- I_a - I_b) \right] \\ &= \frac{1}{3}\left[I_a(1 - h^2) + I_b(h - h^2) \right] \\ &= \frac{1}{3}\left[I_a(\frac{3}{2} + j \frac{\sqrt{3}}{2}) + j\sqrt{3}\ I_b \right] \\ &= \frac{I_a}{2} + \frac{1}{\sqrt{3}}\left[\frac{I_a}{2} + I_b \right] \angle 90^\circ \end{aligned} \tag{8.3}$$

Similarly, the negative phase sequence component is;

$$\begin{aligned} I_{a2} &= \frac{1}{3}\left[I_a + h^2 I_b + hI_c \right] \\ &= \frac{1}{3}\left[I_a + h^2 I_b + h(- I_a - I_b) \right] \\ &= \frac{1}{3}\left[I_a(1 - h) + I_b(h^2 - h) \right] \\ &= \frac{1}{3}\left[I_a(\frac{3}{2} - j \frac{\sqrt{3}}{2}) - j\sqrt{3}\ I_b \right] \\ &= \frac{I_a}{2} - \frac{1}{\sqrt{3}}\left[\frac{I_a}{2} + I_b \right] \angle 90^\circ \end{aligned} \tag{8.4}$$

Graphically, the unbalanced vectors Ia, Ib and Ic may be drawn to form the closed triangle abc as in figure 8.2. The point r is such that;

$$cr = ra = \frac{I_a}{2} \tag{8.5}$$

Then vectorially,

$$rb = \frac{I_a}{2} + I_b \tag{8.6}$$

A triangle brs on br is such that

$$\angle sbr = 30^\circ, \quad and \quad \angle brs = 90^\circ$$

In such a triangle, the ratio of the length of the sides is:

$$rs : rb : sb = 1 : \sqrt{3} : 2 \tag{8.7}$$

In magnitude, therefore,

$$sr = \frac{rb}{\sqrt{3}} \tag{8.8}$$

Since the angle between rb and sr is 90 degrees, the vector relationship is

$$\begin{aligned} sr &= \frac{rb}{\sqrt{3}} \angle 90^\circ \\ &= \frac{1}{\sqrt{3}} \left[\frac{I_a}{2} + I_b \right] \angle 90^\circ \end{aligned} \tag{8.9}$$

The vector sa is now

$$\begin{aligned} sa &= sr + ra \\ &= \frac{1}{\sqrt{3}} \left[\frac{I_a}{2} + I_b \right] \angle 90^\circ + \frac{I_a}{2} \\ &= I_{a1} \end{aligned} \tag{8.10}$$

and the vector cs is

$$\begin{aligned} cs &= cr - sr \\ &= \frac{I_a}{2} - \frac{1}{\sqrt{3}} \left[\frac{I_a}{2} + I_b \right] \angle 90^\circ \\ &= I_{a2} \end{aligned} \tag{8.11}$$

The positive phase sequence sources are the rotating machines in the system[5]. As such the sequence components can be used to provide the desired polarising reference as they

are always present and synchronised to the power system waveforms. The positive phase sequence current is used in this chapter to provide the reference.

8.3 EXTRACTION OF I_{a1} TO FORM THE REFERENCE.

As in equation (8.2), and as discussed in chapter 3 under section 3.2.3 the positive phase sequence current I_1 is given as:-

$$I_1 = \frac{1}{3}\left[I_a + hI_b + h^2 I_c \right]$$

The h-operator in the equation has the effect of rotating the phasor by 120 degrees, the direction of rotation being anti-clockwise by convention. h square thus rotates by 240 degrees anti-clockwise, equivalent to rotating by 120 degrees clockwise. With sinusoidal waveforms, applying the operator is equivalent to shifting, or delaying, the waveform by 120 degrees and 240 for h and h square respectively. In terms of discrete sample values, with n_s samples per power system cycle, the instantaneous values of the positive phase sequence components were given in equation (3.13) of chapter 3 as

$$i_{a1} = \frac{1}{3}\left[i_{a,n} + i_{b,(n-\frac{2}{3}n_s)} + i_{c,(n-\frac{1}{3}n_s)} \right]$$

$$i_{b1} = \frac{1}{3}\left[i_{b,n} + i_{c,(n-\frac{2}{3}n_s)} + i_{a,(n-\frac{1}{3}n_s)} \right]$$

$$i_{c1} = \frac{1}{3}\left[i_{c,n} + i_{a,(n-\frac{2}{3}n_s)} + i_{b,(n-\frac{1}{3}n_s)} \right]$$

where n represents the instant that the last sample was taken. With n_s equals to 24 as the case here, the expression above becomes

$$i_{a1} = \frac{1}{3}\left[i_{a,n} + i_{b,(n-16)} + i_{c,(n-8)} \right]$$

$$i_{b1} = \frac{1}{3}\left[i_{b,n} + i_{c,(n-16)} + i_{a,(n-8)} \right] \qquad (8.12)$$

$$i_{c1} = \frac{1}{3}\left[i_{c,n} + i_{a,(n-16)} + i_{b,(n-8)} \right]$$

In other words, at each instant a positive phase sequence component on a phase is equal to a third of the sum of the corresponding phase signal, the next phase signal in the clockwise direction but delayed by 16 samples, and the remaining phase signal delayed by 8 samples. Thus it is imperative that the number of samples per cycle be divisible by three in order to effect phase delays of 120 and 240 degrees on the signals.

Hence i_{a1}, i_{b1} and i_{c1} are derived on phases a, b and c, respectively at each feeder's terminal.

8.4 ALGORITHM EVALUATION ON OVERHEAD LINE FEEDERS.

The same data cases were used as run when the polarising reference was derived from the three phase voltages in the preceding chapter.

As discussed above in chapter 3 under section 3.3.2, a nominal transmission delay time of 17 milliseconds is introduced between transmitting a signal at one terminal and receiving it at the other. At the local terminal, the delay is compensated for by comparing the received signal with a corresponding local signal delayed by the nominal transmission time.

A simple current differential could be used where the positive phase sequence

components are directly used as the reference. At each feeder's terminal the quantities i_{a1}, i_{b1} and i_{c1} can be directly equalled to the reference phasors s_a, s_b and s_c respectively. The corresponding current measurements I_p and I_q in this case have their units as 'amps squared'. The sequence currents i_{a1}, i_{b1} and i_{c1} can firstly be divided by their maximum value to have the resulting reference phasors with a maximum value of unity. In this case, the corresponding current measurements I_p and I_q will have their units as amps. Either way the reference phasors are disjointed at the instant of the fault and are therefore not sinusoidal. As this polarising reference follows the instantaneous current, there will be no orthogonal component, and therefore the quantity I_q is zero. Only at the point of fault occurrence will there be a significant amount of I_q due to the moving average filter for a period lasting one cycle window. This is illustrated in figure 8.3. One point to note here then is that there is no need to compare I_q in the algorithm.

This simple self polarising method has flaws. As it essentially uses i^2, there are problems with mid-zone faults when contributions of current from the feeder's terminals are the same resulting in no trip conditions. There will be no clear-cut difference between local and remote values after the fault between in-zone and external faults as both will result in current measurement flows in the positive directions. This is illustrated in figure 8.4 for a typical in-zone fault and figure 8.5 for a typical external fault.

Therefore, for the current polarised algorithm, memory assisted current polarised reference phasors were used as have been described in chapter 3. These unit amplitude phasors were derived from I_{a1}, I_{b1} and I_{c1} as described above and a 120 millisecond memory feature was provided by the phase lock loop. The fault currents are therefore locked to the pre-fault positive phase sequence current waveform. This ensures the use of a continuous sinusoidal reference. In this case, with reference to the polarising phasors, an in-zone fault will result in the remote signal flowing in the opposite direction to that before the fault. External faults will result in the local and remote current

measurements flowing in the same direction. The results below illustrate this phenomenon. There is a nominal load current measurement I_p equals 252 Amps. Trip settings of 100 Amps for both $I_{p\text{-}min}$ and $I_{q\text{-}min}$ with the bias settings k_1 and k_2 set at 2 percent satisfy the various fault conditions studied.

8.4.1 SINGLE PHASE FAULTS.

The first series of faults to be studied were those that involve only a single phase. Figure 8.6 shows the input and derived waveforms for a mid-zone fault, clearly indicating the fault inception time. Both Ip and Iq are constants, confirming equations (3.4) and (3.6). Within 20 milliseconds after the fault, both Ip and Iq have settled to new steady values.

Figure 8.7 shows the comparisons between the locally obtained Ip and Iq signals to those received from the remote end of the feeder for a typical in-zone fault. The delays between the two signals which are caused by the communications system delays are shown and also shown are the differences between the measurements during the fault. It is noted that due to the fault the current measurement at the remote terminal flows in the opposite direction to that of the local terminal. The fault results in Ip equals to 362 Amps for the local terminal and 141 Amps for the remote terminal. It also results in Iq equals to 1064 and -1058 Amps for the local and remote terminals, respectively. Using the trip requirement of two subsequent trip indications leads to a trip time of 40.817 milliseconds. The spikes in the trip signal confirms that, as long as the in-zone fault is present, the algorithm always gives a 'yes trip' decision and produces a trip output every time it makes a comparison between the local and remote signals.

Figure 8.8 shows the comparisons between the locally obtained Ip and Iq signals to those received from the remote terminal for a typical external fault. It is noted that, unlike in the in-zone fault condition, the direction of flow of the measurements is the same after

the fault for the local and remote terminals. For this condition, the Ip and Iq currents are relatively small and there is insignificant difference between the local and remote signals with reference to the trip setting. For this fault, the algorithm remains stable and does not trip.

8.4.2 DOUBLE PHASE FAULTS.

The response to a double phase to earth in-zone fault is illustrated in figure 8.9. The differences between the local and remote Ip and Iq led to the algorithm producing a trip output 39.151 milliseconds after the fault. The algorithm keeps producing a trip output whenever it compares the remote and local signals as long as the fault is present, and this is illustrated by the train of spikes in the trip signal.

The response to a similar fault but external to the protected zone is shown in figure 8.10. For this fault condition, the algorithm remained stable and did not trip.

The response of the algorithm to an in-zone phase to phase fault without earth is presented in figure 8.11. The differences between the local and remote Ip and Iq led to the algorithm tripping after 41.65 milliseconds. The response to a similar fault but external to the protected zone is shown in figure 8.12. For this condition, the algorithm remained stable and did not trip.

8.4.3 THREE PHASE FAULTS.

Similar to above, the responses to in-zone and external three phase to earth faults are illustrated in figures 8.13 and 8.14, respectively. For these conditions, the in-zone fault resulted in the algorithm producing a trip output after 40.817 milliseconds. The algorithm remained stable and did not trip for the external fault.

The algorithm was evaluated for a fault at the remote terminal. The corresponding signals are presented in figure 8.15. The disturbance did not cause the algorithm to produce a trip output.

Fault conditions close to a relaying terminal were also studied. Fault conditions were introduced 100 metres from the terminal both inside and external to the protected zone. Figure 8.16 shows the response to such a fault condition inside the protected zone. This condition resulted in the algorithm producing a trip output after 39.151 millisecond. The response to the external fault is shown in figure 8.17. This condition did not cause any trip.

Point-on-wave at fault was considered. A typical response to such a fault condition at 54 degrees on the wave, inside the protected zone, is illustrated in figure 8.18. This condition caused the algorithm to trip after 42.483 milliseconds. Figure 8.19 is for the response to a similar fault condition but external to the protected zone. For this fault condition, the algorithm remained stable and did not produce a trip output.

As a summary of the trip response of the algorithm for a typical in-zone fault condition on a system with overhead line feeders, 100 simulation were run using the most common fault condition which is the single phase fault. Figure 8.20 is the histogram showing the total number of trips against trip times. The trip times lie inside one and half to two and half power system cycles after the fault. A similar number of runs for an external fault did not produce a trip indication.

8.5 ALGORITHM EVALUATION ON UNDERGROUND CABLE FEEDERS.

There is a nominal load Ip of 1152 Amps. An in-zone single phase fault results in Ip equals to 1350 Amps and 949 Amps for the two terminals with Iq equals to 2328 Amps

and -1394 Amps. An external single phase fault condition results in Ip equals to 1182 Amps for both terminals with Iq equals to -230 and -248 Amps for the two terminals. An in-zone three phase to earth fault results in Ip equals to 3674 Amps and -1450 Amps for the two terminals with Iq equals 19287 and -18391 Amps. All these results are clearly illustrated in the figures below. Setting $I_{p\text{-}min}$ and $I_{q\text{-}min}$ both at 750 Amps and k_1 and k_2 at 6 percent satisfies the trip conditions.

8.5.1 SINGLE PHASE FAULTS.

As with the case with overhead lines, the first series of faults to be studied were those that involve only a single phase. Firstly, an in zone single phase fault was introduced. Figure 8.21 shows the comparisons between the locally obtained Ip and Iq signals to those received from the remote terminal. There are dramatic differences between the local and remote measurements after the fault. The algorithm produces a trip output after 41.65 milliseconds.

The response to a typical single phase fault external to the protected zone is shown in figure 8.22. For this condition, the measurements did not cause the algorithm to produce a trip output.

8.5.2 DOUBLE PHASE FAULTS.

The response to a double phase to earth fault inside the protected zone is summarised in figure 8.23. The differences between the local and remote Ip and Iq led to the algorithm tripping after 44.149 milliseconds. However, the algorithm did not produce a trip output for a similar fault condition but external to the protected zone whose typical response is shown in figure 8.24.

The response curves for an in-zone double phase fault without earth is given in figure 8.25. The differences between the local and remote current measurements Ip and Iq resulted in the trip output of the algorithm after 45.815 milliseconds. A typical response to a similar fault but outside the protected zone is shown in figure 8.26. The algorithm remained stable for this fault condition and did not produce a trip output.

8.5.3 THREE PHASE FAULTS.

As above, the responses to in-zone and external faults that involve all three phases are illustrated in figures 8.27 and 8.28 respectively. The in-zone fault resulted in tripping after 39.984 milliseconds. For the external fault, the algorithm remained stable and did not trip.

The performance of the algorithm on a fault at the terminal was evaluated. The response of the algorithm for such a fault is illustrated in figure 8.29. The algorithm remained stable and did not trip.

A summary of the performance of the algorithm for faults on a system with underground cable feeders is illustrated in figure 8.30. This figure is a histogram of number of trips versus trip times for 100 simulation runs for a typical single phase in-zone fault. Tripping occurs within one and half and two and a half power system cycles. There was not tripping for a similar fault but external to the protected zone.

8.6 ALGORITHM EVALUATION ON COMPOSITE FEEDERS.

As feeders in distribution systems may consist of both overhead lines and underground cables, this section presents the responses of the algorithm for such networks. For simplicity as mentioned in chapter 6, equal lengths of sections of overhead lines and

underground cables were used. There was a nominal load current measurement Ip equals to 330 Amps. Trip conditions were satisfied with both $I_{p\text{-}min}$ and $I_{q\text{-}min}$ set at 200 Amps and k_1 and k_2 both set at 6 percent. A summary of the results is given below.

8.6.1 SINGLE PHASE FAULTS.

Similar to above cases, the first series of faults to be studied were those that involve only a single phase. An in-zone single phase fault was introduced. Figure 8.31 shows the comparisons between the locally obtained Ip and Iq signals to those received from the remote end of the feeder. The differences between the local and remote measurements after the fault led to the algorithm tripping after 44.149 milliseconds.

A typical single phase fault external to the protected zone results in the responses summarised in figure 8.32. For this fault condition, the algorithm remained stable and did not trip.

8.6.2 DOUBLE PHASE FAULTS.

The response curves for a double phase to earth in-zone fault are shown in figure 8.33. The differences between the local and remote Ip and Iq led to the algorithm producing a trip output after 39.151 milliseconds. A typical response to a similar fault but external to the protected zone is shown in figure 8.34. The algorithm remained stable and did not trip for this fault condition.

The response to a double phase in-zone fault without earth is illustrated in figure 8.35. The differences between the local and remote Ip and Iq led to the algorithm tripping after 41.65 milliseconds. Figure 8.36 illustrates the responses to a similar fault but external to the protected zone. For this fault condition, the algorithm did not trip.

8.6.3 THREE PHASE FAULTS.

Similarly, the response to an in-zone three phases to earth fault is given in figures 8.37. For this fault condition, the algorithm produced a trip output at 37.485 milliseconds. Figure 8.38 illustrates the response to a three phases to earth fault external to the protected zone. This fault resulted in the algorithm remaining stable and not producing a trip output.

As above, the response of the algorithm to a fault at the terminal is illustrated in figure 8.39. For this fault condition, the algorithm remained stable and did not trip.

As a summary and considering the most common fault conditions on feeder circuits, figure 8.40 is a histogram showing number of trips against trip times for 100 simulation runs of an in-zone single phase fault on the system with composite feeders. The trip times are nearly all under two and half power system cycles after the fault. Only one simulation run resulted in a trip time of 51.646 milliseconds. This was when communications started soon after the fault.

8.7 SUMMARY.

It has been the objective of the research to formulate a current differential protection algorithm that accommodates the modest communications capabilities associated with a robust digital data voice frequency communications channel. The method of using positive phase sequence current to provide the polarising reference phasor used to derive a polarised measurement of the three phase currents offers an effective means of achieving this. One attractive feature in using the positive phase sequence components is that the method still retains the advantage of current differential protection of not using VTs.

Feeders that may exist in a network were modelled. They included those with only overhead lines, with only underground cables, and those with a mixture of both overhead lines and underground cables. A variety of faults were considered at different fault positions. Applied within and outside of the protected zone, these faults involved single phases, double phases and three phases.

Communications would normally be free running and not synchronised with the fault. This was simulated by randomising the start of a simulation run. As in the preceding chapter the variations in the synchronism between fault occurrence and data transmission meant that the tripping times vary within 13.33 milliseconds, as discussed in chapter 3. For the fault conditions presented for which the algorithm should trip, the tripping times were less than 50 milliseconds for in-zone faults. For all external faults, including a terminal fault, the algorithm remained stable and did not trip.

To emphasize the fact that the trip times for in-zone faults are within two and half power system cycles, multiple simulation runs were used and the results were illustrated in the histograms of number of trips plotted against trip times.

8.8 FIGURES.

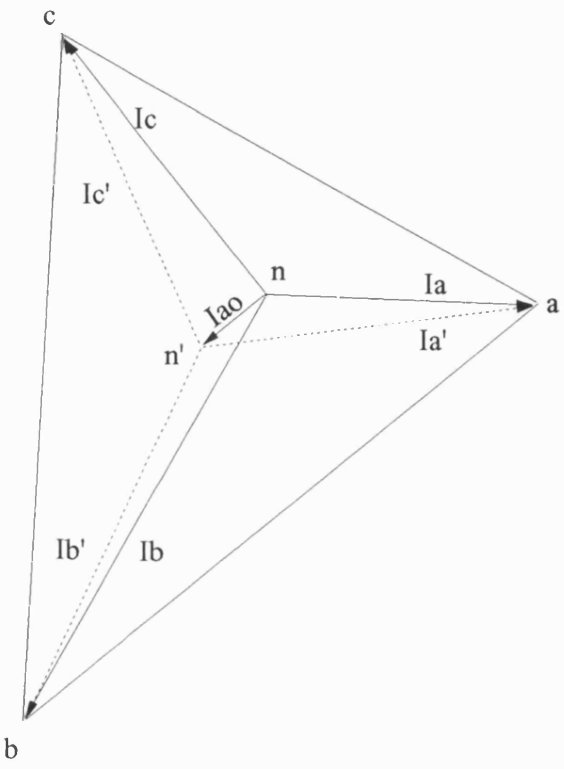

Figure 8.1 Zero Phase Sequence Current graphical determination.

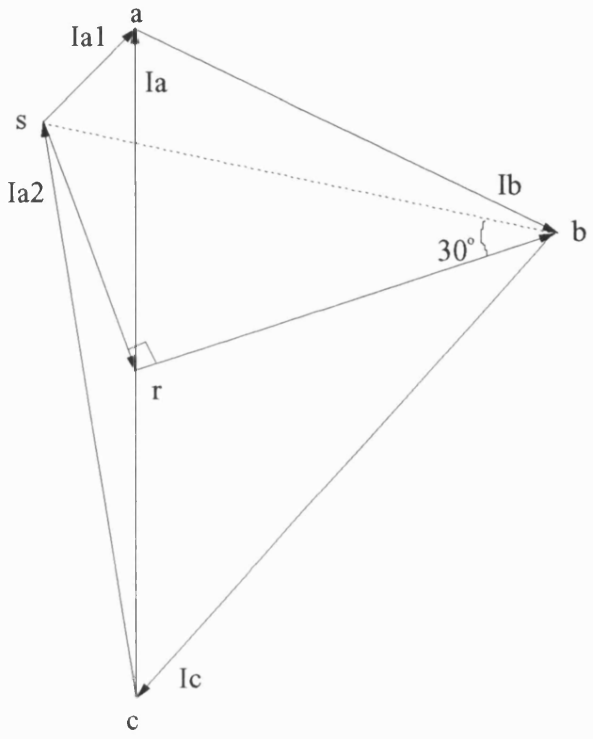

Figure 8.2 Positive and Negative Phase Sequence Current graphical determination.

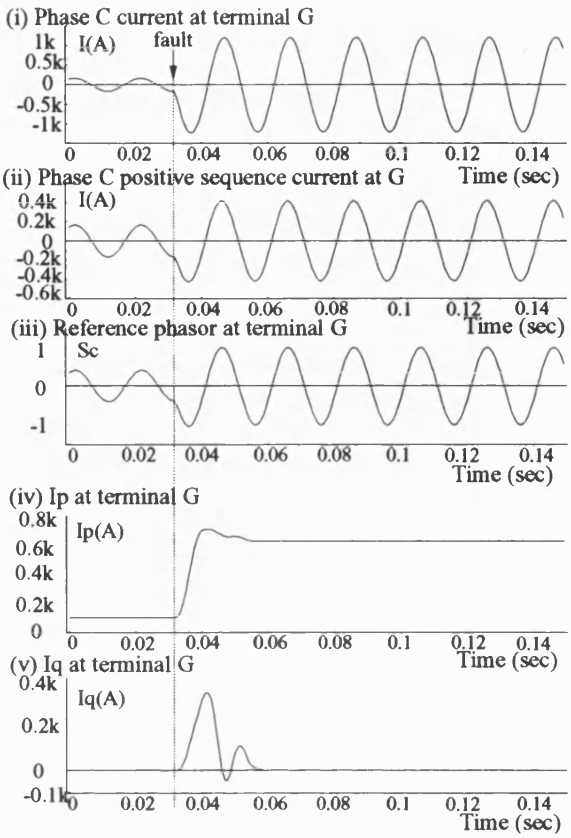

Figure 8.3 Input and Algorithm Derived waveforms for an In-zone Single Phase Fault on the System with Overhead Line Feeders for the simple differential scheme using self polarising method.

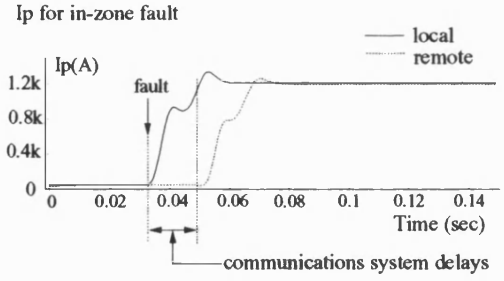

Figure 8.4 Polarised Currents for a typical mid-zone fault on the System with Overhead Line Feeders for the simple differential scheme using self polarising method.

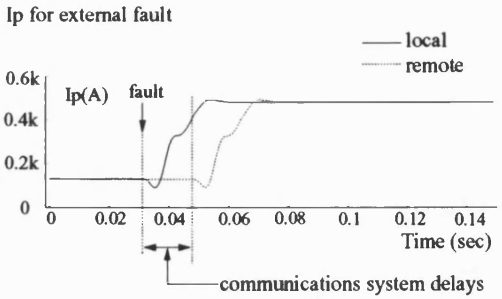

Figure 8.5 Polarised Currents for a typical external fault on the System with Overhead Line Feeders for the simple differential scheme using self polarising method.

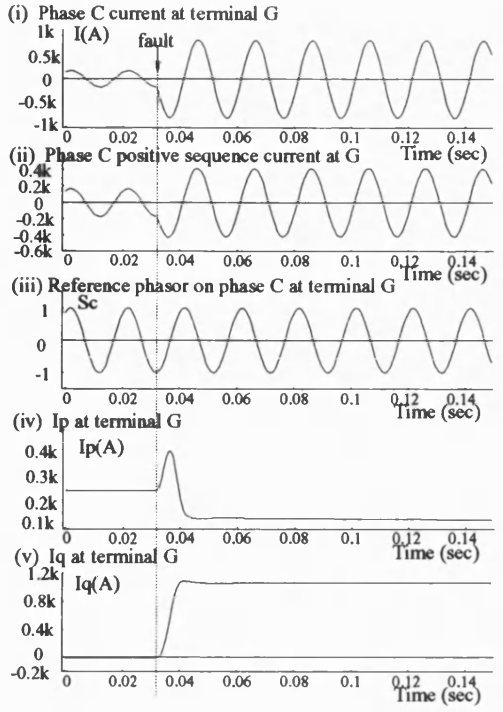

Figure 8.6 Input and Derived waveforms for an In-zone Single Phase fault on the Test System with Overhead Line Feeders.

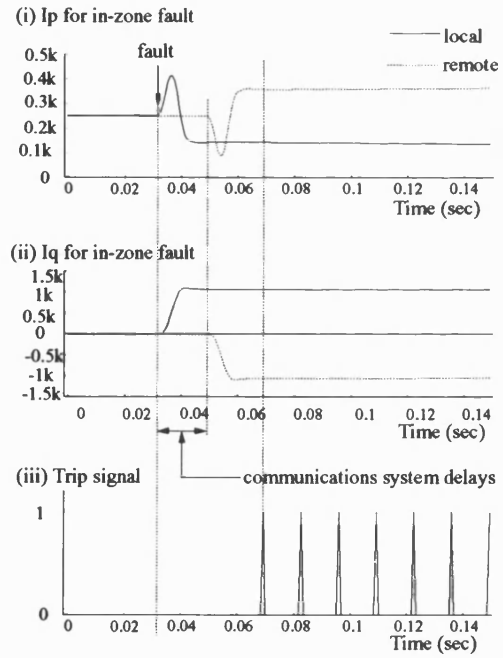

Figure 8.7 Polarised Currents for an In-zone single phase fault on the Test System with Overhead Line Feeders.

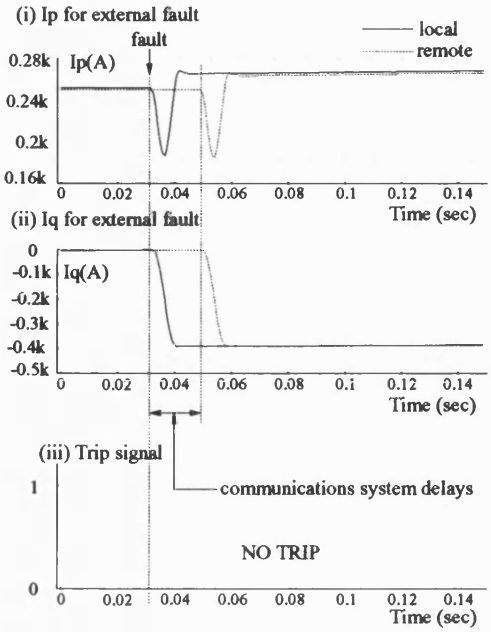

Figure 8.8 Polarised Currents for an External single phase fault on the Test System with Overhead Line Feeders.

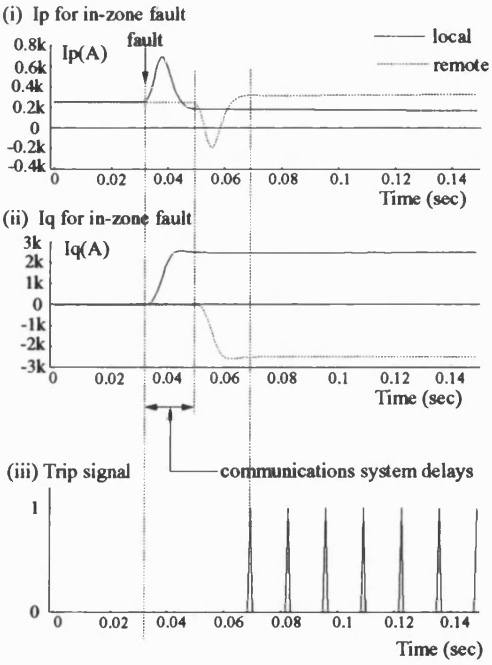

Figure 8.9 Polarised Currents for an In-zone double phase to earth fault on the Test System with Overhead Line Feeders.

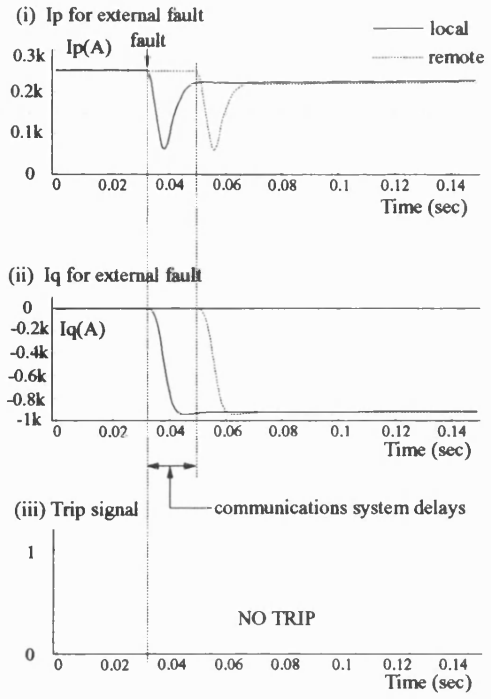

Figure 8.10 Polarised Currents for an External double phase to earth fault on the Test System with Overhead Line Feeders.

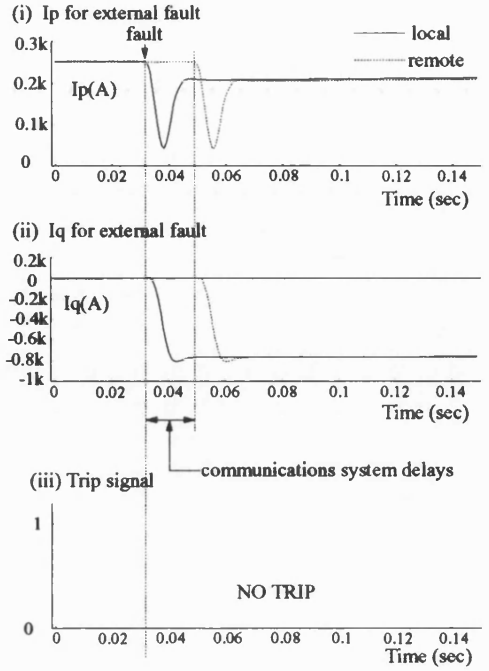

Figure 8.12 Polarised Currents for an External double phase fault, no earth, on the Test System with Overhead Line Feeders.

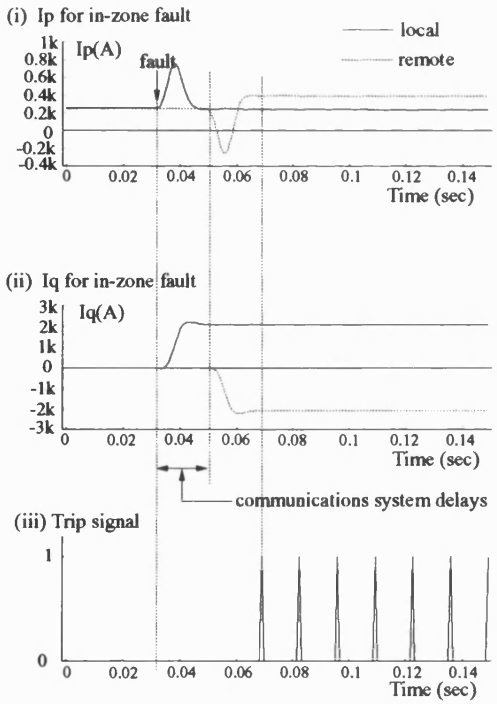

Figure 8.11 Polarised Currents for an In-zone double phase fault, no earth, on the Test System with Overhead Line Feeders.

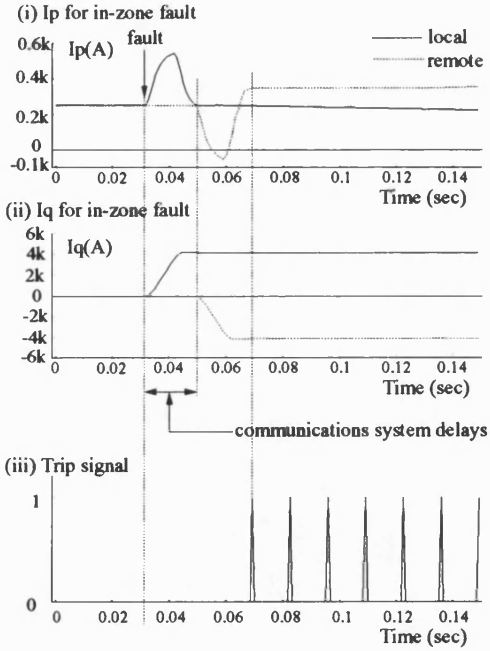

Figure 8.13 Polarised Currents for an In-zone three phases to earth fault on the Test System with Overhead Line Feeders.

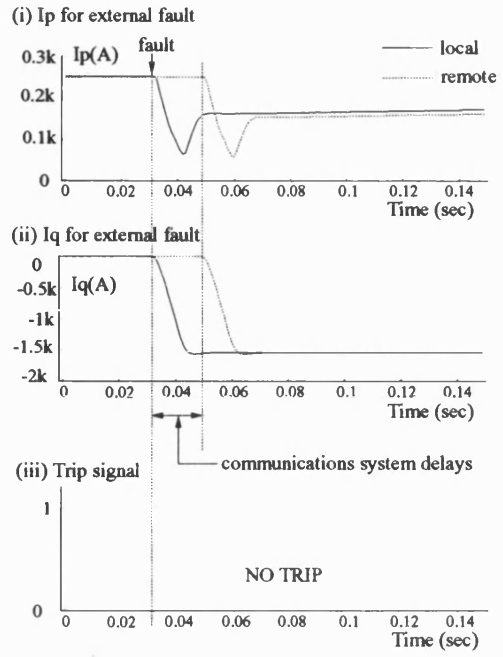

Figure 8.14 Polarised Currents for an External three phases to earth fault on the Test System with Overhead Line Feeders.

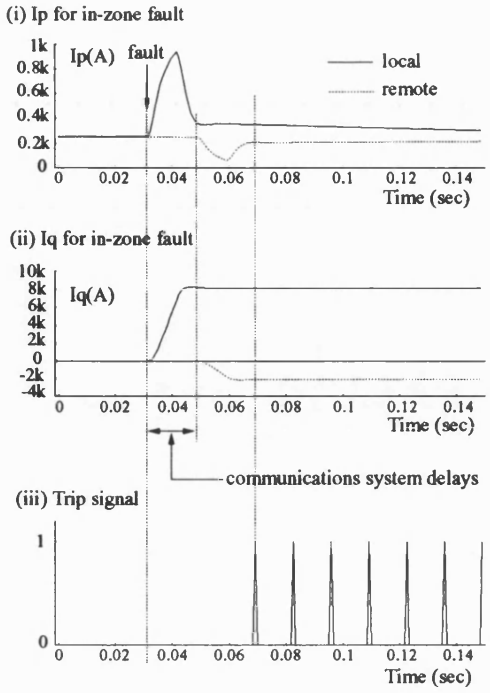

Fig 8.16 Polarised Currents for In-zone three phase to earth fault 100 metres from terminal on the System with Overhead Line Feeders.

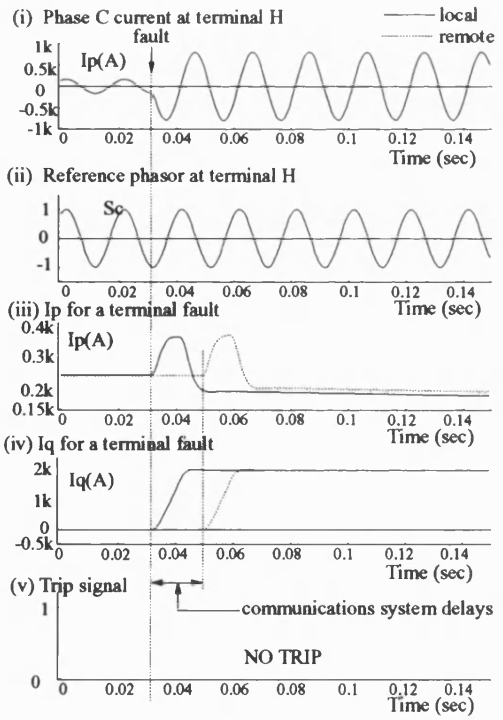

Figure 8.15 Input and Derived waveforms for a three phases to earth fault at terminal H on the Test System with Overhead Line Feeders.

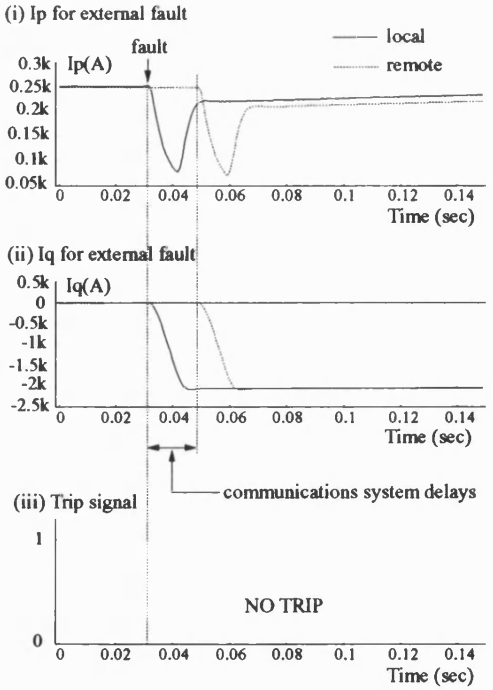

Fig 8.17 Polarised Currents for external three phase to earth fault 100 metres from terminal on the System with Overhead Line Feeders.

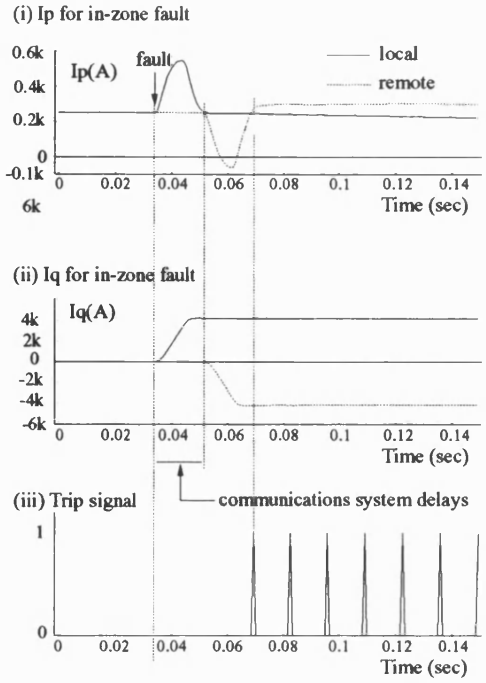

Fig 8.18 Polarised Currents for varied point-on-wave In-zone three phase to earth fault on System with Overhead Line Feeders.

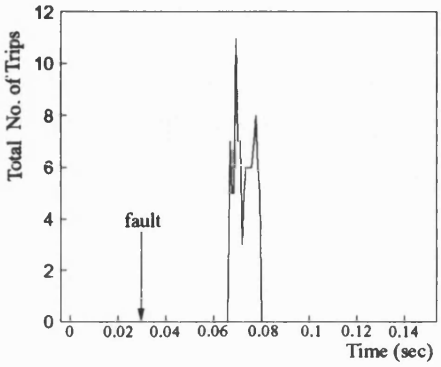

Fig 8.20 Histogram of Trip Response Summary of In-zone faults on System with Overhead Line Feeders using 100 simulation runs.

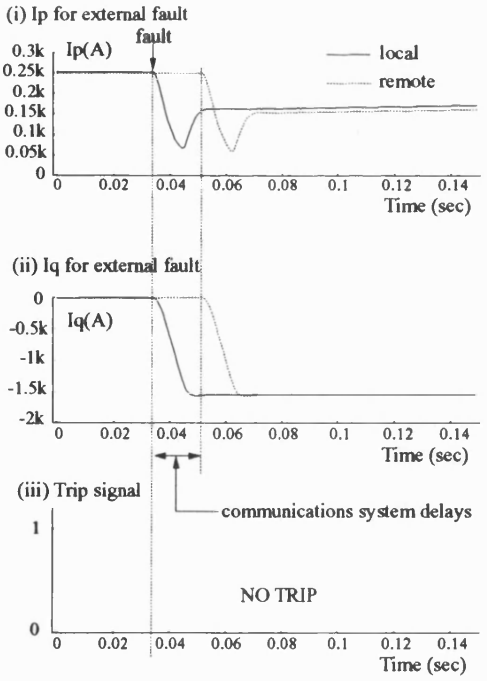

Fig 8.19 Polarised Currents for varied point-on-wave External three phase to earth fault on System with Overhead Line Feeders.

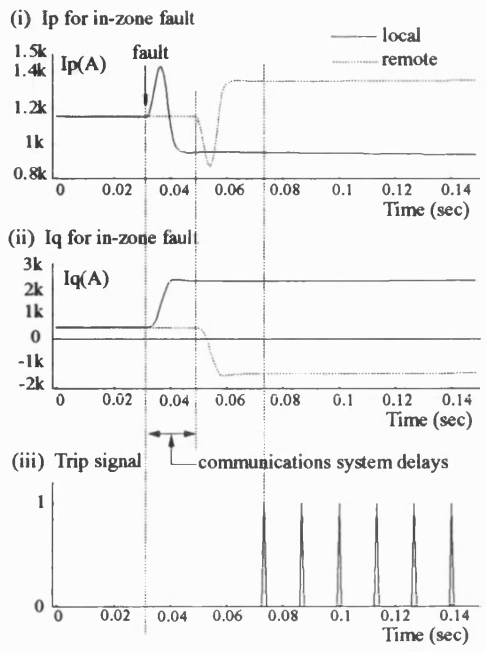

Figure 8.21 Polarised Currents for an In-zone single phase fault on the Test System with Underground Feeders.

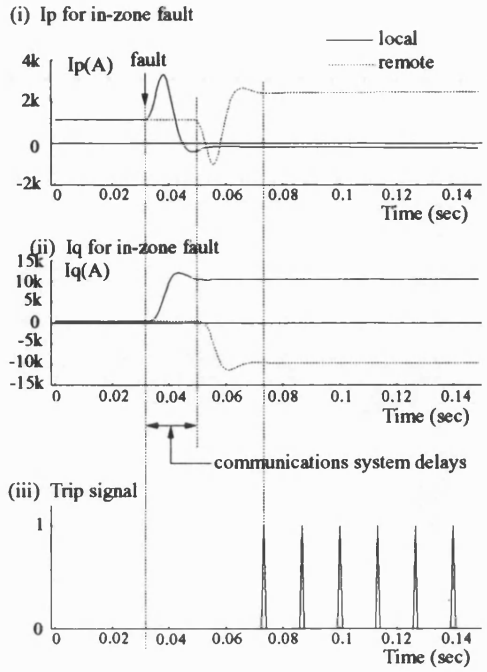

Figure 8.23 Polarised Currents for an In-zone double phase to earth fault on the Test System with Underground Feeders.

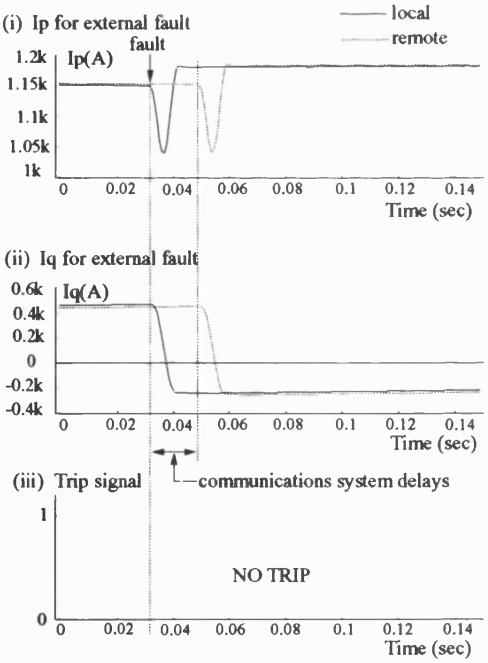

Figure 8.22 Polarised Currents for an External single phase fault on the Test System with Underground Feeders.

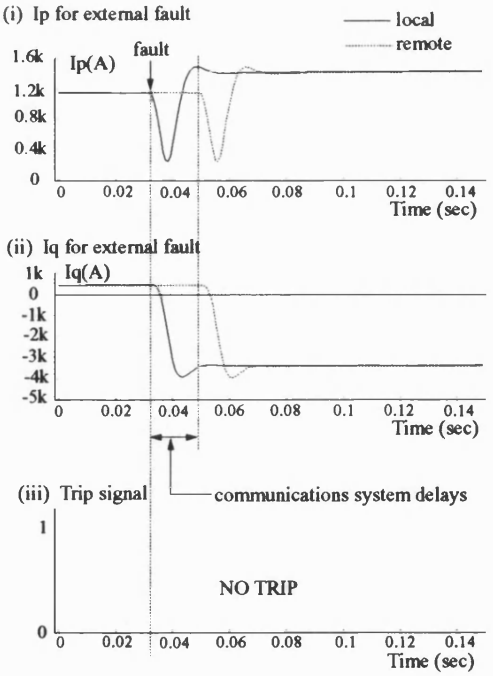

Figure 8.24 Polarised Currents for an External double phase to earth fault on the Test System with Underground Feeders.

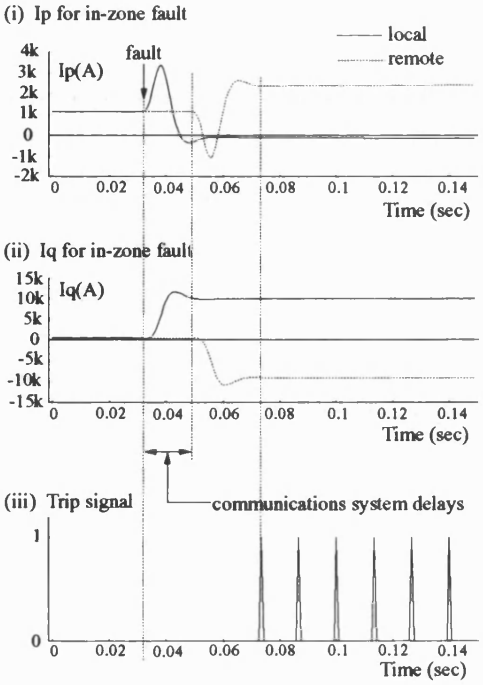

Figure 8.25 Polarised Currents for an In-zone double phase fault, no earth, on the Test System with Underground Feeders.

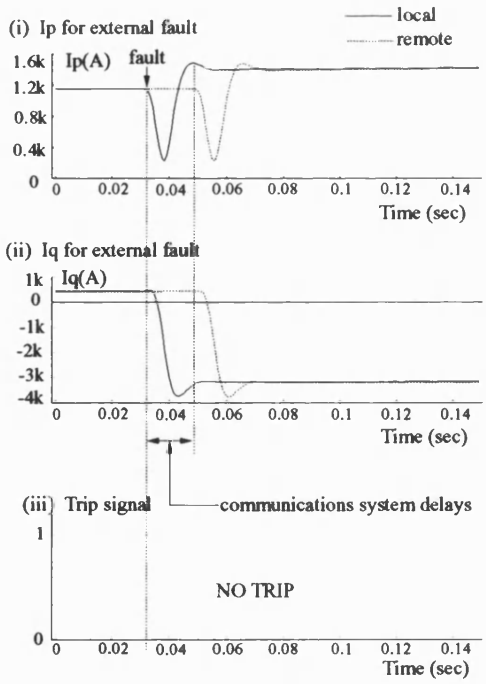

Figure 8.26 Polarised Currents for an External double phase fault,no earth, on the Test System with Underground Feeders.

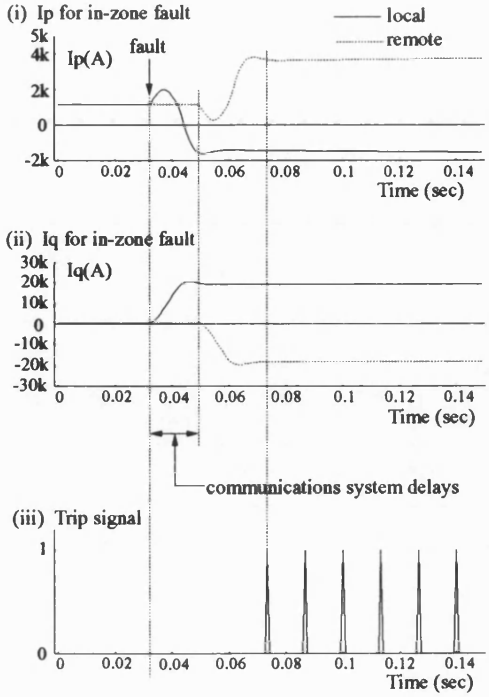

Figure 8.27 Polarised Currents for an In-zone three phases to earth fault on the Test System with Underground Feeders.

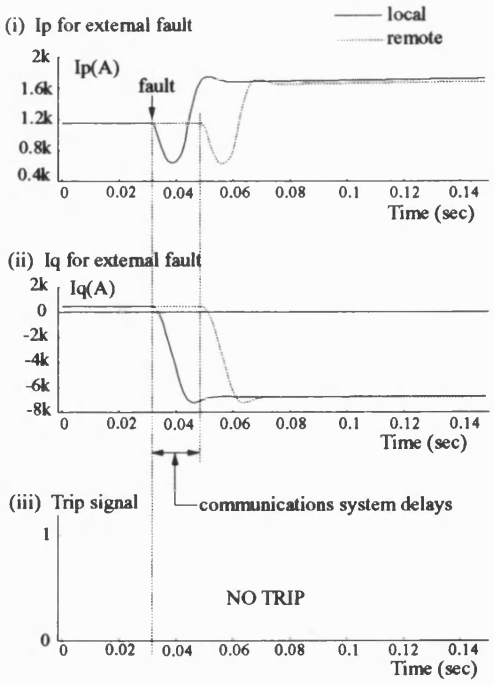

Figure 8.28 Polarised Currents for an External three phases to earth fault on the Test System with Underground Feeders.

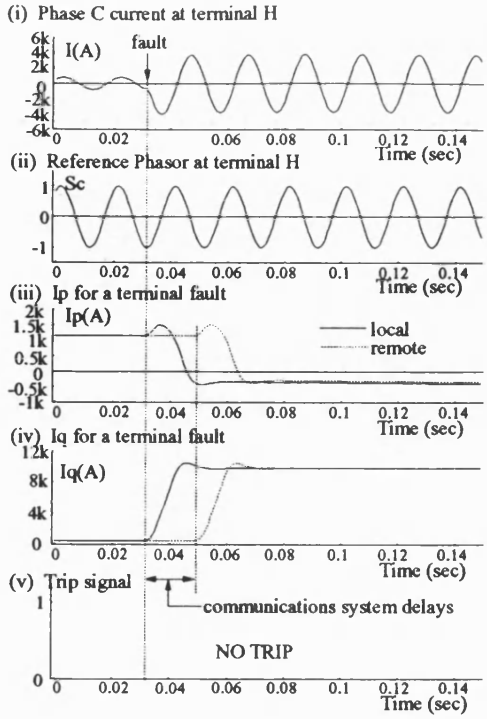

Figure 8.29 Input and derived waveforms for a Three Phase to earth fault at terminal H on the Test System with Underground Feeders.

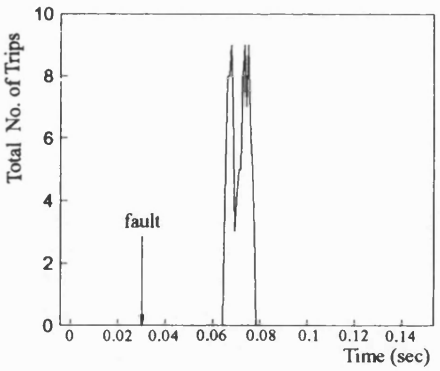

Figure 8.30 Histogram of Trip Response Summary of In-zone faults on System with Underground Feeders using 100 simulation runs.

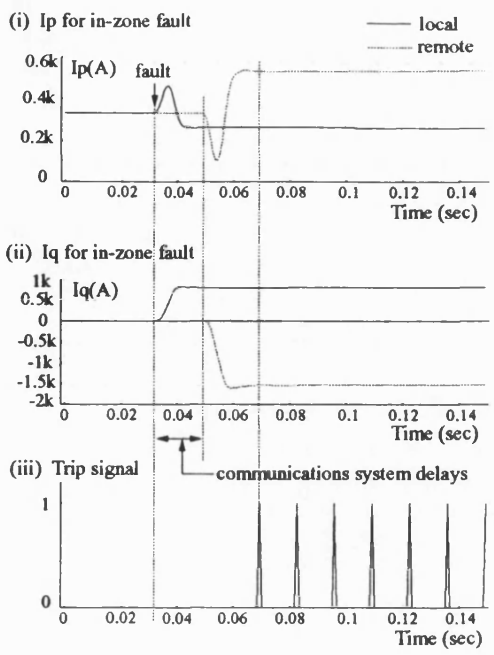

Figure 8.31 Polarised Currents for an In-zone single phase fault on the Test System with Composite Feeders.

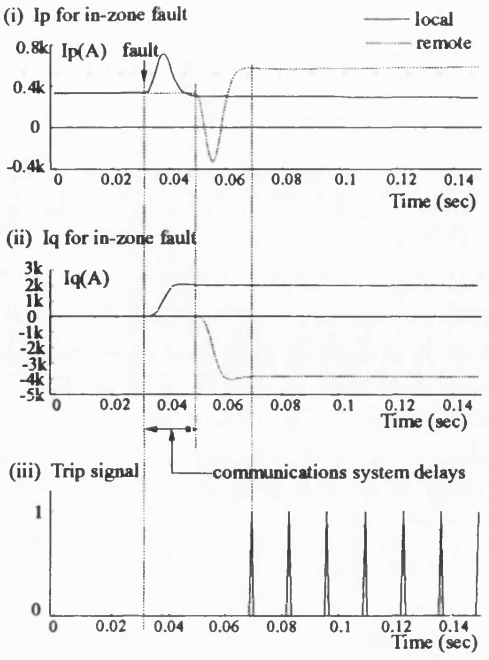

Figure 8.33 Polarised Currents for an In-zone double phase to earth fault on the Test System with Composite Feeders.

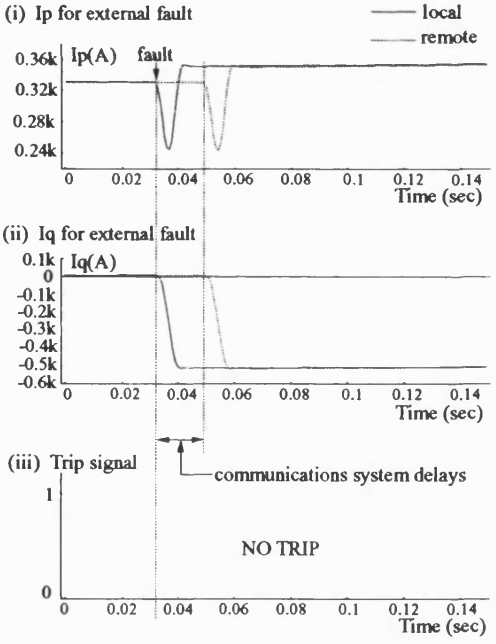

Figure 8.32 Polarised Currents for an External single phase fault on the Test System with Composite Feeders.

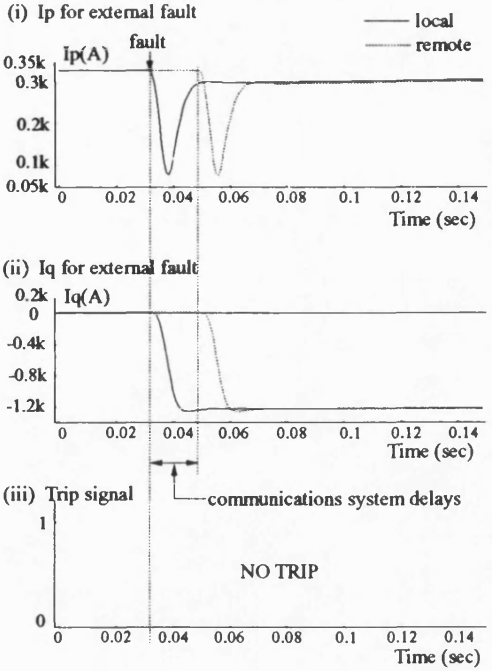

Figure 8.34 Polarised Currents for an External double phase to earth fault on the Test System with Composite Feeders.

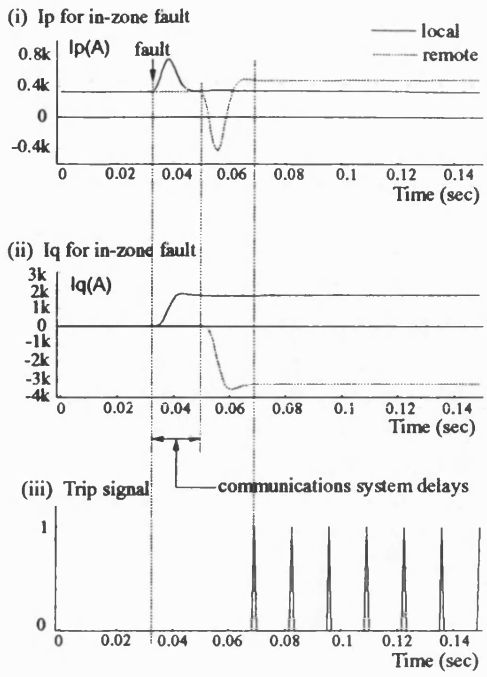

Figure 8.35 Polarised Currents for an In-zone double phase fault, no earth, on the Test System with Composite Feeders.

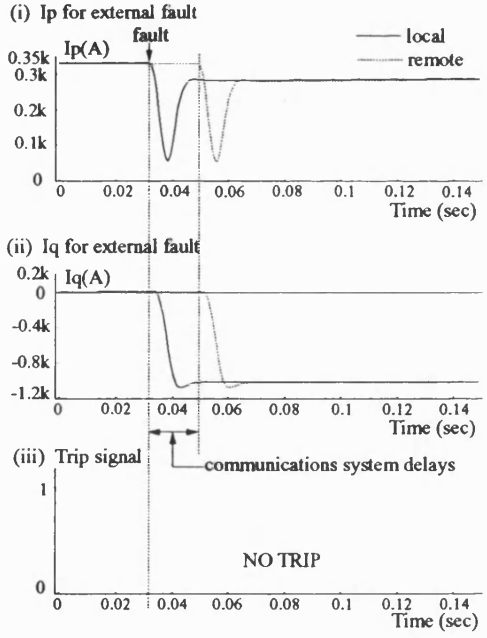

Figure 8.36 Polarised Currents for an External double phase fault, no earth, on the Test System with Composite Feeders.

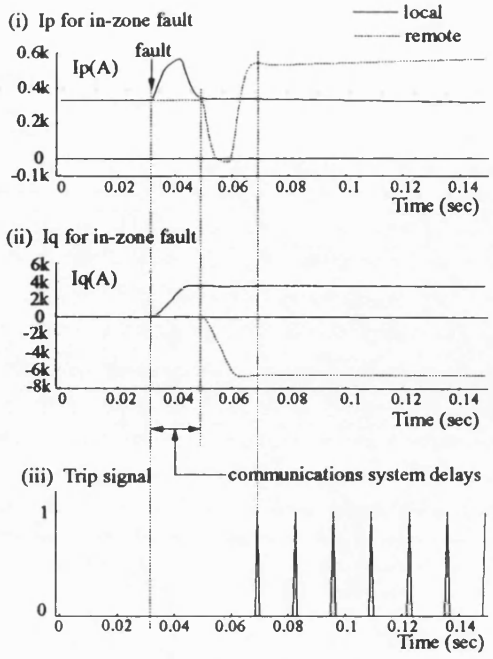

Figure 8.37 Polarised Currents for an In-zone three phase to earth fault on the Test System with Composite Feeders.

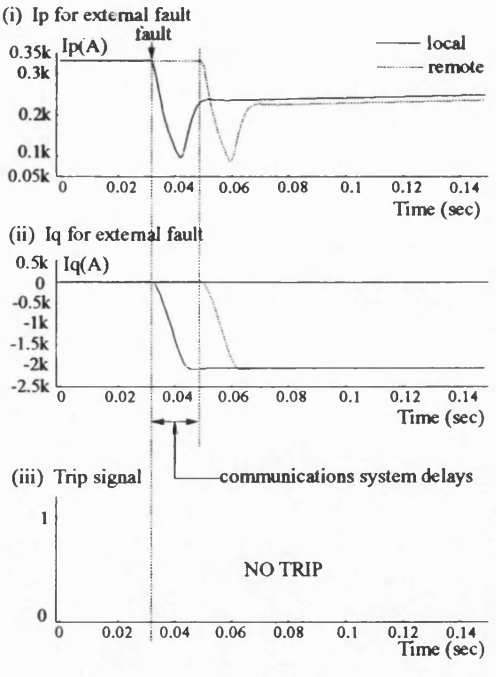

Figure 8.38 Polarised Currents for an External three phase to earth fault on the Test System with Composite Feeders.

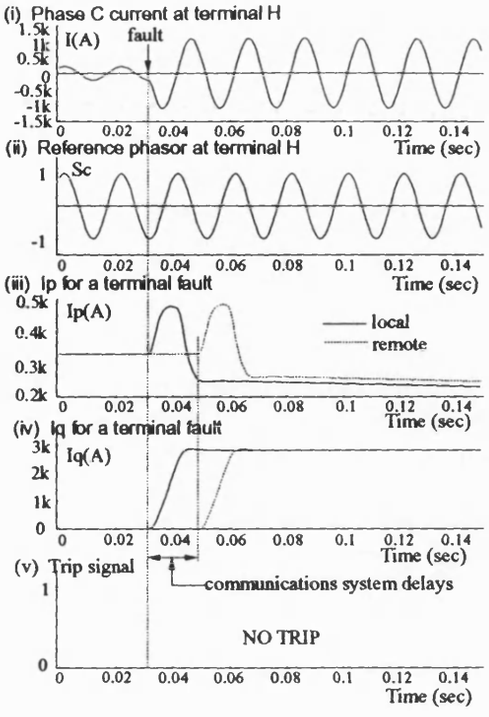

Figure 8.39 Input and derived waveforms for a Three phase to earth fault at terminal H on the Test System with Composite Feeders.

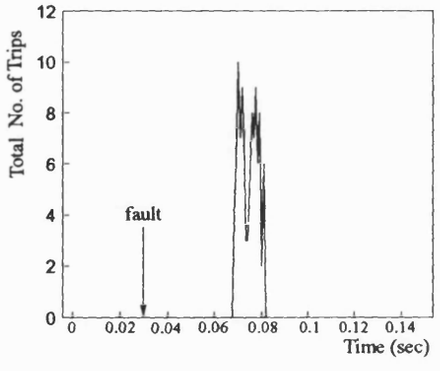

Figure 8.40 Histogram of Trip Response Summary of In-zone faults on System with Composite Feeders using 100 simulation runs.

Chapter 9

CONCLUSIONS AND SUGGESTIONS FOR FURTHER WORK.

9.1 CONCLUSIONS.

The thesis has presented the basis of the protection algorithm, the characteristics of voice frequency channel modems and their importance to the protection requirement. The thesis has also presented details of the relay's performance under a variety of power system fault conditions. Included in the write-up is an overview of feeder current differential protection, giving its weaknesses and strengths, and also an overview of communication systems and its effects.

DATA REDUCTION.

The signal processing is new in this research. Data reduction technique has been used which uses polyphase polarised current measurements derived from current measurements taken at the feeder's terminals to determine whether or not a shunt fault exists on the protected feeder. The technique chosen was based on the equations used to derive the instantaneous power in a three-phase circuit. The algorithm used locally obtained reference phasors as polarising signals to obtain polyphase polarised measurements of the current waveforms at the feeder's terminals. An orthogonal set of reference phasors provided complimentary information. Signals synchronised to the power system frequency and ideally having the same phase at all of the feeder's terminals were used to derive the reference. Since this protection is principally aimed at distribution feeders and assuming a heavily interconnected power system, the phase voltages are in phase with each other at the terminals. These were used to derive the reference phasors. A more attractive method for application in distribution circuits was

not to use VT's but, instead, derive the reference phasors from the positive phase sequence currents. One set of reference phasors is a set of three rotating sinusoidal waveforms, s_a, s_b, and s_c for phases a, b, and c respectively. The orthogonal set of reference phasors is then (s_b-s_c), (s_c-s_a) and (s_a-s_b) for phases a, b, and c respectively.

The summation of the products of instantaneous three-phase currents and instantaneous values of the in-phase reference phasors together with some filtering, produces a constant term I_p representing the amplitude of the current in phase with the reference phasors. The orthogonal set of reference phasors produces a constant term I_q representing the amplitude of the current orthogonal to the reference phasors. The filtering is required for unbalanced fault or load conditions, where because the currents are not balanced, second harmonic terms are introduced.

The immediate advantage of the approach is that the communications requirements are modest. After careful consideration of the characteristics of communication systems, it was thus decided to base the research on a full duplex 2400 bits per second channel.

THE COMMUNICATIONS SYSTEM.

Considerable expertise and investment has been applied to telephone based digital data communication systems. These systems, therefore, provide an almost ready made communications platform which can be used for feeder protection schemes. For this application, a voice frequency channel has been used for the digital data communications, operating with both standard telephone type communication circuits and copper pilot circuits, if they have already been installed. A CCITT V.26 standard modem using 2400 bits per second operating in full duplex mode was used. Thus, on the communications side, the use of such low data rate digital communications is new.

Whenever data is transmitted over a communications channel there is a possibility that the received data will be corrupted. It is important in protection applications that any corrupted blocks of data are properly identified. Since the protection data is continually being updated, corrupted data is best rejected. Coding techniques offer the potential of greatly enhancing a communications system's ability to handle errors in the received signal. However, it is essential to minimise the overheads introduced by the coding strategy so as to ensure maximum throughput of actual data from the communications system. As only a modest communications data rate was used in this work, a Hamming (13,9) code was used, providing an information data stream of 9 bits into a block of 13 bits, with 4 parity bits to handle errors.

The data stream to be transmitted was divided into pairs of consecutive bits as per operation of the V.26 modem. Each block of code started with a six bit header to provide synchronism followed by two Hamming code blocks. Each message block therefore contained eighteen data bits, comprising two identifier bits, two bits reserved for other applications and fourteen data bits relating to the polarised measurements I_p and I_q alternatively. A total of about 17 milliseconds for data transmission between terminals was adopted in the simulation. This was made up of 13.33 milliseconds transmission time for the thirty two bits for a message with a modem at 2400 bits per second bit rate, 2 milliseconds as marshalling time and worst case propagation delay time of 2 milliseconds. It is noted that the total delay time can vary. The 17ms is nominal with a reasonable tolerance dominated by message time.

Data communications would normally be free-running and not synchronised with the fault. This was simulated by randomising the start of transmission for each simulation run. The received value was compared to the corresponding locally measured signal delayed by the total message transmission delay time of 17 milliseconds. From these, bias and operate signals were derived. To provide security against mal-operation due to

the transitions in the polarised measurements after the fault, two trip indications were required before allowing the algorithm to trip.

THE POWER SYSTEM TEST MODEL.

For the evaluation of the algorithm, the EMTP power simulation package was used to model the test power system which consisted of a parallel feeder circuit at 33 kV. With the protection on one of the parallel feeders, external faults would be introduced on the other parallel feeder as well as on the supply feeders. Types of feeders that may exist in a distribution network were modelled. These consisted of overhead lines, underground cables, and a combination of overhead lines and underground cables.

TYPES OF FAULTS.

Various faults were studied on the different types of feeders. The faults involving single phase, double phases and all three phases, were applied both internal and external to the protected zone. With 20 km long feeders, some faults were applied close to the terminal at 100 metres both inside and outside the protected zone. Faults were also applied on the remote terminal. Point-on-wave at fault was varied.

RESULTS WITH PHASE VOLTAGE DERIVED REFERENCE PHASORS.

The technique of using polarised polyphase current measurements in the differential protection of feeders has been very effective in discriminating between in-zone faults and external faults. Generally and simply put, all in-zone faults resulted in increased magnitudes of the polarised measurements at the terminals with change of directional flow for the remote terminal quantity. Thus there were dramatic differences between the local and remote measurements after the fault for all in-zone faults, resulting in trip

outputs in under two and half power system cycles with an average of about 40 milliseconds after the fault. Without the variations in the synchronism between fault occurrence and data transmission, the tripping times would decrease by up to about 13 milliseconds to an average of about 30 milliseconds.

All external faults, including a terminal fault, resulted in relatively small polarised current measurements, with the same direction of flow of the remote terminal quantity after the fault. Although there was a difference between the local and remote signals, this was less than the trip settings. For these faults, the algorithm remained stable and did not trip.

RESULTS WITH POSITIVE PHASE SEQUENCE CURRENTS PROVIDING THE REFERENCE.

One attractive feature in using the positive phase sequence components is that the method still retains the advantage of current differential protection of not using VTs.

As in the voltage polarisation, the current polarisation results in all in-zone faults producing reversal of directional flow for the remote terminal quantity. Thus there were dramatic differences between the local and remote measurements after the fault, resulting in trip times in under two and half power system cycles. Average trip times of these in-zone faults is about 41 milliseconds. Again these times would be smaller by up to about 13 milliseconds without the variations in the synchronism between fault occurrence and data transmission.

For the external faults including terminal faults, there is no reversal of directional flow for any quantity. Thus the differences between the local and remote measurements were less than the trip settings. For these faults, the algorithm remained stable and did not

trip.

Thus, when compared to existing systems, some of the merits of the approach in this research are the choice of using either voltage polarisation or current polarisation.

9.2 SUGGESTIONS FOR FURTHER WORK.

Protection is sometimes defined as 'the science, skill, and art of applying and setting relays and/or fuses to provide maximum sensitivity to faults and undesirable conditions, but to avoid their operation on all permissible or tolerable conditions'[5]. A lot of improvements can thus result from posing and answering the question such as 'what if?

With reference to the work carried out in this research, CT saturation is some problem area. Future work should therefore investigate the performance of the protection under CT saturation. Another problem area involves high impedance faults. Below is a summary of other areas that require investigation.

TEED FEEDERS.

Radial feeders with Tee-offs are also common in distribution systems. Thus the performance of this type of protection to Teed feeders requires investigating. With reference from the local relay, a fault may be introduced beyond the tee-off point but within the protected zone. Conditions can then be studied that give rise to fault current infeed from the tee leg of the circuit. On the other hand, the remote terminal on the tee leg may be linked via another network to the other remote terminal causing fault current outfeed at the tee-off point. This scenario can also be studied. It should be noted that for a Teed feeder, a master-slave philosophy for the scheme may be justifiable as it would reduce the communications and processing requirements.

The above studies should not give problems when the reference phasors are derived from the phase voltages as in-zone faults will be characterised by large magnitudes for all polarised measurements from the terminals and change of direction of flow of the polarised measurements from the remote terminals. However, problems may arise when the reference is derived from the positive phase sequence currents. It should be investigated if a voltage element is needed.

EVENTS OF RANDOM NATURE.

Generally, optimisation of the algorithm is required. A number of points can be investigated. For accuracy, this will involve the use of probability distribution functions for some phenomena of random nature to be investigated, such as measurement errors and communication channel effects. Measurement errors include errors from the primary plant such as CT's and VT's not producing exact replicas of the power system quantities. Moreover, the research so far has assumed ideal transformers which may not be the case in real life. The digital output has only a limited accuracy and therefore a quantisation error may be present in the output. Probably the use of higher bit A/D converters can be investigated. On channel effects, the transmission system delays were modelled as lumped delays. But these may be of some random nature considering that they comprise delays due to analogue to digital conversion, buffering for transmission, as well as channel propagation. Also, there may be some random data drop-outs due to excessive noise on the channel. There may be temporary outages of the channel and these are random events. The effects of these on the algorithm can be investigated using distribution functions.

SPEED OF DATA TRANSMISSION.

One principal constraint for the technique in this research is the time required to transmit data from one terminal to another. Reducing this time, by increasing the data rate, would reduce the tripping time. Whilst not ignoring cost, the use of higher data rates should be investigated, as generally, the more data there is, the better the decision making. Of interest would be the use of a CCITT V.27 modem standard which operates at 2400 or 4800 bits per second in full duplex. Care must be taken however to ensure that the start-up, interruption and collapse characteristics of the modems are fully investigated, together with an investigation of their performance in the presence of both random and burst noise.

REFERENCE PHASORS.

The reference phasors have been sinusoidal waveforms. As digital data is in 1's and 0's, the use of square waveforms as reference phasors should be investigated. Actually, taking the positive phase sequence currents in DADiSP and dividing a phase component by its absolute value results in a square waveform oscillating between +1 and -1. With the reference phasors designated s_a, s_b and s_c for the respective phases, the corresponding orthogonal set is obtained by the subtraction of two subsequent phasors as detailed in the thesis in chapter 3. Thus to ensure that the reference phasors are synchronised to the power system waveforms, the positive phase sequence currents can be used to derive the unit amplitude square waveforms. Alternatively, as the positive phase sequence current for a phase is synchronised to, or say, follow, the phase current, unit amplitude square waveforms can be generated that are synchronised to the phase currents. Similarly unit amplitude square waveforms can be derived from the phase voltages.

Finally, it will be necessary to implement the algorithm in a modern digital relay host

system and to carry out field tests to verify the performance of this new current differential protection algorithm for distribution feeders.

Chapter 10

REFERENCES.

1. G I Atabekov, 'The Relay Protection of High Voltage Networks', Pergamon, New York, 1960, pp. 12 - 13, 471 - 504.

2. D Jones, 'Analysis and Protection of Electrical Power Systems', Pitman, Bath, 1961, ISBN 0 273 43915 4, chapter 7.

3. GEC Alsthom Measurements, 'Protective Relays Application Guide', 3rd edition, 1987, pp. 47 - 59, 115 - 127, 159 - 181, 225 - 233, 297 - 301.

4. J D Glover, M Sarma, 'Power System Analysis and design', 2nd edition, PWS publication, Boston, 1994, ISBN 0-53493-960-0, chapter 5, chapter 10.

5. J W Lewis Blackburn, 'Protective Relaying: Principles and Applications', Marcel Dekker, Inc., New York, 1987, ISBN 0 8247 7445 0, pp. 3, 76, 183, 448 - 478.

6. J H Neher, 'A New Approach to the Pilot-Wire Protection of Transmission Lines Using Leased Pilot Wires Having Relatively Long Electrical Characteristics', AIEE Trans. on Power Apparatus and Systems, vol. 79, No. 48, June 1960, pp 245 - 252.

7. R Aggarwal, P Moore, 'Digital Communications for Protection: Tutorial part 2, Teleprotection Systems', IEE Power Engineering Journal, vol. 8, No. 2, April 1994, pp. 97 - 102.

8. H W Lensner, 'Protective Relaying Systems Using Pilot-Wire Channels', AIEE Trans. on Power Apparatus and Systems, vol. 79 No. 52, February 1961, pp 1107 - 1120.

9. GEC Alsthom Measurements, 'Type MBCI Relay, Translay "S" Differential Feeder Protection', pp. 1 - 15.

10. L P Singh, 'Advanced Power System Analysis and Dynamics', 3rd edition, Wiley Eastern Limited, New Delhi, 1992, ISBN 81-224-0433-2, pp 399 - 470.

11. G D Rockefeller, 'Fault Protection with a Digital Computer', IEEE Trans. on Power Apparatus and Systems, vol. PAS-88, no. 4, April 1969, pp 438 - 464.

12. IEEE Committee Report, 'Local Backup Relaying Protection', IEEE Trans. on Power Apparatus and Systems, vol. PAS 89 July/August 1970, pp. 1061 - 1068.

13. C Russell Mason, 'The Art and Science of Protective Relaying', Wiley and Sons, New York, 1956 pp. 1 - 15.

14. A R van Warrington, 'Protective Relays, Their Theory and Practice', vol. 2, 3rd edition, Chapman and Hall, London, 1977, ISBN 0 421 15380 7, pp. 1 - 4, 150 - 155.

15. L Yee, D C Brownlee, 'Protection and Telecommunications Interface Problems for Digital Data Transfer Relays', Communications, Computers and Power in the Modern Environment, IEEE Wescanex 1993 Conference Proceedings, ch. 60, pp. 7- 14.

16. L J Ernst, W L Hinman, D H Quam, J S Thorp, 'Charge Comparison Protection of Transmission Lines - Relaying Concepts', IEEE Trans. on Power Delivery, vol. 7, No. 4, October 1992, 92 WM 209-7 PWRD, pp. 1834 1842.

17. N P Albrecht, W C Fleck, K J Fodero, R J Ince, 'Charge Comparison Protection of Transmission Lines - Communications Concepts', IEEE Trans. on Power Delivery, vol. 7, No. 4, October 1992, 92 WM 210-5 PWRD, pp. 1853 - 1859.

18. W S Kwong, M J Clayton, A Newbould, 'A Microprocessor-based Current Differential Relay for use with Digital Communication Systems', 3rd International Conference on Developments in Power System Protection, IEE Conference publication 249, 17-19 April 1985, pp. 65 - 69.

19. J Wheatley, 'A Microprocessor-based Current Differential Protection', 4th International Conference on Developments in Power System Protection, IEE Conference publication 302, 11-13 April 1989, pp. 116 - 120.

20. W Stallings, 'Data and Computer Communications', 3rd edition, MacMillan, New York, 1991, ISBN 0-02-415454-7, pp. 40 - 70.

21. M A Redfern, A A W Chiwaya, 'A New Approach to Digital Current Differential Protection for Low and Medium Voltage Feeder Circuits using a Digital Voice Frequency Grade Communications Channel', IEEE Trans. on Power Delivery, Vol. 9, no. 3, July 1994, 94 WM 013 - 3 PWRD, pp. 1352 - 1358.

22. D R Doll, 'Data Communications, Facilities, Networks, and Systems Design', Wiley and Sons, New York, 1978, ISBN 0-471-21768-9, pp. 197 - 203.

23. R L Brewster (editor), 'Data Communications and Networks', Peregrinus, London, 1986, ISBN 0-86341-078-2, pp. 12 - 13.

24. CCITT Recommendations, Blue Book, 'Series V Recommendations, Data Communication over the Telephone Network', Vol. VIII, published by ITU, Geneva, 1989, pp. 65 - 69, 104 - 121, 153 - 180, 252 - 266, and Vol. IV 'Recommendations M800 - M1375, pp. 55 -59, 85 - 89.

25. IEEE Tutorial Course, 'Nonsinusoidal situations: Effects on the Performance of Meters and Definitions of Power', IEEE Power Engineering Society, course text 90EH0327-7-PWR.

26. J Rushton, 'The Fundamental Characteristics of Pilot-Wire Differential Protection Systems', Proceedings IEE, vol. 108, part A, Oct. 1961, pp. 409 - 420.

27. NEI Reyrolle Protection, 'Digital Feeder Protection, Solkor-M', data sheet, published 1991.

28. M Mir, P J McCleer, ' A New Microprocessor-based approach for Pilot Differential Protection of Transmission Lines', International Journal, Computers and Electrical Engineering, Vol. 13, no. 3/4 , Pregamon Journals 1987, pp. 129 - 137.

29. AIEE Relay Committee Report, 'Protection of Multiterminal and Tapped Lines', AIEE Transactions, Part III, Power Apparatus and Systems, vol. 80, April 1961, pp. 55 - 66.

30. GEC ALSTHOM T&D, PROTECTION AND CONTROL 'LFCB Digital Current Differential Relay', publication R-4028B.

31. C R Mason, 'Relay Operation during System Oscillations', AIEE Trans. vol. 56, July 1937, pp 823-832. Disc., vol. 56, Dec. 1937, pp. 1513 - 4; vol. 57, Feb. 1938, pp. 111 - 3.

32. F Ilar, 'Innovations in the Detection of Power Swings in Electrical Networks', Brown Boveri Revue, part 2, 1981, pp. 87 - 93.

33. E H Bancker, E M Hunter, 'Distance Relay action During Oscillations', AIEE Transaction, vol. 53, July 1934, pp 1073 - 1080.

34. J S Thorp, A G Phadke, S H Horowitz, J E Beehler, 'Limits to Impedance Relaying', IEEE Transactions. on Power Apparatus and Systems, vol. PAS 98, no. 1, Jan/Feb 1979, pp. 246 - 260.

35. IEEE Power System Relaying Committee Working Group Report, 'EHV Protection Problems', IEEE Trans. on Power Apparatus and Systems, vol. PAS 100, no. 5, May 1981, pp. 2399 - 2406.

36. A A W Chiwaya, M A Redfern, 'A New Microprocessor Based Current Differential Protection for Distribution Feeders', Universities Power Engineering Conference proceedings, University of Galway, Ireland, September 1994.

37. O Usta, 'A Power Based Digital Algorithm for the Protection of Embedded Generators', PhD Thesis, University of Bath, 1992, pp. 49 - 73.

38. B M Weedy, 'Electric Power Systems', 3rd edition revised, Wiley and Sons, Chichester UK, 1987, ISBN 0 471 91659 5, pp. 59 - 66, 88 - 143, 258 - 262, 419 - 472.

39. M A Redfern, J I Barrett, O Usta, T Yip, 'A New Microprocessor Based Loss of of Grid Protection for Embedded Generation', Proc. 2nd International Conference on Advances in Power System Control, Operation and Management, APSCOM-93, Hong Kong, Conference publication No. 388, pp. 373 - 378.

40. A Blanchard, 'Phase-Locked Loop Behaviour Near Threshold', IEEE Trans. on Aerospace and Electronic Systems, Vol. AES-12, no. 5, Sept 1976, pp. 628 - 638. Corrections AES-12, Nov 1976, page 823.

41. A Blanchard, 'Phase -Locked Loops - Application to Coherent Receiver Design', Wiley and Sons, New York, 1976, ISBN 0-471-07941-3.

42. F M Gardner, 'Phaselock Techniques', Wiley and Sons, New York, 1966, ISBN 0 472 29156 0.

43. EXAR Data Book, Exar Corporation, California, 1987, pp. 6.58 - 6.100.

44. A M Chebbo, M R Irving, M J H Sterling, 'Voltage Collapse Proximity Indicator: Behaviour and Implications', IEE Proceedings-C, Vol. 139, no. 3, May 1992, pp. 241 - 252.

45. M Brucoli, M la Scala, R Sbrizzai, M Trovato, 'Voltage Stability Analysis of Electric Power Systems with Frequency Dependent Loads', IEE Proceedings-C, Vol. 140, no. 1, January 1993, pp. 1 - 6.

46. A O Ekwue, R M Dunnett, N T Hawkins, W D Laing, 'On-Line Voltage Collapse Monitor', National Grid Research and Development Center, ref. NG RDC/TSP/0130/M91, 12 June 1991.

47. F Mercede, J-C Chow, H Yan, R Fischl, 'A Framework to Predict Voltage Collapse in Power Systems', IEEE Transactions on Power Systems, Vol. 3, no. 4, November 1988, pp. 1807 - 1813.

48. C W Taylor, 'Concepts of Underground Load Shedding for Voltage Stability', IEEE Trans. on Power Delivery, Vol. 7, no. 2, April 1992, 480 - 488.

49. DSP development Corporation, 'The DADiSP Worksheet, Signal Analysis Software', Instructional Manual, 1988.

50. H Schildt, 'C: The Complete Reference', 2nd edition, McGraw-Hill, California, 1990, ISBN 0-07-881538-X.

51. H Schildt, 'Teach Yourself C', McGraw-Hill, California, 1990, ISBN 881596-7.

52. Working Group of the Relay Input Sources Subcommittee, 'Transient Response of Coupling Capacitor Voltage Transformers, IEEE Committee Report', IEEE trans. on Power Power Apparatus and Systems, vol. PAS-100, no.12, December 1981, pp.4811 - 4814.

53. M Kezunovic, C W Fromen, F Phillips, 'Experimental Evaluation of EMTP-Based Current Transformer Models for Protective Relay Transient Study', IEEE Trans. on Power Delivery, Vol. 9, no. 1, January 1994, pp. 405 - 413.

54. H Nyquist, 'Certain Factors Affecting Telegraph Speed', Bell System Technical Journal, Vol. 3, no. 2, April 1924, pp. 324 - 346.

55. H Nyquist, 'Certain Topics in Telegraph Transmission Theory', AIEE Transactions, Vol. 47, April 1928, pp. 617 - 627.

56. RS Components book, March - June 1994, pp. 1.683 - 1.687.

57. F de la C Chard, 'Electricity Supply: Transmission and Distribution', Electrical Engineering Series, Longmans, London, 1976, ISBN 0-582-44462-4, pp. 125, 195 - 337.

58. E O Schweitzer III, D Hou, 'Filtering for Protective Relays', paper presented at the 19th Annual IEEE Western Protective Relay Conference, Washington, 20 - 22 Oct. 1992.

59. M A Redfern, D P McGuinness, R F Ormondroyd, Z Q Bo, 'Coding Techniques to Enhance Digital Data Communications for Unit Protection during Power System Fault Conditions', 5th International Conference on Developments in Power System Protection, IEE Conference publication 368, 30 March - 1 April 1993, pp. 21 - 24.

60. R W Hamming, 'Error Detecting and Error Correcting Codes', The Bell System Technical journal, vol. 29, April 1950, pp. 147 - 160.

61. G C Clark, J B Cain, 'Error-Correction Coding for Digital Communications', Plenum Press, New York, 1981, ISBN 0-306-40615-2, pp. 54 - 57.

62. S A Vanstone, P C van Oorschat, 'An Introduction to Error Correcting Codes with Applications', Kluwer Academic publishers, Boston, 1989, ISBN 0-7923-9017-2.

63. H Hupfauer, G Koch, 'An Enhanced Transmission Line Protection Concept for Multi-Circuit Lines', 5th International Conference on Developments in Power System Protection, IEE Conference publication 368, 30 March - 1 April 1993, pp. 149 - 152.

64. P A Crossley, S F Elson, S J Rose, A Williams, 'The Design of a Directional Comparison Protection for EHV Transmission Lines', 4th International Conference on Developments in Power System Protection, IEE Conference publication 302, 11 - 13 April 1989, pp 151 - 155.

65. P T F Kelly, M K Sands, 'An Introduction to Data Communications', British Telecommunications Engineering journal, vol. 3 July 1984, pp. 68 - 75.

66. F Jennings, 'Practical Data Communications; Modems, Networks, and Protocols, Blackwell Scientific publication, Oxford, 1986, ISBN 0-632-01306-0, pp. 31 - 51.

67. A J Swan, 'Data Communications, Protocols', National Computing Centre publication, Manchester, 1978, ISBN 0-85012-203-1, pp. 33 - 49.

68. G Waters (editor), 'Computer Communication Networks', McGraw-Hill publication, 1991, ISBN 0-07-707325-8, pp. 21 - 28.

69. R L Freeman, 'Telecommunication Transmission Handbook', Wiley & Sons publication, New York, 1975, ISBN 0-471-27789-4, pp. 13 - 27, 359 - 366, 382 - 397.

70. J N McMurdo, G C Weller, 'Applications of Digital Differential Protection', 5th International Conference on Developments in Power System Protection, IEE Conference publication 368, 30 March - 1 April 1993, pp 115 - 118.

71. L W Couch II, 'Digital and Analogue Communication Systems', Macmillan press, New York, 1983, ISBN 0-02-325240-5, pp. 76 - 91, 213 - 230.

72. M A Redfern, B H A Ramsden, W Kwong, G V Roberts, 'Pilot Wire Data Communications for Digital Distribution Feeder Protection Schemes', Universities Power Engineering Conference proceedings, September 1989, pp. 211 - 214.

73. R F W Coates, 'Modern Communication Systems', Macmillan press, London, 1975, ISBN 333 15024 4, pp. 193 - 197, 217 - 245.

74. A J Dobson, 'Introduction to Statistical Modelling', Chapman and Hall, London, 1983, ISBN 0-412-24850-6, pp. 5 - 8, 21 - 25.

75. C Chatfield, 'Statistics for Technology, A Course in Applied Statistics', 2nd edition, Chapman and Hall, London 1978, ISBN 0 412 15750 0, chapters 2, 4 and 5.

76. F Halsall, 'Data Communications, Computer Networks, and Open Systems', 3rd edition, Addison-Wesley, 1992, ISBN 0-201-56506-4, pp. 60 - 68.

77. R D Martin-Royle, G H Bennett, 'Optical Fibre Transmission Systems in the British Telecommunications Network: An Overview', British Telecommunications Engineering journal, vol. 1, January 1983, pp. 190 - 199.

78. M A Redfern, Z Q Bo, W Kwong, G V Roberts, 'An Investigation into the Characteristics of HV Distribution Cable Circuits for Digital Protection Data Communication', Universities Power Engineering Conference proceedings, September 1990, pp. 151 - 154.

79. C E Shannon, ' A Mathematical Theory of Communication', The Bell System Technical journal, vol. 27, no. 3, July 1948, pp. 379 - 423; October 1948, pp. 623 - 657.

80. J Dunlop, D G Smith, 'Telecommunication Engineering', 2nd edition, Van Nostrand Reinhold, Hong Kong, 1989, ISBN 0-278-00082-7, pp. 29 - 41.

81. M A Redfern, D P McGuinness, R F Ormondroyd, 'High Security Digital Data Communications for Unit Protection of Distribution Feeders and Local Network Automation', International Conference on New Developments in Power System Protection and Local Control, DPSP & C'94, 25 - 28 May 1994, China, pp. 152 - 156.

82. W J Bonwick, P J Hession, 'Fast Measurement of Real and Reactive Power in Three Phase Circuits', IEE Proceedings-A, vol. 139, No. 2, March 1992, pp. 51 - 56.

83. M A Slomin, J D Van Wyk, 'Power Components in a System with Sinusoidal and Nonsinusoidal Voltages and/or Currents', IEE Proceedings-B, vol. 135, No. 2, March 1988, pp. 76 - 84.

84. W Shepherd, P Zakikhani, 'Suggested Definitions of Reactive Power for Nonsinusoidal Systems', IEE Proceedings-B, vol. 119, 1972, pp. 1361 - 1362.

85. IEEE Power System Harmonics Working Group Report, 'Bibliography of Power Systems Harmonics', IEEE Trans. on Power Apparatus and Systems, PAS-109, part I, 1984, pp. 2460 - 2462, and part II, Ibid.

86. E B Makram, R B Haines, A A Girgis, 'Effect of Harmonic Distortion in Reactive Power Measurement', IEEE Trans., Industry Applications, vol. 28, no. 4, 1992, pp 782-787.

87. A E Emanuel, 'Powers in Nonsinusoidal Situations, A Review of Definitions and Physical Meaning', IEEE Trans. on Power Delivery, vol. 5 No. 3, July 1990, pp. 1377-1383.

88. M A Redfern, R J Hewett, A A W Chiwaya, 'An Investigation into Reverse Power Flow Protection for Small and Medium sized Embedded Generation', Universities Power Engineering Conference proceedings, September 1993, pp. 109 - 112.

89. G S Hope, O P Malik, 'Microprocessor-based Active and Reactive Power Measurement', Electric Power and Energy Systems, vol. 3, No. 2, April 1981, pp. 75 - 83.

90. W Fairney, 'Reactive Power - Real or Imaginary?', IEE Power Engineering Journal, vol. 8, No. 2, April 1994, pp. 69 - 75.

91. P H Buxton, R E Morrison, 'Digital Measurement of Negative Phase Sequence Voltages,' IEEE Trans. on Power Apparatus and Systems, vol. PAS-103, No. 3, March 1984, pp. 581 - 588.

92. C F Wagner, R D Evans, 'Symmetrical Components as applied to the Analysis of Unbalanced Electrical Circuits', McGrawHill, New York, 1933, ISBN 07-067660-7, pp. 9 - 24.

93. A G Warren, 'Mathematics Applied to Electrical Engineering', 2nd edition revised, Chapman and Hall, London, 1958, pp. 137 - 144.

94. H Tropper, 'Electrical Circuit Theory, An Introduction to Steady State and Transient Theory based on the Superposition Principle', Longmans, London, 1963, pp. 53 - 62.

95. Westinghouse Electric Corporation, 'Applied Protective Relaying', 2nd printing, 1979, chapters 2, 6.

96. T Lobos, 'Fast Estimation of Symmetrical Components in Real Time', IEE Proceedings-C, vol. 139, No. 1 January 1992, pp. 27 - 30.

97. C L Fortescue, 'Method of Symmetrical Coordinates Applied to the Solution of Polyphase Networks', AIEE Transactions, vol. 37, part II, July - December 1918, pp. 1027 - 1115.

98. S Y King, N A Hafter, 'Underground Power Cables', Longmans, London, 1982, ISBN 0-582-46344-0, pp. 1 - 5, 15 - 22.

99. E O Taylor, G A Boal, (editors), 'Electric Power Distribution 415V - 33kV', Edward Arnold, London, 1966, pp 1 - 10, 146 - 257.

100. Leuven EMTP Center, 'Alternative Transient Program rule book', July 1987.

101. M Wilkinson, 'Material Progress in Cable Accessories up to 33kV', IEE Power Engineering Journal, vol. 8, No. 2, April 1994, pp. 89 - 91.

102. H Waddicor, 'The Principles of Electric Power Transmission', Chapman and Hall, London, 1964, chapter 11.

103. G E A Hance, 'The Modern Self Contained Oil Filled Cable System for use at Voltages up to 180kV', IEE 2nd International Conference on Power Cables and Accessories, 10kV to 180kV, Conference publication no. 270, November 1986, pp. 198 - 201.

104. British Standard Specification, B.S.480: 1954, 'Impreganted Paper-insulated Cables for Electricity Supply, part 1: Lead or Lead-alloy Sheathed cables for Working Voltages up to and including 33kV'.

105. C C Barnes, 'Power Cables, Their Design and Installation', 2nd edition, Chapman and Hall, 1966, pp. 184 - 187, 286 - 291.

106. P Graneau, 'Underground Power Transmission', Wiley & Sons, 1979, ISBN 0-471-05757-6, pp. 107 - 112, 274 - 275.

107. D G Fink, H W Beaty(editors), 'Standard Handbook for Electrical Engineers', 11th edition, McGraw-Hill, New York, 1978, ISBN 0-07-020974-X, chapter 4.

108. M G Say(editor), 'Electrical Engineer's Reference Book', Butterworths, London, 1973, ISBN 0 408 70289 3, chapter 8.

109. G R Jones, M A Laughton, M G Say, 'Electrical Engineers Reference Book', 15th edition, Butterworths Heinemann, London, 1993, ISBN 7506 1202 9, chapters 13, 23.

110. IEEE Power System Relaying Committee, special publication, 'System Protection and Voltage Stability', 1993, IEEE 93TH0 596-7PWR, ISBN 0-7803-9981-1.

111. E Fesler, J C Maun, S Bassem, 'Development of a Digital EHV Line Differential Protection Relay', International Conference on New Developments on Power System Protection and Local Control, DPSP&C'94, Beijing, China, 25 - 28 May. 1994, pp 126 - 131.

112. M S Sachdev, R Agarwal, 'A Technique for Estimating Transmission Line Fault Locations from Digital Impedance Relay Measurements', IEEE Transactions on Power Delivery, vol. 3, No. 1, January 1988, pp 121 - 129.

113. T Takagi, Y Yamakoshi, M Yamaura, R Kondow, T Matsushima, 'Development of a New Type Fault Locator using the one- terminal Voltage and Current Data', IEEE Tans. on Power Apparatus and Systems, vol. PAS-101, No. 8, August 1982, pp 2892 - 2898.

114. H E Namarika (editor), 'Malawi Statistical Yearbook 1987', National Statistical Office, Zomba, Malawi.

115. 'Encyclopædia Britannica, a new survey of universal knowledge', vol.14, W. Benton publishing, Chicago, 1966, page 674, 674A, 674B.

116. 'The Europa World Year Book 1993', 34th edition, vol. II, Europa publications, London, 1993, ISBN 0-946653-80-1, pp 1839, 2915.

117. Electricity Supply Commission of Malawi, 'Study to Update ESCOM's Least Cost Development Programme', draft copy, 1994.

118. Electricity Supply Commission of Malawi, 'ESCOM Transmission System', drawing no. 7.03/108B, Nov 1993.

119. Electricity Supply Commission of Malawi, 'ESCOM Protection System', drawing no. 7.03/94G, Nov 1993.

120. GEC Alsthom T&D, Protection and Control, 'Biased Differential 'Translay' Relays, HO4 Type', publication R-5145C, Staffold.

121. GEC Alsthom T&D, Protection and Control, 'High Speed Biased Differential Feeder Protection Relay DS7 Type', publication R-5151C, Staffold.

122. L J Myatt, 'Symmetrical Components', Pergamon Press, First edition, 1968.

123. Electricity Supply Commission of Malawi, 'Electricity Supply Commission of Malawi 27th Annual Report and Statement of Accounts, 1991/1992', Blantyre Print and Publishing, Malawi, 1992.

APPENDIX A

AN OVERVIEW OF MALAWI POWER SYSTEM.

A.1 INTRODUCTION.

This appendix gives the current practice of protection of the power system in the Electricity Supply Commission of Malawi, ESCOM. An overview of ESCOM is given and how ESCOM performs in its task of supplying electrical power to the country, Malawi.

Since ESCOM power system is still growing as shown in the load forecast model between 1991 and 2010 in table 9.1, the importance of reliable protection exploiting recent developments in the field of protection can not be over-emphasized. There are plans to introduce a 220 kV power grid connection with the neighbouring countries, Mozambique, Zambia and Tanzania, but at the moment ESCOM's highest voltage is 132 kV. As such it can be said that ESCOM is mainly at low and medium voltage levels, or distribution voltage levels. On the communications side, ESCOM is not as yet using the state-of-the-art optical fibres for protection for example. It uses pilot wire and power line carrier systems for protection and control. These channels are also used in conjunction with radio systems for operations.

With most of the feeders, in fact over 80 percent, being less than 80 km long, and as ESCOM operates at medium and low voltages, nearly the whole network of feeders can be protected using the unit protection schemes. All substations for stepping up the voltage from generation level of 11 kV to transmission levels of 132 kV and 66 kV have VT's and CT's. Similarly, all the substations for stepping down the voltage from the transmission levels to 33 kV and 11 kV have VT's and CT's. 33/11kV substations have

only CT's. Thus with the use of the low cost communications, the new protection can be widely applied to the ESCOM system, whether in the VT polarisation mode or CT polarisation mode.

A.2 GENERAL STRUCTURE OF E.S.C.O.M.

Electricity Supply Commission of Malawi (ESCOM) is a parastatal organisation, established in 1958 to generate, transmit and distribute electricity in Malawi.

As illustrated in the electricity supply network in ESCOM in figure 9.1, Malawi, situated in Central Africa, is surrounded by Zambia, Mozambique and Tanzania. It covers an area of 118,484 sq km[114, 115, 116], roughly the size of England which covers 130,423 sq km or half of Great Britain which has area of 228,269 sq km[116]. Water mass occupies 24,208 sq km which is 20.43 per cent of the total area. Its population which was 7982607 in 1987[114] is now close to 10 million.

ESCOM employs about 2,400 permanent members of staff and has power generation capacity comprising 164 MW from hydro-generation at three power stations, 15 MW from standby gas turbine, 8.5 MW standby diesel plant and 2 MW isolated diesel plant. There are 921 km of 132 kV lines, 815 km of 66 kV lines and 452000 kVA of step-down system transformers. At low voltage levels there are about 1780 km of 33 kV lines, 2020 km of 11 kV lines and 290000 kVA of step-down substations. The above statistics were as at 31 March 1994[117].

As at 31 March 1994, the number of metering points totalled 51000, comprising 39371 domestic, 11065 commercial, 560 industrial and 4 export (to Mozambique). These figures represent about 3 per cent of Malawi's population having direct access to electricity.

The country is presently self-sufficient in electricity supply and exports a small amount to one of its neighbours, Mozambique. In the fiscal year 1993/94 (1 April 1993 to 31 March 1994) the peak demand was 140.2 MW, units sent out amounted to 822.7 GWh and total losses were at 14.6 per cent[117].

Currently, major system development work in ESCOM includes the construction of a 50 MW hydro-power station (Tedzani III), the construction of a 128 MW hydro-power station (Kapichira) in two phases of 64 MW each and the construction of a mini-hydro station of 4.5 MW (Wovwe). The planned commissioning dates of these projects are 1995, 1998-2001 and 1995, respectively. Together with these projects are several transmission and distribution expansion and reinforcement projects. The main ones are rehabilitation of about 350 km of 132 kV lines and construction of several 33 kV and 11 kV injection points in two major load centres (Blantyre and Lilongwe). Table 9.2 gives a summary of the transmission and distribution systems.

A.3 CURRENT POWER SYSTEM PROTECTION PRACTICE IN ESCOM.

Figure 9.2[118] shows the ESCOM transmission system at present, with 132 kV and 66 kV as the transmission voltages. It shows the main step-up transformers from the generating stations and also step-down transformers towards the load centres. Various types of conductors are used such as the ACSR and AAA conductor types with the physical characteristics of such conductor names as the racoon, lynx, elm and tiger[107]. Lines are as long as 250 km and as short as 0.4 km. As seen from figure 9.2, there are seven lines of less than 20 km and four lines of between 20 km and 30 km connecting major substations.

Overcurrent and earth fault protection is widely used both as main protection and also as back-up protection. This is shown in the system protection diagram given in figure

9.3[119]. Distance protection is the main protection on the transmission network. Some short feeders are protected using current differential schemes. Such schemes exist between Tedzani and Nkula for example, with feeder line distances of 7.4 km, where the biased differential 'Translay' relays type HO4[120] are used. Private pilot wires are used to provide the communications link between the relays at each end of the protected feeder. Least sensitive earth fault setting of 40% is used. Also used on the system are the high speed biased differential feeder protection relay types DS7[121]. These can use least sensitive earth fault setting of 20% of rating.

ESCOM's performance over the years has been good. However, with the current power system expansion comes an increase in the degree of complexity. Consequently, there is an increase in the number of faults as illustrated in table 9.3 which summarises ESCOM's performance for the years 1986 to 1994[123]. The importance of the protection system is thus even more pronounced as the power system expands.

Problems have been that during the rainy seasons, some areas are extremely difficult to get to due to the state of the roads. Yet this is the season that ESCOM experiences a lot of faults. The faults could be simply due to lightning, but may also be due to washed away poles or tree branches being blown onto the conductors. The number of faults is expected to reduce as network reinforcement progresses.

A.4 IMPACT OF THE NEW PROTECTION ON THE ESCOM SYSTEM.

Although most of the feeders have short lengths, unit protection is not widely used. A common excuse is the cost and complexity of supplying communication channels. However, with the system development, many projects are being carried out, and thus there is a potential to attract the use of the much desired unit protection schemes of the feeders using low cost communications channels. These developments include hydro

electric projects with finance commitments from the International Development Agency (IDA) of the World Bank, Commonwealth Development Corporation (CDC), European Investment Bank (EIB) and African Development Bank (ADB)[123]. There are also developments in the transmission rehabilitation, distribution reinforcement, and rural electrification.

As mentioned above, over 80 percent of the feeders are of short lengths. With such a small system and operating at voltages of only up to 132 kV, the use of the new current differential protection would be welcome, especially so as it uses low cost communications. With some substations having only CT's and others having both CT's and VT's, the new protection can use either the VT polarisation mode or the CT polarisation mode. Tests can firstly be carried out on feeders connecting substations Nkula 'A' and Tedzani, Nkula 'B' and Tedzani, or Dedza and Mtendere.

There are many associated benefits for the system. Integrated Non-unit protection schemes can be included as back-up. Also included can be integrated auto-reclosure schemes. As there will be the communication channels, associated SCADA schemes can be used on all the major substations. With this as a standard protection unit for the whole feeder network, construction and installation will be standard, and this is desirable in a power system. There will now be no need for the costly routine and regular maintenance and checking as applies with the conventional relays. There will be no need to take the power system out of service when evaluating the relays performance as this exercise can be done on line. Thus, there is no requirement for a lot of highly skilled staff for maintenance and servicing. As there will be one supplier, the spares holding will be good as parts can be interchanged.

A.5 SUMMARY.

This appendix has briefly given a summary of the Electricity Supply Commission of Malawi, ESCOM. Briefly, the transmission system has been described, its performance outlined, and the protection practice summarised.

The suitability of the new unit protection has been highlighted. ESCOM operates at low and medium voltages with the distances involved being mostly short. As such, the use of the new current differential protection is attractive. The associated benefits include cost effectiveness, standardised protection, and the inclusion of integrated Non-unit protection and auto-reclosure schemes.

A.6 FIGURES

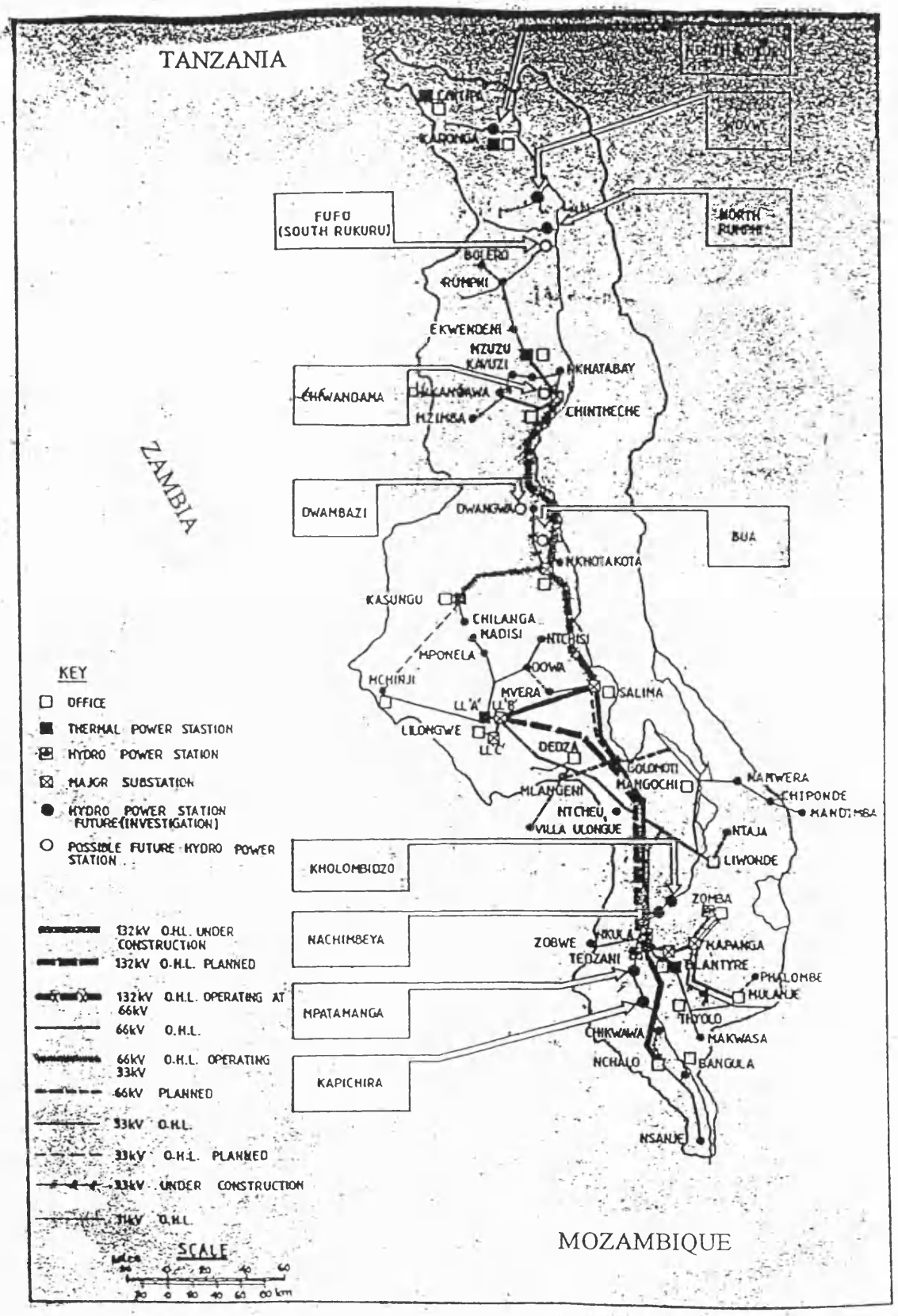

Figure 9.1 Map of Malawi showing the Electrical Network.

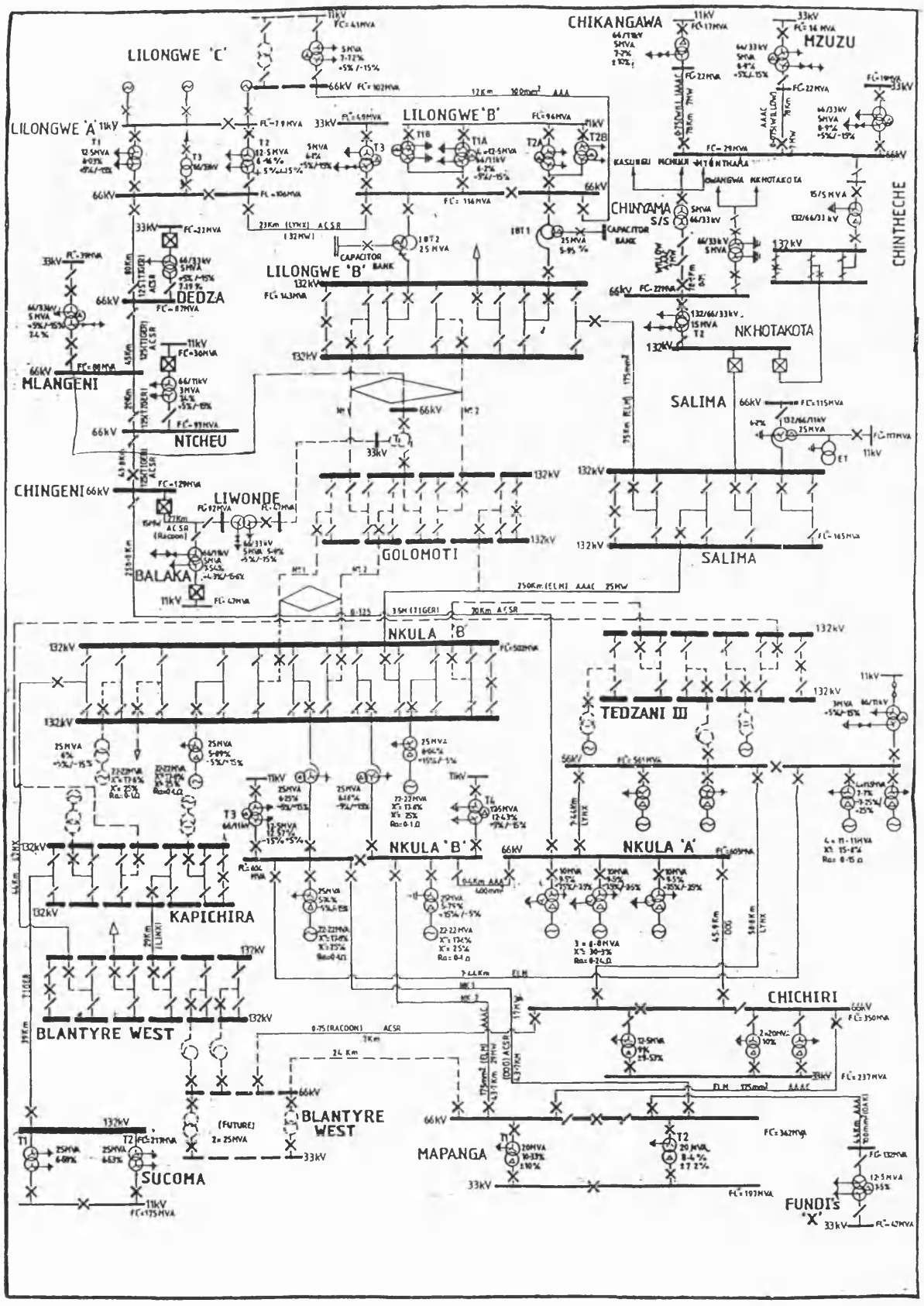

Figure 9.2 E.S.C.O.M Transmission system.

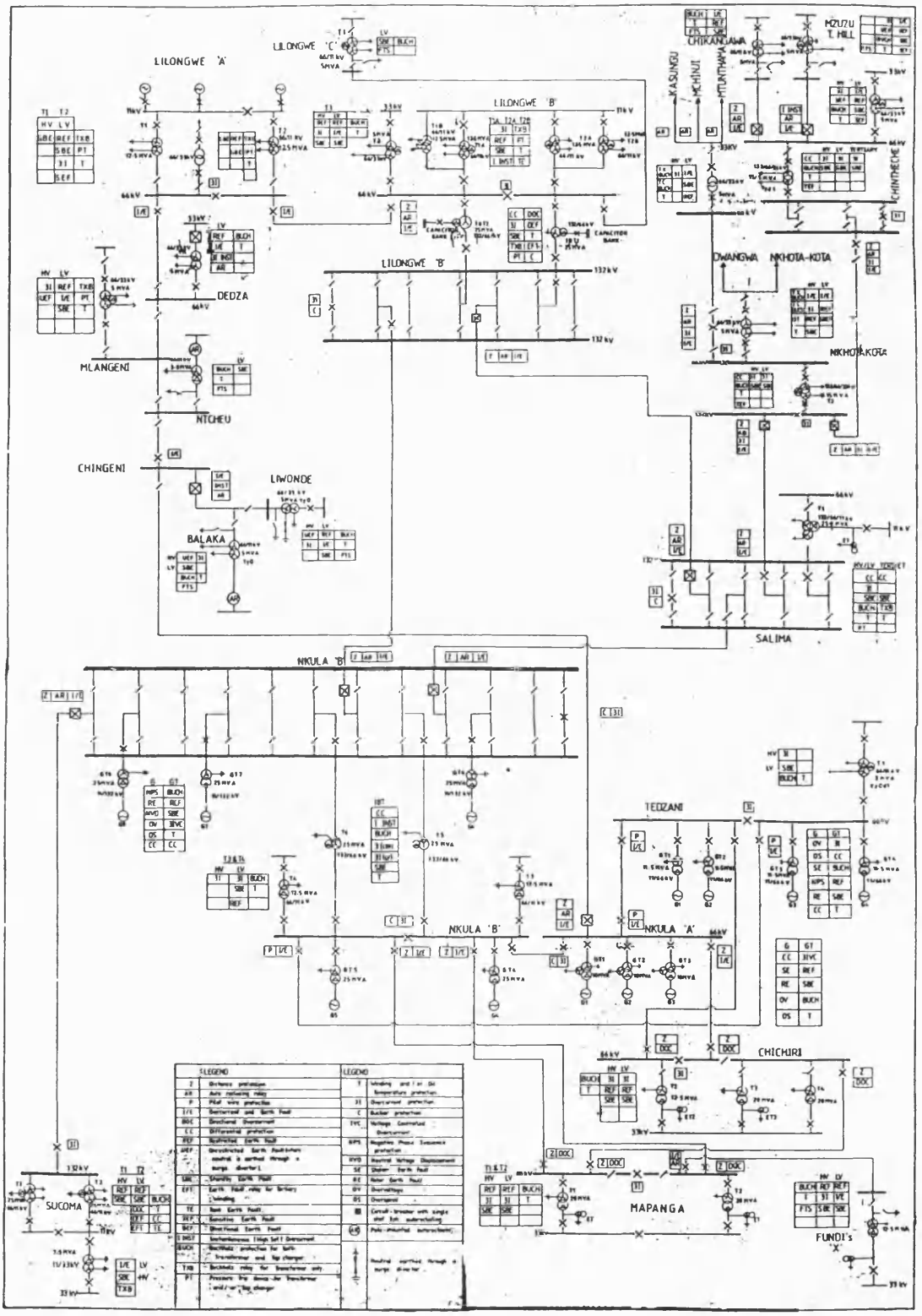

Figure 9.3 E.S.C.O.M. Power System Protection Diagram.

A.7 TABLES.

Basic Scenario	1991/92	1992/93	1993/94	1994/95	1995/96	1996/97	1997/98	1998/99	1999/00	2000/01	2001/02	2002/03	2003/04	2004/05	2005/06	2006/07	2007/08	2008/09	2009/10
DEMAND (MW)																			
Low Density	13.96	16.26	16.12	17.14	18.34	19.67	21.11	22.65	24.31	26.09	28.00	30.05	32.25	34.61	37.14	39.85	42.77	45.90	49.26
High Density	2.85	3.22	3.01	3.26	3.54	3.84	4.16	4.51	4.89	5.30	5.75	6.23	6.75	7.32	7.93	8.60	9.32	10.11	10.95
General	20.88	19.03	22.04	24.65	27.14	29.67	32.35	35.22	38.33	41.70	45.36	49.35	53.68	58.39	63.52	69.10	75.16	81.76	88.94
Small Power	49.49	48.65	49.71	51.76	55.11	59.16	63.88	69.24	75.24	81.90	89.25	97.34	106.21	115.93	126.57	138.20	150.93	164.83	180.02
Large Power																			
– SUCOMA	9.32	9.60	9.89	10.19	10.49	10.81	11.13	11.46	11.81	12.16	12.53	12.90	13.29	13.69	14.10	14.52	14.96	15.41	15.87
– Blantyre Water Board	7.37	7.60	7.82	8.09	8.49	8.73	9.22	9.42	9.66	9.91	10.18	10.45	10.73	11.02	11.32	11.32	11.32	11.32	11.32
– Portland Cement	3.56	3.71	3.79	3.88	3.97	4.07	4.17	4.28	4.39	4.51	4.69	4.86	5.07	5.28	5.49	5.71	5.93	6.17	6.42
– David Whitehead	4.21	4.21	4.21	4.21	4.21	4.21	4.21	4.21	4.21	4.21	4.21	4.21	4.21	4.21	4.21	4.21	4.21	4.21	4.21
– Viphya Saw Mill	1.00	1.13	1.24	1.37	1.51	1.66	1.82	2.00	2.20	2.42	2.67	2.93	3.23	3.55	3.91	4.30	4.73	5.20	5.72
– Central Leaf	1.14	1.15	1.24	1.28	1.48	1.69	1.69	1.69	1.69	1.69	1.69	1.69	1.69	1.69	1.69	1.69	1.69	1.69	1.69
– Tobacco Processors	0.40	0.36	0.95	0.95	0.95	0.95	0.95	0.95	0.95	0.95	0.95	0.95	0.95	0.95	0.95	0.95	0.95	0.95	0.95
– Limbe Leaf	1.04	1.47	1.63	1.63	1.63	1.63	1.63	1.63	1.63	1.63	1.63	1.63	1.63	1.63	1.63	1.63	1.63	1.63	1.63
– David Whitehead (Salima)	0.94	0.94	1.18	1.47	1.88	1.88	1.88	1.88	1.88	1.88	1.88	1.88	1.88	1.88	1.88	1.88	1.88	1.88	1.88
– DWASCO	1.66	1.41	2.08	2.34	2.50	2.50	2.50	2.50	2.50	2.50	2.50	2.50	2.50	2.50	2.50	2.50	2.50	2.50	2.50
– Lilongwe Water Board	1.11	1.01	1.26	1.58	1.97	2.21	2.21	2.21	2.21	2.21	2.21	2.21	2.21	2.21	2.21	2.21	2.21	2.21	2.21
– State House (Lilongwe)	0.65	0.72	0.79	1.19	1.19	1.19	1.19	1.19	1.19	1.19	1.19	1.19	1.19	1.19	1.19	1.19	1.19	1.19	1.19
– Irrigation (Mchinji)	0.00	0.00	0.00	0.00	0.00	0.00	0.00	0.00	0.00	0.00	0.00	0.00	0.00	0.00	0.00	0.00	0.00	0.00	0.00
– VIPCOR	0.00	0.00	0.00	0.00	0.00	0.00	0.00	0.00	0.00	0.00	0.00	0.00	0.00	0.00	0.00	0.00	0.00	0.00	0.00
– Other	0.00	0.00	0.00	0.00	0.00	0.00	0.00	0.00	0.00	0.00	0.00	0.00	0.00	0.00	0.00	0.00	0.00	0.00	0.00
Sub – total	32.40	33.31	36.09	38.18	40.28	41.52	42.60	43.42	44.32	45.26	46.32	47.42	48.58	49.79	51.07	52.10	53.19	54.35	55.58
Export	0.15	0.18	0.19	0.20	0.31	0.32	0.34	0.36	0.39	0.41	0.43	0.46	0.49	0.52	0.55	0.58	0.61	0.65	0.69
INTERCONNECTED SYSTEM																			
Correction to Calc Demand (MW)	−14.57	−8.36																	
Total (MW)	119.73	120.65	127.15	135.19	144.71	154.19	164.45	175.41	187.48	200.66	215.11	230.84	247.95	266.55	286.77	308.43	331.95	357.60	385.44
Auxilary Consumption (MW)	0.68	0.69	0.75	0.79	0.85	0.90	0.96	1.02	1.09	1.17	1.25	1.34	1.44	1.54	1.66	1.79	1.92	2.07	2.22
Tx. & Dbn. Losses (%)	20.7%	16.5%	16.5%	17.2%	17.2%	17.2%	17.2%	17.2%	17.2%	17.2%	17.2%	17.2%	17.2%	17.2%	17.2%	17.2%	17.2%	17.2%	17.2%
Losses (MW)	27.56	25.72	29.08	28.26	30.24	32.23	34.37	36.66	39.18	41.94	44.96	48.25	51.82	55.71	59.93	64.46	69.36	74.74	80.56
Generated (MW)	133.40	138.70	156.85	164.10	175.65	187.16	199.61	212.92	227.56	243.57	261.11	280.19	300.96	323.54	348.08	374.37	402.96	434.05	467.85
Growth rate in maximum demand	11.7%	4.0%	13.1%	4.6%	7.0%	6.6%	6.6%	6.7%	6.9%	7.0%	7.2%	7.3%	7.4%	7.5%	7.6%	7.6%	7.6%	7.7%	7.8%
Load Factor (generated)	66.1%	64.3%	62.2%	62.6%	62.6%	62.7%	62.5%	62.5%	62.4%	62.3%	62.3%	62.2%	62.1%	62.0%	62.0%	62.0%	62.0%	62.0%	62.0%

Basic Scenario	1991/92	1992/93	1993/94	1994/95	1995/96	1996/97	1997/98	1998/99	1999/00	2000/01	2001/02	2002/03	2003/04	2004/05	2005/06	2006/07	2007/08	2008/09	2009/10
CONSUMER NUMBERS																			
Low Density	21032	22609	24305	26128	28088	30194	32459	34893	37510	40323	43348	46599	50094	53851	57889	62231	66898	71916	77310
High Density	14372	14771	15892	16971	18151	19384	20701	22108	23610	25214	26927	28756	30710	32796	35024	37404	39945	42659	45557
kWh/CONSUMER																			
Low Density	4845	4955	4764	4712	4691	4681	4672	4664	4656	4648	4640	4632	4624	4616	4608	4600	4592	4584	4577
High Density	1191	1156	1177	1195	1213	1232	1250	1269	1288	1307	1327	1347	1367	1386	1409	1430	1451	1473	1496
SALES (GWh)																			
Low Density	100.25	116.92	115.79	123.10	131.76	141.33	151.65	162.74	174.64	187.41	201.13	215.84	231.63	248.58	266.76	286.28	307.22	329.70	353.82
High Density	17.73	20.00	18.71	20.28	22.02	23.87	25.88	28.05	30.41	32.96	35.73	38.74	41.99	45.52	49.34	53.49	57.98	62.85	68.13
General	102.44	93.34	108.11	120.92	133.12	145.55	158.68	172.77	188.02	204.56	222.54	242.08	263.33	286.45	311.60	338.96	368.71	401.08	436.29
Small Power	281.80	276.98	283.04	294.73	313.77	336.88	363.75	394.27	428.43	466.35	508.20	554.23	604.75	660.09	720.67	786.93	859.37	938.54	1025.06
Large Power																			
– SUCOMA	62.70	57.89	60.78	65.00	68.00	71.00	71.00	71.00	71.00	71.00	71.00	71.00	71.00	71.00	71.00	71.00	71.00	71.00	71.00
– Blantyre Water Board	67.10	45.81	47.65	49.55	51.53	53.60	55.74	57.97	60.29	62.70	65.21	67.82	70.53	73.35	76.28	79.34	82.51	85.81	89.24
– Portland Cement	16.74	17.76	18.47	19.21	19.98	20.77	21.61	22.47	23.37	24.30	25.28	26.29	27.34	28.43	29.57	30.75	31.98	33.26	34.59
– David Whitehead	25.43	25.43	25.43	25.43	25.43	25.43	25.43	25.43	25.43	25.43	25.43	25.43	25.43	25.43	25.43	25.43	25.43	25.43	25.43
– Viphya Saw Mill	5.25	5.95	6.54	7.19	7.91	8.71	9.58	10.53	11.59	12.75	14.02	15.42	16.96	18.66	20.53	22.58	24.84	27.32	30.05
– Central Leaf	3.00	6.06	6.54	6.73	7.80	8.87	8.87	8.87	8.87	8.87	8.87	8.87	8.87	8.87	8.87	8.87	8.87	8.87	8.87
– Tobacco Processors	1.77	1.58	4.17	4.17	4.17	4.17	4.17	4.17	4.17	4.17	4.17	4.17	4.17	4.17	4.17	4.17	4.17	4.17	4.17
– Limbe Leaf	5.44	7.71	8.57	8.57	8.57	8.57	8.57	8.57	8.57	8.57	8.57	8.57	8.57	8.57	8.57	8.57	8.57	8.57	8.57
– David Whitehead (Salima)	2.85	5.69	7.12	8.90	11.39	11.39	11.39	11.39	11.39	11.39	11.39	11.39	11.39	11.39	11.39	11.39	11.39	11.39	11.39
– DWASCO	5.83	4.92	7.29	8.20	8.74	8.74	8.74	8.74	8.74	8.74	8.74	8.74	8.74	8.74	8.74	8.74	8.74	8.74	8.74
– Lilongwe Water Board	7.36	6.73	8.41	10.51	13.14	14.72	14.72	14.72	14.72	14.72	14.72	14.72	14.72	14.72	14.72	14.72	14.72	14.72	14.72
– State House (Lilongwe)	2.69	2.96	3.26	4.89	4.89	4.89	4.89	4.89	4.89	4.89	4.89	4.89	4.89	4.89	4.89	4.89	4.89	4.89	4.89
– Irrigation (Mchinji)	0.00	0.00	0.00	0.00	0.00	0.00	0.00	0.00	0.00	0.00	0.00	0.00	0.00	0.00	0.00	0.00	0.00	0.00	0.00
– VIPCOR	0.00	0.00	0.00	0.00	0.00	0.00	0.00	0.00	0.00	0.00	0.00	0.00	0.00	0.00	0.00	0.00	0.00	0.00	0.00
– Other	0.00	0.00	0.00	0.00	0.00	0.00	0.00	0.00	0.00	0.00	0.00	0.00	0.00	0.00	0.00	0.00	0.00	0.00	0.00
Sub – total	206.17	188.49	204.21	218.35	231.56	240.86	244.71	248.76	253.03	257.53	262.29	267.31	272.61	278.23	284.16	290.45	297.11	304.18	311.67
Export	0.61	0.75	0.79	0.84	1.26	1.33	1.41	1.50	1.59	1.68	1.78	1.89	2.00	2.12	2.25	2.38	2.53	2.68	2.84
INTERCONNECTED SYSTEM																			
Total Sales (GWh)	648.64	654.98	730.64	778.22	833.48	889.62	946.08	1008.08	1076.11	1150.50	1231.66	1320.08	1416.32	1520.99	1634.79	1758.48	1892.92	2039.02	2197.80
Auxilary Consumption (GWh)	3.86	3.91	4.27	4.50	4.82	5.14	5.47	5.83	6.22	6.65	7.12	7.63	8.19	8.79	9.45	10.16	10.94	11.79	12.70
Tx. & Dbn. Losses (%)	15.6%	14.0%	14.0%	13.0%	13.0%	13.0%	13.0%	13.0%	13.0%	13.0%	13.0%	13.0%	13.0%	13.0%	13.0%	13.0%	13.0%	13.0%	13.0%
Losses (GWh)	120.56	109.42	119.64	116.96	125.26	133.73	142.18	151.50	161.73	172.91	185.11	198.39	212.86	228.59	245.69	264.28	284.49	306.44	330.31
Generated (GWh)	772.80	781.60	854.55	899.67	963.56	1028.70	1093.73	1165.41	1244.06	1330.05	1423.89	1526.11	1637.36	1758.37	1889.93	2032.93	2188.35	2357.25	2540.81

Table 9.1 E.S.C.O.M. Load Forecasting Model
(updated May 1993).

Plant		Quantity
132 kV Overhead Lines (steel towers)	(km)	362
132 kV Overhead Lines (wooden poles)	(km)	593
66 kV Overhead Lines	(km)	820
33 kV Overhead Lines	(km)	1,766
11 kV Overhead Lines	(km)	2,010
400 / 230 Volts Overhead Lines	(km)	2,245
33 kV Underground Cable	(km)	6.9
11 kV Underground Cable	(km)	89.6
400 / 230 Volts Underground Cable	(km)	178
Step-up 11/132 kV Substations	(kVA)	75,000
Step-up 11/66 kV Substations	(kVA)	126,000
Step-up 11/33 kV Substations	(kVA)	8,500
Step-up 0.4/11 kV Substations	(kVA)	8,100
Step-up 3.3/11 kV Substations	(kVA)	3,380
Step-down 33/11 kV Substations	(kVA)	100,000
Step-down 33/0.4/0.23 kV Substations	(kVA)	55,410
Step-down 11/0.4/0.23 kV Substations	(kVA)	244,666
Step-down 66/11 kV Substations	(kVA)	101,000
Step-down 66/33 kV Substations	(kVA)	145,000
Step-down 132/11 kV Substations	(kVA)	50,000
Step-down 132/66/11 kV Substations	(kVA)	25,000
Step-down 132/66/33 kV Substations	(kVA)	30,000
Interbus Transformers 132/66 kV	(kVA)	50,000
Interbus Transformers 132/66/11 kV	(kVA)	50,000

Table 9.2 Summary of Transmission and Distribution Systems in E.S.C.O.M.

		1986	1987	1988	1989 /90	1990 /91	1991 /92	1992 /93	1993/ 94
System peak demand	Mw	94.8	97.2	101.	114.	119.	133.	143.	158
System losses	%	16.2	16.6	17.5	16.3	15.0	15.6	14.1	13.5
Plant availability (hydro)	%	85.6	85.2	85.2	87.4	85.0	92.7	90.0	90.0
Faults per 100 consumers	No.	-	22.0	22.0	30.0	29.0	29.7	30.0	30.0
Average connection period	Days	14.0	14.0	14.0	14.0	14.0	14.0	14.0	14.0

Table 9.3 E.S.C.O.M.'s Performance from 1986.

PUBLISHED WORK.

1. M A Redfern, A A W Chiwaya, 'A New Approach to Digital Current Differential Protection for Low and Medium Voltage feeder Circuits using a Digital Voice-Frequency Grade Communications Channel', IEEE Transactions on Power Delivery, Vol. 9, no. 3, July 1994, pp. 1352 - 1358.

2. M A Redfern, R J Hewett, A A W Chiwaya, 'An Investigation into Reverse Power Flow Protection for Small and Medium sized Embedded Generation', Proceedings of the 28th Universities Power Engineering Conference, Stafforshire University, September, 1993.

3. M A Redfern, A A W Chiwaya, 'A Digital Current Differential Protection for Distribution Feeders using Voice Frequency Data Communications', International Conference on New Developments in Power System Protection and Local Control, Beijing, China, May 1994.

4. A A W Chiwaya, M A Redfern, 'A New Microprocessor based Current Differential Protection for Distribution Feeders', Proceedings of the 29th Universities Power Engineering Conference, University of Galway, Ireland, September, 1994.

5. A A W Chiwaya, M A Redfern, 'A Novel Technique in Digital Current Differential Protection for Distribution Feeders', International Power Engineering Conference, Singapore, 1995.

PAPER 1

M A Redfern, A A W Chiwaya, 'A New Approach to Digital Current Differential Protection for Low and Medium Voltage feeder Circuits using a Digital Voice-Frequency Grade Communications Channel', IEEE Transactions on Power Delivery, Vol. 9, no. 3, July 1994, pp. 1352 - 1358.

94 WM 013-3 PWRD

A NEW APPROACH TO DIGITAL CURRENT DIFFERENTIAL PROTECTION FOR LOW AND MEDIUM VOLTAGE FEEDER CIRCUITS USING A DIGITAL VOICE-FREQUENCY GRADE COMMUNICATIONS CHANNEL.

M A Redfern, Member IEEE and A A W Chiwaya

School of Electronic and Electrical Engineering,
University of Bath,
Bath, BA2 7AY, UK.

Abstract:- A new approach to digital current differential protection is described which provides the capabilities of conventional pilot wire differential protection while using the limited data transfer capabilities of a digital data voice-frequency grade communications channel. This approach compares polyphase polarised current measurements taken at the feeder's terminals to detect faults and can trip in under two power system cycles. The algorithms decouple the measurements from the power system frequency and its waveform, and thereby have a high inherent tolerance to the complications introduced by communication channel delays and their fluctuations. For this project, the communications requirements have been limited to a full duplex 2400 bits/sec system suitable for operation over a voice-frequency grade channel. Naturally a higher data rate would have provided less problems, but the object of the exercise was to tackle these problems.

Keywords:- Power System Protection, Unit Protection, Differential Protection, Feeder Protection, Digital Relaying, Digital Data Communications, and Voice-Frequency Grade Communications Channel.

1. INTRODUCTION.

The concepts behind current differential relaying are both simple and elegant. They therefore provide the basis for efficient and effective power system protection relaying. When applied to feeder circuits, the separation between the terminals of the protected feeder introduces the need for a communications system. Ideally, the communications system should instantaneously transfer all the data required for the protection between the relays which constitute the scheme. Unfortunately, in the real world, instantaneous, high volume data communications is not possible.

Practical communications systems are limited in the quantity of data that they can handle in a specified time period, and they introduce time delays from when the data is made available for transfer at one terminal and provided for use at the others. This has led to investigations into new approaches to differential relaying to formulate algorithms which are tolerant to the limited capacity and associated time delays of practical communications systems.

Communications systems are principally characterised by their data carrying capacity. In general, the higher the data rate the higher the cost. The communications system may use metallic conductors, optical fibres, or free space via radio or microwave as the communications medium. The system may be dedicated to one user or shared between several. The choice depends on availability, costs and geography.

Voice-frequency grade communication channels are the most commonly used systems having been developed for telephone communications. They provide a standardised communications environment operating over a variety of media. With an operating bandwidth of 4 kHz, they can use a dedicated medium or share a medium with other channels. Having been extensively developed commercially for mass communications, they provide a convenient standard for use with distribution system protection schemes. Since the available bandwidth is limited, the volume of data which can be handled is also limited. Standard data rates cover a wide range varying from 75 bits/sec to 14.4 kbits/sec operating in full or half duplex.

94 WM 013-3 PWRD A paper recommended and approved by the IEEE Power System Relaying Committee of the IEEE Power Engineering Society for presentation at the IEEE/PES 1994 Winter Meeting, New York, New York, January 30 - February 3, 1994. Manuscript submitted July 22, 1993; made available for printing November 29, 1993.

The commercial importance of voice-frequency grade communication channels is prompting continual research by the communications industry to increase channel capacity. For this study, a full duplex digital data capacity of 2400 bits/sec has been used. Although this may be considered modest in light of currently available systems, the inherent communications security and its tolerance to interference generally vary with the inverse of the data rate. It also provides a useful challenge to examine the level of performance which can be achieved with the system.

2. FEEDER CURRENT DIFFERENTIAL RELAYING.

The concepts behind current differential relaying were established by Merz and Price in the early 1900's. To protect feeder circuits, relays are located at the terminals of the protected feeder to monitor the electrical quantities required for the trip decision, to provide data for other relays in the scheme, and to initiate local circuit breaker operation. For the decision making, data relating to the state of the power system must be transferred from the remote terminal(s) to the local terminal and then compared with data obtained at that terminal. This requires use of a communications channel for the transfer of data.

Traditional current differential relaying[1] uses either electro-mechanical or analogue static relays together with copper pilot wires to provide the communications circuit. In these schemes, the pilot circuit is an integral part of the decision making process since it provides the electrical signal summation circuit. This applies equally for the circulating current and balanced voltage schemes. The typical operating time of these relays varies from one and a half to three cycles depending on the type of relay, its settings and the fault.

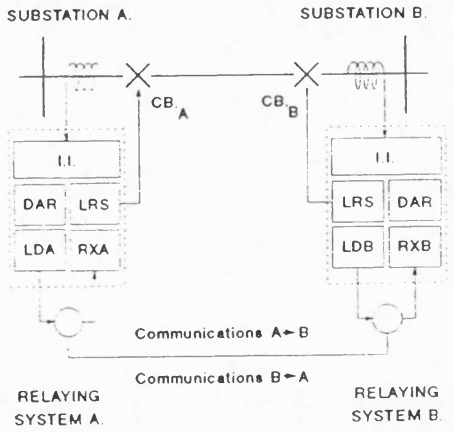

I.I. INPUT INTERFACE.
DAR DATA ACQUISITION FOR REMOTE RELAY.
LRS LOCAL RELAY SYSTEM.
LDA LINE DRIVER - RELAY A (B).
RXA RECEIVER - RELAY A (B).

FIGURE 1. SIMPLIFIED BLOCK DIAGRAM OF A DIGITAL CURRENT DIFFERENTIAL PROTECTION SCHEME.

For digital relaying, where digital data is transferred between relays, the data can not be summated in the communications media in the manner used with traditional relays. For simultaneous decision making by the relays at the feeder's terminals, full duplex data transmission is required and independent decision making is made at each terminal. A simplified representation of a typical digital current differential scheme is shown in figure 1.

The operation of the classical digital current differential scheme is similar to that described by Kwong et al[2]. The volume of data together with the communications

system protocols and error detection coding demanded the use of a wideband communications system. The system described used a CCITT standard 64 kbits/sec full duplex communications. Taking eight samples per cycle, the resulting average relay operating time was about 26 msec, for a 50 Hz system.

A different approach was adopted by Wheatley[3]. He described a system which could use either Pulse Coded Modulation (PCM) digital or Frequency Modulated (FM) analogue communications. The PCM option used a 64 kbits/sec channel whereas in the FM option could operate over voice-frequency grade communication channels. Using this later option, the power system waveform was frequency modulated onto a 1750 Hz audio tone carrier frequency. This represents the flattest part of the voice-frequency grade channel's group delay characteristic and hence provided the least probability of distortion in the demodulated signal.

Several researchers have examined techniques to reduce the volume of data required to be transferred between relays in a current differential scheme. The charge comparison technique described by Ernst et al[4] and Albrecht et al[5] provided a new solution to the difficulties of limited communications capabilities. They highlighted the critical disadvantages of digital current differential relaying and described a phase and magnitude comparison scheme for which the communications requirements were satisfied using a 7.2 kbits/sec data rate suitable for transmission over a voice-frequency grade communications channel.

An important and inherent advantage of using digital techniques, as highlighted by several authors, is the opportunity to include other protection algorithms in the package in addition to the current differential scheme. These other algorithms can overcome the non-operation of the unit protection should the communications channel be lost. Since local data relating to the operation of the power system is available, these additional schemes can include non-unit protection functions providing stand-alone and back-up protection features.

3. THE CURRENT DIFFERENTIAL ALGORITHM.

3.1. Data Reduction.

The new current differential algorithms were formulated to accommodate a relatively low data rate and the fluctuating channel delay times of a voice-frequency grade communications channel. As stated earlier, the communications offered a data rate of 2400 bits/sec operating in a full duplex scheme. This data rate corresponds to a data transfer rate of 48 bits of data for each cycle of a 50 Hz power system frequency. Allowing for a nominal fifty percent overhead for communications protocols and error detection coding, this reduces the data transfer capacity to a modest 24 bits per cycle. Channel delay times depend on the communications equipment used and the communications medium, but can be assumed to be of the order of a few milliseconds.

To overcome the need to transmit the mass of data required to define the sampled current waveform and operate with a data transfer capacity of 24 bits/cycle, techniques were examined which would dramatically reduce the data used to define the current signals. Instead of using the sampled data, the locally obtained data samples were compared with locally obtained reference data, polarising signals, to produce a non-sinusoidal signal which characterised the locally measured three-phase currents. To provide both phase and magnitude data, two signals were derived, using similar processing but with orthogonal reference waveforms.

The technique chosen was based on the equations used to derive the instantaneous power in a three-phase circuit. Multiplying the instantaneous values of the sampled phase currents with the instantaneous values of three-phase reference phasors provides a measurement which contains a steady component plus second harmonic terms. This steady, or dc, component contains both amplitude and phase information of the monitored three-phase currents with respect to the reference phasors. A second measurement, using an orthogonal set of phasors, provides complimentary information, and hence these two measurements fully characterise the monitored terminal currents.

A variety of power system derived signals could have been used for the reference phasors. These should be synchronised to the power system frequency and ideally have the same phase at all of the feeder's terminals. Since this protection is principally aimed at distribution feeders and assuming an interconnected power system, the most useful signals are the terminal's three phase voltages, a single phase voltage, and the positive phase sequence current. For the results presented below, the terminal's three-phase voltages have been used to derive the reference.

The reference phasors are a set of three unit amplitude rotating sinusoidal waveforms, 120 degrees apart. The principal set corresponds to the phase to ground voltages and the second set to the phase to phase voltages. Selecting the appropriate voltage derived reference waveforms to be used with the sampled currents produces two orthogonal reference sets. Since the protection is required to operate during faults causing voltage collapse, a memory feature is included

With balanced three-phase currents, the summation of the products of instantaneous three-phase currents, i_a, i_b and i_c, and instantaneous values of the reference phasors, s_a, s_b and s_c, together with some filtering, produces a constant term I_p representing the amplitude of the current in phase with the reference phasors[6]. The orthogonal set of reference phasors, (s_a-s_b), (s_b-s_c) and (s_c-s_a) produces a constant term I_q representing the amplitude of the current orthogonal to the reference phasors.

$$I_p = i_a s_a + i_b s_b + i_c s_c \tag{1}$$

$$I_p = 3\, I \cos(\phi) \tag{2}$$

and,

$$I_q = i_a(s_b - s_c) + i_b(s_c - s_a) + i_c(s_a - s_b) \tag{3}$$

$$I_q = 3\sqrt{3}\, I \sin(\phi) \tag{4}$$

where I_p and I_q are nonoscillating constants.

The filtering is required for unbalanced fault or load conditions, where because the currents are not balanced, second harmonic terms are introduced. Analysis of equation (1) to consider unbalance currents involves replacing the three-phase currents by three balanced systems containing positive, negative and zero phase sequence components.

Letting;-

$$i_{a0} = i_{b0} = i_{c0} = I_0 \sin(\omega t + \Theta_0 + \phi_0) \tag{5}$$

$$\begin{aligned} i_{c1} &= I_1 \sin(\omega t + \Theta_1 + \phi_1) \\ i_{b1} &= I_1 \sin(\omega t + \Theta_1 + \phi_1 + \tfrac{4\pi}{3}) \\ i_{c1} &= I_1 \sin(\omega t + \Theta_1 + \phi_1 + \tfrac{2\pi}{3}) \end{aligned} \tag{6}$$

$$\begin{aligned} i_{a2} &= I_2 \sin(\omega t + \Theta_2 + \phi_2) \\ i_{b2} &= I_2 \sin(\omega t + \Theta_2 + \phi_2 + \tfrac{2\pi}{3}) \\ i_{c2} &= I_2 \sin(\omega t + \Theta_2 + \phi_2 + \tfrac{4\pi}{3}) \end{aligned} \tag{7}$$

and,

$$\begin{aligned} s_a &= \sin(\omega t + \Theta) \\ s_b &= \sin(\omega t + \Theta + \tfrac{4\pi}{3}) \\ s_c &= \sin(\omega t + \Theta + \tfrac{2\pi}{3}) \end{aligned} \tag{8}$$

equation 1 becomes;

$$I_p = 3\, I_1 \cos(\phi_1) - 3\, I_2 \cos(2\omega t + \Theta + \Theta_2 + \phi_2) \tag{9}$$

Although this technique removes the zero phase sequence currents immediately, the negative phase sequence components produce the second harmonic term. Averaging the measurements of I_p and I_q over half a power system cycle, removes these terms leaving the steady, dc term.

3.2. The Communications Systems.

Considerable expertise and investment has been applied to telephone based digital data communication systems, and therefore these systems provide an almost ready made communications platform which can be used for feeder protection schemes.

The basis of the interface between the digital protection system and the communications medium is the modem. These operate at a wide variety of different operating speeds and offer different advantages for different applications. To ensure connectivity between different equipments, a host of national and international standards have been agreed to define the characteristics of the different systems[7], some of which are illustrated in figure 2.

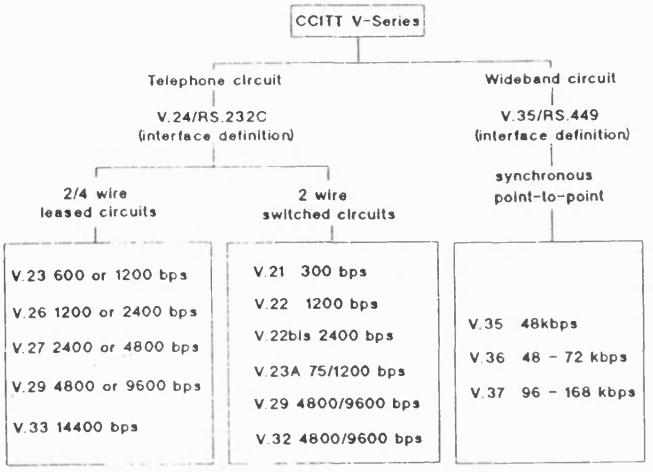

FIGURE 2. SUMMARY OF CCITT V-SERIES MODEM STANDARDS.

The V26 standard was chosen for this application because of its short initialisation time and its tolerance to noise. This can be illustrated by comparing the V26 standard to V33. Although the V33 offers a higher data rate, its idling time is greater than 50 msec compared to the 15 msec of the V26[8]. The tolerance to interference is related to the system's energy per bit to noise ratio, E_b/N_o[9], defined by:-

$$\frac{E_b}{N_o} = \frac{\left(\frac{S}{R}\right)}{N_o} \qquad (10)$$

where,

E_b is the signal energy per bit
N_o is the noise energy per hertz
S is sending signal strength

and,

R is data bit rate.

For a constant sending signal strength and interference level, an increase in the data rate decreases the energy per bit to interference energy ratio and hence increases the possibility of data corruption.

The data stream used for the relaying scheme was organised as shown in figure 3. Each block of code was started with an six bit header followed by two Hamming (13,9) code blocks. The six bit header is a defined set of bits which provides data synchronism. Each Hamming code block contains thirteen bits, nine of which are data bits. Each message block therefore contains eighteen data bits. These comprised of two identifier bits, two bits reserved for other applications and fourteen data bits relating to I_p and I_q alternatively. The identifier bits were used to define the measurement as corresponding to I_p ('0' '0') or I_q ('1' '1'). The remaining eight bits were used for error detection such that should data be corrupted, the security of the protection would not be compromised.

Each thirty-two bit message requires 13.33 milliseconds transmission time and hence this delay must be included in the protection algorithm. Since the data stream could be considered to be continuous, although marshalling, decoding and propagation delays had to be accommodated in the algorithms, data was available each 13.33 milliseconds. Marshalling times and propagation delays were assessed to be within 3.66 milliseconds and hence the data communications delay was taken to be 17 milliseconds in total.

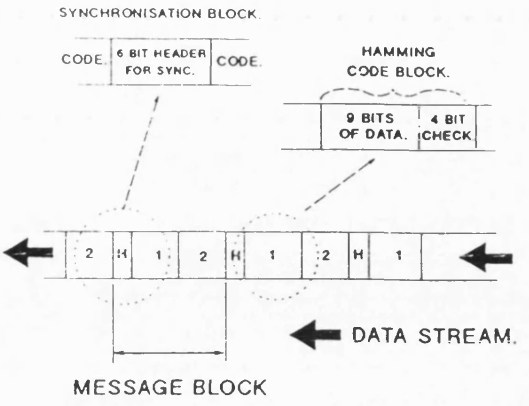

FIGURE 3. DATA STREAM ORGANISATION.

3.3. Algorithm Operation.

The general operation of the algorithm is shown in figure 4. The input signals were filtered using anti-aliasing filters and then sampled using the A/D converter. For the results presented the samples were taken every millisecond, using a 50 Hz power system. The voltage samples were used to generate the reference phasors and the current samples were used with these to generate the basic I_p and I_q signals. These were then filtered using a half cycle filter to remove any second harmonic terms.

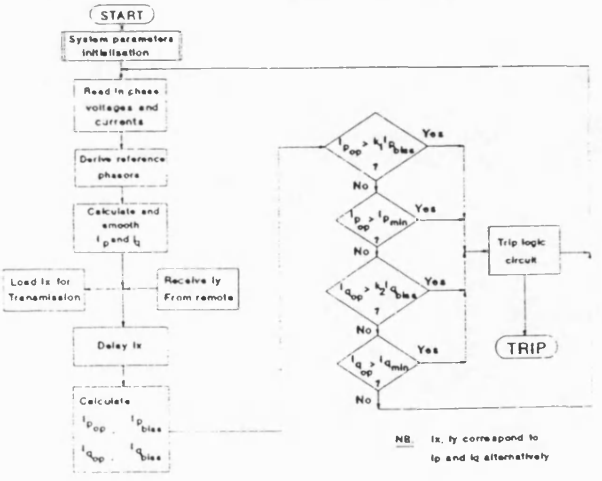

FIGURE 4. GENERAL OPERATION OF THE PROTECTION ALGORITHM.

Shortly before the end of one message's transmission period, the next value of I_p or I_q was provided in rotation to the data sending unit for coding and transmission. If the last transmission was of the measurement I_p, the next would be I_q and vice versa.

As soon as an incoming message had been received and decoded, its value together with the value obtained from local measurements was provided for the trip comparator. This received value was compared to the corresponding locally measured signal delayed by the message transmission delay together with an allowance for signal propagation delays and marshalling. With the message structure described above, a 17 millisecond delay was introduced to the locally derived measurement, and the decision process was executed after receipt of a message, i.e. every 13.33 milliseconds.

A similar trip algorithm is used for both I_p and I_q, namely:-

$$\begin{aligned} (I_p)_{op} &= | I_{p_L} - I_{p_R} | \\ (I_p)_{bias} &= \frac{1}{2} (| I_{p_L} | + | I_{p_R} |) \\ (I_q)_{op} &= | I_{q_L} - I_{q_R} | \\ (I_q)_{bias} &= \frac{1}{2} (| I_{q_L} | + | I_{q_R} |) \end{aligned} \qquad (11)$$

and the trip indication was given when either of the following applied:-

$$\begin{aligned} (I_p)_{op} > (I_p)_{min} \quad AND \quad (I_p)_{op} > k_p (I_p)_{bias} \\ (I_q)_{op} > (I_q)_{min} \quad AND \quad (I_q)_{op} > k_q (I_q)_{bias} \end{aligned} \qquad (12)$$

The trip settings were set at 200 Amps for both $(I_p)_{min}$ and $(I_q)_{min}$ and the bias settings were 2.0 percent for both $(I_p)_{bias}$ and $(I_q)_{bias}$.

Two trip conditions were required before the relay trip is given. These could either be consecutive trip decisions, i.e. I_p and then I_q, or vice versa, or alternatively two subsequent I_p or I_q trips. The theoretical relay tripping time was therefore a minimum of 30 milliseconds, varying up to 50 milliseconds where the fault occurred just after the marshalling process for the next transmission had begun.

Separating the trip decisions so that they were based on I_p or I_q, and requiring two trip decisions before tripping the relay provided a faster trip output than combining the two measurements.

4. ALGORITHM EVALUATION.

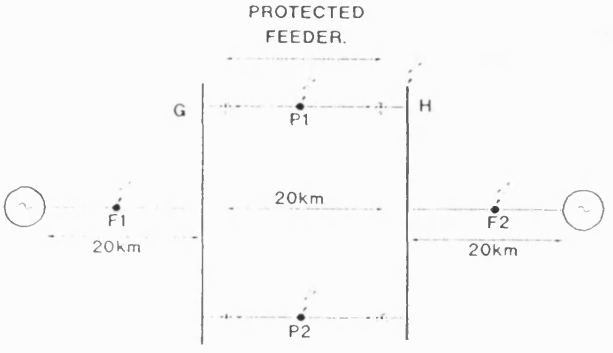

FIGURE 5. MODEL POWER SYSTEM USED FOR ALGORITHM EVALUATION.

Evaluation of the protection algorithm was performed using the EMTP power system simulation package. The power system model was of a typical 33 kV feeder network containing parallel feeders, as shown in figure 5. Both overhead lines and underground cables were modelled together with a variety of faults at different fault positions to examine the algorithm's response. Both internal and external faults were considered, with external faults being applied both on the parallel feeder and the supply feeders.

The most common type of fault in sub-transmission and distribution systems is the single phase to ground fault. Figure 6 shows the current, the C-phase voltage, the C-phase reference signal, and the polarised currents measured at the local terminal for a mid-zone fault on an overhead line system. Within twenty milliseconds after the fault, both I_p and I_q have settled to a new steady value. Figure 7 shows the comparisons between the locally obtained I_p and I_q signals to those received from the remote end of the feeder. This clearly shows the delays between the two signals which are caused by the communications system delays and the differences between the measurements during the fault. Using the trip requirement of two subsequent trip indications, leads to a trip time of 36 milliseconds.

Figure 8 shows the comparisons between the locally obtained I_p and I_q signals for an external single phase to ground fault. For this situation, the I_p currents are relatively small and although there is a difference between the local and remote signals, this is less than the trip setting. For this fault, the algorithm remains stable and does not trip.

A similar fault to that used in figure 7 but for an underground cable network is shown in figure 9. There are dramatic differences between the local and remote measurements after the fault and the algorithm tripped after 33 milliseconds. The response to an external single phase to ground fault on the underground cable system is shown in figure 10. The differences in the post fault local and remote measurements were within the trip setting, and the algorithm remained stable.

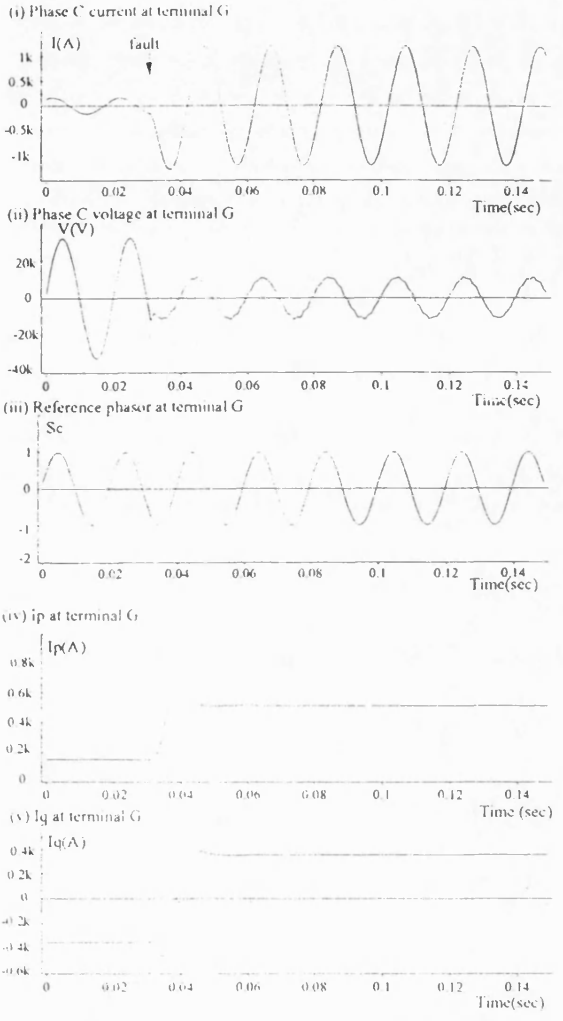

FIGURE 6. INPUT AND ALGORITHM DERIVED WAVEFORMS FOR AN INTERNAL SINGLE PHASE FAULT AT POINT P1 ON THE TEST SYSTEM.

The response curves for phase to phase faults on an overhead line is illustrated in figure 11. The differences between the local and remote measurements of I_p and I_q led to the algorithm tripping after 33 milliseconds. The response to a similar fault but external to the protected zone is shown in figure 12. For this the algorithm remained stable and did not trip.

The responses to internal and external three phase to ground faults are shown in figures 13 and 14 respectively. For these the internal fault resulted in tripping after 35 milliseconds but the algorithm remained stable for the external fault.

A more demanding fault is illustrated in figure 15, which shows a terminal fault resulting in voltage collapse at the remote terminal. For this the memory feature of the reference phasors was required. Although the disturbance was detected, the

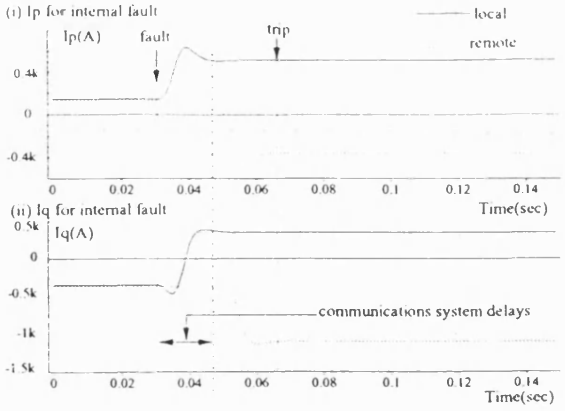

FIGURE 7. POLARISED CURRENTS FOR AN INTERNAL SINGLE PHASE FAULT AT POINT P1 ON THE SYSTEM WITH OVERHEAD LINE FEEDERS.

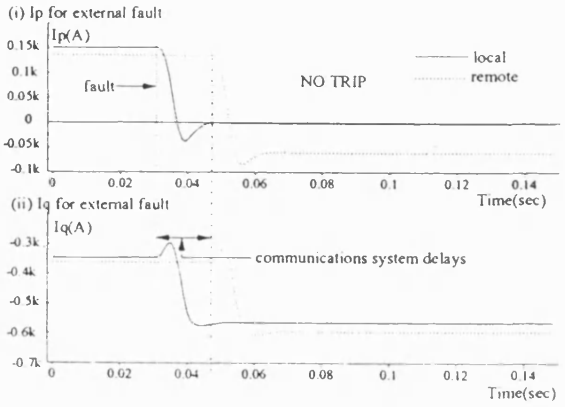

FIGURE 8. POLARISED CURRENTS FOR AN EXTERNAL SINGLE PHASE FAULT AT POINT F1 ON THE SYSTEM WITH OVERHEAD LINE FEEDERS.

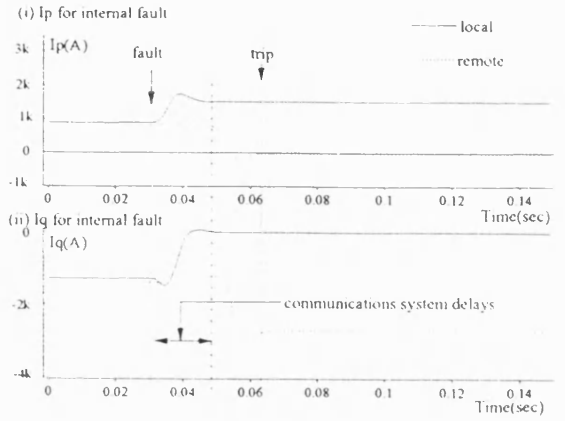

FIGURE 9. POLARISED CURRENTS FOR AN INTERNAL SINGLE PHASE FAULT AT POINT P1 ON THE SYSTEM WITH UNDERGROUND FEEDERS.

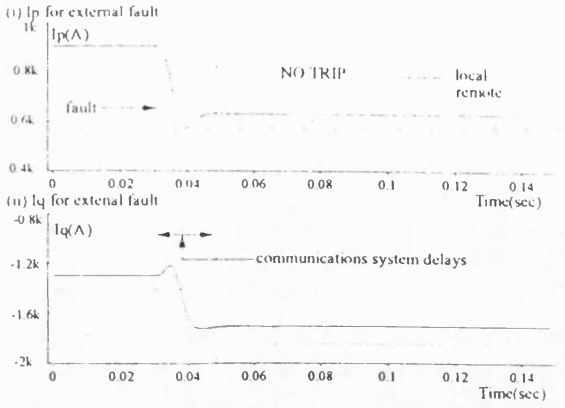

FIGURE 10. POLARISED CURRENTS FOR AN EXTERNAL SINGLE PHASE FAULT AT POINT F1 ON THE SYSTEM WITH UNDERGROUND FEEDERS.

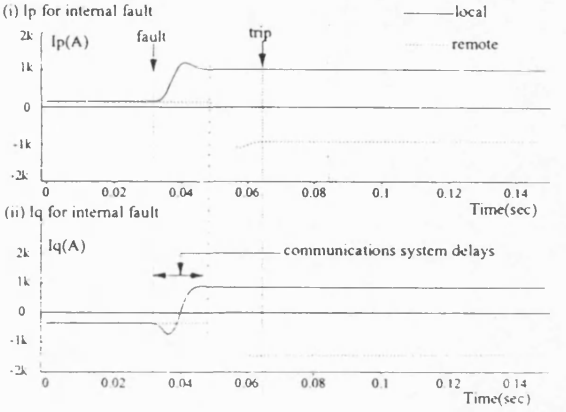

FIGURE 11. POLARISED CURRENTS FOR AN INTERNAL PHASE TO PHASE FAULT AT POINT P1 ON THE SYSTEM WITH OVERHEAD LINE FEEDERS

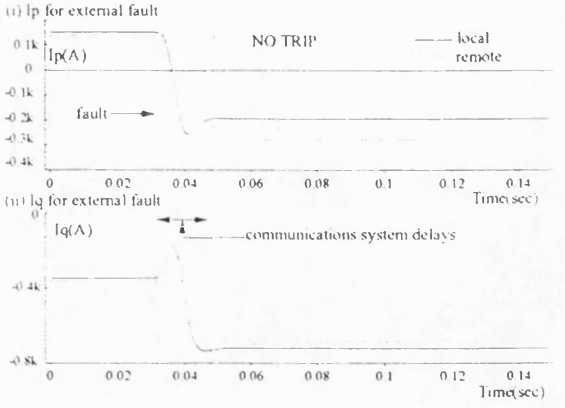

FIGURE 12. POLARISED CURRENTS FOR AN EXTERNAL PHASE TO PHASE FAULT AT POINT F1 ON THE TEST SYSTEM WITH OVERHEAD LINE FEEDERS.

algorithm remained stable since it did not receive the second trip indication.

For all of the above tests, the trip times have been measured with the communications system collecting data soon after the fault occurrence. However, the communications would normally be free running and not synchronised with the fault and therefore the trip times could vary from those recorded, to those plus 13.33 milliseconds giving typical maximum tripping times of 50 milliseconds.

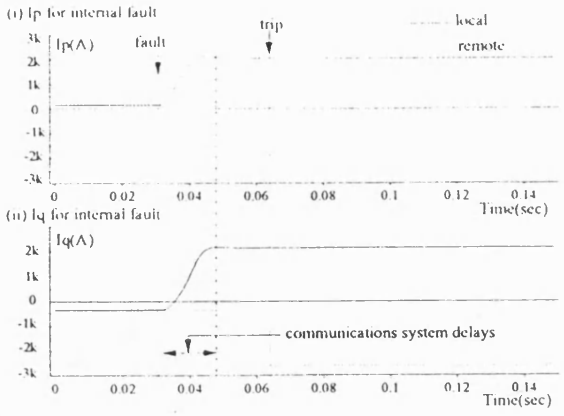

FIGURE 13. POLARISED CURRENTS FOR AN INTERNAL THREE PHASE TO GROUND FAULT AT POINT P1 ON THE TEST SYSTEM WITH OVERHEAD LINE FEEDERS.

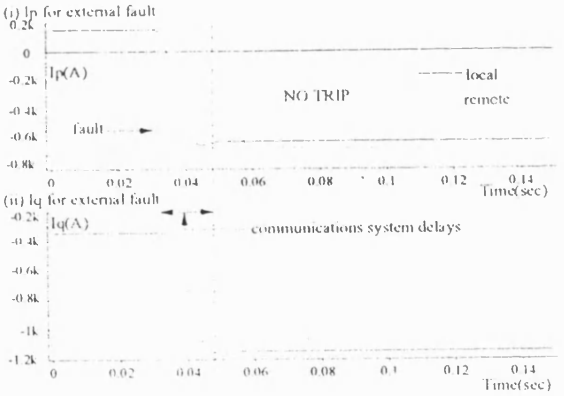

FIGURE 14. POLARISED CURRENTS FOR AN EXTERNAL THREE PHASE TO GROUND FAULT AT POINT F1 ON THE TEST SYSTEM WITH OVERHEAD LINE FEEDERS.

5. CONCLUSION.

This current differential protection algorithm has been developed to accommodate the modest communications capabilities associated with a robust digital data voice-frequency grade communications channel. To avoid the need to accurately synchronise the data at the local and remote ends of the feeder, two reference phasor sets are derived which are used to provide a polarised measurement of the three phase currents.

The current measurement system, when coupled with a half cycle filter to remove second harmonic terms, provides a steady, dc, output. Using two orthogonal reference phasor sets, provides the data required to characterise the currents measured. Requiring two trip indications before allowing the algorithm to trip provides security against mal-operation due to the transitions in the measured *Ip* and *Iq* signals after the fault.

For the fault conditions presented for which the algorithm should trip, the tripping times were all about 35 milliseconds for in-zone faults. Variations in the synchronism between fault occurrence and data transmission could increase these times to approximately 50 milliseconds. For all external faults, including a terminal fault, the algorithm remained stable and did not trip.

The principal constraint for this technique is the time required to transmit data from one terminal to another. Reducing this time, by increasing the data rate, would reduce the tripping time. The power system frequency period, was not so significant, and similar tripping times would have been obtained with a 60 Hz power system.

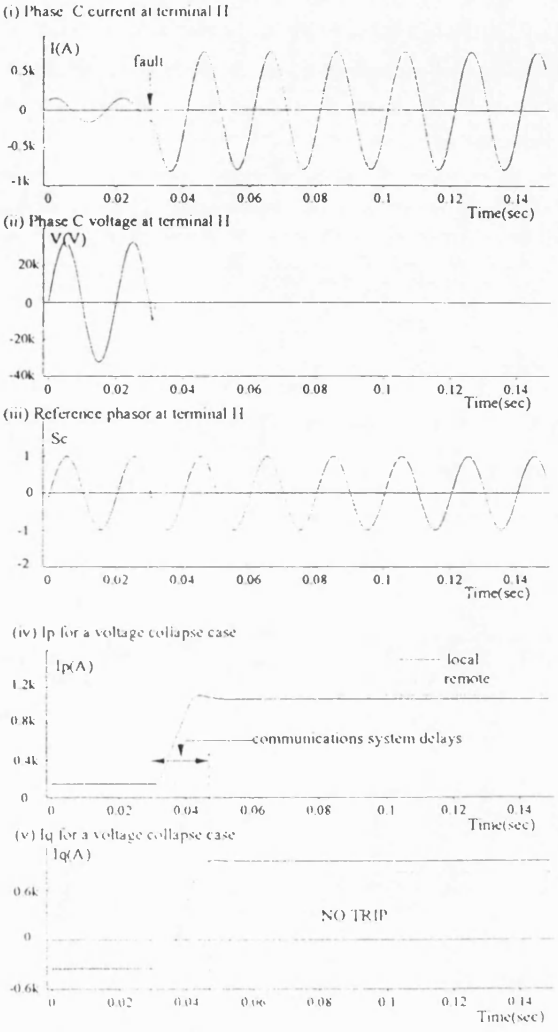

FIGURE 15. INPUT AND ALGORITHM DERIVED WAVEFORMS FOR A THREE PHASE TO GROUND FAULT AT TERMINAL H ON THE TEST SYSTEM.

6. REFERENCES.

1. GEC MEASUREMENTS, 'Protective Relays Application Guide', 3rd edition, 1987, pp 159 - 181.

2. W. S. Kwong, M. J. Clayton, A. Newbould, 'A Micropocessor-based Current Differential Relay for use with Digital Communication Systems', 3rd International Conference on Developments in Power System Protection, IEE Conference publication 249, 17-19 April 1985, pp 65 - 69.

3. J. Wheatley, 'A Microproccessor-based Current Differential Protection', 4th International Conference on Developments in Power System Protection, IEE Conference publication 302, 11-13 April 1989, pp 116 - 120.

4. L J Ernst, W L Hinman, D H Quam, J S Thorp, 'Charge Comparison Protection of Transmission Lines - Relaying Concepts', IEEE transactions on Power Delivery, Vol. 7, No. 4, October 1992, 92 WM 209-7 PWRD, pp 1834 - 1842.
5. N P Albrecht, W C Fleck, K J Fodero, R J Ince, ' Charge Comparison Protection of Transmission Lines - Communications Concepts', IEEE transanctions on Power Delivery, Vol. 7, No. 4, October 1992, 92 WM 210-5 PWRD, pp 1853 - 1859.
6. IEEE Tutorial Course, 'Nonsinusoidal situations: Effects on the Performance of Meters and Definitions of Power', IEEE Power Engineering Society, course text 9OEH0327-7-PWR.
7. R L Brewster (editor), 'Data Communications and Networks', Peregrinus book publication 1986, pp 12 - 13, ISBN 0-86341-078-2.
8. D R Doll, 'Data Communications, Facilities, Networks, and Systems Design', Wiley and Sons book publication 1978, pp 197 - 203, ISBN 0-471-21768-9.
9. W Stallings, 'Data and Computer Communications', MacMillan book publication 1985, pp 42 - 47, ISBN 0-02-415440-7.

Miles A Redfern (M'79) received his BSc degree from the University of Nottingham and his PhD degree from the University of Cambridge in 1970 and 1976 respectively. In 1970 he joined British Railways Research Division, and in 1975 joined the then GEC Measurements. In GEC he held various posts including Head of Research and Long Term Development, and Overseas Sales Manager. In 1986 he joined the University of Bath with interests in Power System Protection and Industrial Management. He is currently a member of IEE Professional Group P11, the IEE Management and Design Divisional Board, the IEE Western Centre Board and has been a corresponding member of the IEEE Line Protection Sub-committee, particularly interested in Working Group D13.

Allexon A W Chiwaya received his BSc in Mathematics and Physics from University of Malawi in 1977, and BSc in Electronics and Electrical Engineering from University of Glasgow (U. K.) in 1980. He holds the position of Technical Services Manager at the Electricity Supply Commission of Malawi (ESCOM). Mr Chiwaya joined the University of Bath in 1991 to study for his PhD degree. His research interests are in power system simulation, protection and communications for protection.

PAPER 2

M A Redfern, R J Hewett, A A W Chiwaya, 'An Investigation into Reverse Power Flow Protection for Small and Medium sized Embedded Generation', Proceedings of the 28th Universities Power Engineering Conference, Stafforshire University, September, 1993.

AN INVESTIGATION INTO REVERSE POWER FLOW PROTECTION FOR SMALL AND MEDIUM SIZED EMBEDDED GENERATION

M A Redfern, R J Hewett and A A W Chiwaya.

University of Bath, UK.

This paper introduces a new protection algorithm for reverse power relaying. It was formulated to be included into a microprocessor based integrated generator protection package for small to medium sized embedded generators. The algorithm's decision to trip is based on measurements of the three phase power flowing in the connections to the generator. The principal considerations in its formulation are the definition of power in three phase ac systems and the errors introduced by the transducers. The algorithm's response to power changes resulting from the loss of prime mover in a laboratory model power system are used to demonstrate its operation.

1. INTRODUCTION.

Embedded generator motoring occurs for a variety of conditions including power system instability and tripping of the prime mover. During motoring, the generator takes power from the utility supply system with the possibility of damage to itself and its prime mover. Reverse power protection can prevent serious damage by tripping the circuit breaker connecting the machine to the utility supply as soon as the situation is recognised and hence removing the source of motoring power.

Reverse power and under power relays have been available for many years. They have included both electro-mechanical and static designs, and more recently, digital relays have been introduced.

Existing reverse power relays have been based on induction cup, induction disk elements, or electronic comparators. Since different applications require different operating characteristics, sensitive reverse power, under power and low forward power relays are available together with instantaneous, definite time and inverse definite minimum time delay timing characteristics[1,2].

The two main approaches to determining the direction of power flow are to use poly-phase or single-phase power direction measurements. The poly-phase induction cup relays use the cup element as a small motor which is driven by the transducer secondary voltages and currents to determine the direction of power flow. Single-phase designs generally use the phase angle between the measured voltage and current inputs to determine the direction of power flow and are hence referred to as cos(Φ) relays.

The challenge for relay designers in designing power direction relays is first the choice of parameter for determining the direction of power flow and secondly accommodation of errors. Whereas the dramatic change from generating watts to absorbing watts is not particularly difficult to detect, conditions where the machine is operating at low power factors make accurate discrimination difficult.

2. THE POWER BASED ALGORITHM.

The new algorithm which has been formulated is intended to be included into a microprocessor based digital relaying protection package for small and medium sized embedded generation units. The microprocessor based relay hardware provides the platform onto which several protection functions are added using software routines. Previous work on other functions[3,4,5] needed in this package have also used power based algorithms and hence the necessary inputs for poly-phase power measurements are already available.

The first question raised by the investigation was "What is power?". Although the question appears to be straightforward the answer is far from simple. In 1990, the IEEE ran a tutorial course on 'Nonsinusoidal Situations: Effects on the Performance of Meters and Definitions of Power[6]' with twelve selected papers which attempted to resolve this subject for metering engineers. The principal power definitions include Instantaneous Power, Real Power, Reactive Power, Apparent Power, Distortion Power, Fictitious Power, Non-Reactive Power, Complex Power and Vector Power.

The immediate interest for power directional relaying is the Real Power flowing at the generator's terminals., i.e. the rate at which energy is provided or absorbed by the machine. If time were not a constraint, this could be measured accurately with an integrating algorithm, however for protection applications, minimising the decision making time of the algorithm is an important criterion of the systems success. If the power system was balanced, an instantaneous measurement is possible since under these conditions the Real Power is the same as the Instantaneous Power, i.e.:-

$$P = i_a v_a + i_b v_b + i_c v_c$$

where,

i_a, i_b, i_c, v_a, v_b, and v_c are the instantaneous values of the three phase currents and voltages measured at the generator's terminals.

Unfortunately power systems cannot be assumed to be balanced. Also, it is desirable for the power direction algorithm to discriminate correctly under adverse system conditions, the most notable being power system fault conditions.

Using symmetrical components, the current and voltage waveforms at the generator terminals can be broken down into positive, negative and zero phase sequence components. Evaluating the instantaneous power for an unbalanced system provides;-

$$\begin{aligned} P = \; & 3[V_{a0}I_{a0}\cos(\Phi_0) + V_{a1}I_{a1}\cos(\Phi_1) + V_{a2}I_{a2}\cos(\Phi_2)] \\ & -3V_{a0}I_{a0}\cos(2\omega t + 2\theta_0 + \Phi_0) \\ & -3V_{a1}I_{a2}\cos(2\omega t + \theta_1 + \theta_2 + \Phi_2) \\ & -3V_{a2}I_{a1}\cos(2\omega t + \theta_1 + \theta_2 + \Phi_1) \end{aligned}$$

where Φ are the phase angles between the voltage and current phasors and θ are the phase displacements of the positive, negative and zero sequence components measured at time zero.

Although filtering could remove the sinusoidal terms, extraction of the positive phase sequence components and using these alone would concentrate the power measurement onto the positive phase sequence power, such that:-

$$P_1 = 3V_{a1}I_{a1}\cos(\Phi_1) = V_{a1}I_{a1} + V_{b1}I_{b1} + V_{c1}I_{c1}$$

where,

I_{a1}, I_{b1}, I_{c1}, V_{a1}, V_{b1}, and V_{c1} are the positive phase sequence components referenced to phases 'a', 'b' and 'c'.

The instantaneous values for these are derived from equations similar to those for the 'a' phase values shown below.

$$V_{a1} = \frac{[V_{a,n} + V_{b,(n-16)} + V_{c,(n-8)}]}{3}$$

and,

$$I_{a1} = \frac{[I_{a,n} + I_{b,(n-16)} + I_{c,(n-8)}]}{3}$$

where,

n represents the instant that the last sample was taken.

For the reverse power application, the relay will trip if:-

$$P_1 \leq 0$$

High frequency interference on the power system is also expected and since it must not cause maloperation, a half cycle FIR low pass filter is used on the derived values of the positive sequence components.

Errors in the primary transducers and the relay interface circuits consist of both amplitude and phase errors. For both current and voltage transducers, errors are not linear but vary with respect to the magnitude of the measured signal. To provide an automatic accommodation of errors, especially when the decision making became critical, a parameter was sought which varied in line with the correction required. The positive phase sequence reactive power, Q_1, provided the error accommodation required, and detailed analysis of the non-linearities involved led to the use of αQ_1^2, where α is the error compensation coefficient. When P_1 is large with respect to Q_1, the decision making process is relatively straight forward. Difficulties arise when Q_1 is large with respect to P_1, i.e. the power system is operating at low power factor. Using this error accommodation increases the security of the decision. The trip criterion therefore becomes:-

$$P_1 \leq \alpha Q_1^2$$

The positive phase sequence reactive power is derived from:-

$$Q_1 = \frac{1}{\sqrt{3}}[\, I_{a1}(V_{b1} - V_{c1}) + I_{b1}(V_{c1} - C_{a1}) + I_{c1}(V_{a1} - V_{b1}) \,]$$

The flow diagram used to evaluate the algorithm is shown in figure 1 and the relay's trip characteristic is shown in figure 2.

3. ALGORITHM EVALUATION

The reverse power protection algorithm was evaluated using both computer based power system simulation and laboratory model power system[7]. The computer simulation allowed fundamental analysis of the speed of the algorithm to detect any changes in the direction of power flow, whereas the laboratory model enabled practical loss of prime mover tests to be undertaken with a three-phase synchronous generator. The laboratory power system model was built around two 5 kVA synchronous machines coupled to dc machines. The ac machines could be connected to incoming 200 V ac supplies through a series of circuit breakers and isolators via main busbars. The block diagram of the laboratory system is shown in figure 3.

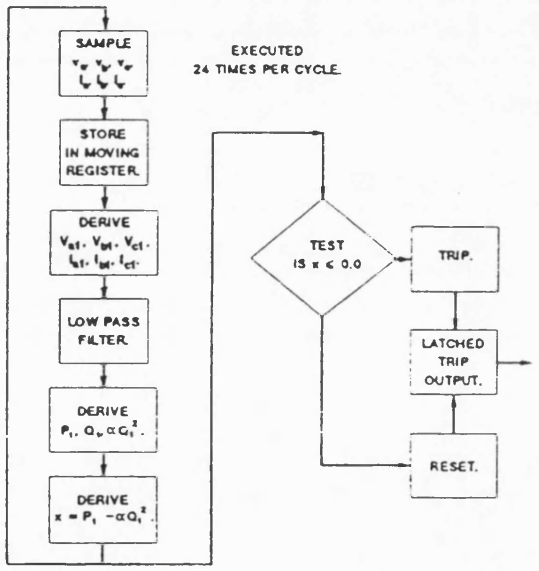

FIGURE 1. Flow Diagram for the New Reverse Power Algorithm.

The digital relaying platform was provided by a desk top personal computer fitted with input interface circuitry and A/D converters. The block diagram of this system is shown in figure 4. To facilitate a detailed analysis of the workings of the algorithm, data acquired from the tests was stored and later processed using a digital signal processing package. The sampling rate was set to 24 samples per cycle, and the A/D convertors provided 12 bit conversion.

From tests on the current and voltage transducers used in the laboratory system, the error compensation coefficient, α, was set at 0.002 percent. This provided a five degree compensation at the machines rated output at near zero power factor. Although the computer simulation assumed ideal transducers, this value was also used in the computer studies.

Computer tests to demonstrate the speed of the algorithm revealed that an instantaneous power reversal with a system operating at unity power factor and at an advantageous point on wave gave an algorithm tripping time of six samples, i.e. a quarter of a cycle. For more demanding cases, where the power factors before and after the direction reversal were low, the algorithm tripping times were up to thirty samples, i.e. one and a quarter cycles.

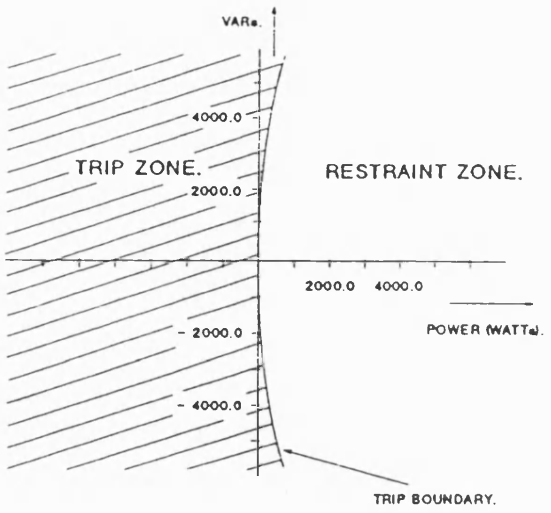

FIGURE 2. Reverse Power Protection Relay Trip Characteristic.

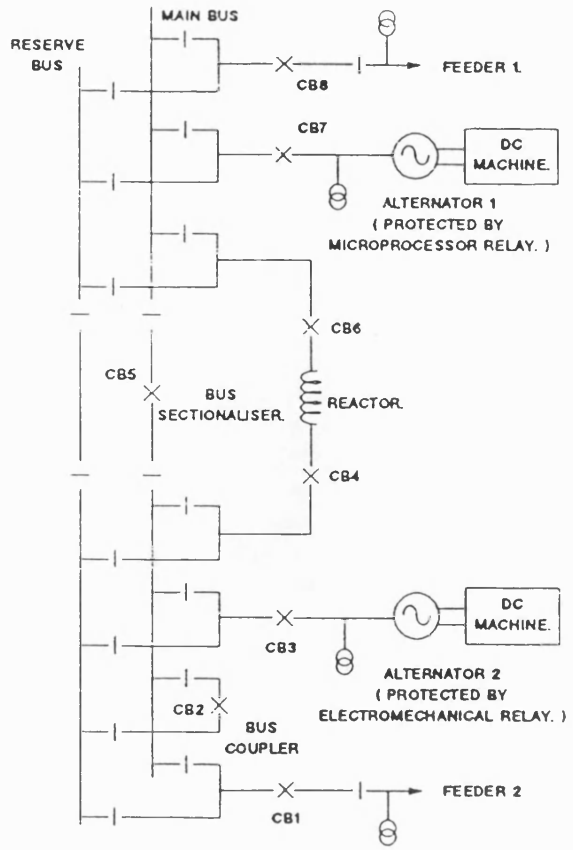

FIGURE 3. Laboratory Model Power System.

The algorithm's response to loss of prime mover tests using the laboratory model are shown in figures 5 and 6. The tests were conducted with the synchronous generator loaded to 80% of its rated capacity, with a power factor of 0.8 for the first test and unity for the second. Loss of prime mover power was implemented by disconnecting the dc supply with a circuit breaker. System inertia provided some forward power flow, and the algorithm tripped after 0.172 seconds for the first test and 0.230 seconds for the second.

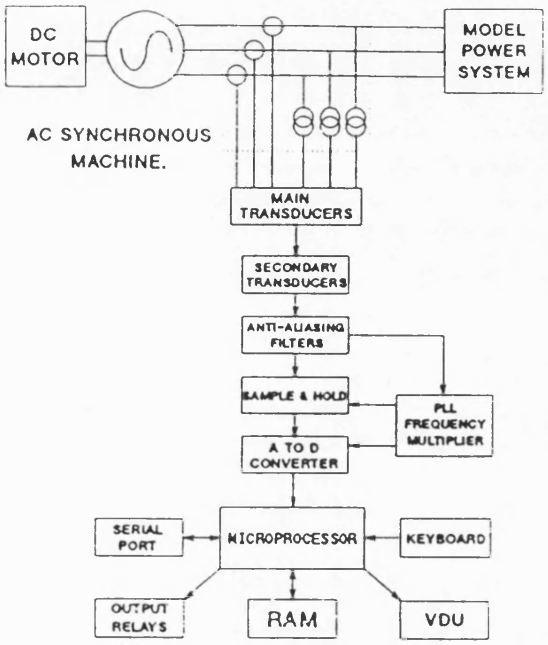

FIGURE 4. Protection Algorithm Investigation Platform.

The response to the disturbance introduced by a power system fault is demonstrated in figure 7. This considers a single phase to earth fault at the generator's busbar. A fault impedance of one ohm was used to prevent the laboratory supplies from tripping. Although there are violent disturbances in the measured real power waveform, the algorithm does not trip and there are no suggestions that this type of fault would cause tripping. A selection of other fault combinations at the busbar were tested and in all cases the algorithm remained stable.

4. CONCLUSIONS.

The concept of power measurement in three-phase ac systems is not straightforward, and there are a variety of definitions which describe the different 'powers' involved. For the detection of direction of power flow during generator motoring, the positive phase sequence power was chosen to be of greatest importance, and therefore provided the basis for the reverse power algorithm investigated.

Three-phase positive phase sequence phasors were derived from the input currents and voltages and used to provide a measure of the positive phase sequence power flowing into the protected generator. To accommodate errors, the tripping algorithm used an error correction coefficient based on the positive phase sequence reactive power flow measured at the generator terminals.

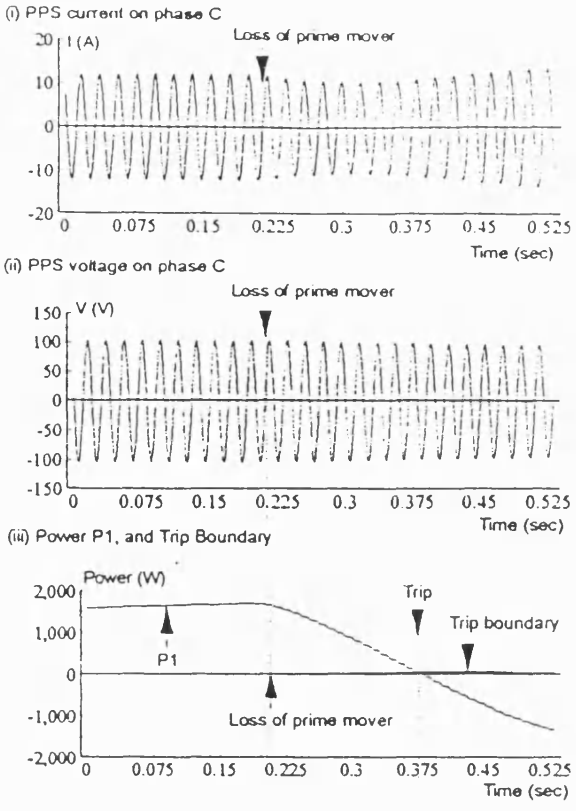

FIGURE 5. Loss of Prime Mover Test with Generator Initial Power Factor of 0.8.

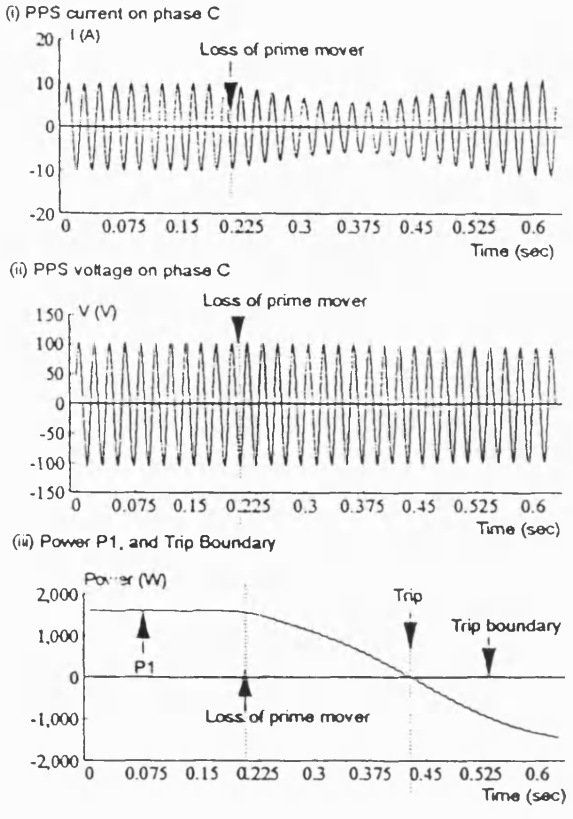

FIGURE 6. Loss of Prime Mover Test with Generator Initial Power Factor Unity.

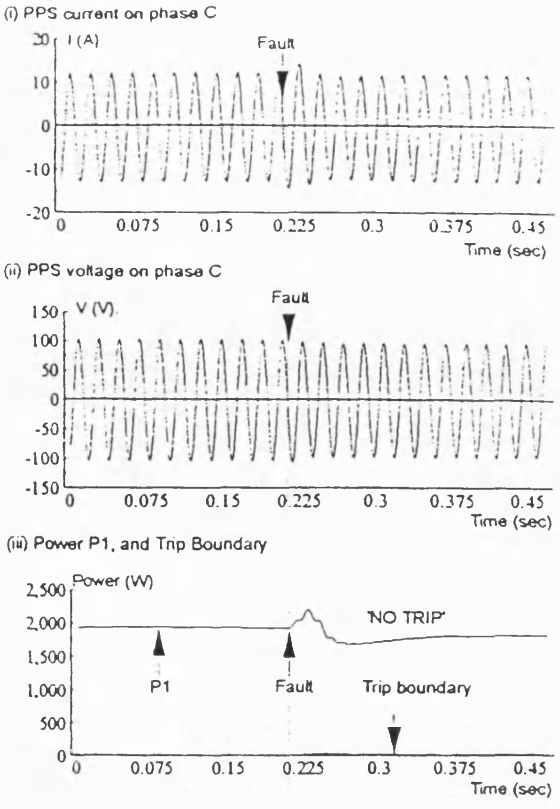

FIGURE 7. Response to a Single Phase Fault at the Generator Busbar.

The protection algorithm was found to provide an acceptable tripping time and was shown to respond well for laboratory loss of prime mover tests. It was also shown to discriminate correctly during short circuit fault conditions for faults on the generator's busbar.

5. REFERENCES.

1. HARRISON C K, FELTES J W, 'Industrial and Cogeneration Problems Requiring Simulation '. IEEE Trans Ind Apps , vol 25, 1989, no 4 , 766 - 775 .

2. GEC ALSTHOM, 'Protective Relays Application Guide ', Stafford : GEC Alsthom Protection and Control, 1990, pp 319-322.

3. REDFERN M A, USTA O, FENG B and FIELDING G, 'Loss of Mains Protection for Private Generation Operating in Parallel with the Utility Supply.' UPEC 1990, pp 89-92.

4. REDFERN M A, USTA O and FIELDING G, 'Protection Against Loss of Utility Grid Supply for a Dispersed Storage and Generation Unit.' IEEE paper 92 SM 376-4 PWRD presented to the PES Summer Meeting, Seattle, 1992.

5. CHECKSFIELD M J and REDFERN M A, 'An Investigation into Pole Slipping Protection for Small and Medium Sized Embedded Generation.' UPEC 1993.

6. IEEE TUTORIAL COURSE, 'Nonsinusoidal situations: Effects on the Performance of Meters and Definitions of Power', IEEE Power Engineering Society, course text 90EH0327-7-PWR

7. REDFERN M A, BARRETT J, HEWINGS D, USTA O, 'A laboratory facility for research into Digital Protection Algorithms used for the Protection of small and medium sized Synchronous Generators', UPEC 1991, pp 457-460.

PAPER 3

M A Redfern, A A W Chiwaya, 'A Digital Current Differential Protection for Distribution Feeders using Voice Frequency Data Communications', International Conference on New Developments in Power System Protection and Local Control, Beijing, China, May 1994.

A DIGITAL CURRENT DIFFERENTIAL PROTECTION FOR DISTRIBUTION FEEDERS USING VOICE FREQUENCY DATA COMMUNICATIONS.

M A Redfern and A A W Chiwaya

School of Electronic and Electrical Engineering,
University of Bath,
Bath, BA2 7AY, UK.

Abstract:- This paper presents a new digital current differential protection for distribution feeders which uses polyphase, polarised current measurements. The current measurements are taken at the feeder's terminals and are used to detect shunt faults on the feeder. The algorithm produces a trip output within two and a half power system cycles. A particular feature of these measurements is that they are divorced from the power system frequency and its waveform. This overcomes the complications introduced by communication channel delays and their possible fluctuations. An immediate advantage of the technique is that communications requirements are modest. The algorithms have been developed to operate using a full duplex 2400 bits/sec modem. Higher data rates can be provided with superior encoding, but care must be taken to ensure that they are not less tolerant to interference on the communications system. Moreover, considering that the protection is for a distribution feeder network, higher data rates may not be economically justifiable.

INTRODUCTION

The use of current differential relaying is well established. When applied to feeder circuits, the separation between the terminals of the protected feeder introduces the need for a communications system. Ideally, the communications system would instantaneously transfer all the data required for the protection between the relays which constitute the scheme. Instantaneous, high volume data communications is, however, not possible because practical communications systems are limited in the quantity of data that they can handle in a specified time period. They therefore introduce time delays between transmitting and receiving a signal. This has led to research into new differential relaying algorithms which can tolerate the limited capacity and associated time delays of practical communications systems.

Voice-frequency communication channels are the most widely used because they have been developed for telephone communications. They provide a standardised environment for communications operating over a variety of media. With a channel bandwidth of 4 kHz, they can use a dedicated medium or share a medium with other channels. Having been extensively developed commercially for mass communications, they provide a convenient standard for use in distribution system relaying. With only a limited bandwidth available, the volume of data which can be handled is also limited. Standard data rates cover a wide range varying from 75 bits/sec to 14.4 kbits/sec operating in both full and half duplex modes. In this work, a full duplex digital data capacity of 2400 bits/sec (CCITT Recommendations, 1989). This modest data transfer rate has favourable tolerance to interference and inherent communications security.

CURRENT DIFFERENTIAL RELAYING IN FEEDERS.

Current differential relaying concepts established by Merz and Price in the early 1900's form the basis for effective protection of power systems. In feeder protection, relays are located at the terminals of the protected feeder to monitor the electrical quantities required for the trip decision, to provide data for other relays in the scheme, and to initiate local circuit breaker operation. A communications channel is required to transfer data relating to the state of the power system from the remote terminal(s) to the local terminal where it is compared with data obtained at that terminal in order to make a trip decision.

The simplicity and elegance of the concepts are used in a wide range of electro-mechanical and static relays. In these schemes, copper pilot wires are generally used for communications. These pilots connect the relays at the feeder's terminals in either the circulating current mode or balanced voltage mode, and form an integral part of the decision making process as they provide the electrical signal summation circuit. Depending on the type of relay, its settings and the fault, the typical operating time of these relays varies from one and a half to three cycles.

In digital relaying, digital data can not be summated in the communications media in the same manner as used with traditional relays. For simultaneous decision making by the relays at the feeder's terminals, full duplex data transmission is required and independent decision making is made at each terminal. A simplified representation of a typical digital current differential scheme is shown in Fig. 1.

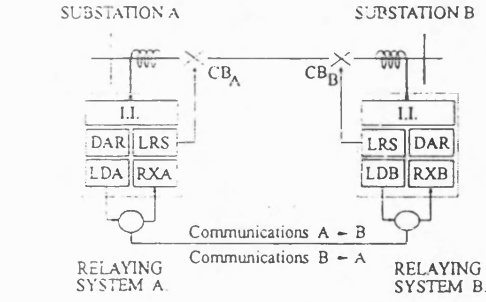

Fig. 1. Simplified block diagram of a digital current differential protection scheme.

Classical digital current differential schemes operate in a manner similar to that described by Kwong, Clayton, and Newbould (1985). Several researchers have considered techniques to provide the advantages of digital relaying without compromising the simplicity of the concept. The charge comparison technique described by Ernst and others (1992) presented a technique to reduce the volume of data required to be transferred between relays in a current differential scheme.

A paper by Yee and Brownlee (1993) highlighted protection and telecommunications interface problems for relays using digital data transfer. Relays are designed assuming that bidirectional propagation times are essentially equal in each direction. Bidirectional time symmetry is, unfortunately, not a critical requirement for normal data transfer. The V.35 CCITT standard, for example, has no restriction to the amount of propagation time asymmetry for communications equipment. The communications may

thus produce some significant difference between transmit signal delays and receive signal delays causing misalignment of the data and resulting in calculation of a non existent spill current by the difference process.

An inherent advantage of using digital techniques highlighted by several authors is the ability to use advanced analytical techniques leading to improvements in the protection. This paper presents the new technique for relaying that provides the protection capabilities of conventional pilot wire differential protection while using the limited data transfer capabilities of a digital data voice frequency communications channel.

THE ALGORITHM.

Techniques to Reduce Data.

As stated earlier, the communications system chosen offered a data rate of 2400 bits/sec operating in full duplex and this corresponds to a data transfer rate of 48 bits of data for each cycle of a 50 Hz power system frequency. Allowing a fifty percent overhead for communications protocols and error detection coding reduces this data transfer capacity to only 24 bits per cycle. The communications equipment and the medium would determine channel delay times. In this application the delay can be assumed to be of the order of a few milliseconds.

It was thus essential to dramatically reduce the data used to define the current signals so as to overcome the need to transmit the mass of data required to define the sampled current waveform and thereby operate with a data transfer capacity of 24 bits/cycle. The method chosen was based on the equations used to derive the instantaneous power in a three-phase circuit. Multiplying the instantaneous values of the sampled three phase currents with the instantaneous values of three-phase reference phasors provides a measurement which contains a steady d.c. component plus second harmonic terms. This steady component contains the amplitude of the monitored three-phase currents with respect to the reference phasors. A second measurement, using an orthogonal set of phasors, provides complimentary information, and hence used together these two measurements fully characterise the monitored terminal currents. The principle set of three phase reference phasors corresponds to the phase to ground voltages and the second set to the phase to phase voltages.

Signals synchronised to the power system frequency and ideally having the same phase relationship at all of the feeder's terminals could be used to derive the references. Since this protection is principally aimed at short distribution feeders and assuming a heavily interconnected power system, the terminals' three phase voltages will be in phase with each other at the terminals of the feeder and therefore were used to derive the reference phasors. The reference phasors are a set of three unit amplitude rotating sinusoidal waveforms, 120 degrees apart. A memory feature is included in the algorithm to accommodate faults that cause voltage collapse.

The summation of the products of instantaneous three-phase currents, i_a, i_b and i_c, and instantaneous values of the reference phasors, s_a, s_b and s_c, together with filtering of the twice frequency terms, produces a constant term I_p representing the amplitude of the currents in phase with the reference phasors. Using the instantaneous values of the orthogonal set of reference phasors, (s_a-s_b), (s_b-s_c) and (s_c-s_a) together with the terminal currents produces a constant term I_q representing the amplitude of the current orthogonal to the reference phasors, thus;-

$$I_p = i_a s_a + i_b s_b + i_c s_c \qquad (1)$$

$$I_p = 3\ I \cos(\ \phi\ ) \qquad (2)$$

and,

$$I_q = i_a(\ s_b - s_c\ ) + i_b(\ s_c - s_a\ ) + i_c(\ s_a - s_b\ ) \qquad (3)$$

$$I_q = 3\sqrt{3}\ I \sin(\ \phi\ ) \qquad (4)$$

where I_p and I_q are nonoscillating constants.

The filtering is required for unbalanced fault or load conditions, where because the currents are not balanced, second harmonic terms are introduced. Equation (1) can be analysed to consider unbalance currents by replacing the three-phase currents with three balanced systems containing positive, negative and zero phase sequence components (Redfern and Chiwaya, 1994).

Representing the reference phasors by:-

$$\begin{aligned} s_a &= \sin(\ \omega t + \theta\ ) \\ s_b &= \sin\left(\ \omega t + \theta + \frac{4\pi}{3}\ \right) \\ s_c &= \sin\left(\ \omega t + \theta + \frac{2\pi}{3}\ \right) \end{aligned} \qquad (5)$$

equation 1 becomes;

$$I_p = 3\ I_1 \cos(\ \phi_1\ ) - 3\ I_2 \cos(\ 2\omega t + \theta + \theta_2 + \phi_2\ ) \qquad (6)$$

This technique removes the zero phase sequence currents immediately, but leaves the negative phase sequence components which produce a second harmonic term. In the protection algorithm this term is removed by averaging I_p and I_q over half a power system cycle.

Communications Concepts.

Modems form the basis of the interface between the digital protection system and the communications medium. These operate at a wide variety of different operating speeds and offer different advantages for different applications. A host of national and international standards have been agreed to define the characteristics of the different systems (CCITT Recommendations, 1989) to ensure connectivity between different equipments,

The V26 modem standard was chosen (Redfern and Chiwaya, 1994) to provide the 2400 bits/sec data transfer rate because of its advantages over other modems. For example, the V21 modem is too slow at 300 bits/sec. Although the V33 offers a higher data rate of 14.4 bits/sec, its recovery time to a disturbance in the communications system is greater than 50 msec compared to 15 msec for the V26 (Doll, 1978).

The data stream used for the relaying scheme has a six bit header followed by two Hamming (13,9) code blocks. The six bit header is a pre-defined set of bits which provides data synchronism. Each Hamming code block contains thirteen bits, nine of which are data bits. Each message block therefore contains eighteen data bits. These comprise two identifier bits, two bits reserved for other applications and fourteen data bits relating to I_p and I_q alternatively. The identifier bits are used to define the measurement as corresponding to I_p ('0' '0') or I_q ('1' '1'). The remaining eight parity bits are used for error detection such that the security of the protection is not compromised should the data be corrupted.

At 2400 bits/sec bit rate, each thirty-two bit message requires 13.33 milliseconds transmission time and this delay is included in the protection algorithm. Since the data stream is continuous, data was available each 13.33 milliseconds. Marshalling times and propagation delays were assessed to be within 3.66 milliseconds and hence the absolute data communications delay was taken to be 17 milliseconds. In order to confirm the response of the algorithm to varying propagation delays tests were conducted in which one millisecond was first added and then subtracted from the 17 milliseconds data transit delay between the terminals.

Operation of the Algorithm.

The general operation of the algorithm is shown in Fig. 2. Anti-aliasing filters were used to filter the input signals before being sampled using the A/D converter. The samples were taken every millisecond. Voltage samples were used to generate the reference phasors and the current samples were used with these to generate the basic I_p and I_q signals. These were then filtered using a half cycle filter to remove any second harmonic terms.

For these tests, the communications is free running and was therefore not synchronised with the fault inception. This was done by randomising the start of data transmission for each simulation. Shortly before the end of one message's transmission period, the next value of I_p or I_q was provided in rotation to the data sending unit for coding and transmission. If the last transmission was of the measurement I_p, the next would be I_q and vice versa.

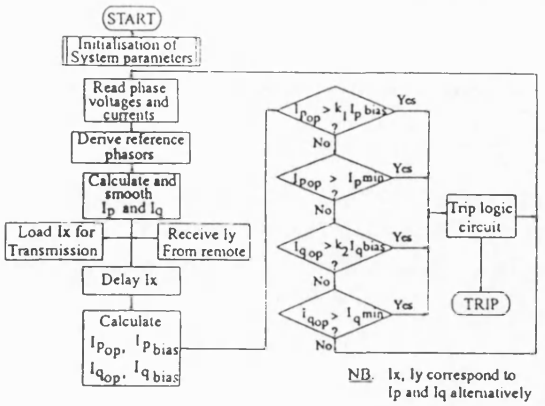

Fig. 2. General operation of the protection algorithm.

Once an incoming message had been received and decoded, its value was compared with the value obtained from local measurements. This received value was compared to the corresponding locally measured signal delayed by the total communications system delay time as detailed earlier. If the difference was above the trip setting, a trip decision was noted. With the message structure described above, the decision process was executed after receipt of a message, i.e. every 13.33 milliseconds.

A similar trip algorithm is used for both I_p and I_q, namely:-

$$\begin{aligned} (I_p)_{op} &= | I_{p_L} - I_{p_R} | \\ (I_p)_{bias} &= \frac{1}{2} (| I_{p_L} | + | I_{p_R} |) \\ (I_q)_{op} &= | I_{q_L} - I_{q_R} | \\ (I_q)_{bias} &= \frac{1}{2} (| I_{q_L} | + | I_{q_R} |) \end{aligned} \qquad (7)$$

and the trip indication was given when either of the following applied:-

$$\begin{aligned} (I_p)_{op} > (I_p)_{min} \quad AND \quad (I_p)_{op} > k_p\ (I_p)_{bias} \\ (I_q)_{op} > (I_q)_{min} \quad AND \quad (I_q)_{op} > k_q\ (I_q)_{bias} \end{aligned} \qquad (8)$$

The trip settings were set at 200 Amps for both $(I_p)_{min}$ and $(I_q)_{min}$ and the bias settings were 2.0 percent for both $(I_p)_{bias}$ and $(I_q)_{bias}$.

Two consecutive trip decisions, i.e. I_p and then I_q, or vice versa, or alternatively two subsequent I_p or I_q trips were required before the trip output is given. The theoretical relay tripping time was therefore a minimum of 30 milliseconds, varying up to 50 milliseconds where the fault occurred just after the marshalling process for the next data transmission had begun. Separating the trip decisions so that they were based on I_p or I_q, and requiring two trip decisions before the relay tripped provided a faster trip output than combining the two measurements into a composite current measurement.

ALGORITHM EVALUATION.

The EMTP power system simulation package was used to evaluate the protection algorithm. Figure 3 shows the power system model of a typical 33 kV feeder network containing parallel feeders used in the evaluation. Both overhead lines and underground cables were modelled together with a variety of faults at different fault positions. Internal, as well as external faults were considered, with external faults being applied both on the parallel feeder and the supply feeders. A selection of the results are given.

The first series of faults to be studied were those that involve only a single phase.

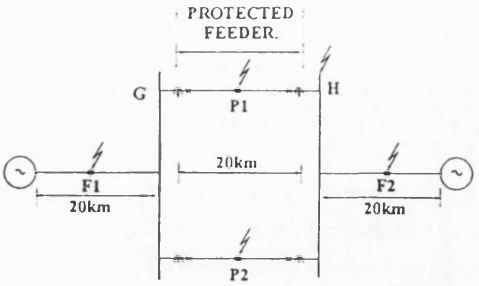

Fig. 3. Test power system model.

Figure 4 shows the current, the C-phase voltage, and the C-phase reference signal at one terminal for an in-zone fault on an overhead line system. Figure 5 shows the comparisons between the locally obtained I_p and I_q signals to those received from the remote end of the feeder. For the remote signals, the instances that show solid lines are when the signals are actually received,whereas the dashed lines are when they are not received. Within twenty milliseconds after the fault, both I_p and I_q have settled to new steady values. The delays between the two signals which are caused by the communications system delays and the differences between the measurements during the fault are clearly shown. Using the trip requirement of two subsequent trip indications, leads to a trip time of 38 milliseconds.

Figure 6 shows the comparisons between the locally obtained I_p and I_q signals for an external single phase to ground fault. For this situation, the measurements are relatively small and although there is a difference between the local and remote signals, this is less than the trip setting. For this fault, the algorithm remains stable and does not trip.

A similar fault to that used in Fig. 4 but for an underground cable network is shown in Fig. 7. Here again there are dramatic differences between the local and remote measurements after the fault and the algorithm tripped after 35 milliseconds. The response to an external single phase to ground fault on the underground cable system is shown in Fig. 8. The differences in the post fault local and remote measurements were within the trip setting, and the algorithm remained stable.

The response to an in-zone phase to phase fault on an overhead line is illustrated in Fig. 9. The differences between the local and remote measurements of I_p and I_q led to the algorithm tripping after 40 milliseconds. The response to a similar fault but external to the protected zone is shown in Fig. 10. For this the algorithm remained stable and did not trip.

Figures 11 and 12 respectively show the responses to internal and external three phase to ground faults. For these the in-zone fault resulted in tripping after 37 milliseconds but the algorithm remained stable for the external fault.

A terminal fault condition resulting in voltage collapse at the remote terminal is shown in Fig. 13. For this the memory feature of the reference phasors was required. Although the disturbance was detected, the algorithm remained stable and did not trip since it did not receive the second trip indication.

CONCLUSION.

A new current differential protection algorithm has been developed to accommodate the modest communications capabilities associated with digital data voice frequency communications channel while at the same time providing a protection capability suitable for LV feeders. Two reference phasor sets are derived which are used to provide polarised measurements of the three phase currents at the terminals of the feeder. In order to avoid the need to accurately synchronise the data at the local and remote ends of the protected feeder this process produces a steady d.c. signal for comparison. The use of two trip indications before allowing the algorithm to trip provides security against mal-operation due to the transitions in the measured Ip and Iq signals after the fault.

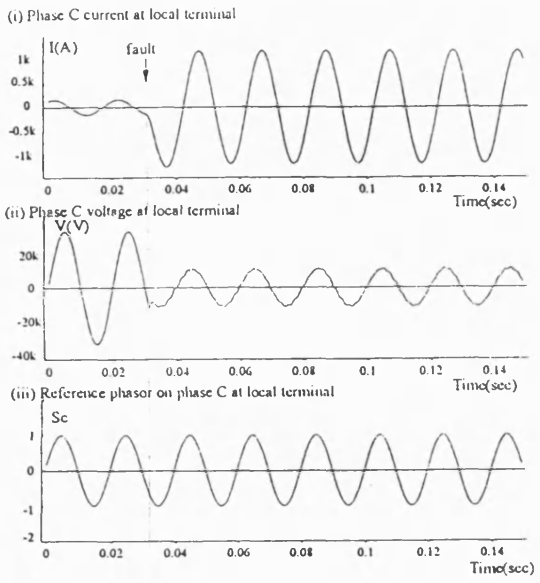

Fig. 4. Input and derived reference waveforms for an in-zone single phase fault on the system with overhead lines.

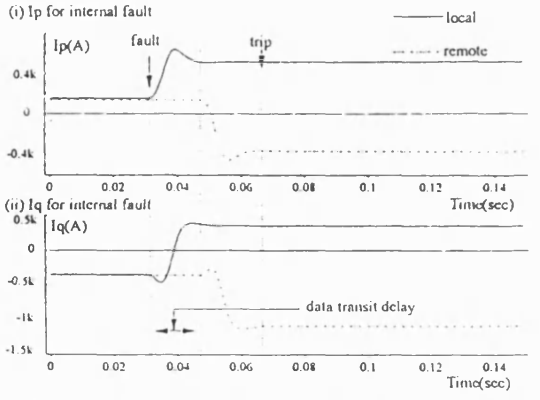

Fig. 5. Polarised currents for an in-zone single phase fault on the system with overhead line feeders.

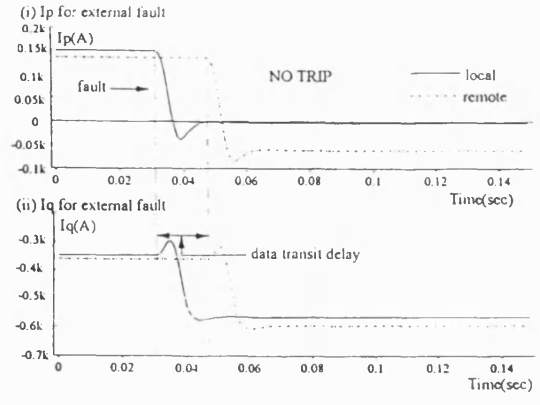

Fig. 6. Polarised currents for an external single phase fault at point F1 on the system with overhead line feeders.

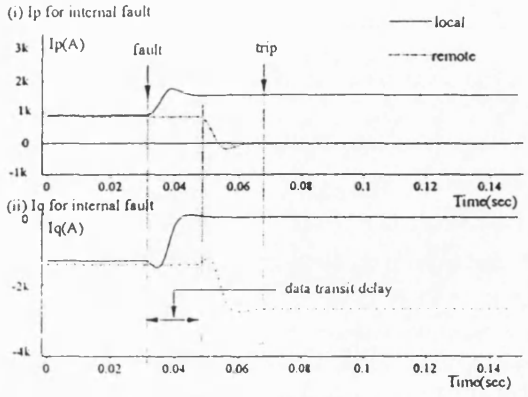

Fig. 7. Polarised currents for an in-zone single phase fault on the system with underground feeders.

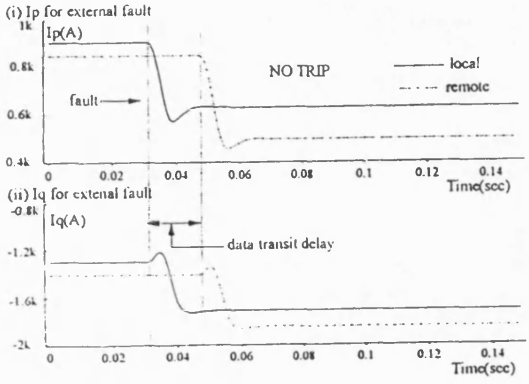

Fig. 8. Polarised currents for an external single phase fault at point F1 on the system with underground feeders.

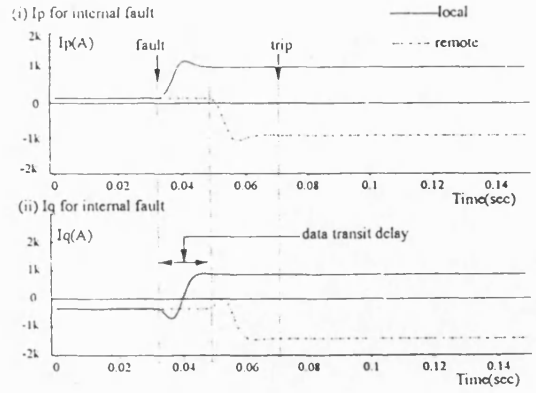

Fig. 9. Polarised currents for an in-zone phase to phase fault on the system with overhead line feeders.

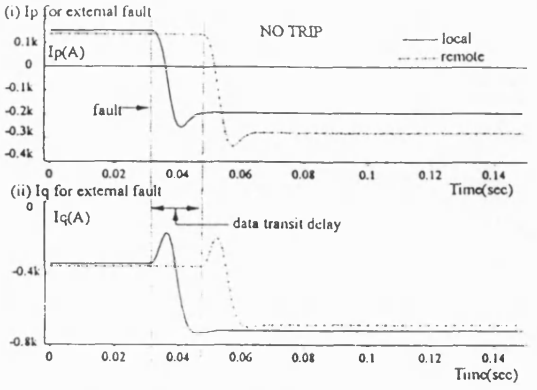

Fig. 10. Polarised currents for an external phase to phase fault at point F1 on the test system with overhead line feeders.

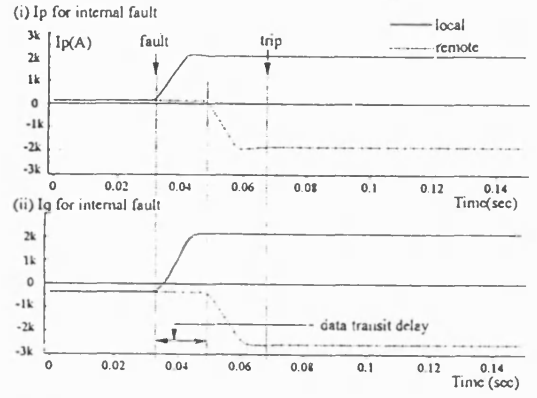

Fig. 11. Polarised currents for an in-zone three phase to ground fault on the test system with overhead line feeders.

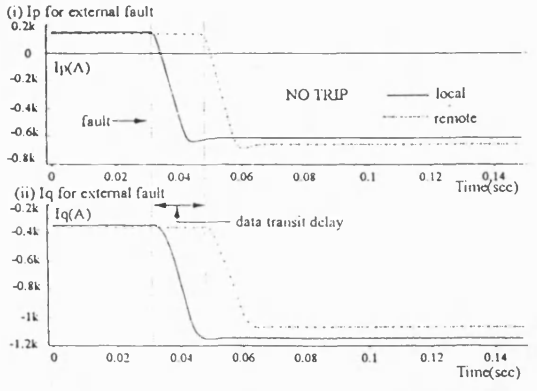

Fig. 12. Polarised currents for an external three phase to ground fault at point F1 on the test system with overhead line feeders.

Variations in the synchronism between fault occurrence and data transmission were simulated. The algorithm produced tripping times of about 37.5 milliseconds for all in-zone faults. For all external faults, including a terminal fault, the algorithm remained stable and did not trip.

As the algorithm was based on steady d.c. current measurements, the power system frequency was not so significant to the tripping times, and similar tripping times would have been obtained for both 50 Hz and 60 Hz power systems. The time required to transmit data from one terminal to another is a major constraint for this technique. Increasing the data rate would reduce the tripping time.

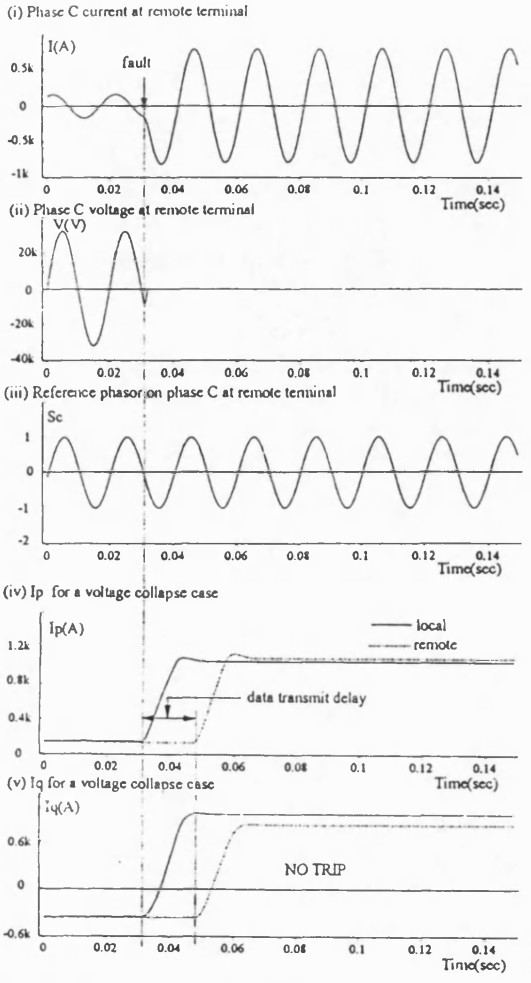

Fig. 13. Input and algorithm derived waveforms for a three phase to ground fault at terminal H on the test system.

REFERENCES.

CCITT Recommendations (1989). Series V recommendations. Data Communication over the Telephone Network, Vol. VIII, Fascicle VIII.1. ITU. pp. 65 - 69, 153 - 180, 252 - 266.

Doll, D. R. (1978). Data Communications, Facilities, Networks, and Systems Design. Wiley and Sons. pp. 197 - 203.

Ernst, L. J., W. L. Hinman, D. H. Quam, and J. S. Thorp (1992). Charge comparison protection of transmission lines - relaying concepts. IEEE Transactions on Power Delivery, 7, 92 WM 209-7 PWRD, pp. 1834 - 1842.

Kwong, W. S., M. J. Clayton, and A. Newbould (1985). A microprocessor-based current differential relay for use with digital communication systems. 3rd International Conference on Developments in Power System Protection, IEE Conference publication, 249, pp. 65 - 69.

Redfern, M. A., and A. A. W. Chiwaya (1994). A new approach to digital current differential protection for low and medium voltage feeder circuits using a digital voice-frequency grade communications channel. IEEE/PES Winter Meeting, New York, Feb 1994, paper number 94 WM 013-3 PWRD.

Yee, L., and D. C. Brownlee (1993). Protection and telecommunications interface problems for digital data transfer relays. Communications, Computers and Power in the Modern Environment, IEEE Wescanex 93, Conference Proceedings, 60, pp. 7-14.

PAPER 4

A A W Chiwaya, M A Redfern, 'A New Microprocessor based Current Differential Protection for Distribution Feeders', Proceedings of the 29th Universities Power Engineering Conference, University of Galway, Ireland, September, 1994.

A NEW MICROPROCESSOR BASED CURRENT DIFFERENTIAL PROTECTION FOR DISTRIBUTION FEEDERS.

A A W Chiwaya and M A Redfern.

University of Bath, UK.

Polarised polyphase current measurements taken at the feeder's terminals are used in this current differential protection for distribution feeder circuits to determine whether a shunt fault exists on the feeder or not. The algorithms make these measurements independent of the power system frequency and its waveform, and therefore overcome the normal requirement in digital differential relaying for precise time-alignment of the sampled waveforms. As the mass of data required to accurately define a sampled current waveform is thus reduced, the communications requirements are modest and are satisfied with a voice frequency channel operating at 2400 bits/sec in full duplex. Tripping time is generally provided in about one and half power system cycles after the fault. This paper discusses the basis for the protection algorithms, the choice of the modems, and presents the relay's performance under a variety of power system fault conditions.

1. INTRODUCTION.

The Merz and Price principles of current differential protection provide the basis for a wide range of highly successful electro-mechanical and static relays. For distribution feeder protection, the simplicity and elegance of these relays have ensured that they are universally accepted as an industry standard. Their communications requirements are modest. The copper links generally used to connect the relays at the feeder's terminals in either circulating current mode or balanced voltage mode provide the electrical signal summation circuit and, hence, in addition to providing communications, form an integral part of the decision making process.

Unfortunately, the move to microprocessor relaying and in particular the use of digital data communications have complicated rather than simplified the design of current differential relaying. The data can not be summated in the communications media in the manner used with traditional relays. Bidirectional data transmission is required. To take into account communications system delays, the normal requirement in digital differential relaying is to effect precise time-alignment of the sampled data from the feeder's terminals. This avoids calculating non-existent spill current which will cause relay mal-operation. The mass of data that correctly defines a sampled sinusoidal waveform at a terminal with any accuracy and is required to be transmitted between the terminals is thus very high. Several researchers[1, 2] are working on techniques to reduce the volume of data required to be transferred between relays in a current differential scheme.

This paper is about a technique that dramatically reduces the amount of data used to define the current signals and provides very effective feeder current differential protection. For data transmission between the feeder's terminals, a voice frequency channel operating at 2400 bits/sec in full duplex is used. These channels have been targeted because they are the most commonly used systems having been extensively developed commercially for mass communications. They operate using a 4 kHz bandwidth. One advantage is that most media (optical fibres, power line carrier, microwave, and pilot wires) can be used with voice frequency communications. These channels thus provide a convenient standard for use with distribution system protection. For this protection, the system can operate with both standard telephone type communications circuits and copper pilot circuits, if these have already been installed.

2. OVERVIEW OF CURRENT DIFFERENTIAL RELAYING.

Current differential relaying provides unit protection of a plant item such as a generator, a transformer, and a busbar, as illustrated in Figure 1. The elements in the trip decision making are the operate and restrain currents. The operate current is the phasor sum of the terminal currents. To provide security in the wake of errors that increase with current, such as current transformer (CT) mismatch, a restrain current, which is the algebraic mean of the terminal currents, is used to provide increased restraint as the current levels get larger.

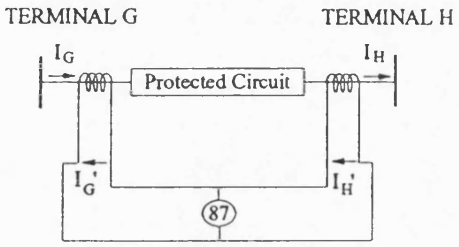

FIGURE 1. Typical Merz-Price Differential Protection.

To protect feeder circuits, a communications channel is required to transmit current information between the relays at the feeder's terminals. Relays located at the terminals of the protected feeder monitor the local electrical quantities, compare local with received quantities from other relays in order to make a trip decision, provide data for other relays in the scheme, and initiate local circuit breaker operation. Figure 2 illustrates this system.

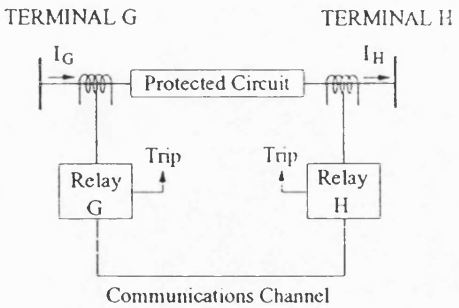

FIGURE 2. Typical Current Differential Protection Scheme of Feeder Circuits.

3. COMMUNICATIONS.

Channel compensation[3] is a normal requirement in digital differential relaying in order to prevent false tripping due to the comparison of wrong samples. Error control coding is used in data transmission because, as perceived by the relay at the local terminal, the channel introduces possible errors in the remote current. Thus considering the communications system protocols, error control coding, and channel compensation, the amount of data to accurately define a sampled current signal is high.

Naturally, wideband communication channels would offer good opportunities to transmit the mass of data required for the protection. However, as this protection is for distribution feeder networks, an economical communications system is required. This new protection for distribution feeders only requires a voice frequency channel for digital data communications.

Choice of Voice Frequency Channel Modem.

Communications systems use modems to provide the interface between the digital protection system and the communications medium. Offering different advantages for different applications, modems operate at different speeds ranging from 75 bits/sec to 14400 bits/sec operating in full or half duplex mode. Standards have been agreed upon to ensure connectivity between various equipments[4].

The 2400 bits/sec full duplex V.26 modem CCITT standard[5] was chosen for this application. This may be considered modest in light of currently available systems. However, its inherent communications security and tolerance to noise is favourable according to the relationship between the system's energy per bit to noise ratio, E_b/N_o, defined as:-

$$\frac{E_b}{N_o} = \frac{\left(\frac{S}{R}\right)}{N_o} \qquad (1)$$

where,

E_b is the signal energy per bit
N_o is the noise energy per hertz
S is the sending signal strength
R is the data bit rate.

Equation (1) depicts that for a constant interference level and sending signal strength, the possibility of data corruption increases with an increase in the data rate because the energy per bit to interference energy ratio decreases. Thus, the V.26 modem standard scores favourably against, for example, the V.33 which operates at 14400 bits/sec. In addition, the V.26 has a short initialisation time after a disturbance in the communications. Its initialisation time is 15 milliseconds as compared to more than 50 milliseconds for V.33[4].

4. THE PROTECTION ALGORITHM.

The use of such a low data transfer rate of 2400 bits/sec introduces problems. The data rate corresponds to a data transfer rate of 48 bits for each power system cycle. If communications protocols and error detection coding account for nominal fifty percent overheads, the data transfer capacity becomes 24 bits per cycle.

The mass of data required to define the sampled current waveform must therefore be reduced so as to operate with the low data transfer capacity. The algorithm achieves this by using locally obtained reference phasors as polarising signals to obtain polyphase polarised measurements of the current waveforms at the feeder's terminals. An orthogonal set of reference phasors provides complimentary information. The polarised current measurements are non-sinusoidal steady signals containing both amplitude and phase information of the monitored three-phase currents with respect to the reference phasors.

The equations used to derive instantaneous power in a three-phase circuit form the basis of the algorithm. Equations[6] for real power P and reactive power Q are given as:-

$$P = i_a v_a + i_b v_b + i_c v_c \qquad (2)$$

$$Q = \frac{1}{\sqrt{3}} \left[i_a(v_b - v_c) + i_b(v_c - v_a) + i_c(v_a - v_b) \right] \qquad (3)$$

Equations (2) and (3) are constants under balanced conditions.

Unfortunately there are inherent limitations in using a power differential scheme and therefore in the algorithm, the instantaneous values of the sampled phase currents are multiplied by instantaneous values of three phase reference phasors to provide a measurement which contains the steady dc component. The reference phasors should be derived from signals that are synchronised to the power system frequency and ideally have the same phase at all the feeder's terminals. Assuming a heavily interconnected power system, and as the protection is aimed at short distribution feeders, the phase voltages are in phase with each other at the terminals. These were used to derive the reference phasors which are a set of three unit amplitude rotating sinusoidal waveforms, s_a, s_b and s_c, equally spaced and synchronised to the phase voltages. The orthogonal set of reference phasors, (s_a-s_b), (s_b-s_c) and (s_c-s_a), therefore corresponds to the phase to phase voltages. A memory feature is included to maintain the polarising reference during a terminal fault.

As in equations (2) and (3), the reference set s_a, s_b, and s_c produces a constant polarised measurement I_p under balanced conditions, and the orthogonal set produces I_q:-

$$I_p = i_a s_a + i_b s_b + i_c s_c \qquad (4)$$
$$I_p = 3 I \cos(\phi)$$

$$I_q = i_a(s_b - s_c) + i_b(s_c - s_a) + i_c(s_a - s_b) \qquad (5)$$
$$I_q = 3 \sqrt{3} I \sin(\phi)$$

Unbalanced conditions introduce second harmonics[4]. Therefore a low pass filter is introduced by averaging I_p and I_q over half a power system cycle, to remove these terms leaving the steady, dc term.

At each terminal, the relay system uses the voltage samples to generate the reference phasors and uses the current samples with these to generate the basic I_p and I_q measurements. These are then filtered using a half cycle filter to remove any second harmonic terms. I_p and I_q are provided alternatively for coding and transmission.

For transmission, a six bit header starts each code block to provide data synchronism, followed by two Hamming (13,9) code blocks. The eighteen data bits thus available comprise two identifier bits, two bits reserved for other applications, and fourteen data bits relating to I_p and I_q alternatively. The eight bits for error detection ensure that the security of the protection is not compromised should data be corrupted.

The total message therefore has thirty two bits, and with a modem operating at 2400 bits/sec, it requires 13.33 milliseconds transmission time. There are also delays due to signal propagation and marshalling, making a typical data communications delay of

17 milliseconds. When an incoming message has been received and decoded, its value together with that obtained from local measurements is provided for the trip comparator. For comparison, the remote data is compared with the locally measured signal which has been delayed by the communications system delay time.

The relay calculates the operate and bias signals to use in the trip criteria:-

$$
\begin{aligned}
(I_p)_{op} &= |I_{p_L} - I_{p_R}| \\
(I_p)_{bias} &= \frac{1}{2}(|I_{p_L}| + |I_{p_R}|) \\
(I_q)_{op} &= |I_{q_L} - I_{q_R}| \\
(I_q)_{bias} &= \frac{1}{2}(|I_{q_L}| + |I_{q_R}|)
\end{aligned}
\qquad (6)
$$

A trip indication is given when either of the following applies:-

$$
\begin{aligned}
(I_p)_{op} &> (I_p)_{min} \quad AND \quad (I_p)_{op} > k_p (I_p)_{bias} \\
(I_q)_{op} &> (I_q)_{min} \quad AND \quad (I_q)_{op} > k_q (I_q)_{bias}
\end{aligned}
\qquad (7)
$$

The relay trip output is given after two trip conditions. The trip conditions can either be consecutive trip decisions, I_p and then I_q, or vice versa, or alternatively two subsequent I_p or I_q trips. Separating the trip decisions so that they are based on I_p or I_q, and requiring two trip decisions before tripping the relay provides a faster trip output than combining the two measurements.

5. POWER SYSTEM MODEL.

The power system model used to evaluate the protection algorithm was that of a typical 33 kV feeder network containing parallel feeders, as shown in Figure 3.

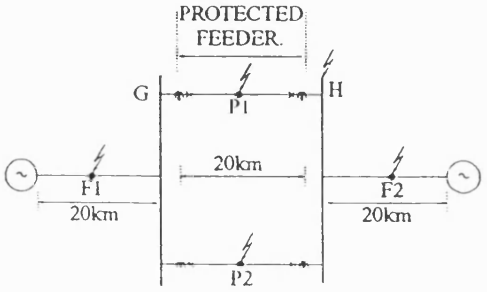

FIGURE 3. Power System Model.

The EMTP power system simulation package was used. Overhead lines and underground cables were modelled together with a variety of faults at different fault positions to examine the algorithm's response. Also modelled were composite feeders containing both underground cables and overhead lines. Faults included single phase to earth, phase to phase with and without earth, and three phases with and without earth. Point P1 on the figure represents an arbitrary point within the protected zone. Internal faults were studied on points mid-zone and also 100 meters away from the CT's. External faults were considered both on the parallel feeder and the supply feeders, with some faults 100 meters away from the CT's.

6. RESULTS.

For the results presented, fault occurrence and data transmission are not in synchronism. The communications was made free running by randomising the start of data transmission for each simulation. Also considered were fault points on wave.

In the summary of the results, single phase faults have mainly been referred to because they are the most common type of fault in distribution feeder circuits. Figure 4 is a typical representation of phase current, phase voltage and reference signal at one terminal. This is for an in-zone single phase fault condition on overhead lines. Fault incidence is clearly marked, and shows that there is an increase in the current after the fault while the voltage is reduced, with the reference signal still providing an effective polarising element.

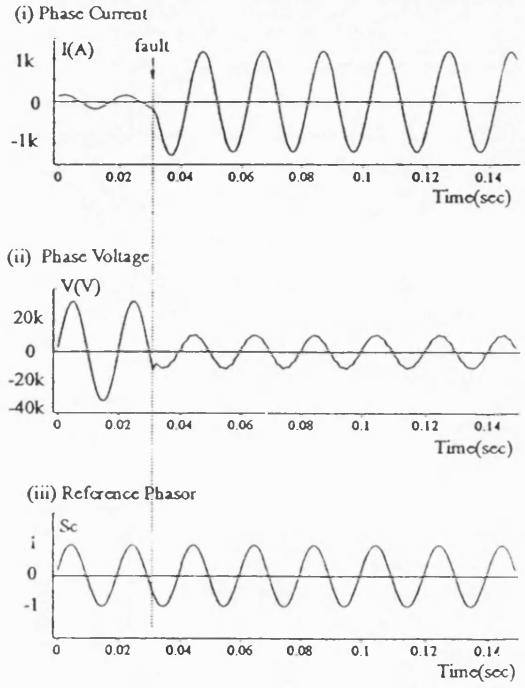

FIGURE 4. Input and Reference Signals for an In-zone Single phase Fault on the Test System.

All in-zone fault conditions show similar characteristics. For these faults, the algorithm derived measurements of I_p and I_q for both local and remote terminals, but at the local terminal, are summarised in Figure 5 which is actually for the in-zone single phase fault condition on overhead lines. This figure shows that both I_p and I_q settle to a new steady value inside 20 milliseconds. The figure also shows the differences between the measurements due to the fault, with the communications system delays marked. The trip time for this fault is 34 milliseconds.

Figure 6 summarises the comparisons of the measurements for similar faults but this time external to the protected zone. The I_p measurements are relatively small. There is a difference between the local and remote signals, but it is less than the trip level. The algorithm remained stable and did not produce a relay trip output.

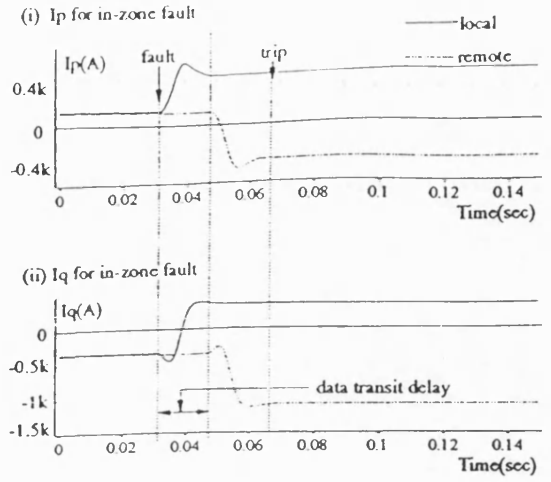

FIGURE 5. Polarised Currents for a typical In-zone Fault on the Test System.

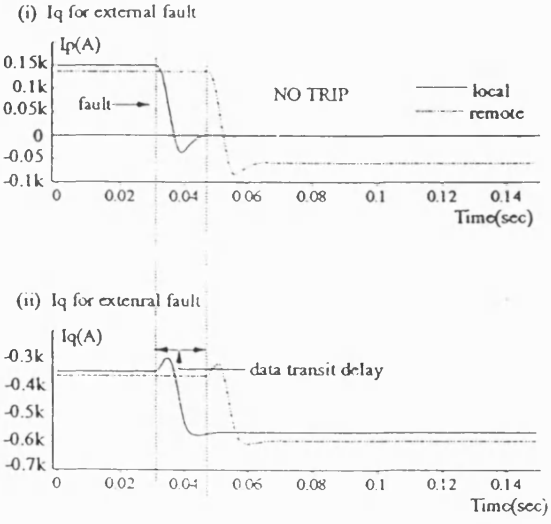

FIGURE 6. Polarised Currents for a typical External Fault on the Test System.

A terminal fault condition was introduced at terminal H to introduce voltage collapse at that terminal. The role of the memory feature is appreciated here as shown in Figure 7. I_p and I_q have the same characteristics as an external fault. Although the fault was detected, the algorithm did not produce a relay trip output.

7. CONCLUSION.

This polyphase polarised current differential protection provides effective protection for distribution feeder circuits. It uses orthogonal reference phasor sets to provide the polarised current measurements which are used in the trip decision. As the measurements are independent of the power system frequency and its waveform, the communications requirements are modest. The immediate advantage is that low data rates of voice frequency channels are sufficient for the protection requirements.

The algorithm is sensitive to in-zone faults, producing trip outputs in about 34 milliseconds. It remains stable and produces no relay trip output for all external faults including a terminal fault.

8. REFERENCES.

[1]. Ernst L J, Hinman W L, Quam D H, Thorp J S, 'Charge Comparison Protection of Transmission Lines - Relaying Concepts', IEEE Transactions on Power Delivery, Vol. 7, No. 4, 92 WM 209-7 PWRD, pp. 1834 - 1842, October 1992.

[2]. Albrecht N P, Fleck W C, Fodero K J, Ince R J, 'Charge Comparison Protection of Transmission Lines - Communications Concepts', IEEE Transactions on Power Delivery, Vol. 7, No. 4, 92 WM 210 - 5 PWRD, pp. 1853 - 1859, October 1992.

[3]. Yee L, Brownlee D C, 'Protection and Telecommunications Interface Problems for Digital Data Transfer Relays', Communications, Computers and Power in the Modern Environment, IEEE Wescanex 93, Conference Proceedings, ch. 60, pp. 7-14, 1993.

[4]. Redfern M A, Chiwaya A A W, 'A New Approach to Digital Current Differential Protection for Low and Medium Voltage Feeder Circuits Using a Digital Voice-Frequency Grade Communications Channel', IEEE/PES Winter Meeting, New York, 94 WM 013-3 PWRD, Feb 1994.

[5]. CCITT Recommendations, 'Series V Recommendations: Data Communication Over the Telephone Network',Vol. VIII, Fascicle VIII.1, ITU, pp. 65 - 69, 153 - 180, 252 - 266, 1989.

[6]. Redfern M A, Hewett R J, Chiwaya A A W, 'An Investigation into Reverse Power Flow Protection for Small and Medium sized Embedded Generation', UPEC Proceedings, pp. 109 - 112, Sept 1993.

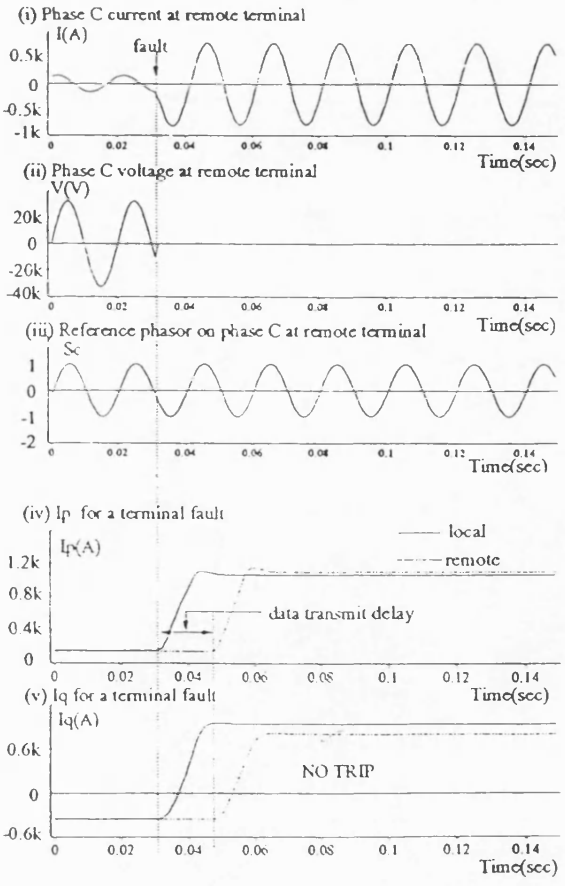

FIGURE 7. Signals for a Terminal Fault on the Test System.

PAPER 5

A A W Chiwaya, M A Redfern, 'A Novel Technique in Digital Current Differential Protection for Distribution Feeders', International Power Engineering Conference, Singapore,1995.

A NOVEL TECHNIQUE IN DIGITAL CURRENT DIFFERENTIAL PROTECTION FOR DISTRIBUTION FEEDERS.

A. A. Chiwaya and M. A. Redfern.
University of Bath
UK.

Abstract

This paper presents a new technique for current differential relaying of distribution feeders that compares polarised polyphase current measurements taken at the feeder's terminals to detect faults. The signal processing reduces the requirements of the communications system by transforming the current measurements into nominally dc values. Voice frequency channels are therefore able to satisfy the communications requirements which have been limited to a full duplex 2400 bits per second system. With variations in the synchronism between fault occurrence and data transmission, tripping times vary from one and a half to two and half power system cycles.

Keywords

Current differential relaying, distribution feeder protection, digital relaying, voice frequency communications channels.

1 INTRODUCTION

To detect faults, current differential protection involves the comparison of electrical quantities at the boundaries of the protected zone. In the comparison of the zone boundaries of a feeder circuit, the separation between the terminals necessitates the use of a communications channel to transfer the electrical quantities from the remote terminal to the local terminal. The communications should ideally instantaneously transfer all the data required for the protection between the relays in the scheme.

However, practical communications systems introduce complications. There is a significant delay associated with transmission of data due to analogue to digital conversion, buffering for transmission, channel propagation delays, and transmitting the message. Effective protection therefore normally requires precise time-alignment of the sampled waveforms from the feeder terminals. Combining raw data, communication protocols and error control coding, the volume of data required to correctly define the measured quantities and to be transferred between the relays is high. Although wideband communications would satisfy these requirements, their use in short distribution feeders may not be attractive on financial grounds.

The technique presented has been formulated to use a voice frequency communications channel for data transmission. It resolves the problems of precise time alignment of data from the terminals and the requirement of large channel capacity by dramatically reducing the amount of data used to define the current signals. At each feeder's terminal, instead of using the raw sampled data, these were compared with locally obtained reference data, polarising signals, to produce a non-sinusoidal signal which characterised the locally measured three phase currents. Being nominally dc signals, the demands on the communications are dramatically reduced.

The communications requirements are satisfied with a voice frequency channel operating at 2400 bits per second in full duplex mode. With an operating bandwidth of 4 kHz, the channel can use a dedicated medium or share a medium with other channels. Voice frequency communications can use most media including pilot wires, microwave and optical fibres. Having been extensively developed for the mass communications market, they provide a convenient and economic standard for use with distribution system relaying.

2 CURRENT DIFFERENTIAL RELAYING

In feeder circuit applications, relays located at the terminals monitor the electrical quantities and compare local with received quantities from other relays in order to make a trip decision. They also provide data for other relays in the scheme. An overview of a typical relay located at one terminal is summarised in figure 1.

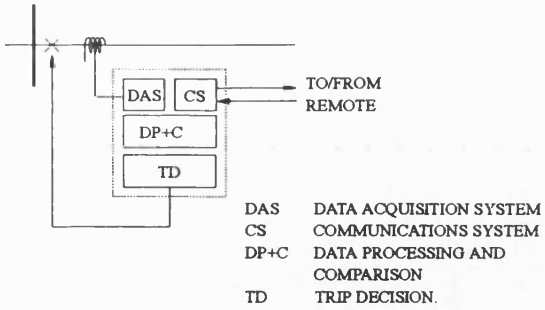

Figure 1: Overview of current differential relaying located at one of the feeder's terminals

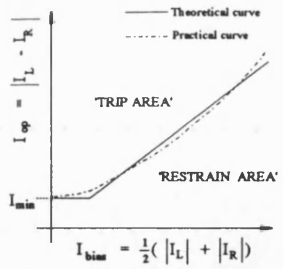

Figure 2: Biased current differential trip characteristic

The input signals are filtered using anti-aliasing filters and then sampled using a 12 bit Analogue to Digital converter. The digitised signals are provided to the data sending unit for coding and transmission. As soon as an incoming message has been received and decoded, its value is compared to the locally measured signal taking into consideration the communications system delays. Using the principle that the current flowing into the fault in the protected zone is the difference between the local and remote currents, data processing and comparison involves calculating the difference or operate current. To cater for such effects as line charging currents, a minimum difference current is allowed for. As CT mismatch results in different excitation for the same inputs, and particularly so during through faults, a restrain or bias term is calculated. With the local current as I_L and the remote current as I_R, the operate and bias currents are given as:-

$$I_{op} = |I_L - I_R|$$
$$I_{bias} = \frac{1}{2}(|I_L| + |I_R|) \quad (1)$$

A percentage bias setting k is introduced to overcome CT mismatch. It indicates the operate current required to operate the relay as a percentage of the restraint current [1]. Generally, the trip criterion is summarised as:-

$$I_{op} > I_{min} \quad AND \quad I_{op} > k\, I_{bias} \quad (2)$$

Figure 2 shows the typical trip characteristic for a differential protection scheme.

3 THE NEW ALGORITHM

As mentioned above, the new protection scheme uses a 2400 bits/sec full duplex data communications system. Assuming communications protocols and error detection coding account for nominal fifty percent overheads, the practical data transfer capacity is equivalent to a modest 24 bits per cycle.

Techniques were therefore examined which would dramatically reduce the data required to define the current signals. This overcomes the need to transmit the mass of data required to define the sampled current waveform and enables the system to operate with a data transfer capacity of 24 bits per cycle. The technique chosen was based on the equations used to derive instantaneous power in a three phase circuit [2]. Multiplying the instantaneous values of the sampled phase currents with the instantaneous values of three-phase reference phasors provides a measurement which contains a steady dc component and second harmonic terms. The steady component contains both amplitude and phase information of the monitored three phase currents with respect to the reference phasors.

The reference phasors are derived from signals that are synchronised to the power system frequency and ideally have the same phase at all the feeder's terminals. As the protection is intended for relatively short feeders in heavily interconnected power systems, the phase voltage signals provide suitable references. To cater for conditions when there are no VT's, as may be common in distribution circuits, reference phasors were also derived from the positive phase sequence currents.

The three phase reference phasors are a set of three unit amplitude rotating sinusoidal waveforms 120 degrees apart and designated s_a, s_b and s_c for phases a, b and c respectively. To maintain the sinusoidal nature of the reference following a system disturbance, a 120 millisecond memory feature is provided.

The sum of the products of the instantaneous three phase currents i_a, i_b, and i_c and the instantaneous values of the reference phasors s_a, s_b, and s_c, together with some filtering, produces a constant term I_p. The measurement I_p represents the amplitude of the current in phase with the reference phasors. An orthogonal set of reference phasors, (s_a-s_b), (s_b-s_c) and (s_c-s_a) produces a second measurement I_q which provides complimentary information. Hence the two measurements fully characterise the monitored terminal currents. I_p and I_q are

given as:-

$$I_p = i_a s_a + i_b s_b + i_c s_c \quad (3)$$

$$I_p = 3\ I \cos(\phi) \quad (4)$$

and

$$I_q = i_a(s_b - s_c) + i_b(s_c - s_a) + i_c(s_a - s_b) \quad (5)$$

$$I_q = 3\sqrt{3}\ I \sin(\phi) \quad (6)$$

Using either the phase voltages or the positive phase sequence currents, the relay system at each terminal derives the reference phasors and uses the current samples with these to generate the basic I_p and I_q measurements as in Equations (3) and (5). Averaging the measurements I_p and I_q over half a power system cycle removes any second harmonic terms, leaving the nominally steady dc term.

3.1 Communications Systems

Telephone-based digital data communication systems provide an almost ready made communications platform which can be used for distribution feeder protection relaying. To interface the communications medium with the digital protection system requires a modem. Operating at different speeds ranging from 75 bits/sec to 14400 bits/sec in full or half duplex, modems offer different advantages for different applications. A host of standards have been agreed which define the characteristics of the different systems and ensure connectivity between different equipments. Figure 3 gives a summary CCITT V-series modem standards [3].

After careful consideration of the characteristics of the communications systems, it was decided to base the research on a V.26 modem standard operating at 2400 bits/sec in full duplex. The V.26 offers an acceptable tolerance to system disturbances with an idle time of about 15 milliseconds. This is better than the 50 milliseconds for the V.33 [4].

For the transfer of data between the terminals of the protected feeder, the data stream is marshalled into messages such that each block of data is started with a six bit header followed by two Hamming (13,9) code blocks [5]. The six bit header is a defined set of bits which provide data synchronism. The two Hamming code blocks provide eighteen data bits comprising two identifier bits, two bits reserved for other applications, and fourteen data bits relating to I_p or I_q. They also provide eight bits for error detection. A total message thus has thirty two bits. With a modem operating at 2400 bits/sec, the message requires 13.33 milliseconds transmission time. Together with the delays due to signal propagation and marshalling, a typical communications system delay time of 17 milliseconds has been used. In the algorithm, therefore, when the remote data has been received and decoded, it is compared with the local data delayed by this communications system delay time.

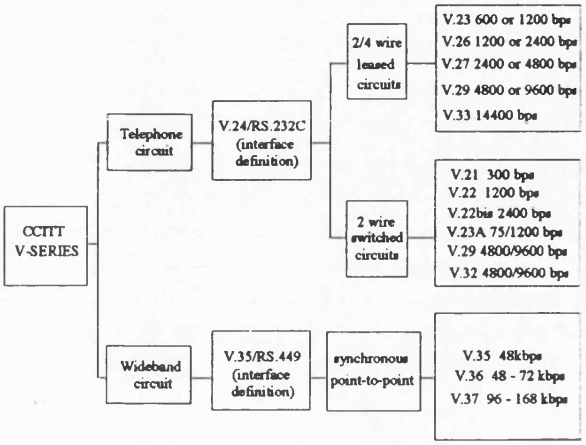

Figure 3: Summary of CCITT V-series modem standards

The relay calculates $(I_p)_{op}$, $(I_p)_{bias}$, $(I_q)_{op}$ and $(I_q)_{bias}$ using Equation (1). A trip indication is given when either I_p or I_q satisfies Equation (2). The algorithm produces a trip output after two trip indications. The trip conditions can either be consecutive trip decisions, I_p and then I_q, or vice versa, or alternatively two subsequent I_p or I_q trips.

4 EVALUATION OF THE ALGORITHM

The test power system model for evaluation was modelled using the EMTP power simulation package. A typical 33 kV feeder circuit containing parallel lines was modelled using firstly overhead lines, then underground cables, and finally a combination of overhead lines and underground cables. Distances of the feeders were limited to 20km. With the protection scheme on one of the parallel lines, a variety of internal faults and external faults were studied, with external faults applied on the parallel feeder as well as on the supply feeders. Balanced faults involving three phases and unbalanced faults involving single phase and double phases were considered. Also considered were variations of points-on-wave at fault for both in-zone and external to the protected zone. Terminal faults and faults close to the terminals were also considered.

4.1 RESULTS WITH POLARISING REFERENCE PHASORS FROM PHASE VOLTAGES

Sinusoidal unit amplitude reference phasors were synchronised to the phase voltages. Input and derived waveforms are illustrated in figure 4 for a typical fault condition on the test system.

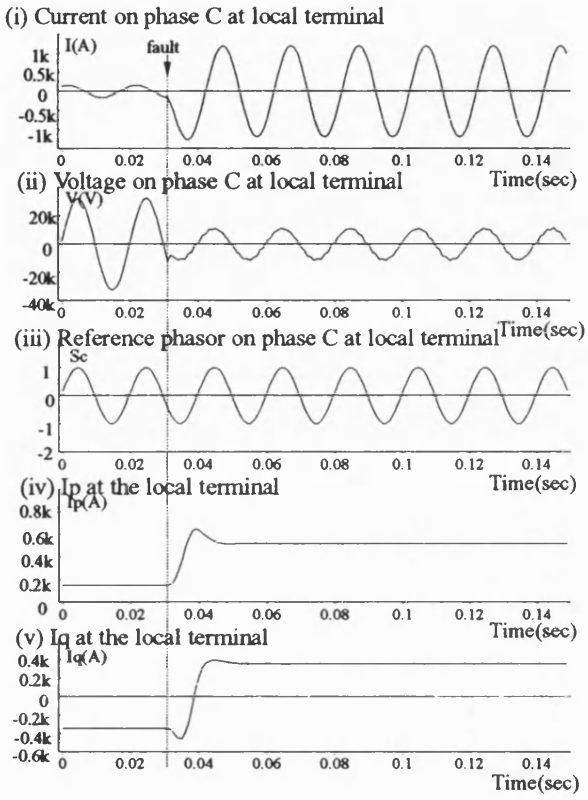

Figure 4: Input and derived waveforms for a typical fault when reference is derived from phase voltages

Both I_p and I_q are constants confirming Equations (4) and (6). The fault results in large measurements for both I_p and I_q. Within 20 milliseconds after the fault, both I_p and I_q have settled to new steady values.

Figure 5 shows the comparisons between the locally obtained I_p and I_q signals to those received from the remote end of the feeder for a typical in-zone fault. This figure clearly shows the difference between the measurements during the fault, and the delays between the two signals which are caused by the communications system. Bias settings k of 2 percent for both I_p and I_q were used with trip settings $(I_p)_{min}$ and $(I_q)_{min}$ of 200 Amps. Using the trip requirement of two subsequent trip indications, in-zone faults lead to an average trip time of 40 milliseconds. The train of spikes on the trip signal indicates that as long as the fault is on, the algorithm produces a trip output every time it makes a comparison between the local and received signals.

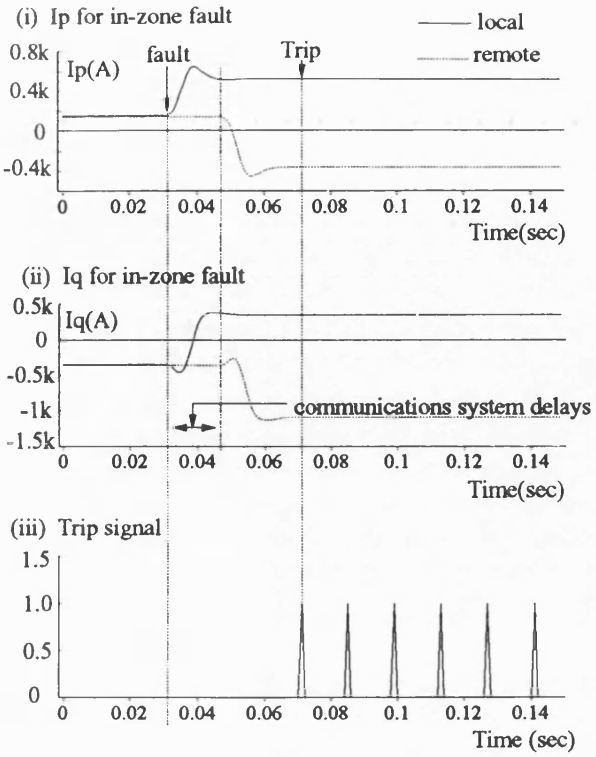

Figure 5: Polarised currents for a typical in-zone fault when reference is derived from phase voltages

Figure 6 shows the comparison between the locally obtained I_p and I_q signals to those received from the remote end of the feeder for an external fault. For this condition, the measurements are relatively small and although there is a difference between the local and remote signals, this is less than the trip setting. The algorithm therefore remains stable and does not trip.

The response to a terminal fault condition resulting in voltage collapse at one terminal is illustrated in figure 7. For this condition, although the disturbance was detected, the algorithm remained stable and did not trip.

4.2 RESULTS WITH POLARISING REFERENCE PHASORS FROM POSITIVE PHASE SEQUENCE CURRENTS

The positive phase sequence currents referenced to the phases a,b and c are I_{a1}, I_{b1} and I_{c1}, respectively. In terms of discrete sample values, with n_s samples per power system cycle, the instantaneous values for these are derived from equations similar to those for the 'a' phase value shown below:-

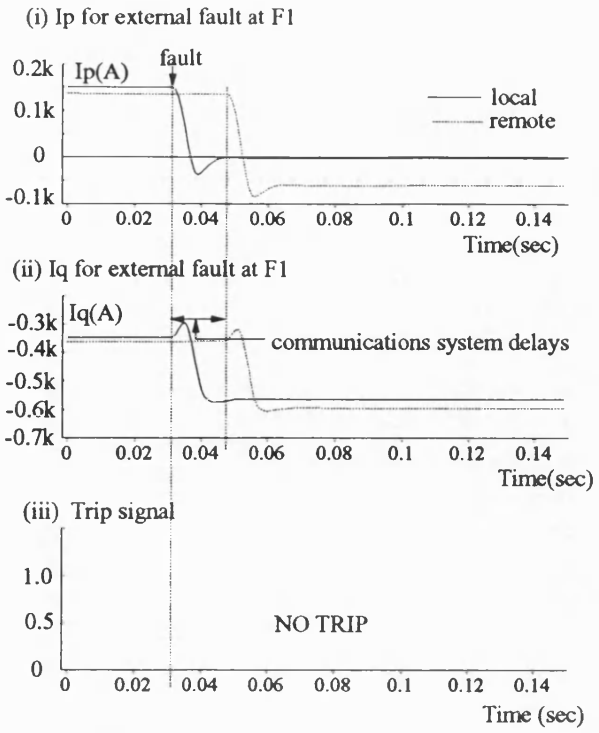

Figure 6: Polarised currents for a typical external fault when reference is derived from phase voltages

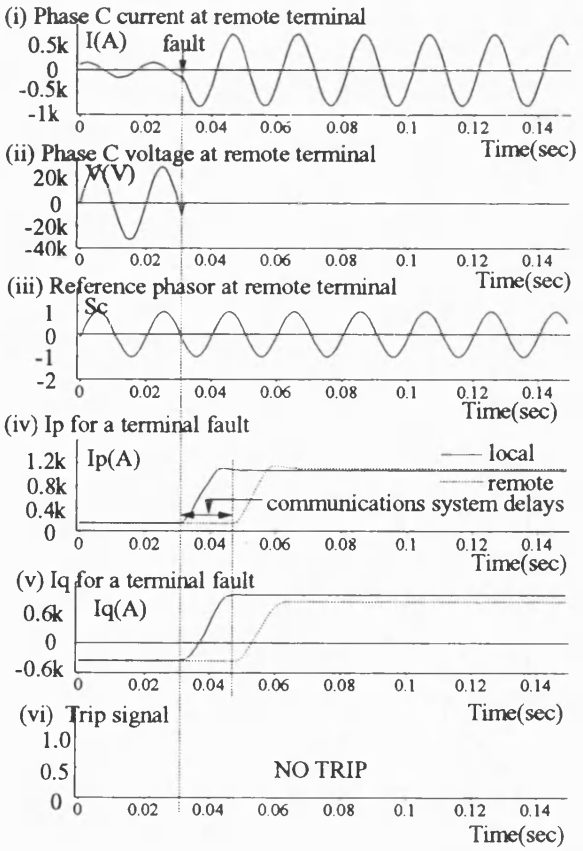

Figure 7: Input and derived waveforms for a terminal fault at a remote terminal on the test system

$$i_{al} = \frac{1}{3}\left[i_{a,n} + i_{b,(n-\frac{2}{3}n_s)} + i_{c,(n-\frac{1}{3}n_s)} \right] \quad (7)$$

where n represents the instant that the last sample was taken. With n_s equals to 24, Equation (7) becomes

$$i_{al} = \frac{1}{3}\left[i_{a,n} + i_{b,(n-16)} + i_{c,(n-8)} \right] \quad (8)$$

Sinusoidal unit amplitude reference phasors synchronised to i_{a1}, i_{b1} and i_{c1} were derived using a phase locked loop which included a memory feature. Input and derived waveforms for a typical application with a fault condition are shown in figure 8.

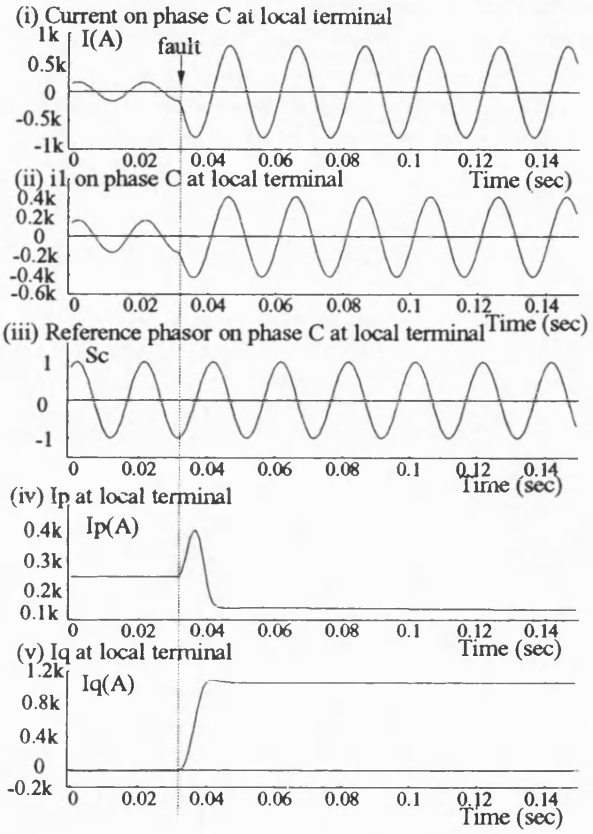

Figure 8: Signals for a typical fault when reference phasors are derived from positive phase currents

Figure 9 shows the algorithm's response to an in-zone fault condition. The average trip time was 38 milliseconds, measured over 100 fault applications.

The responses to a typical external fault are illustrated in figure 10. For this fault condition the algorithm did not produce a trip output.

5 CONCLUSION

This paper has presented the new technique for current differential protection that uses polarised polyphase current measurements taken at the feeder's terminals to detect if a shunt fault exists in the protected zone. The need for large channel capacity and accurate time alignment of the data from the terminals of the feeder is avoided by using polyphase measurements of the three phase currents which are referenced to two orthogonal reference waveforms. A half cycle moving average filter is used to remove any second harmonic terms and provide nominally steady outputs. This technique reduces the demands on the communications and allows the use of low data rates associated with voice frequency channels.

In the first algorithm, phase voltages are used to derive the reference. As the protection is for distribution feeders, the use of VT's may be unattractive. An alternative method therefore uses the positive phase sequence current to derive the reference. Both methods provide effective protection and trip for in-zone faults while restraining for out of zone faults.

For the fault conditions presented for which the algorithm should trip, the algorithm tripped with tripping times varying between one and a half and two and a half cycles. There was no trip for external faults including terminal faults.

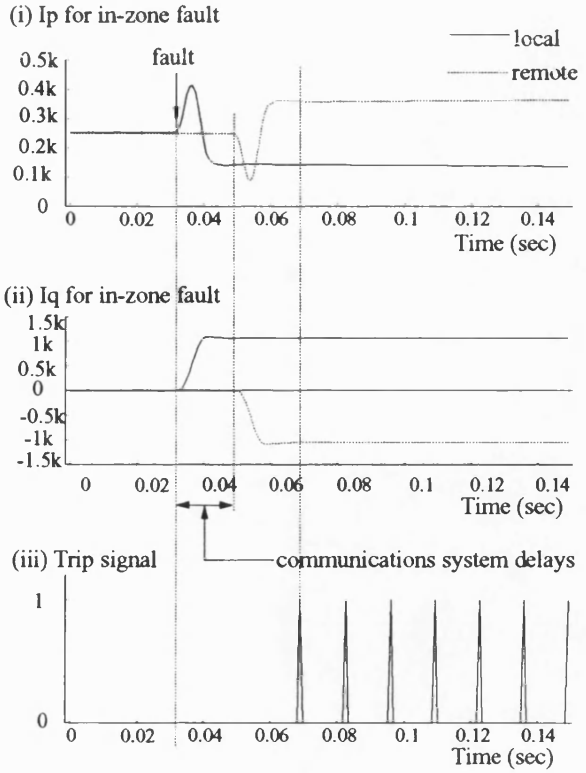

Figure 9: Polarised currents for a typical in-zone fault when reference is derived from I1

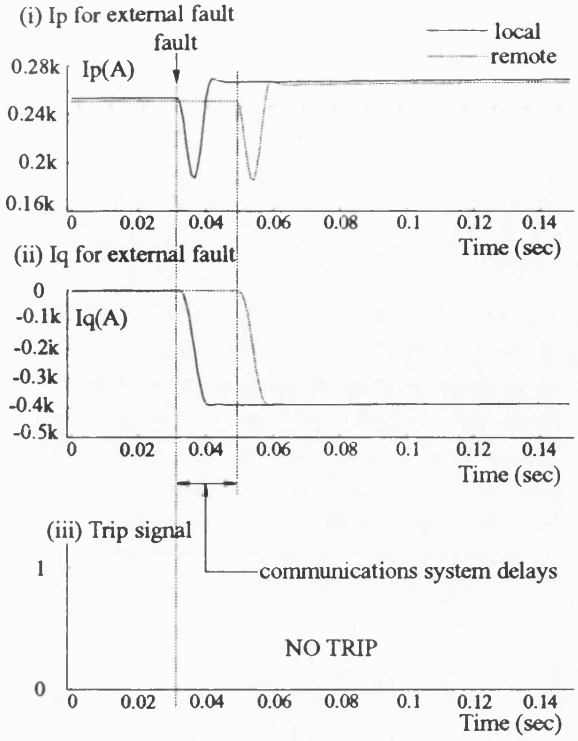

Figure 10: Polarised currents for a typical external fault when reference is derived from I1

REFERENCES

[1] Westinghouse Electric Corporation. *Applied Protective Relaying*. 2nd printing, 1979.

[2] IEEE Tutorial Course on Power. Nonsinusoidal situations: Effects on the Performance of Meters and Definitions of Power. *IEEE Power Engineering Society, course text*. 90EH0327-7-PWR.

[3] CCITT Recommendations, Blue Book. *Series V Recommendations, Data Communication over the Telephone Network*. Vol. VIII, ITU, 1989.

[4] D.R. Doll. *Data Communications, Facilities, Networks, and Systems Design*. Wiley and Sons, 1978.

[5] M.A. Redfern, D.P. McGuinness and R.F. Ormondroyd. High security digital data communications for unit protection of distribution feeders and local network automation. *Pro. Int. Conf. on New Developments in Power System Protection & Local Control*. China, 1994.